The Dissertation Committee for Alexander Asterios Plionis

certifies that this is the approved version

of the following dissertation:

Automated Multi-Radionuclide Separation and Analysis with

Combined Detection Capability

Committee:

Sheldon Landsberger, Supervisor

Kendra Biegalski

Steven R. Biegalski

Erich A. Schneider

Dominic Peterson

Automated Multi-Radionuclide Separation and Analysis with Combined Detection Capability

by

Alexander Asterios Plionis, B.A., M.S.E.

Dissertation

Presented to the Faculty of the Graduate School of

The University of Texas at Austin

in Partial Fulfillment

of the Requirements

for the Degree of

Doctor of Philosophy

The University of Texas at Austin

December, 2007

Dedication

I would like to dedicate this dissertation to my wife, Krista Scott Plionis. Her love and support provide me with the strength and confidence I need to accomplish any task.

Acknowledgements

I would like to thank Dr. Sheldon Landsberger for guiding me to this research project and for all the advice and encouragement he has provided me during the course of its research and writing. From him I have learned not only the academics of Nuclear Engineering, but also the traits of a professional scientist.

I would also like to thank Dr. Dominic Peterson for his supervision of my research during my time at the Los Alamos National Laboratory. From him I have learned how to function as a scientist within the national lab complex.

In addition, I would like to express my deepest gratitude to Edward Gonzales for mentoring and supporting me throughout my tenure at Los Alamos. His recent mentor of the year award is a well-deserved honor.

I am very grateful to my entire family and especially my wife for all of their love and support in getting me though all of life's difficulties.

Special appreciation is given the entire faculty and staff of the Nuclear Engineering Program for their time, advice, and patience during my studies at the University of Texas at Austin. This appreciation is also extended to the entire Chemical Sciences and Engineering group at the Los Alamos National Laboratory for their generous financial, technical, and moral support throughout this project.

Automated Multi-Radionuclide Separation and Analysis with Combined Detection Capability

Publication No._____

Alexander Asterios Plionis, PhD

The University of Texas at Austin, 2007

Supervisor: Sheldon Landsberger

The radiological dispersal device (RDD) is a weapon of great concern to those agencies responsible for protecting the public from the modern age of terrorism. In order to effectively respond to an RDD event, these agencies need to possess the capability to rapidly identify the radiological agents involved in the incident and assess the uptake of each individual victim. Since medical treatment for internal radiation poisoning is radionuclide-specific, it is critical to identify and quantify the radiological uptake of each individual victim. This dissertation describes the development of automated analytical components that could be used to determine and quantify multiple radionuclides in human urine bioassays. This is accomplished through the use of extraction chromatography that is plumbed in-line with one of a variety of detection instruments. Flow scintillation analysis is used for ^{90}Sr and ^{210}Po determination, flow gamma analysis is used assess ^{60}Co and ^{137}Cs, and inductively coupled plasma mass spectrometry is used to determine actinides. Detection limits for these analytes were determined for the appropriate technique and related to their implications for health physics.

Table of Contents

List of Tables

List of Figures

Chapter 1: Introduction

The radiological dispersal device (RDD) is a weapon of concern to those agencies responsible for protecting the public from the modern age of terrorism. The Centers for Disease Control and Prevention (CDC) is charged with promoting health and quality of public life by preventing and controlling disease, injury, and disability. It would be the frontline institution for administering to the health and well being of victims of an RDD attack. In order to effectively respond to an RDD event, an agency like the CDC needs to possess the capability to rapidly identify the radiological agents involved in the incident and assess the uptake of each potential victim. This task is made more daunting by two factors: one, the prospect that a densely populated area will be targeted and two, the fact that an RDD can be comprised of one or any number of the thousands of radionuclides that exist. Since medical treatment for internal radiation poisoning is radionuclide-specific, it is critical to identify and quantify the radiological uptake of each individual victim as quickly as possible.

While over 3,100 radionuclides are known to exist, most have too short a half-life to be produced in macro quantities, thus they are not suitable for use in any type of weapon (KAPL 2002). Several dozen radionuclides *do* exist in significant quantities and many of these are accessible in consumer products, industrial sites, and research institutions. In assessing the threat posed by these accessible radionuclides, CDC has come up with a short list of radionuclides of greatest concern, shown in Table 1.1. The purpose of this research is to develop analytical components that could be utilized in a proto-type system that will analyze and quantify radionuclides from urine samples of RDD victims in a rapid and automated manor. This will be accomplished by the chemical separation of analytes using extraction chromatography and multiple counting

techniques including: flow scintillation analysis, flow gamma analysis, mass spectrometer, and optional off-line alpha spectrometry.

Table 1.1: Isotopes of Concern for Use in an RDD.

ISOTOPE	DECAYS BY	HALF-LIFE
^{51}Cr	β/γ	27.702 d
^{57}Co	β/γ	271.8 d
^{60}Co	β/γ	5.271 y
^{90}Sr	β	28.78 y
^{131}I	β/γ	8.020 d
^{137}Cs	β/γ	30.07 y
$^{192/192m}Ir$	β/γ	240 y
^{210}Po	α	138.38 d
^{226}Ra	α	1599 y
^{233}U	α	1.59E5 y
^{235}U	α	7.04E8 y
^{237}Np	α	2.14E6 y
^{238}Pu	α	87.7 y
^{239}Pu	α	2.41E4 y
^{242}Pu	α	3.75E5 y
^{241}Am	α	432.7 y
^{243}Am	α	7.37E3 y

RESEARCH OBJECTIVES

The creation of a system capable of multiple radionuclide separation and analysis is extremely complex due to the number of individual components that need to be developed and optimized. Multiple detection methods are required for different types of radiations and to accommodate the vast differences in half-lives and emission type of the associated nuclides shown in Table 1. This research attempts to identify, create and optimize the necessary components of such a system.

The detection of ^{90}Sr is difficult because it is a pure beta emitter and has a sufficiently high specific activity to preclude detection via inductively coupled mass spectrometry (ICP-MS) at biologically important activities. Liquid scintillation is the preferred method of detection for ^{90}Sr, but the technique is problematic in that it requires the quantitative separation of ^{90}Sr from virtually all other beta emitters to prevent interferences. To perform this separation, a high pressure gradient pump and an extractive chromatographic resin is employed in a technique called high pressure extraction chromatography (HPEC). And while traditional liquid scintillation counting is done off-line with a dedicated instrument, this research shows that on-line detection of ^{90}Sr can be accomplished using flow scintillation analysis (FSA), whereby the HPEC effluent is mixed on the fly with scintillating cocktail and counted with a detector that is plumbed on-line.

^{210}Po is an isotope that presents many challenges to its separation chemistry and detection. It is a virtually pure alpha emitter with a very high specific activity. Identification and detection are traditionally accomplished by a chemical separation followed by deposition onto a planchette for alpha spectrometry. The same HPEC technique employed for ^{90}Sr can be utilized for ^{210}Po by varying the loading and stripping

conditions. This research will show that ^{210}Po may also be detected using FSA—a completely novel approach for counting this isotope.

Among the isotopes in Table 1 are a number of relatively short-lived β/γ emitters (^{51}Cr, ^{57}Co, ^{60}Co, ^{131}I, ^{137}Cs, and $^{192/192m}$Ir). These isotopes are most easily quantified by their high intensity characteristic γ-ray energies. The isotopes ^{60}Co and ^{137}Cs, are representative of this group. It is, therefore, prudent to use these isotopes to demonstrate proof of principle in developing novel counting methods for identification and quantization of the short-lived β/γ isotope group. Traditionally, these isotopes are quantified off-line by high purity germanium detectors. However, automation for these off-line systems usually consists of one-of-a-kind custom sample changers that do not interface with automated chemistry techniques. In order to further automate the separation and detection of the short-lived β/γ emitter group, they must be incorporated into a flowing system. These isotopes are typically not well retained by HPEC, which results in their being separated *en mass* from the many isotopes that are well retained by HPEC. Detection is accomplished using flow gamma analysis (FGA), whereby a well-type sodium iodide (NaI) detector is used to provide rudimentary spectral analysis of the isotopes in the flowing system. This research shows that this novel technique is a suitable method for quantifying ^{60}Co, ^{137}Cs, and other similar isotopes.

Another significant isotope group in Table 1 is the long-lived actinide group (^{233}U, ^{235}U, ^{237}Np, ^{238}Pu, ^{239}Pu, ^{242}Pu, ^{241}Am, ^{243}Am). These isotopes are most easily quantified using alpha spectrometry and their characteristic alpha radiation energies. Alpha spectrometry requires extensive source preparation methods that can only be accomplished by off-line radiochemistry (ASTM 2005a; 2005b). Automated analysis of this group is more easily accomplished by mass counting with an ICP-MS. Since all of these isotopes have low specific activities, fast ion counting is usually more efficient than

radiometric counting techniques. In addition, mass spectrometry easily accommodates automated separation methods, such as HPEC.

It is conceivable that one might want the flexibility to utilize the automated separation techniques to facilitate off-line detection methods. For this reason, HPEC was examined as source preparation tool for traditional alpha spectrometry. This is accomplished by plumbing a fraction collector on-line with the HPEC system to collect the column effluent into different beakers. In this manor, alpha emitters with spectral interferences, e.g. ^{234}U and ^{237}Np, can be collected into different beakers and electrodeposited separately. This novel application of HPEC can reduce the typical alpha source preparation time by several hours.

When assessing the detection limits of the techniques that have been evaluated, it is important to not lose sight of the health physics implications, as they apply to internal dosimetry. By knowing the effective dose coefficients of the isotopes studied and the established detection limits, we can determine the effectiveness of each technique as a screening method for determining the level of radiological uptake for the victims that produced the sample. We can therefore determine the committed dose of a given victim, and relate this dose to a prognosis in terms of chances of a fatalality . Such knowledge may provide medical professionals with the information they need to determine what, if any, treatment is needed for a given patient.

As outlined above, the research objectives of this work can be concisely stated to be to develop and optimize the individual components of an automated radionuclide separation and detection system. These components include ^{90}Sr analysis by FSA, ^{210}Po analysis by FSA, ^{60}Co and ^{137}Cs analysis by FGA, actinide analysis by mass spectrometry, optional on-line actinide separation for off-line alpha spectrometry, and the determination of the health physics implications of the individual component capabilities.

LITERATURE REVIEW

Due to the multifaceted nature of the proposed system, a complete review of the literature pertaining to the topics covered in this project would be quite extensive, easily comprising thousands of publications. Among the many components of the proposal are: actinide chemistry, synthetic extractive ligands, chromatography, liquid scintillation counting, gamma spectroscopy, mass spectrometry, automation techniques, and the health physics of bioassays. In order for this literature review to be concise and relevant, it will focus on the intersection of two or more of these topics—extractive resins for chromatography, flow scintillation analysis (FSA), flow gamma analysis (FGA), polonium chemistry and detection, mass spectrometry for the detection of radionuclide, and automated actinide separations for electrodeposition. The reader is encouraged to investigate the works cited herein for a more detailed accounting of specific topics when the desired understanding is beyond the scope of that presented within this review.

Extractive Resins for Chromatography

Extractive chromatography for the purpose of radiochemistry came into existence in the early 1990s through the efforts of a research team comprised of Horwitz *et al.* at Argonne National Laboratory. Building on the previous success (Horwitz 1984; 1985) of a liquid-liquid extraction process using the key ingredient octyl(phenyl)-N, N-diisobutylcarbamoylmethylphosphine oxide (CMPO), the team began investigating more convenient uses for the compound as it pertained to actinide separations. The result was a publication describing a method of extracting actinides from an aqueous solution onto a column that had been packed with inert polymer beads coated with CMPO and then eluting the actinides as a group (Horwitz 1990). The same methodology was explored in subsequent publications using other extractive compounds (Horwitz 1991; 1992a; 1992b; Chiarizia 1993; Horwitz 1993a; 1993b; 1997). Realizing the commercial potential of

pre-packed extraction columns, Horwitz launched Eichrom Inc. in 1990 and now supplies a variety of selective columns for radioanalytical chemistry. Extractive chromatography soon surpassed ion exchange resins as the medium of choice for radinuclide extraction, preconcentration, and separation.

One of the most successful of these extractive resins was Sr-Spec, a crown ether molecule (bis-4,4'(5')-[tert.-butylcyclohexano]-18-crown-6) that is selective for Sr, Pb, Po, Tc, Pu, and to a lesser extent, Th, U, Np, and Am (Horwitz 1992b). This resin is used extensively in this research for its ability to selectively retain and elute ^{90}Sr and ^{210}Po. Another successful resin is the TRU-Spec resin, which is COMPO dissolved in TBP (Horwitz 1990). This resin is selective for Th, U, Np, Pu, Am, Bi, Fe, and to a lesser extent, Tc. This resin is used in this research for its ability to retain a mixture of actinides and to selectively elute them under specific conditions.

Flow Scintillation Analysis

Despite a history dating back to the 1970s of flow scintillation analysis (FSA) in the biosciences (Parvez 1988), a report as late as 1989 notes the fact that, "the application of FIA [FSA] for the automation of radioanalytical methods has not been reported"(Kuca 1989). Two years later the first radioanalytical application of FSA was attempted to detect radioactive silver displaced from a preloaded column (Grudpan 1991). Other publications were seen that touted the potential benefits of FSA, but no separations were performed to evaluate such systems (Tolgyessy 1993; U 1994a; 1994b; 1994c; 1995). The first radionuclide separations with on-line scintillation detection were conducted on reactor coolant water for a variety of radionuclides and in nuclear waste for ^{90}Sr, both involving very high sample activity (Fjeld 1995; Grate 1996). The first use of FSA for bioassay purposes was for ^{90}Sr where a MDA in the rage of nCi/L was achieved (Desmartin 1997). The next year there were a series of publications by Egorov and

Grate, who were working with a Radiomatic FSA at Pacific Northwest National Laboratory, including: the first coupling of an FSA and Eichrom's TRU extractive chromatographic column (Egorov 1998a), determination of ^{99}Tc from nuclear waste using a TEVA column (Egorov 1998b), and optimization of FSA analysis for ^{238}Pu and ^{241}Am from a TRU column (Grate 1998). Subsequent publications investigated the detection and optimization of other radionuclides (Egorov 1999a; 1999b; Grate 1999a; 1999b; 2005). Another team—DeVol *et al.*, based out of Clemson University—conducted similar work, with an emphasis on environmental monitoring, using a β-RAM FSA by IN/US Systems (Fjeld 1995; Coates 2001; Roane 2002; Hughes 2003; Roane 2003; Fjeld 2005; Hughes 2006a; 2006b)

The combination of automated chemical separations with on-line detection capability make FSA an ideal technique for determining the pure beta emitter, ^{90}Sr, and the high specific activity alpha emitter, ^{210}Po. The ability to enhance FSA detection limits using a stopped flow detection technique has also been described and is used in this research (Grate 1996; Egorov 1998b; Grate 1999b).

Flow Gamma Analysis

The body of publications pertaining to flow gamma analysis (FGA) is small when compared to that which exists for FSA. The study on reactor coolant water, cited in the above paragraph, does evaluate the chromatographic separation and detection of several gamma emitters (^{55}Fe, ^{60}Co, ^{137}Cs), though it does not mention whether the detection was accomplished by an on-line detector (Fjeld 1995). The paucity of publications relating to FGA is most likely the result of the fact that off-line gamma counting is easy and yields better results (with an HPGe vs. an on-line NaI). Many off-line gamma counters are also partnered with an automated sample changer that facilitates high sample throughput.

Thus, there would be no need to develop an on-line gamma counting capability for routine gamma analysis. The exceptions to this statement would be:

1) If one were committed to an on-line detection system for the sake of having a more automated system while producing less waste

2) If one wanted to use chromatographic separations in order to sequentially analyze mixed gamma-emitters in order to lower background counts

3) If one wanted to analyze a mixture of gamma and non-gamma emitters in a single system

There seems to be room for research on all three of the above scenarios, indicating a direction for further development of the proposed system. Despite the lack of interest in the journals, there is extensive coverage of FGA instrumentation, gamma flow cells, and techniques in the Flow Scintillation Analysis chapter of the Handbook of Radioactivity Analysis (L'Annunziata 2003).

Polonium Chemistry and Detection

The element polonium (specifically the isotope ^{210}Po) was the first new element discovered in pitchblende by Marie Curie and was later named for her home country of Poland. Since its discovery, polonium has been widely studied and was utilized in the early days of the Manhattan Project as a neutron generator (Pearlman 1944). In 1945 the first comprehensive paper on polonium volatility, production, purification, electrodeposition, migration, and health concerns was produced (Dodson 1945). At the time, the tolerance for hand contamination was 1000 cpm and semiweekly urine bioassays were screened for a maximum permissible level of 3000 cpm per 24 hour voiding. Since the 1940s, the health hazards of ^{210}Po were further studied, and bioassay methods were further refined (Fink 1950; Anonymous 1951; Robbins 1955; Stannard 1964). After the 1960s, polonium bioassay studies shifted from studying the effects of

large work-related exposures of inorganic polonium in favor of assays of organic polonium from natural sources and tobacco products. An excellent review of ^{210}Po determination in environmental materials was recently published (Matthews 2007). The consensus among the literature is that ^{210}Po is considered to be one of the most toxic naturally occurring radionuclides (Al-Masri 2004).

The three principle methods of separating ^{210}Po from radioactive interferences and matrix ions are solvent extraction, ion-exchange chromatography, and extraction chromatography (Matthews 2007). The increasing popularity of extraction chromatography is due to the commercially available and proprietary Sr-Spec extractant by Eichrom Technologies. This is known to retain ^{210}Po from acid solutions with recoveries of approximately 70% (Vajda 1997). Several publications utilize a method whereby ^{210}Po is loaded onto the column with a hydrochloric acid solution and stripped with nitric acid (Vajda 1997; Biggin 2002; Obara 2003; Vreček 2003). This method and variations on it were employed in this research. The method of detection used in the all of the above references was traditional alpha spectroscopy. There is only one modern reference in the literature of using liquid scintillation to determine ^{210}Po activity (Brown 2005). In the paper, Brown was using a standard Tri-Carb liquid scintillation unit in combination with ICP atomic emission mass spectrometer to analyze hydrometallurgical samples that were known to be concentrated in ^{210}Pb, ^{210}Bi, and ^{210}Po relative to other uranium daughters. This research is the first to use flow scintillation analysis to detect ^{210}Po.

Mass Spectrometry for Radionuclide Detection

The routine use of mass spectrometery in the nuclear sciences is still less frequent than the use of radiometric methods. The improvement in sensitivity, coupled with the reduction of background noise and interferences, has accentuated the fact that mass

spectrometry is a complementary companion to radiometric techniques for radionuclide detection (Lariviere 2006). The first attempt to measure long-lived anthropogenic radionuclides in environmental samples by ICP-MS an analysis of ^{99}Tc seaweed and ^{129}I in rainwater at the ng level, collected after the Chernobyl accident (Brown 1988). The first use of an extractive chromatography to preconcentrate actinides to enhance mass spectrometry analysis came several years later (Hollenbach 1994). Very high concentrations of fission products and actinides from spent nuclear fuel were also determined by preconcentration of a sample stream with a high pressure liquid chromatography (HPLC) system feeding a mass spectrometer (Alonso 1995). A method for determining the ultra-trace concentrations of long-lived U, Np, and Pu isotopes found in urine bioassays was later determined using a similar HPLC and TRU column system and an ICP-MS (Wyse 1998). Further development and improvement of column loading and elution schemes optimized ICP-MS detection by lowering detection limits and improving actinide separations (Boulyga 2001; Egorov 2001). Work done in the Chemistry Division at the Los Alamos National Laboratory (LANL) used a single TRU column to demonstrate the detection of ^{238}U, ^{232}Th, ^{237}Np, ^{239}Pu, and ^{241}Am in urine bioassays (Hang 2004; 2005).

However, the great limitation of mass spectrometry for radionuclide determination is that the technique is not effective for high specific activity isotopes, where there is simply not enough mass present to be detected at the desired activity levels. A theoretical evaluation of the limitations of mass spectrometry to detect high specific activity isotopes, and of radiometric methods for detecting very low specific activity isotopes was also done in the Chemical Sciences and Engineering group at LANL (Gonzales 2005).

Automated Actinide Separation for Electrodeposition

The past 10 years have witnessed a number of publications on the automated analysis of actinides. The driving factor behind these publications is that the source preparation for alpha spectrometry is lengthy and labor-intensive. One of the most challenging factors is the separation of the actinides from their matrices and from each other, where they may interfere spectrometrically (this process can take a full day's work). Many of these research efforts employ high pressure chromatography driven mass spectrometry (Thompson 1986; Alonso 1995; Aldstadt 1996; Egorov 2001; Unsworth 2001; Hang 2004; 2005; Lariviere 2006). However, mass spectrometric techniques are limited in their ability to detect relatively high specific activity actinides. The second most prevalent technique is flow scintillation analysis that is driven by flow injection (Aldstadt 1996; Egorov 1998a), sequential injection (Grate 1996; Egorov 1998b; 1999a; Grate 1999a; 1999b; Egorov 2001), and high pressure chromatography (Fjeld 1995; Smith 1995; Desmartin 1997; Reboul 2002; Roane 2002; Fjeld 2005; Grate 2005). One publication employs a high pressure chromatography system to preconcentrate and determine ^{235}U and ^{241}Am by gamma spectroscopy (Stricklin 2002).

Source preparation by electrodeposition, and isotopic determination by alpha spectroscopy remain the method of choice for several relatively short-lived alpha emitters such as: ^{228Th}, ^{232}U, ^{238}Pu, ^{241}Am, and various curium and californium isotopes. For this reason, a system that permits the automated separation of actinides, while facilitating off-line electrodeposition and alpha spectrometry, could be useful for field-deployable emergency response activities, routine bioassays, or routine radioanalytical work.

The bridge between automated chromatographic separations and off-line electrodeposition is fraction collection (which also has many other uses). With fraction collection, a device called a fraction collector receives the column effluent and distributes

portions of it into different containers. The fraction distribution may be accomplished by pre-set time windows, or some method of detecting when an analyte is present in the effluent stream, such as the signal from a UV-Vis spectrometer. Fraction collectors have been employed in a few publications regarding automated actinide analysis (Egorov 1998a; Grate 1999b; Grate 2001). One publication employed manual effluent collection after flow scintillation analysis for alpha spectrometry, but the method of alpha source preparation was a neodymium fluoride precipitation (Grate 1999a). The precipitation was necessary because the sample was mixed with scintillation cocktail, precluding the chemical workup needed for electrodepositon. However, the technique of using a fraction collector to collect HPEC effluents for the explicit purpose of electrodeposition is novel and described in this research.

INSTRUMENTATION

Here, a brief overview of the instrumentation used in this work is provided. Pictured are: the flow scintillation/gamma system (Figure 1.1); inside the tandem flow gamma detector (Figure 1.2); the mass spectrometry system (Figure 1.3); the fraction collector (Figure 1.4); the electrodeposition system (Figure 1.5); an electrodeposition cell (Figure 1.6); and the alpha spectrometry system (Figure 1.7).

Figure 1.1: The flow scintillation/gamma system. 1) The computer system. 2) The gradient pump. 3) The reagent bottles. 4) The analytical injector (syringe port). 5) The 2000 µL sample loop. 6) The extraction chromatography column. 7) The β-RAM model 4B flow scintillation unit. 8) The tandem flow gamma detector.

The flow scintillation system, featured in chapters 3 and 4, is comprised of components 1-7. The flow gamma system, discussed in chapter 5, is comprised of components 1-8.

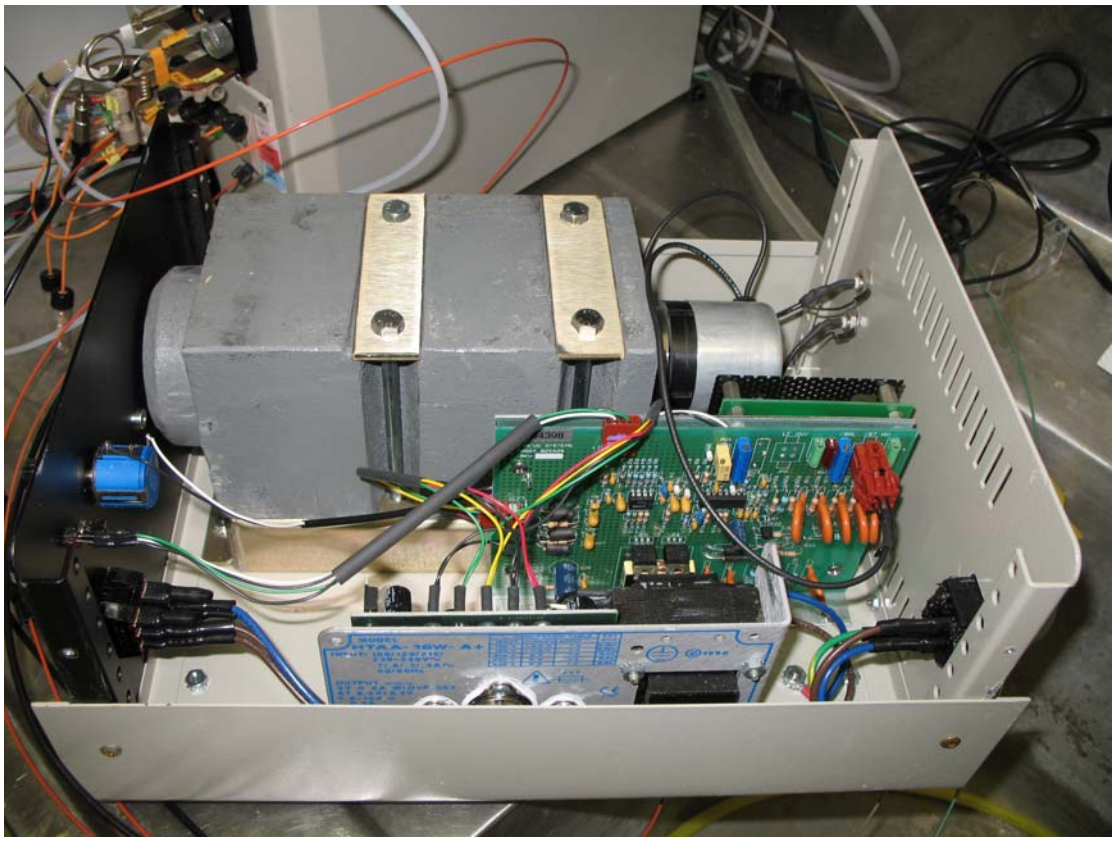

Figure 1.2: Inside the tandem flow gamma detector. The well-type NaI detector is housed within a formed lead casing. The high voltage source and pre-amplifier are housed within unit casing. Not pictured is the DSpec Pro MCA and positive NaI interface module.

As sold, the tandem flow gamma unit was intended to be a "black box" gross gamma counter for generating radio-HPLC chromatograms. The unit was not designed to provide energy discrimination of the detected γ-rays. Since the project goals of radionuclide identification necessitated the need for energy discrimination, the unit output signal was split and configured with a MCA. This allowed for the unit to provide both chromatographic and spectral information of the radionuclides detected.

Figure 1.3: The mass spectrometry system. 1) The computer system. 2) The ion chromatography unit. 3) The reagent bottles. 4) The autosampler. 5) The nebulizer. 6) The mass spectrometer. Not pictured is the chromatography column.

The mass spectrometry system used in the work featured in chapters 6 and 7. The ion chromatography unit used with this system is like the gradient pump in Figure 1.1, except that it is controlled by the Chromeleon IC management system, which coordinates this unit with the autosampler, the mass spectrometer, and the computer. The autosampler allows for the automated injection of multiple samples into the IC system. The nebulizer pictured in Figure 1.3 is not the concentric cyclonic spray chamber used in this work. It is a specialized nebulizer that allows for improved sensitivity by condensing the solvent molecules out of the sample stream.

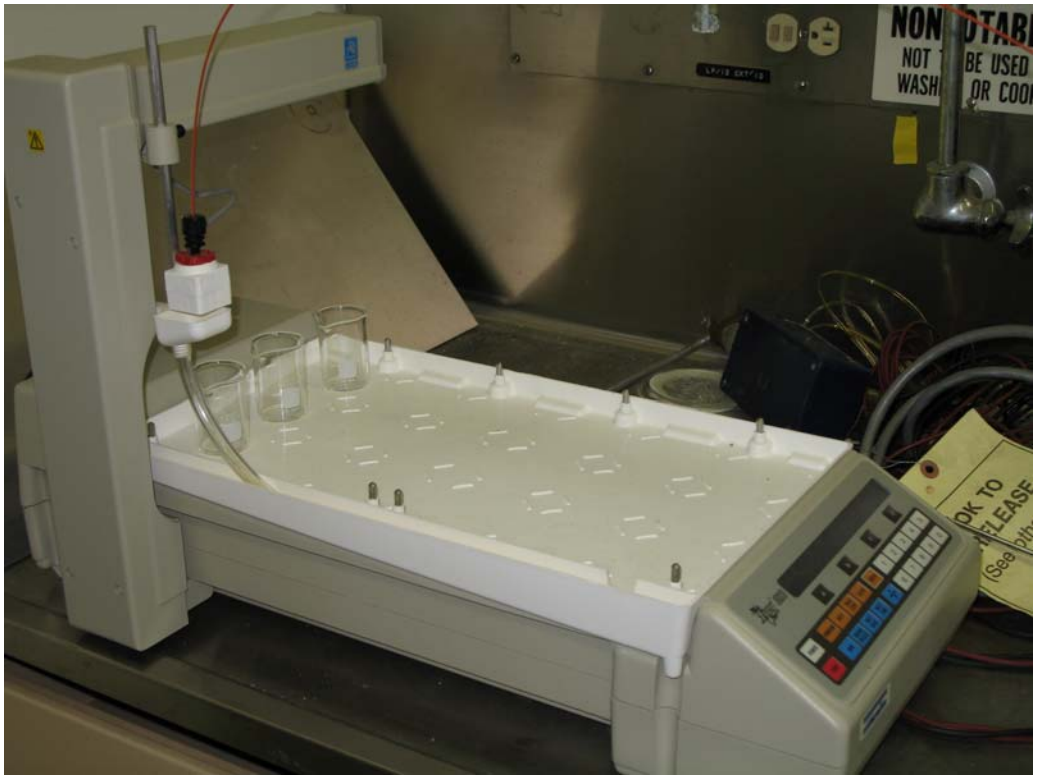

Figure 1.4: The fraction collector. Plumbed into the column exit, this system distributes the effluent into one of several containers according to a pre-programmed protocol.

The fraction collector pictured in Figure 1.4 was used in chapter 7 of this work. The system is used in combination with components 1-6 of Figure 1.1, where it is plumbed in-line with the column exit. The purpose of the system is to distribute the column effluent into various collection vessels according to a pre-programmed collection protocol. Here the vessels are 30 mL Pyrex beakers. The dripper of the fraction collector is free to move in the x and y-direction to access the beakers. As pictured, the fraction collector is draining to waste.

Figure 1.5: The electrodeposition system. 1) The constant current power supply. 2) The cell holder. 3) An electrodeposition cell.

The electrodeposition system seen in the above figure was used in create counting sources for the experiments of chapter 7. The power supply is capable of delivering 0.6 Amps of constant current to each of 16 cells during the course of the deposition time. The cell holder allows for uniform deposition parameters for each of the 16 cell positions. A deposition cell is shown in the context of the entire electrodeposition system.

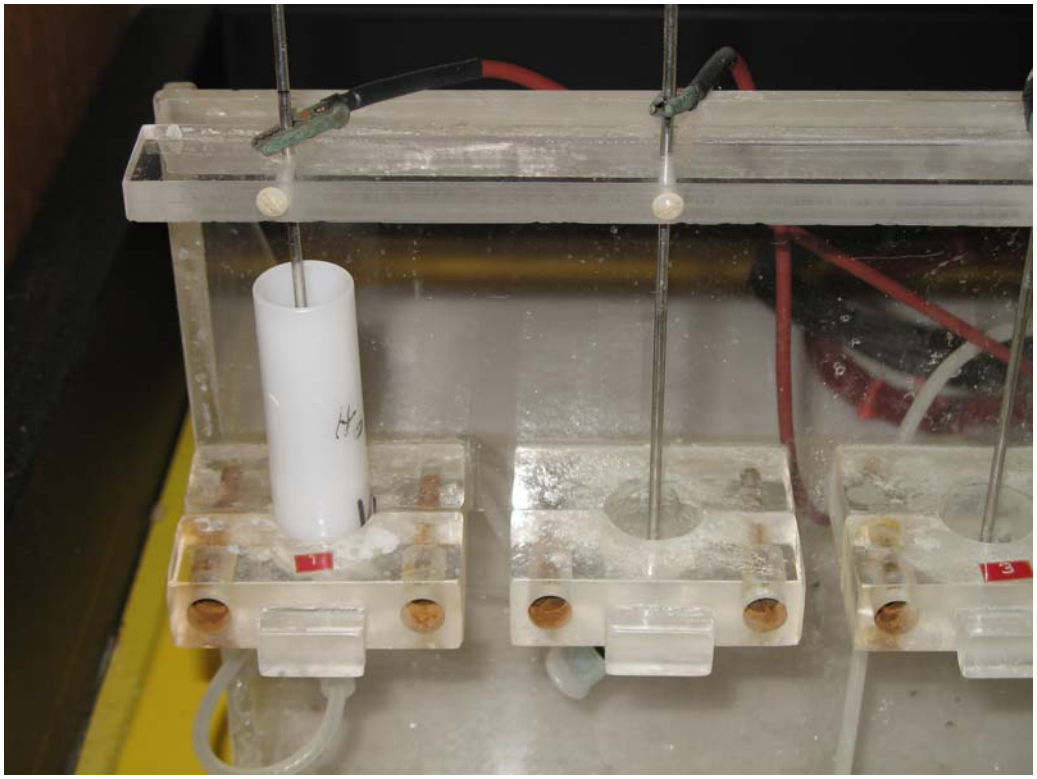

Figure 1.6: An electrodeposition cell. The cell is comprised of a platinum wire anode that is connected to the power supply, an attachable cathode cap that fits onto the bottom of the cell, and the plastic holding cell, itself. Not pictured is a 5/8" diameter stainless steel planchette, onto which the actinides are deposited.

Each cell is assembled with a 5/8" diameter stainless steel planchette that fits into a cathode cap that screws onto the bottom of plastic cell. The electrolyte solution (containing the actinides) is then poured into the cell. The cell is then inserted into the holder, which positions the planchette with respect to the platinum wire anode. The anode is connected to the constant current power supply. When activated, the actinides in solution are driven to the cathode where they are deposited in a thin uniform layer.

Figure 1.7: The alpha spectrometry system. This system features 44 individual alpha spectrometers that are managed by one of four input MCB Ethernims. Not pictured is the vacuum pump and manifold that allows all of the counting chambers to be pumped down to the desired pressure. Also not pictured is the computer system which collects and analyzes the spectra.

Once the counting sources have been prepared by electrodeposition, they can be counted with the alpha spectrometry system. This system was used to count the samples produced in chapter 7 of this work. Within each counting chamber is a 450 mm detector face, and a sample pedestal that allows the sample to be positioned relative to the detector. Signals from each detector are acquired and analyzed using commercially available software.

Chapter 2: Relevant Theory

This section provides the theoretical foundation for the various topics featured within this research. A common feature of all projects described herein is high pressure extraction chromatography (HPEC). HPEC system components, extractive resins, and column packing techniques will be discussed in detail. Flow analysis is another important topic that will be discussed, including: system components, flow scintillation analysis, and flow gamma analysis. The use of mass spectrometry as a radioanalytical tool will also feature prominently, with topics to include: elementary principles, system components, and analytical procedures. Finally, a brief discussion of the process and instrumentation of fraction collection will be given.

HIGH PRESSURE EXTRACTION CHROMATOGRAPHY (HPEC), PRINCIPLES AND PRACTICES

HPEC is a variation classical chromatographic methods that have been used by chemists since the beginning of the 20th century. The driving principle behind all chromatographic techniques is that different substance move through a medium at different rates depending on their chemical affinity for the molecules that comprise the medium. Thus, a mixture of substances may be separated by passing the mixture through the chromatographic medium and noting the rate at which each individual substance emerges from the medium.

An analogy that has often been used to describe chromatography is to imagine a swarm of bees and wasps that are carried by the wind over a flower bed. As the swarm encounters the flowers, the bees, which are attracted to the nectar, slow to browse among the flowers. The wasps, which are uninterested in nectar, pass over the flower bed without slowing down. To a casual observer down wind of the flower bed it would seem

that two distinct swarms exist; the first, consisting of only wasps and the second, only bees. This analogy illustrates the four principle components of most chromatography systems, the analytes (bees and wasps), the mobile phase (the wind), the stationary phase (the flowers), and a method of detection (the observer). Two key principles are also demonstrated. The first is that the relative differences in affinity of the analytes for the stationary phase result in a separation of the analytes. The second is that if one has prior knowledge of the analytes and their retention factors on a medium, one does not need a detector capable of itself discriminating among the analytes, since the analytes have become separate and recognizable before encountering the detector. Thus, the product of chromatographic detection is typically a plot of gross signal peaks as a factor of time, called a chromatogram. A generic chromatogram is shown in Figure 2.1. Ideally, peaks are sharp and well resolved, such as the first 3 peaks. However, in practice, peaks often overlap (as the analytes co-eluet) or are broadened due to multiple factors, such as resin mesh size, flow rate, and resin retention characteristics. It is also possible to have a single analyte elute into two or more different peaks due to the existence of multiple oxidation states of the analyte and the formation of various analyte complexes.

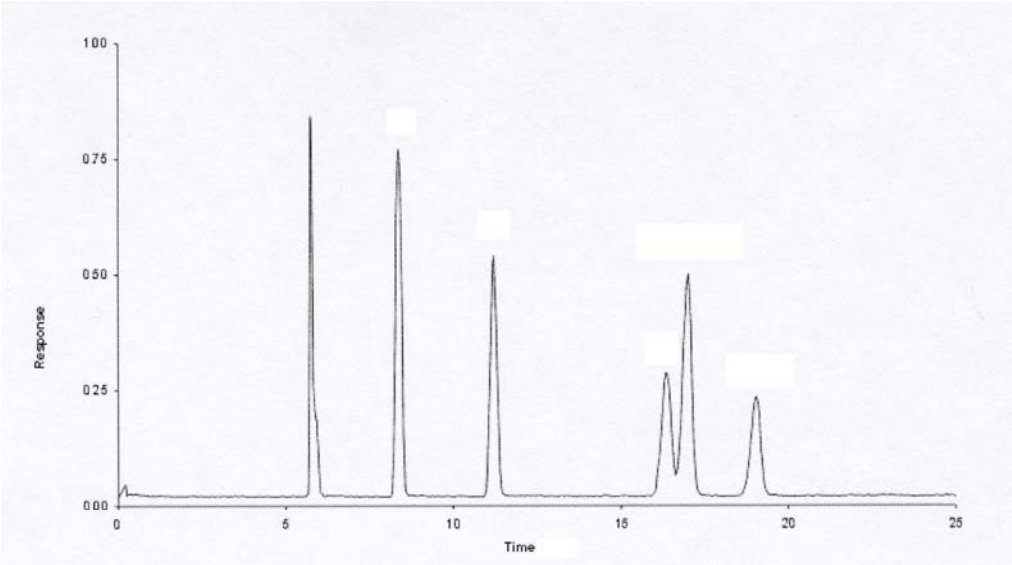

Figure 2.1: A generic chromatogram. This chromatogram shows six eluent peaks over the course of the run time and their normalized detector response (adapted from c2v.nl).

Retention of analytes in a chromatographic system may be based on charge (ion-ion interactions or ion-dipole interactions), van der Waal's forces, relative solubility, or adsorption. Two major theories exist to describe the resulting analyte behavior. The first theory employs retention factors, R_f. Retention factor is a measure of the speed at which an analyte moves through the chromatographic system and may be described by:

$$R_f = \frac{D_A}{D_S} \tag{2.1}$$

where D_A is the distance moved by the analyte and D_s is the distance moved by the solvent. Retention factors can vary considerably for a given analyte due to variations in the elute composition, changes within the stationary phase, temperature, sample matrix, and system setup. Therefore, retention factors can only be compared under absolutely identical run conditions.

The other theory of describing analyte behavior is plate theory which supposes that the chromatographic column contains a large number of separate layers, called

theoretical plates. Separate equilibrations of the sample between the stationary and mobile phase occur in these "plates" and the analyte moves down the column by transfer of equilibrated mobile phase from one plate to the next. These plates do not actually exist, but provide a means of conceptualizing how sample zones can equilibrate with the medium as they travel through the column. The number of theoretical plates that a real column possesses can be found by examining a chromatographic peak after elution and using the following equation:

$$N = \frac{5.55 t_R^2}{FWHM^2} \tag{2.2}$$

where the number of theoretical plates, N, is proportional to the square of the retention time, t_R, and inversely proportional to the square of the full-width-half-max, FWHM, of the peak. The retention time, t_R, is further defined as the time between sample injection and the analyte peak reaching the detector. The larger the number of theoretical peaks the better the efficiency of the column. This method of evaluating column performance is more easily comparable from method to method. However, this work will use an acid dependency factor, k', to describe analyte behavior within the column. Details of method will follow in the next section of this chapter.

The most common chromatography system configuration contains the stationary phase within a column. The pure form of the stationary phase molecules is often not permeable enough to accommodate the passage of the mobile phase, so stationary phase molecules are often bound to a substrate, which is packed into the column. One popular substrate is a micro bead made of an inert polymer, which sieved to uniform in size to within a specified tolerance. These beads can then be coated with the stationary phase molecule so that the entire surface area of the bead becomes the stationary phase site. A slurry of these beads (called a resin) can then be loaded into a column and packed under

pressure. This way all of the internal space of the column is filled with the stationary phase, leaving very little void space within the column.

Early column chromatography experiments fixed the column in a vertical position and utilized a reagent reservoir and the force of gravity to force the mobile phase through the column. While this type of setup is still used today, pressurized systems for administering the mobile phase are now common. A pressurized system allows for quicker processing of a sample and sharper eluent peaks because diffusion of the analyte plug is minimized. The broad application of this technique has become known as high performance/pressure liquid chromatography (HPLC).

Chromatography systems are also categorized by their specific separation mechanism. One very popular mechanism is ion exchange, in which the stationary phase contains molecules with a functional group that is opposite in charge of the analyte. Thus, exchange resins are typically either of the anion or cation variety. Anion exchange resin is most often used for radionuclide determination because metal ions will form negatively charged complexes under certain acid concentrations.

EXTRACTIVE RESINS

Extraction chromatography is a technique that is ideally suited to the separation of radionuclides from a wide range of sample types. This technique, which was developed by Horwitz in the late 1980s and early 1990s, combines the selectivity of liquid-liquid extraction with the ease of operation of column chromatography. During this time a number of resins with selectivities for various radionuclides were developed and commercialized by the company Horwitz founded, Eichrom Industries. Most of Eichrom's resins have been used extensively over the last 20 years for research in radioanalytical chemistry, in publications too numerous to detail. As such, there is much

data on the behavior of radionuclides with these resins that are available in publications or on Eichroms's website, (eichrom.com).

The key statistic that details the affinity of an analyte for a particular resin is the acid dependency factor, k'. As its name suggests, the factor relates the analyte-resin affinity to the type and molarity of acid used in the mobile phase of a chromatography experiment. More simply, k', is the number of free column volumes (FCVs) of an acid solution one must pass through the column onto which an element is sorbed to obtain the peak maximum from the column exit.

$$k' = D\frac{v_s}{v_m} \tag{2.3}$$

D, is the distribution ratio of the analyte, v_s, is the volume of the stationary phase, and v_m, is the volume of the mobile phase. Values for k' and D are not directly measured in extraction chromatography. Rather, the weight distribution ratio, D_w, is determined by conducting an experiment that measures the amount of a given metal ion taken up by a measured weight of resin from a given volume of aqueous solution.

$$D_w = \frac{A_0 - A_s}{A_s}\left(\frac{mL}{g}\right) \tag{2.4}$$

In these experiments a known activity and volume of a radioactive isotope, A_0 , is added to a known mass of resin and shaken until equilibrium is established. The activity of the isotope remaining in solution, A_s, is then measured. The activity of the isotope adsorbed onto the known mass of resin is A_0-A_s. Eichrom then provides conversion factors for converting values of D_w to k' (shown in Table 2.1) by a process that is detailed elsewhere and is beyond the scope of this basic theory section (Horwitz 1992; 1995; 1997).

Table 2.1: Converting D_w to k' (eichrom.com/products/extraction.cfm)

RESIN	V_S/V_M	TO CONVERT D_W TO K' DIVIDE BY
TEVA	0.23	1.9
UTEVA	0.25	1.7
TRU	0.22	1.8
Actinide	0.20	1.9
Sr	0.22	2.0

By conducting numerous batch distribution experiments with a particular analyte/resin combination and various acid solutions, one can plot how k' changes with respect to acid concentration. This data is invaluable to the creation of methods for radionuclide separation. Two of the resins listed in Table 2.1 were used in the experimental section of this work: Sr Spec resin (chapeters 3-5) and TRU Spec resin (Chapters 6 and 7). Therefore, we will examine the data relating to the acid dependency factors for these resins in the following sections.

Sr-Spec Resin

Sr Spec resin consists of the compound, 4,4'(5')-bis(tert-butylcyclohexano)-18-crown-6, dissolved in octanol and impregnated on polymer support beads. It serves as the stationary phase in columns used in this work to concentrate ^{90}Sr (chapter 3) and ^{210}Po (chapter 4) from their sample matrices and potential interferences. Figure 2.2 shows a drawing of this molecule. These analytes were subsequently eluted into the mobile phase as pure sample zone, which could then be detected by FSA. This resin was also used in chapter 5, where ^{60}Co, ^{137}Cs, and $^{192/192m}Ir$ were detected by FGA, though

that research was used to demonstrate that these analytes are not retained by the Sr resin and therefore could be separated from solutions that contained Sr and Po.

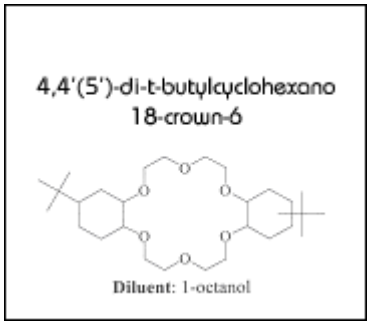

Figure 2.2: The extractive crown ether molecule that gives Sr Spec resin its properties (eichrom.com).

^{90}Sr is increasingly well retained by Sr resin for mobile phases with nitric acid concentrations of 2-8M, as seen in Figure 2.3. In 8M nitric acid, k' for Sr is ~100; that is, it takes about 100 FCVs of 8M nitric acid for the Sr peak to elute. However, potential interferences, like Ca, which has a k' of ~0.3, will elute within the first FCV of 8M nitric. Once adsorped, Sr can be eluted from the column by changing the mobile phase to weak nitric acid; since k' is 0.2 for Sr at a nitric acid concentration of 0.02M. Water can also be used as an eluent for Sr in an HPEC system, since it will mix with the residual nitric acid in the system to form a mobile phase which is dilute in nitric acid (Grate 1996; Grate 1999b). Therefore, an elution scheme, such as the one developed in chapter 3, can be created where a solution containing Sr is loaded on the column with several FCVs of 8M nitric acid. This load solution will retain Sr but will wash out other metals such as K, Ca, Na, and Cs. A Striping solution of several FCVs of water can then be applied to remove the Sr. In this manor ^{90}Sr can be concentrated on the column and eluted as a sample zone which can be detected.

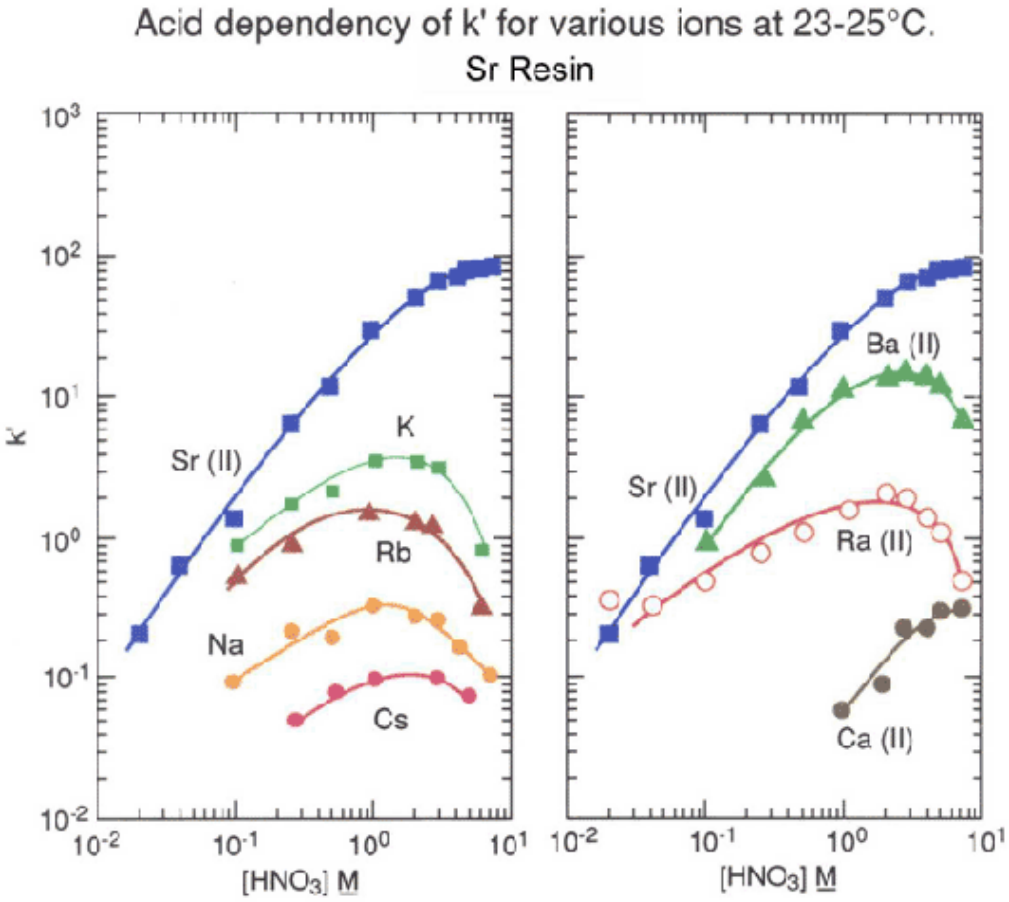

Figure 2.3: Acid dependency of Sr on Sr Spec resin. Sr is well retained from high concentrations of nitric acid and is not well retained for low concentrations (Eichrom.com).

Figure 2.4 shows that several other elements are also well retained by Sr resin. Among those is polonium, which well retained from ~1M nitric acid solutions. Po is not well retained for either high or low concentrations of nitric acid, which may be used to strip Po once it is adsorped. We can also note that Pu (IV) and Pb(II) are also very well retained by the Sr resin from high molarity nitric acid. If present in the sample at a high activity, these analytes may co-elute with ^{90}Sr and cause interferences in FSA.

Fortunately, we do not expect these nuclides to be found in bioassay samples at activity levels that are high enough to interfere with ^{90}Sr.

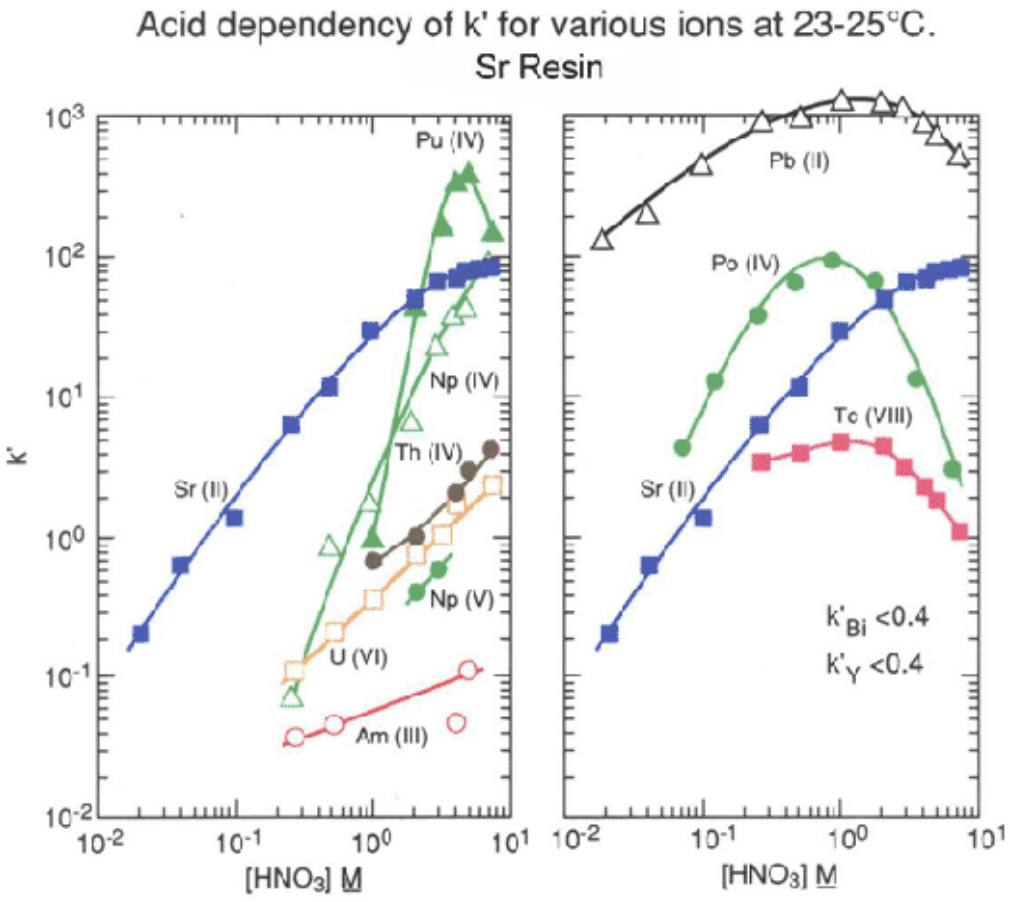

Figure 2.4: Acid dependency of Po on Sr Spec resin. Po is well retained from ~1M nitric acid. Po is not well retained for high or low concentrations of HNO_3 (Eichrom.com).

Data for the retention of Po on Sr resin from HCl solutions also exists, Figure 2.5. This data shows that Po is increasingly well retained on the resin with increasing molarities of HCl. The distribution ratio for Po in 2M HCl is ~ 100 FCVs, which is adequate to perform a separation. Therefore, a alternative load solution for samples containing Po would be 1-8M HCl.

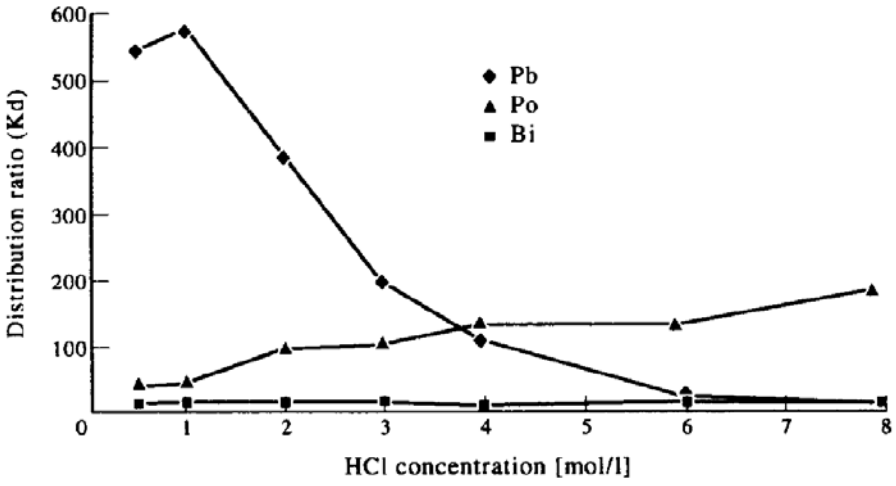

Figure 2.5: HCl dependency of Po and Sr resin (Vajda 1997).

Principle interferences for ^{90}Sr and ^{210}Po that we can expect to encounter in urine bioassay samples are not other radionuclides, but stable matrix ions. Of particular concern are potassium (which competes with Sr for binding sites within the resin) and nitrate salts, both of which are found at significant concentrations in urine. Figure 2.6 shows how the retention of Sr is affected by the presence of various nitrate salts. As can be seen, increasing concentrations of these salts has a deleterious effect on Sr retention. Samples with a range of urine concentrations can be studied to determine how urine matrix components affect analyte retention. In cases where retention is seriously inhibited, it may be necessary to dilute urine samples for processing or to perform some type of sample pretreatment to remove these species.

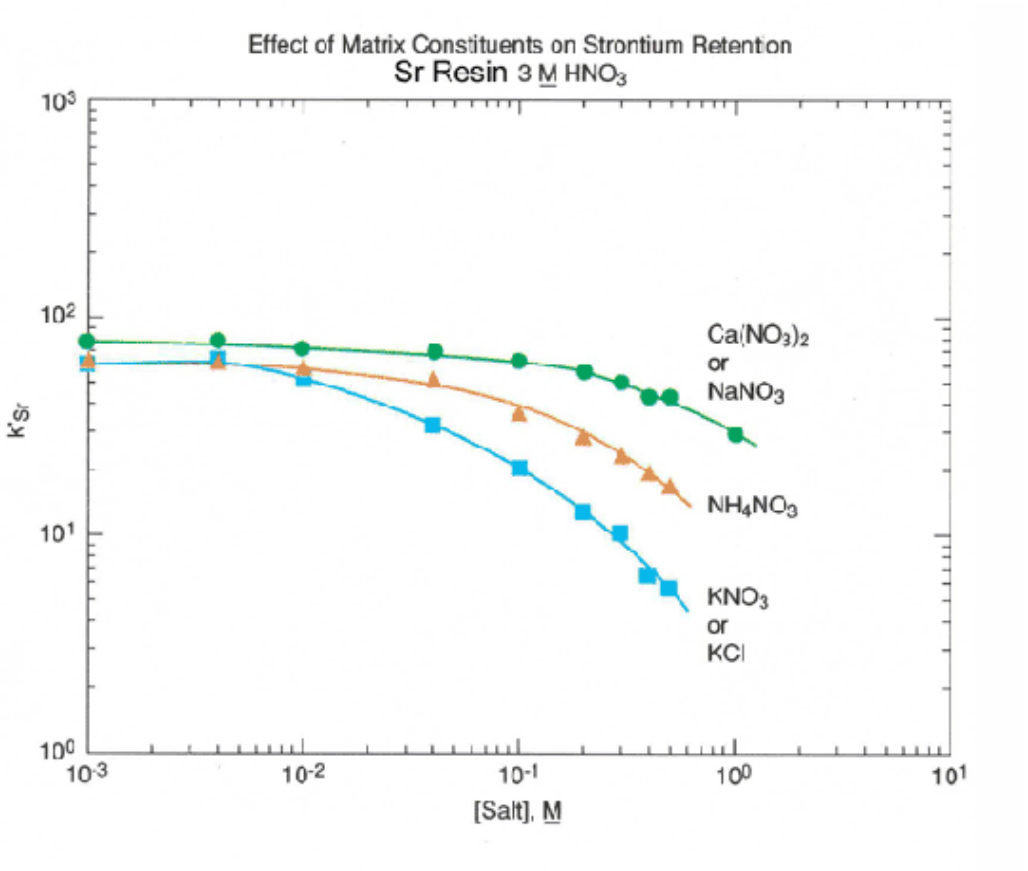

Figure 2.6: Effects of nitrate salt concentration on Sr retention on the Sr resin (Eichrom.com).

Finally, it is helpful to examine retention data for other elements that may be encountered, but for which more specific acid dependency data is not available. Figure 2.7 tabulates this data. Many of the short-lived gamma emitters of concern are not retained by the Sr resin.

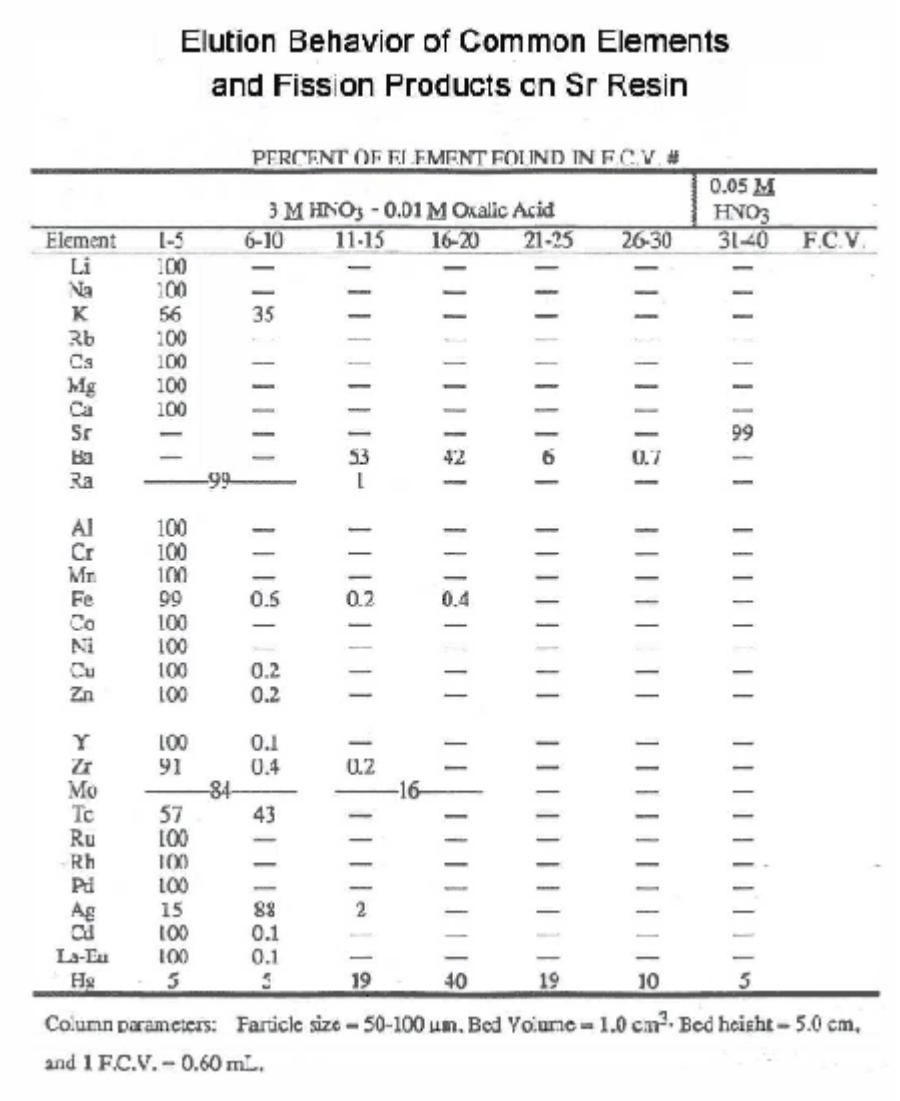

Elution Behavior of Common Elements and Fission Products on Sr Resin

PERCENT OF ELEMENT FOUND IN F.C.V. #

	3 M HNO_3 - 0.01 M Oxalic Acid						0.05 M HNO_3	
Element	1-5	6-10	11-15	16-20	21-25	26-30	31-40	F.C.V.
Li	100	—	—	—	—	—	—	
Na	100	—	—	—	—	—	—	
K	56	35	—	—	—	—	—	
Rb	100	—	—	—	—	—	—	
Cs	100	—	—	—	—	—	—	
Mg	100	—	—	—	—	—	—	
Ca	100	—	—	—	—	—	—	
Sr	—	—	—	—	—	—	99	
Ba	—	—	53	42	6	0.7	—	
Ra	99		1	—	—	—	—	
Al	100	—	—	—	—	—	—	
Cr	100	—	—	—	—	—	—	
Mn	100	—	—	—	—	—	—	
Fe	99	0.5	0.2	0.4	—	—	—	
Co	100	—	—	—	—	—	—	
Ni	100	—	—	—	—	—	—	
Cu	100	0.2	—	—	—	—	—	
Zn	100	0.2	—	—	—	—	—	
Y	100	0.1	—	—	—	—	—	
Zr	91	0.4	0.2	—	—	—	—	
Mo	84		16		—	—	—	
Tc	57	43	—	—	—	—	—	
Ru	100	—	—	—	—	—	—	
Rh	100	—	—	—	—	—	—	
Pd	100	—	—	—	—	—	—	
Ag	15	88	2	—	—	—	—	
Cd	100	0.1	—	—	—	—	—	
La-Eu	100	0.1	—	—	—	—	—	
Hg	5	5	19	40	19	10	5	

Column parameters: Particle size = 50-100 µm, Bed Volume = 1.0 cm^3, Bed height = 5.0 cm, and 1 F.C.V. = 0.60 mL.

Figure 2.7: Elution behavior of common elements and fission products on the Sr resin. Dilute oxalic acid can be added to the load solution to prevent the adsorption of actinides (Eichrom.com).

TRU-Spec Resin

TRU-Spec resin consists of the compound, octylphenyl-N,N-di-isobutyl carbamoylphosphine oxide (CMPO), dissolved in tri-n-butyl phosphate and impregnated on polymer support beads, and serves as the stationary phase in columns used in this work to concentrate actinides from their sample matrices and potential interferences (chapters 6 and 7). Figure 2.8 shows a drawing of this molecule. The actinides were subsequently eluted into the mobile phase as pure sample zones, which could then be detected by mass spectrometry or collected for electrodeposition and alpha spectrometry.

Figure 2.8: The extractive CPMO molecule that gives TRU resin its properties (Eichrom.com).

The acid dependency factors for the actinides on this resin vary considerably from actinide to actinide and even for different oxidation states of the same actinide as shown in Figure 2.9. Pu(IV), Np(IV), Th(IV) and U(VI) are very well retained for a range nitric acid concentrations. Am (III) is retained from 3M nitric acid, and eluted by lower molarities of HNO_3. Np(V) is not well retained from any concentration of nitric acid.

Retention of Pu(IV), Np(IV), Th(IV) and U(VI) is also very high from 10M HCl solutions but drops off rapidly with lower molarities of HCl.

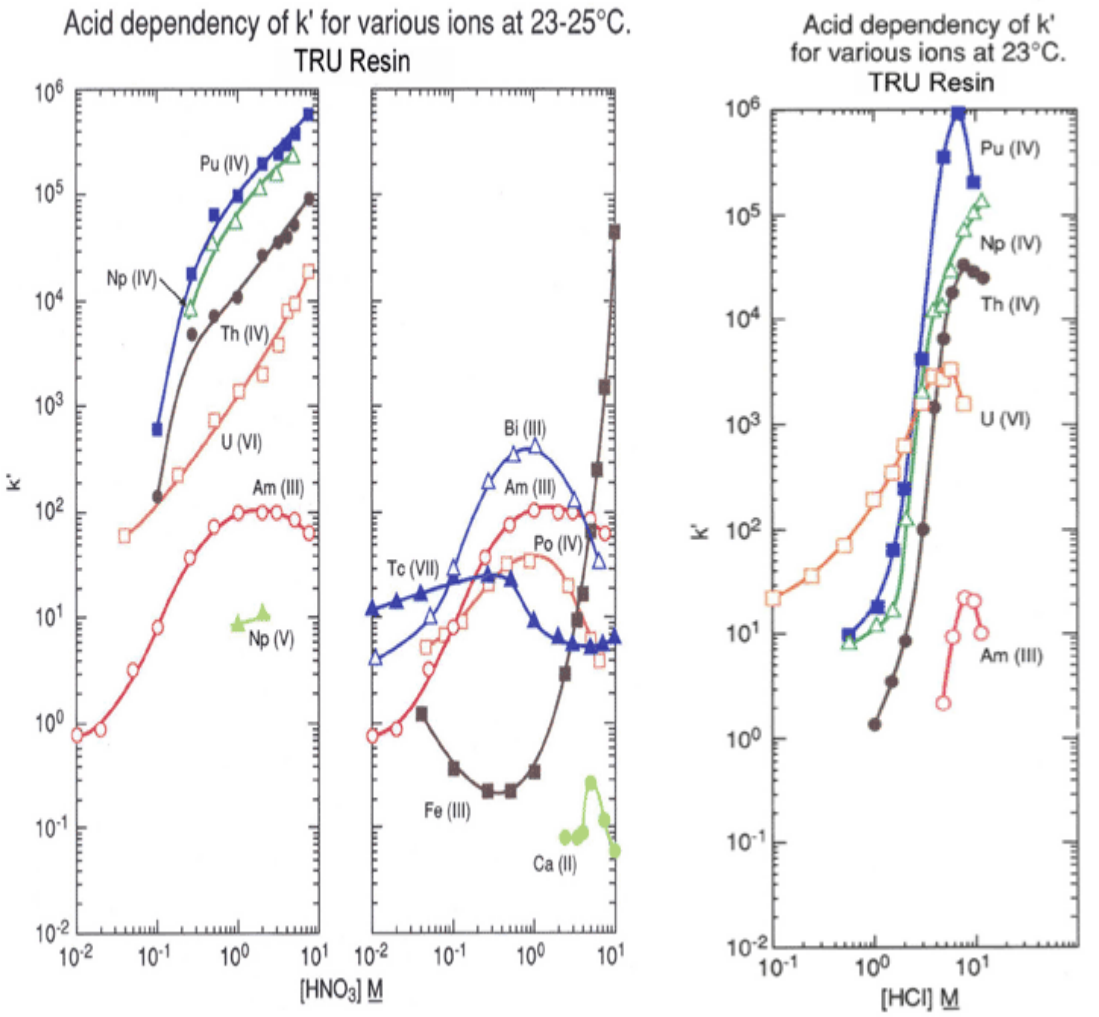

Figure 2.9: Acid dependency factors for actinides on TRU resin (Eichrom.com).

Using this data we can conceive of a scheme by which a solution of mixed actinides may be separated using a TRU column. By loading the mixture with 3M nitric acid, Th, U, Pu, and Am can be retained on the column, while Np (V) is not retained and

passed through the column in a few FCVs. By changing the mobile phase over to dilute HCl, Am will quickly elute. In time, Th (IV) will also elute, followed by Pu (IV). Uranium is still somewhat retained from even dilute HCl. The timely elution of uranium can be facilitated by the addition of oxalic acid, as seen in Figure 2.10. A variation of this basic elution scheme can sequentially elute Th, U, Np, Pu, and Am in a quick and effective manor for instantaneous detection by mass spectrometry (chapter 6) or for alpha spectrometry (chapter 7).

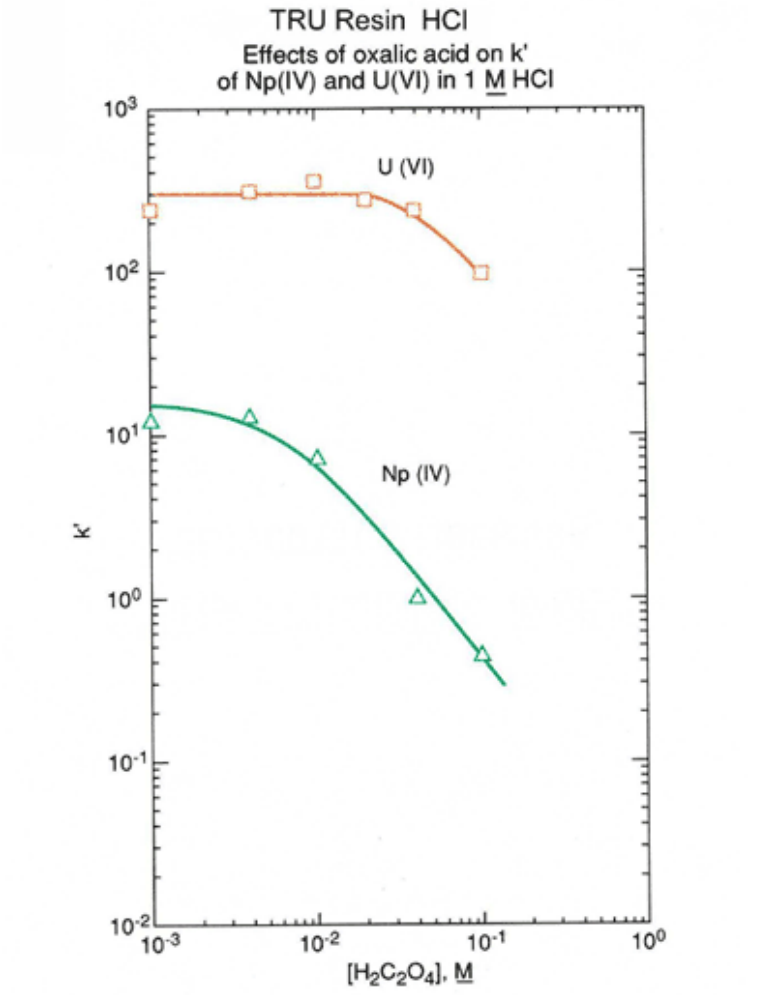

Figure 2.10: Acid dependency factors for uranium on TRU resin with varying concentrations of oxalic acid (Eichrom.com).

Applications of such an elution scheme to urine bioassays are subject to potential interferences from the urine matrix components. The most significant of these interferences is Fe(III), as seen in Figure 2.11. Fe(III) is expected to be found in significant quantities in urine. Fortunately, the simple solution to the problem is sample pretreatment with a few drops of ascorbic acid. This agent reduces Fe(III) to Fe(II), which does not interfere with the retention of Am.

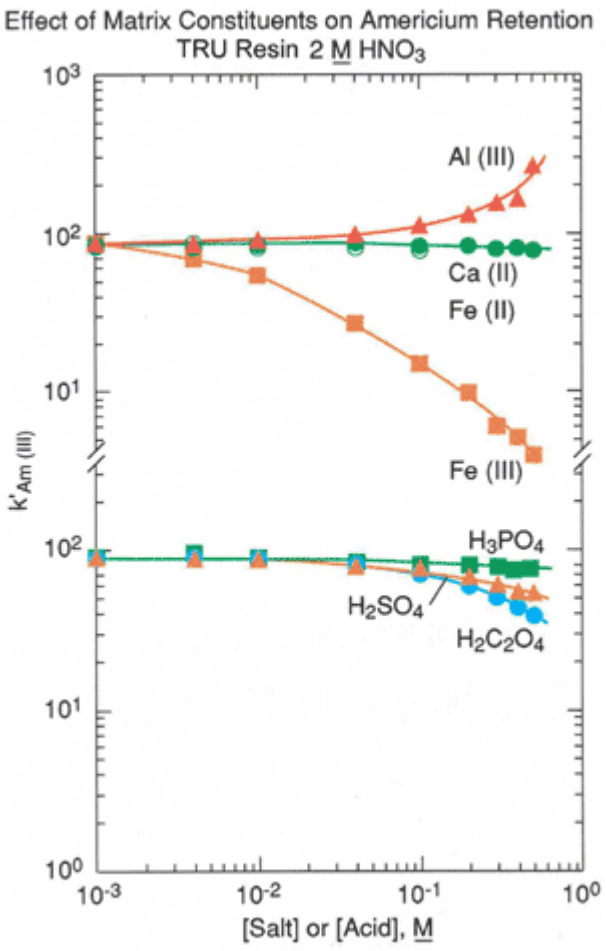

Figure 2.11: Effects of matrix interferences with Am retention on TRU resin. Fe(III) is the principle interference (Eichrom.com).

Finally, it is useful to examine retention data for other elements that may be encountered, but for which more specific acid dependency data is not available. Figure 2.12 tabulates this data. Most of the elements tabulated in Figure 2.12 are expected to be present in significant quantities in urine bioassays. Those that would be present (e.g. Na, Mg, Al, K, Ca, Cr, Co, Sr) would not interfere with actinide detection either by mass spectrometry or by alpha spectrometry.

Elution of Selected Elements on a TRU Resin Column

(fine particles)

Element	Fraction Eluting (%) by number of free column volumes						
	1-5	6-10	11-15	16-20	21-25	26-30	31-40
Li	98.4	<1.9	–	–	–	–	–
Na	92.8	<1.2	–	–	–	–	–
Mg	100	–	–	–	–	–	–
Al	99.8	<2.9	–	–	–	–	–
K	81.8	40.9	–	–	–	–	–
Ca	100	–	–	–	–	–	–
Cr	100	–	–	–	–	–	–
Mn	100	–	–	–	–	–	–
Fe	102	12.3	–	–	–	–	–
Co	100	–	–	–	–	–	–
Ni	100	–	–	–	–	–	–
Cu	100	–	–	–	–	–	–
Zn	100	–	–	–	–	–	–
Sr	100	–	–	–	–	–	–
Y	23.4	76.8	3.5	–	–	–	–
Zr	–	–	–	–	–	–	75.0
Ru	82.6	<19.2	–	–	–	–	–
Rh	100	–	–	–	–	–	–
Ag	100	–	–	–	–	–	–
Cd	100	–	–	–	–	–	–
Ba	100	–	–	–	–	–	–
La	–	–	–	–	–	30.0	72.0
Ce	–	–	–	–	–	<25.0	75.0
Pr	–	–	–	–	–	–	100
Nd	–	–	–	–	–	–	96.0
Sm	–	–	–	–	–	–	100
Eu	–	–	–	–	–	–	>99
Hg	(100)	(60)	(19)	–	–	–	–
Pb	100	–	–	–	–	–	–
Am*	–	–	–	–	–	–	>99

* radiometric
1–30 f.c.v. : 2M HNO_3
31–40 f.c.v. : 0.05M HNO_3

note: Because of uncertainties inherent in the ICP-AES method, the fractions shown for each element may not total to 100%. Values in parentheses are subject to considerable uncertainty and are intended only as a rough guide.

Figure 2.12: Elution behavior of common elements and fission products on the TRU resin (Eichrom.com).

FLOW SCINTILLATION/GAMMA COUNTS, PRINCIPLES AND APPLICATIONS

Flow scintillation analysis has been an established technique for detecting high activity radiolabeled compounds in bioscience research for many decades. However, the use of this technique for radionalytical chemistry has been brief. The application of flow gamma analysis is even less well-known; therefore an understanding of the capabilities and limitations of these systems is needed to evaluate their suitability for this project.

Flow Scintillation Analysis

Flow scintillation analysis is the application of scintillation detection methods for the quantitative analysis of radioactivity in a flowing system. There are two basic types of FSAs, homogeneous and heterogeneous, which involve somewhat different types of instrumentation, as will be discussed below. All FSAs rely on the pump of an HPLC to propel column effluent through the instrument. Common to both types of FSAs is an interchangeable flow cell that serves as the sampling point for interaction of the sample and the detector. Also common is the detector itself, which typically includes two shielded PMTs, coincidence counting electronics, a pulse height analyzer, a multi-channel analyzer, a computer, and analysis software. Detection during flow scintillation analysis is typically accomplished in a transient mode, where there is continuous flow of sample through the cell. However, a stopped-flow detection mode is also possible to enhance the detection of samples that have activity close to background.

A homogeneous FSA consists of all the features described above, but also possesses a cocktail pump and mixing tee so that the column effluent is uniformly mixed with scintillation cocktail before entering the flow cell. The flow cell for this instrument is simple Teflon tubing, coiled between two transparent windows, see Figure 2.13.

Figure 2.13: A Typical Homogenous Flow Cell.

Prior to operation, the selected flow cell is slid into place between the PMTs of the detector as seen in Figure 2.14:

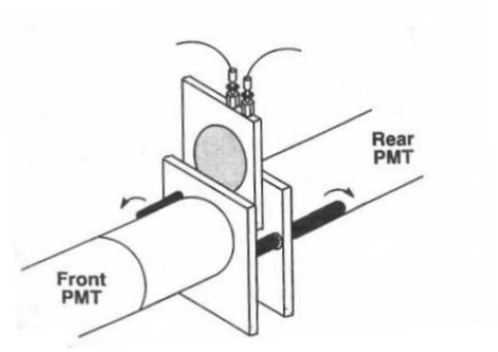

Figure 2.14: Proper Placement of the Flow Cell within an FSA (modified from L'Annunziata 2003)

The major advantage of the homogeneous flow cell is that it provides the highest counting efficiencies (20-60%) for low-energy beta-emitters such as ^{3}H (L'Annunziata 2003). There are two major disadvantages to using a homogeneous system: one, the wide range of chemicals used as eluates and the changing characteristics of the effluent will cause variable quench (though this is less significant for higher energy betas and alphas) and two, by mixing the HPLC effluents with cocktail, they are rendered useless for further chemical separations or analysis. The primary goal of the proposed system is to detect ^{90}Sr and ^{210}Po, both of which should be detected with high efficiency by any scintillator.

Heterogeneous FSAs are different from homogeneous models in that they do not use a cocktail pump, but instead employ a flow cell packed with a solid scintillating material. Such heterogeneous flow cells are manufactured with fine beads of an insoluble solid scintillator packed within the Teflon tubing of the flow cell. The HPLC effluent stream makes intimate contact with the solid scintillator beads as it moves through the flow cell. The PMTs measure the scintillation photons generated as the radioactive fraction of the effluent stream enters the flow cell. There are several types of solid scintillators used in flow cells including yttrium glass, europium-activated calcium fluoride, and lithium glass. The counting efficiencies of these scintillators varies, but are generally low (1.5-5%) for ^{3}H but high for ^{90}Sr and actinides (L'Annunziata 2003). The major advantages to heterogeneous FSA are that the sample integrity is preserved because no cocktail is used and that there is no chemical quench effect. A disadvantage to this method is that there is the potential for analytes to irreversibly bind to the solid scintillating material over time, causing elevated backgrounds. Early experiments with heterogeneous flow cells did show significant problems with carryover from one run to

the next for ^{90}Sr (data not shown). Therefore, a homogeneous flow cell was used for all FSA experiments in this work.

Radionuclide detection in an FSA is accomplished by peaks in the radioactivity of the column effluent as it passes through the flow cell. Confidence in the knowledge of what analyte is eluting from the column at a particular time is crucial, since isotopic identification by emission energy is usually difficult with beta emitters. In transient flow counting, the sample count time is a function of the flow rate and flow cell volume. The radioactive sample is only "seen" by the detector for the time the sample resides in the flow cell. This residence time can be determined as followed:

$$T_R = \frac{V}{F} \tag{2.5}$$

where, V, is the volume of the cell in ml and F is the flow rate in ml/min. Further, the count rate in CPM can be calculated by dividing the observed counts by the residence time:

$$CPM = \frac{Counts}{T_R} \tag{2.6}$$

However, background counts resulting from cosmic radiation and electronic noise must also be accounted for by running a blank sample through the FSA. Net CPM can be determined as follows:

$$Net(CPM) = \frac{gross - background}{T_R} \tag{2.7}$$

Determination of the counting efficiency for a particular isotope is needed to convert the observed CPM into DPM. This is accomplished by passing a solution containing an isotope of certified activity though the flow cell for each isotope to be studied;

$$\%E = \frac{CPM}{DPM}(100) \tag{2.8}$$

Peaks that are sharp, well above the baseline, and separated from each other by significant time are easier to detect than those that are broad, near background, and display tailing behavior. These factors contribute to the minimum detectable activity (MDA) of an FSA for a given radionuclide separation.

$$MDA = \frac{(B)(W)}{(T_R)(E)} \tag{2.9}$$

Where B is the background count rate and W is the width of the peak in minutes and E is the %E/100. As a general rule, the best flow cell volume for a given HPLC application would be a cell with a volume of ½ to ¼ the volume of the smallest peak of interest (L'Annunziata 2003). One can easily conclude that slowing the flow rate and increasing the residence time of a sample in the flow cell will result in more counts and a lower MDA. If the sample activity is near background, short sample residence times may preclude detection. In this case, the practice of stopped-flow detection, described by Gate and Egorov (Grate 1996; Egorov 1998b; Grate 1999b), may be helpful. If the flow is stopped at the peak maximum and the background is subtracted, the radionuclide activity may be determined as followes:

$$C_{CPM} = (D_m)(E_d)(E_{rec})(A_{DPM}) \tag{2.10}$$

where E_d is the detection efficiency, E_{rec} is the recovery efficiency from the HPLC and D_m is the fraction of the sample zone present in the flow cell, determined as follows:

$$D_m = \frac{(C_{\max})(T_R)}{(T_i)(C_n)} \tag{2.11}$$

where C_{max} is the number of counts at the peak maximum, T_i is the pulse summation update time, and C_n is the net peak area counts. The disadvantage of very slow or stopped-flow counting or using a larger flow cell is that peaks from the HPLC are

broadened and peak resolution is lowered, precluding the separation of close peaks. However, peaks resulting from the proposed separations are expected to be broad and well separated (by general HPLC standards), therefore stopped-flow counting will be the anticipated method of counting and flow cell sizes will be as large as possible to enhance the detection of near-background peaks.

Flow Gamma Analysis

Much of the information pertaining to FSA is also applicable to FGA. Traditionally, a heterogeneous-type flow analyzer is used with a special gamma counting cell. The FGA is plumbed similarly to a heterogeneous FSA and counting and radionuclide identification methods are the same. The flow cell configuration and detector system are the only differences between FGA and heterogeneous FSA.

Gamma flow cells are available in three main types: high-eneregy gamma cells, low-energy gamma cells, and positron cells. Positron cells are designed to produce annihilation gamma rays when positrons interact with the flow cell. The primary interest in FGA for this project is for certain high-energy gamma emitters with intensities of around 100%. Existing high-energy gamma cells consist of Teflon tubing coiled flat between two 6 mm thick bismuth germanate (BGO) solid scintillator windows. The BGO has a high density (7.13 g/cc) and is made of high Z material resulting in high stopping power for high-energy gamma radiation. BGO also has a high degree of light output per interaction and a short scintillation decay time. Detection is usually accomplished by the same PMT system as the FSA.

However, there are now commercially available flow gamma detectors that have built in NaI detectors for more effective gamma spectroscopy. This component, shown in Figure 1.2, will no doubt provide better gamma analysis capabilities than the traditional method of FGA. As the FGA unit is sold, its detection capabilities are restricted to gross

gamma counting only since the system lacks a multichannel analyzer. This unit is designed to interface with existing FSA software to create a chromatogram of gross gamma peaks. While this information is useful in that it allows the user to observe the timing and shape of the analyte peaks as they travel through the system, isotopic identification of the peak must be accomplished by advanced knowledge of the analyte elution characteristics. In the event that a mixture of gamma emitters may co-elute (such as is expected for most of the short-lived gamma emitters of concern with the Sr and TRU resins), there is no way to resolve the peak into the contributions of individual analytes.

We have modified the commercial unit by splitting the output signal of the detector and routing one of the signals to a DSpec Pro multi-channel analyzer. This allows us to utilize the gross gamma chromatography to observe analyte peaks, but also allows use to acquire an energy spectrum of the analyte gammas for positive isotopic identification. This set up provides us with a much more detailed analysis of the sample than simple chromatography techniques.

The system is described in greater detail in chapter 5, along with experimental data the shows the effectiveness of this technique for determining ^{60}Co, ^{137}Cs, and $^{192/192m}$Ir in simulated urine bioassay samples. We believe that this system is unique and that the novel experimental techniques are applicable to a number of analytical scenarios. While there are many gamma spectrometry systems that utilize automated sample changers, we believe that this system is the first to incorporate online separation and detection to facilitate batch sample processing.

MASS SPECTROMETRY, PRINCIPLES AND APPLICATIONS

There are many different types of mass spectrometers that provide detection capability for niche analysis needs. These include: thermal ionization mass spectrometry

(TIMS), glow discharge mass spectrometry (GDMS), secondary ion mass spectrometry (SIMS), resonance ion mass spectrometry (RIMS), accelerator mass spectrometry (AMS), and inductively-coupled mass spectrometry (ICP-MS). TIMS, AMS, and ICP-MS are the most utilized types of mass spectrometry for radionuclide determination. While TIMS and AMS provide unparalleled sensitivity, the cost of acquiring and operating these instruments puts them out of reach of all but the best financed institutions. The best sensitivity for the money is the ICP-MS; consequently, this is the instrument most utilized for routine radionuclide analysis.

The basic ICP-MS system consists of a sample introduction system (often the HPLC), a nebulizer to turn the liquid sample into a fine aerosol by mixing it with argon gas, a plasma torch to atomize and ionize the sample, a skimmer to create a collimated beam on ions, ion optics and a magnetic quadrupole to direct the ion beam and separate the beam by mass, and a detector that turns the incident ions into a signal. A schematic diagram of an ICP-MS is shown in Figure 2.15.

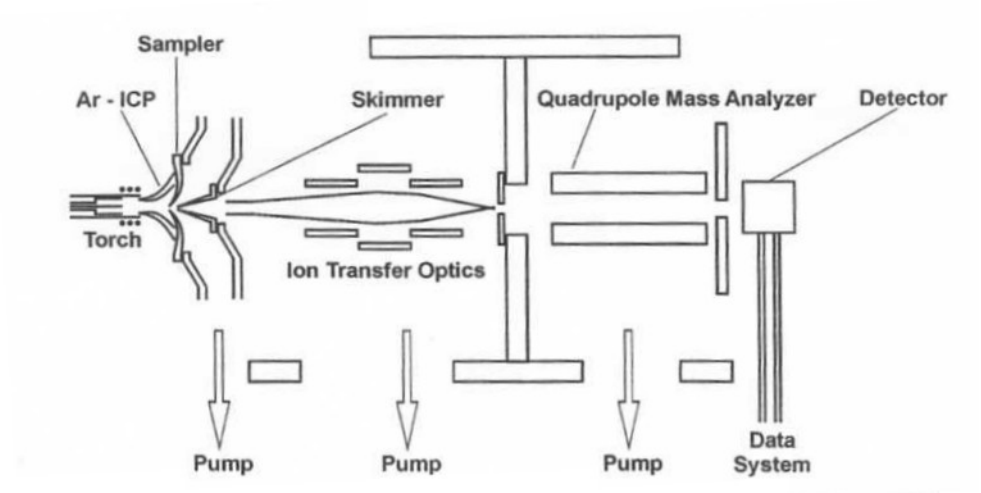

Figure 2.15: Schematic Diagram of an the Internal Structure of an ICP-MS (L'Annunziata 2003)

There are many parameters affecting the performance of the mass spectrometer. The first among these is the sample matrix, which should be in a completely dissolved, aqueous state with no suspended particles. There are several types of nebulizers that specialize in aerosolizing specific types of sample matrices, but suffice it to say that they all accomplish the same stated task. The argon gas flow to the system can be adjusted to provide maximum or minimal sample suspension and to provide maximum or minimal contact with the plasma. The plasma must be hot enough to ionize all elements (elemental ionization potentials can vary greatly) but not hot enough that a significant fraction of atoms are doubly ionized. The skimmer, which collimates the beam, must be kept clean and free of deposited material so that the beam can traverse to the optics. The ion optics have an applied voltage that can be adjusted to guide the ion beam through the device. The quadrupole mass analyzer is tuned so that it can apply a varying magnetic field that will direct ions to the detector based on their mass to charge ratio (m/z). For singly ionized ions (z=1), the m/z is equal to the ion mass in amu. The mass analyzer is programmed by the operator to rapidly scan the range of m/z from 1 to 260 (or any other desired upper limit), dwelling on each increment for a set period of time. In this manor the entire m/z range can be analyzed in less than a second for given count time. The intensity of the signal is given in counts per second for each m/z. A sample spectrum is shown in Figure 2.16.

The detection limit of mass spectrometry as it applies to radionuclides is dependent on the half-life of the isotope. Since radionuclide hazards are often dictated by the level of radioactivity in a sample, rather than the total mass or concentration of the radionuclide, high specific activity isotopes are disproportionately hazardous. In this way, a 50ppt solution of ^{232}Th would have an activity of 0.003 dpm/mL, while a 50ppt solution of ^{244}Cm would have an activity of 8800 dpm/mL. Thus, mass spectrometry is

an excellent technique for determining trace and ultratrace levels of long-lived radionuclides, making it far superior to radiometric techniques, such as alpha or gamma spectrometry. However, mass spectrometry fails to determine the same trace and ultratrace activities of shorter-lived radionuclides because there is simply not enough mass present to be detected.

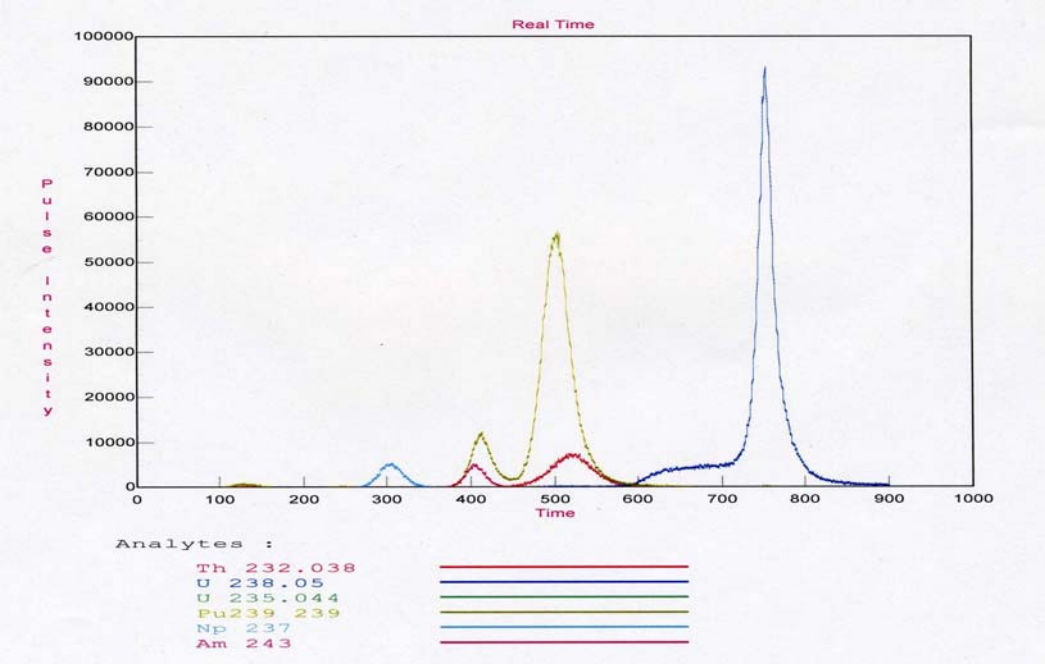

Figure 2.16: Sample Spectrum from a Mass Spectrometer. Each actinide is represented by a different color. The time is in seconds after the start of an elution scheme. Pulse intensity is in counts per second.

Research has shown that under ideal conditions ICP-MS is superior to radiometric techniques for isotopes with half-live longer than 70 years (Gonzales 2005). However, under most practical conditions ICP-MS is only useful for determining trace and ultratrace activities of radionuclides with half-lives of greater than 500 years. Figure 2.17 shows the relationship between radionuclide half-life and mass equivalence for a 1 Bq

sample of the isotope. The dashed line represents the ^{239}Pu detection limits for the various mass spectrometers.

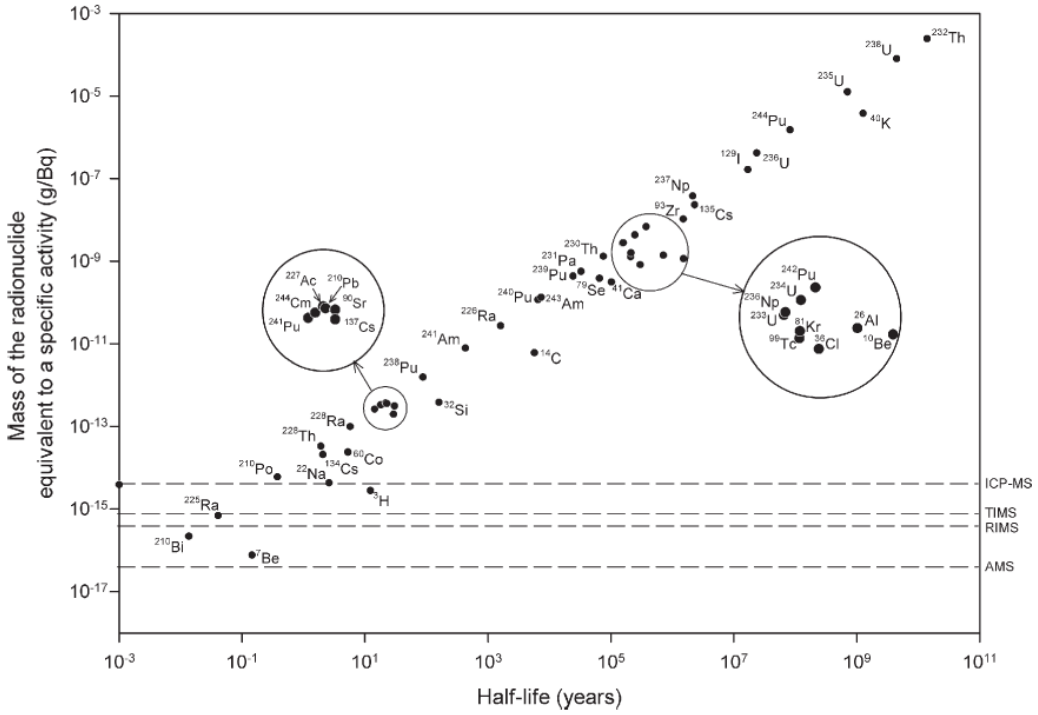

Figure 2.17: The relationship between isotope half-life and mass equivalence for a 1 Bq sample. The dashed line represents the detection limits for ^{239}Pu with the indicated mass spectrometer (McAninch 1999).

The ability to detect trace levels of actinides in biological samples has long been a concern and analytical techniques that can determine the isotopic composition of internally deposited actinides are critically important because isotopic information is most useful in determining dose calculations and where and when the uptake occurred. Isotopic determination of actinides is also valuable for a number of other purposes, such as nuclear forensics and nonproliferation monitoring.

Inductively coupled plasma mass spectrometry (ICP-MS) is a lower cost, commonly available technique that is extremely useful and widely used for actinide analysis. This technique has the advantage of requiring very little sample preparation (for

aqueous samples) and producing fast multi-isotopic analysis, with detection limits reported into the low ppq levels for several actinides, including: ^{232}Th, ^{238}U, ^{237}Np, ^{239}Pu, and ^{241}Am. However, the capabilities of ICP-MS are often limited by the presence of isobars (which produce unresolvable interferences) and polyatomic interferences (some of which are shown in Table 2.2).

Table 2.2: Commonly encountered actinide polyatomic interferences.

ISOBARS	POLYATOMIC IONS
^{236}U and ^{236}Np	^{230}ThH and ^{231}Pa
^{238}U and ^{238}Pu	^{236}UH and ^{237}Np
^{241}Pu and ^{241}Am	^{237}NpH and ^{238}U
^{242}Pu and ^{242}Am	^{238}UH and ^{239}Pu
	^{240}PuH and ^{241}Am
	^{242}PuH and ^{243}Am

While the best sensitivities are realized only in "neat" solutions, samples with complex matrices such as environmental (soil, seawater) or biological (urine) samples reduce sensitivities. This is because an increase in the number of matrix molecules in the sample stream leads to increasing interferences. Therefore, it is necessary to remove as many matrix components as possible prior to analysis, and to use techniques which separate isobars and potential polyatomic interferences. This necessitates the separation of the actinide elements in the sample stream to as large a degree as possible prior to detection.

Chapter 6 shows the optimization of one separation scheme for actinides. This scheme is based on the actinide retention properties of TRU resin, which was detailed earlier in this chapter. While this technique has not yet been optimized for urine bioassays, it does allow us to achieve the detection limits we desire for the actinides of concern set forth in this work.

Chapter 3: Flow Scintillation Analysis of ^{90}Sr

An automated procedure for the determination of ^{90}Sr was adapted from existing methods of flow scintillation analysis (FSA) for use on aqueous samples with low levels of activity (<1000 dpm per sample). This technique employs high performance extraction chromatography (HPEC) and an on-line liquid scintillation counter to provide automated separation and simultaneous detection of ^{90}Sr. Using Sr-Spec resin, ^{90}Sr was concentrated on the column from the matrix and potential radiological interferences with 8M HNO_3 and selectively eluted with water and instantly quantified by FSA. The lowest limit of quantification achieved by this technique was 156 dpm, or 2.6 Bq per sample. The total analysis time is 30 min per sample. A counting technique called stopped-flow detection was used to improve detection limits. Dilute urine samples, spiked with ^{90}Sr, were also processed by this method to test the application of this technique for bioassay monitoring. The advantages of FSA are faster analysis, greater precision, reduced labor commitment, and improved safety due to the fact that chemical and radiological hazards are mostly contained and automated.

INTRODUCTION

Significant quantities of ^{90}Sr are produced by the fission of ^{235}U and ^{239}Pu in nuclear reactors, and is therefore found at high levels in spent nuclear fuel, reprocessing plants, and DOE weapons complexes. ^{90}Sr has been used extensively as a radioactive tracer in medical and agricultural studies and is also used in a variety of industrial applications. The heat generated by the decay of ^{90}Sr can be converted to electricity for long-lived, portable power supplies, which are often used in remote locations, such as in navigational beacons, weather stations, and space vehicles. ^{90}Sr is also used in electron

tubes, as a radiation source in industrial thickness gauges, and for the treatment of eye diseases. Controlled amounts of ^{90}Sr have also been used as a treatment for bone cancer.

^{90}Sr is a pure β-emitter (546 keV max, 100% intensity) with a half-life of 28.79 years and a specific activity of 138 Ci/g, which decays to the isotope ^{90}Y, which is also a pure β-emitter (2280 keV max, 100% intensity) with a half-life of 64.0 hours. (KAPL 2002). The decay product of ^{90}Y is the stable isotope, ^{90}Zr. Because the half-life of the yttrium daughter, ^{90}Sr and ^{90}Y are found in a state of secular equilibrium in aged samples. ^{90}Sr poses a high health hazard as it has the same valance shell electron configuration as calcium and is, therefore, easily metabolized by the body, where it is incorporated into the skeletal system. For this reason, there is a great interest in procedures that can rapidly detect ^{90}Sr in urine bioassay samples for emergency preparedness scenarios.

The nature of β-emitter detection necessitates that need to remove ^{90}Sr from all accompanying radionuclides prior to analysis. Established standard methods consist of a series of precipitation steps (Piltingsrud 1972). While a detection limit of 1mBq/kg is possible, 2-3 weeks of analysis time are needed (Alfaro 1995). After the Chernobyl accident, there were no analytical techniques for the determination of ^{90}Sr that were sufficiently fast and reliable to estimate the spread and extent of ^{90}Sr contamination (Alfaro 1995). The separation of strontium by personnel unaccustomed to the technique was especially problematic, where, even in the presence of additional equipment, sample throughput could not be increased to meet the short-term need (Workshop 1986).

Flow scintillation analysis (FSA) with high performance extraction chromatography (HPEC) is a technique that has evolved from its progenitors, sequential injection (Ruzicka 1990; Ivaska 1993; Christian 1994) and flow injection (Ruzicka 1988; 1994). This technique employs a gradient pump and a column packed with an extractive resin, coupled with an on-line liquid scintillation counter. In this manor, the wet

chemistry of the separation is combined with the detection instrumentation. The process allows for the analyte to be concentrated on the stationary phase, which is housed in a chromatography column, and eluted in a sample zone that is carried by the mobile phase to the detector flow cell. Variations on this technique for the analysis of several radionuclides are numerous: ^{90}Sr (Grate 1996; Grate 1999b; Paulenova 2001; Roane 2003; Fjeld 2005), ^{99}Tc (Egorov 1998; Grate 2005), actinides (Reboul 2002; Roane 2002; Hughes 2003; Fjeld 2005). The advantages of FSA include automated sample pre-treatment, removal of interferences and matrix components, preconcentration, the ability to change solvents on- the-fly, increased sample throughput, and reduced reagent consumption (Luque de Castro 1992). A full, detailed description of flow scintillation analysis principles and applications is available in a chapter of the *Handbook of Radioactivity Analysis* (L'Annunziata 2003). However, to our knowledge, there is no literature dedicated to the determination of ^{90}Sr at low levels (<1000 DPM per sample) or in urine bioassay samples by these techniques.

In this research, we describe the development of an FSA by HPEC method for the separation and quantification of ^{90}Sr from various dilutions of urine matices. The extractive resin used in this work was Sr-Spec resin, developed and previously described by Horwitz (Horwitz 1992). The resin consists of the compound, 4,4'(5')-bis(tert-butylcyclohexano)-18-crown-6, impregnated on polymer support beads, and serves as the stationary phase where the strontium is retained and eluted. A stopped-flow counting technique developed by Grate and Egorov was used to improve the detection limits (Grate 1996; Egorov 1998b; Grate 1999b). The stopped-flow technique improves method sensitivity by extending, indefinitely, the residence time of the largest part of the sample zone within the flow cell, allowing a statistically meaningful number of counts to accumulate before the sample is permitted to exit the detector. An automated column

packing device, described in a previous work by the authors, was used to maintain the reproducibility of resin packing from column to column (Peterson 2007). This work characterizes the effectiveness of the technique for low level ^{90}Sr detection while optimizing several counting parameters for the determination of ^{90}So in simulated urine bioassay samples. Using the techniques and methods described here, there is no need for ^{90}Y ingrowth correction, sample handling is minimized, and radioactive samples are not moved from one room to another. The method presented also has the advantage of being much easier to operate.

EXPERIMENTAL

High Performance Extraction Chromatography System: A Dionex GP50 gradient pump (Dionex, Sunnyvale, CA) was configured with a Rheodyne 7725i dual mode analytical injector and a 2000 µL sample loop (Precision Flow Products, Lake Elsinore, CA). A 2500 µL Gastight syringe (Hamilton Co, Reno, NV) was used to inject samples into the loop. Sr-Spec resin (EIChroM Industries, Inc., Darren, IL) of bead size 50-100 µm was slurried overnight with deionized water (18 MΩ..Nanopure Water System, Barnstead, Dubuque, IA) and packed into one of two PEEK lined columns, 4.6mm I.D. x 30mm or 150mm, hardware (Alltech Associates, Deeerfield, IL) using an Alltech Model 1666 slurry packer. The packing pressure was 1000 psi and the calculated volume of the resin was 0.499 mL for the 3cm columns, and 2.49 mL for the 15cm columns. Elution schemes for the HPEC system were manually programmed into the gradient pump and controlled through the instrument interface. The scheme used for this procedure was adapted from established methods (Grate 1996; Grate 1999b) and can be seen in Table 4.1. The separation of ^{90}Sr from other ions using Sr-Spec resin has been previously characterized, showing that Sr can be loaded onto the resin with 2-8M HNO_3 (Horwitz 1992). While it is desirable to use the lowest molarity of nitric acid possible to preserve

the life of the column, the presence of potassium at concentrations ≥ 0.03M can have a significant suppressing effect on Sr retention (Horwitz 1992). Since K is expected to be present in significant quantities in urine samples, 8M nitric must be used to load the Sr, since the selectivity of the resin for Sr over potassium is highest for this molarity.

Table 3.1: Gradient used in this study.

t(MIN)	ELUENT(mL/MIN)	COMPOSITION	C.TAIL(mL/MIN)	COMMENTS
0	1.00	8M HNO_3	0.0	Inject/Load
4	1.00	Water	2.0	Stripping
28	2.50	8M HNO_3	0.0	Re-condition
30	0	N/A	0.0	End Cycle

On-Line Liquid Scintillation Counting: Flow scintillation analysis was accomplished using a β-Ram 4B (IN/US Systems Inc., Tampa, FL). This model possesses an internal cocktail pump and can be fitted with flow cells of various types and sizes. All experiments in this work were done using a 2500 μL liquid flow cell. The device was configured with the HPEC so that the column effluent was mixed with the scintillator in controllable ratios. The detector counting parameters were controlled using Scint Flow SA software (IN/US) and Laura Lite 3.4 (IN/US) run on desktop PC and connected to the detector by a serial port. The detector was signaled to begin cocktail flow and counting by a closed contact connection to the analytical injector when it was turned to the "inject" position. The detector integration time, t_i, was 6s to allow enough counts to accumulate for each data point. Figure 3.1 shows a block diagram of the flow scintillation analysis system.

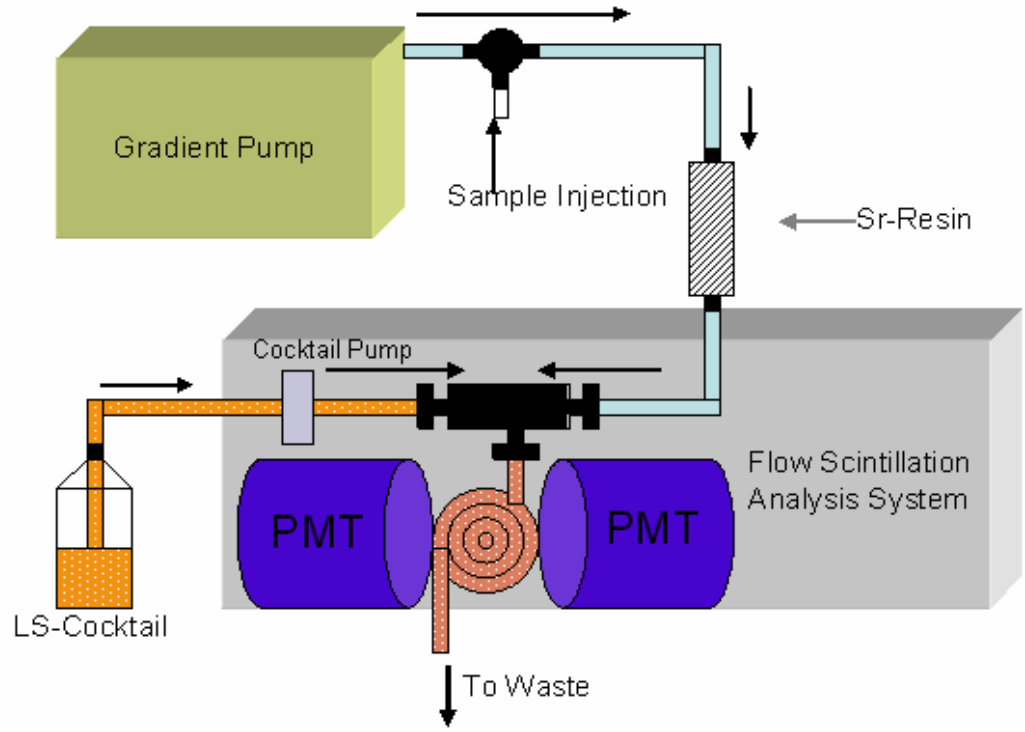

Figure 3.1: A Block Diagram of the Flow Analysis System

Off-Line Liquid Scintillation Counting: All off-line liquid scintillation counting was performed using a Tri Carb 2750 TR/LL Liquid Scintillation Analyzer (Packard Instrument Co., Meriden, CT).

Reagents and Standards: All chemicals used were analytical grade. Deionized water was used in all dilutions. A low-viscosity liquid scintillation cocktail (In-Flow 2:1, IN/US) was used for all flow scintillation measurements because this cocktail can be mixed with eluents at low ratios without gelling. Ultima Gold LLT (Packard) cocktail was used for all off-line liquid scintillation counting. Standard $^{90}Sr/^{90}Y$ solutions were prepared by evaporating aliquots of in-house standards to dryness and dissolving the residue in measured volumes of 8M nitric acid.

Urine Matrix Preparation: Samples were prepared to simulate urine bioassay from patients with ^{90}Sr exposure by mixing portions of water spiked with ^{90}Sr with a urine base

(provided by the Centers for Disease Control and Prevention, Atlanta, GA). The resulting samples contained the desired levels of ^{90}Sr and dilute concentrations of other urine matrix components. Even at a dilute strength, there are still significant levels of salts and organic compounds present to reasonably simulate bioassay samples.

RESULTS AND DISCUSSION

^{90}Sr Observation: The first setting that requires optimization is ^{90}Sr channel window setting so that the ^{90}Sr peak area is counted, minimizing the contribution from ^{90}Y and background noise. 2500 µL of a solution of a known activity of ^{90}Sr/Y was mixed with cocktail at a 2:1 ratio and manually injected directly into the flow cell. The pulse hight analysis feature of the β-RAM was used to determine the spectral appearance of the ^{90}Sr/Y within the instrument. This spectrum is shown below in Figure 3.2.

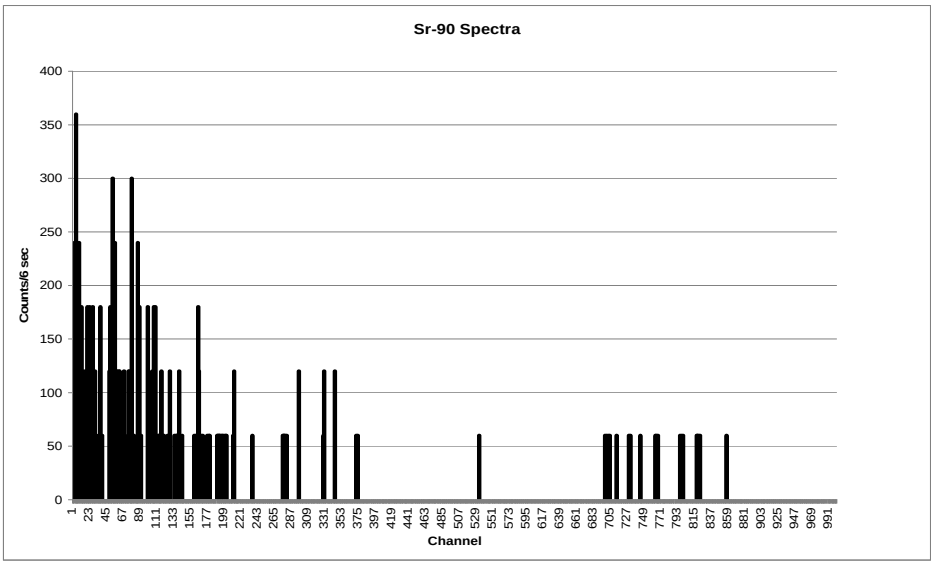

Figure 3.2: The spectral appearance of ^{90}Sr/Y within the β-RAM. Most of the signal occurs within channels 0-600.

The bulk of the activity can be found in channels 0-600, with some high energy counts registering in channels 700-900 (presumably from ^{90}Y). Since the energy spectrum of beta particle emissions is a continuum from 0-β_{Max}, we cannot expect to fully resolve the emissions from ^{90}Sr and ^{90}Y. Nevertheless, the contribution of ^{90}Y to the ^{90}Sr can be minimized by setting the upper channel threshold at channel 600. While ^{90}Sr counts can be expected to register in all channels <600, it is practical to exclude channels 0 and 1 because a significant amount of background signal can be found in these channels (data not shown). Therefore, we have concluded that the optimum ^{90}Sr counting window is 2-600 channels and this counting window was used for all subsequent experiments.

In order to determine the time at which the ^{90}Sr peak elutes from the column under the gradient scheme shown in Table 4.1, a test injections of the analyte were made. In this test, 2112 dpm of ^{90}Sr was injected with a volume of 2mL. Unfortunately, our first attempts to profile the ^{90}Sr peak position using the 3cm columns were not reproducible. The peak position was found to drift from 10 minutes on the first run, to 14 minutes on the second run, to 19 minutes for the third run. On the fourth run the column failed to retain the ^{90}Sr, which eluted with the unretained ^{90}Y. Figure 3.3 depicts four analysis cycles of identical $^{90}Sr/Y$ traces and shows how the peak drifts until the column fails. The reason for the variation of the column performance and failure is likely that the extractive ligand is lost as its octanol solvent dissolves into the mobile aqueous phase. This theory was first postulated by Grate when his group noticed a similar effect following their 1996 work. Their subsequent 1999 publication on the optimization of ^{90}Sr determination by FSA demonstrated that the saturation of the reagents with octanol inhibited the loss of the extractive ligand and promoted reproducible peak positions.

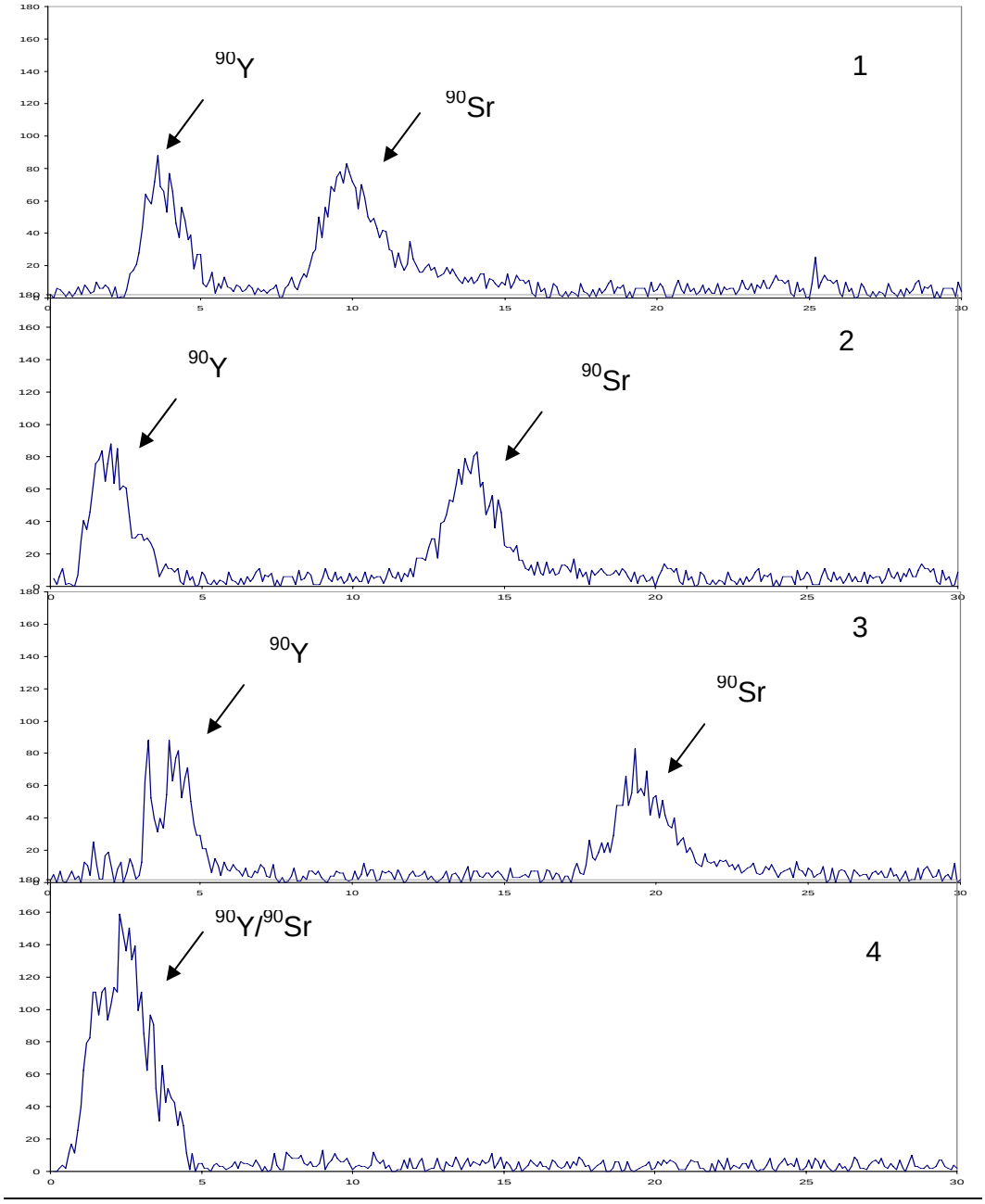

Figure 3.3: Sample chromatograms showing the ^{90}Y and ^{90}Sr peak locations over the course of 4 analysis cycles for a 3cm column. The ^{90}Y peak is more or less consistent, while the ^{90}Sr peak drifts. The column finally fails on the 4th cycle, when ^{90}Sr is not retained and co-elutes with ^{90}Y in one large peak.

The use of reagents saturated in octanol was not desirable in this research because of the added complexity of creating, maintaining, and storing mixed phased reagents. There is also the potential problem of creating a mixed waste stream that is hazardous and radioactive. Therefore, we decided to try larger 15cm columns, which would contain more resin, to obtain more reproducible results and longer column life.

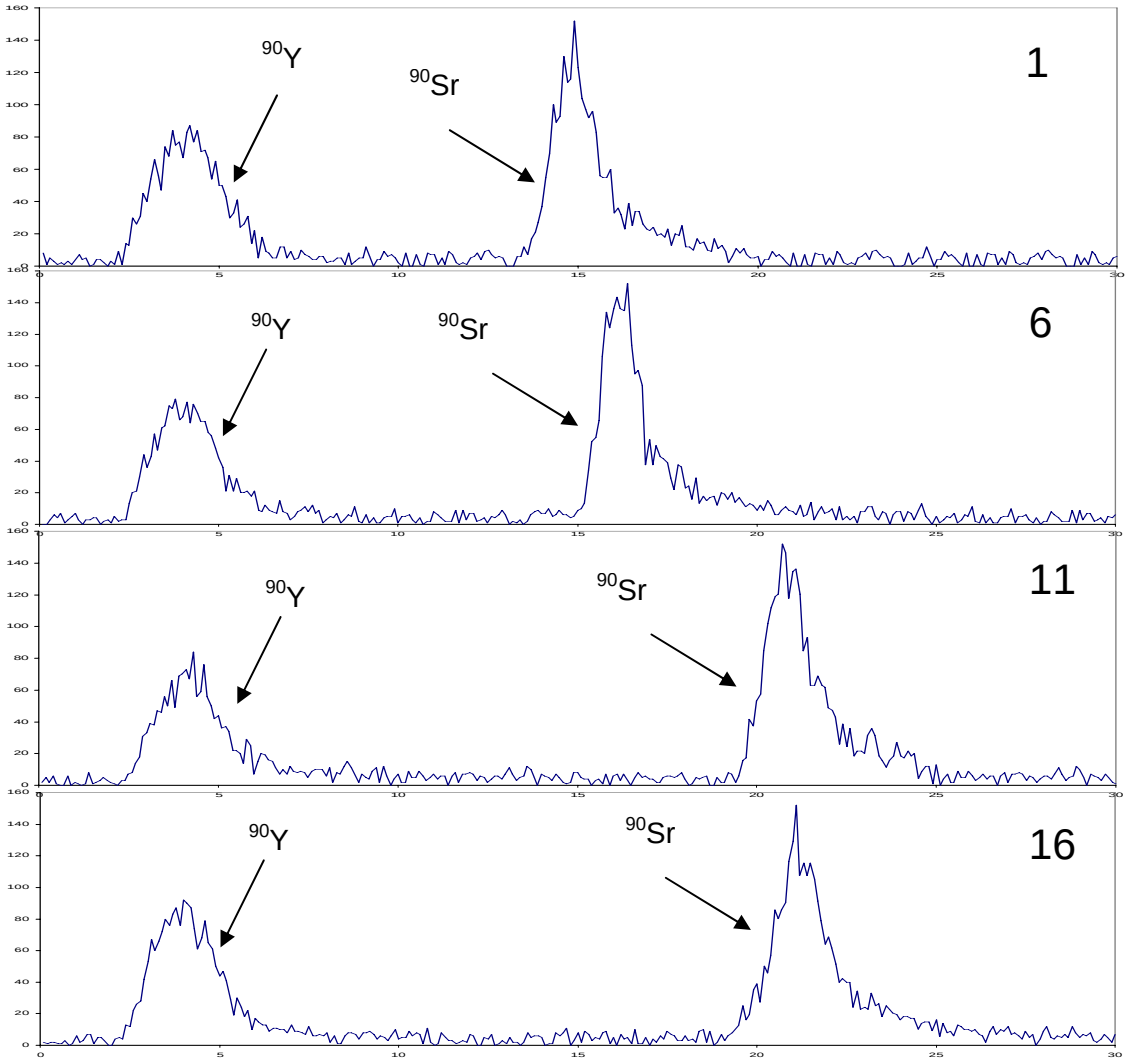

Figure 3.4: Sample chromatograms showing the ^{90}Y and ^{90}Sr peak locations over the course of 16 analysis cycles for a 15cm column. The ^{90}Y peak is more or less consistent, while the ^{90}Sr peak drifts slightly. The column finally, failed on the 17th cycle (not shown).

The timing and level of drift of the ^{90}Sr peak in the 15cm is not ideal, but it is acceptable for our purposed of timely and consistent analysis. On a new 15cm column, the ^{90}Sr peak occurs at approximately 15 minutes. This is longer than the 10 minute time for the 3cm column, which will lead to a longer analytical cycle. Nevertheless, the column lifetime is extended by more than five fold. We therefore deem the trade off between increased analysis time and reduced column consumption acceptable. An added benefit of using the larger column was that the peak shape was improved compared to the shorter column. Figure 3.5 shows the number of counts for the peak 6 seconds versus various activities of ^{90}Sr for the 3cm and 15cm columns.

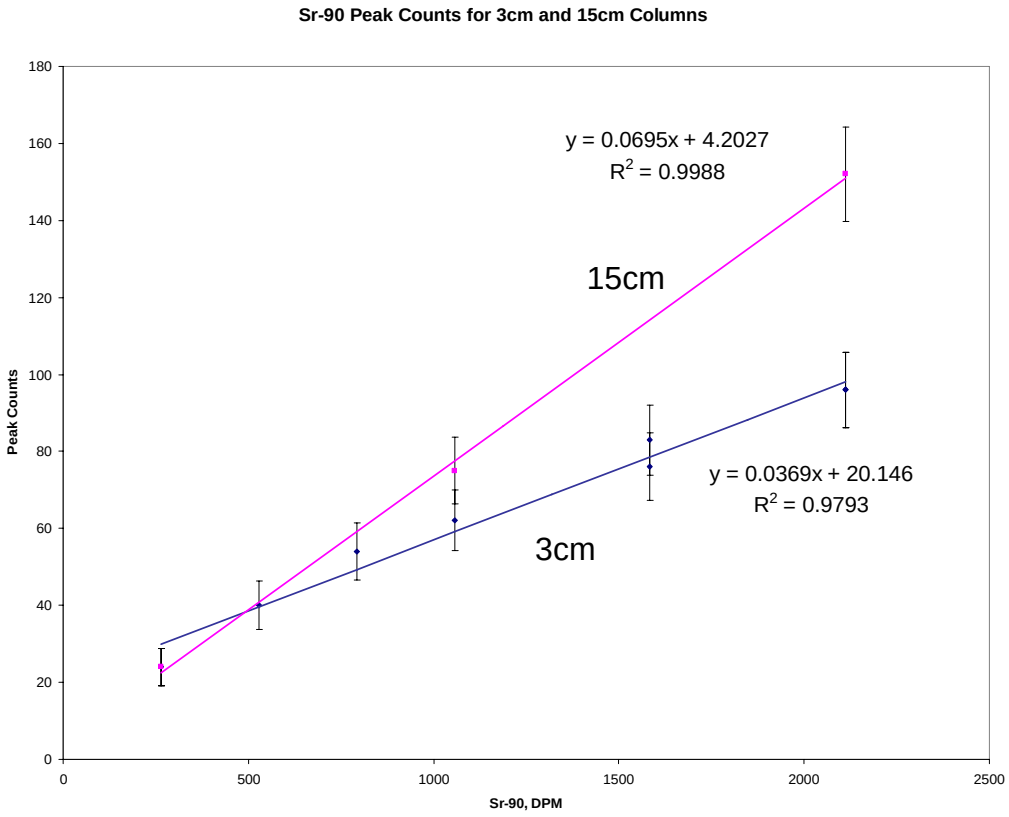

Figure 3.5: Peak heights versus various activities of ^{90}Sr for 3cm and 15cm columns.

Transient-Flow ^{90}Sr Quantification: The strontium elutes from the column in a sample zone, where it is mixed on-the-fly with scintillation cocktail at the recommended ratio of 2:1 prior to entering the detector flow cell (Grate 1996; Grate 1999b). The flow cell consists of a calibrated volume of optically transparent Teflon tubing that is placed within a fixed geometry between two photomultiplier tubes. Scintillations from the radiation are "seen" by the detector only when the sample zone present in the flow cell. Assuming that there is no secondary mixing in the flow cell, the residence time, t_r, of the eluted sample zone in the flow cell is described by:

$$t_r = \frac{V_c}{F} \tag{3.1}$$

where, V_c, is the volume of the flow cell and, F, is the combined flow rate of the eluent/cockatil mixture. In this work, a 2500 μL flow cell was used with a combined scintillator/eluent flow rate of 3mL/min. Therefore, the residence time used in all calculations is 50s, or 0.83 min. For transient flow counting the peak area is summed and the background count for the area is subtracted to derive a net number of counts for the peak, C_n. The net CPM for the peak can then be determined by:

$$C_{CPM} = \frac{C_n}{t_r} \quad \text{(Transient-Flow)} \tag{3.2}$$

If a known activity of ^{90}Sr is introduced to the system, the net count rate can be related to the sample activity, A_{dpm}, to determine the effective efficiency, E_{es} (which combines the efficiency of the separation and the detector).

$$C_{CPM} = E_{es} A_{dpm} \quad \text{(Transient-Flow)} \tag{3.3}$$

Using the above relations, we can create a calibration curve for the detector and analyte of interest by injecting various ^{90}Sr activities and plotting the resulting net peak areas, see Figure 3.6. The slope of the line is related to the effective efficiency, E_{es}, by dividing the slope by the sample residence time, t_r.

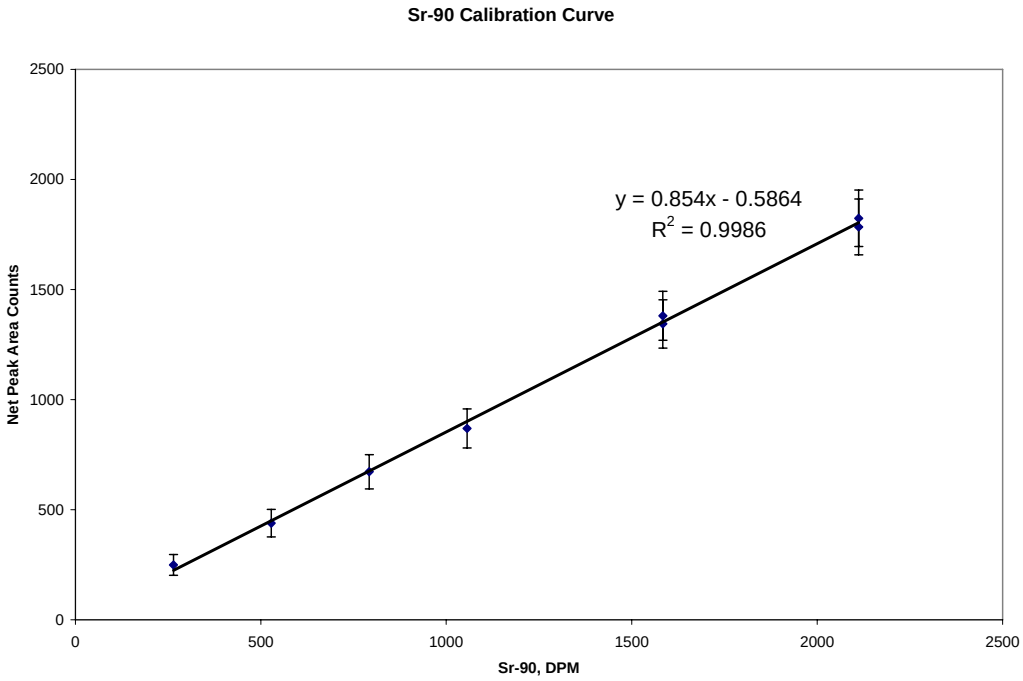

Figure 3.6: A calibration curve of detector response to various levels of ^{90}Sr activity as determined by transient-flow counting. The fact that the value for R^2 is close to unity and that the intercept is near zero indicates that there is a highly linear detector response for this analyte. Error bars represent 3σ.

The efficiency as determined by the slope of the calibration curve was found to be 102.5 (± 6)%. Thus, ^{90}Sr is detected with very high efficiency. Any real value of the effective efficiency >100% may be due to diffusion of the sample zone within the flow cell, or residual luminescence within the cell for a short time after the sample zone has left. Nevertheless, detection of ^{90}Sr by transient counting methods can be considered highly efficient and accurate.

Due to the high detection efficiency, transient flow counting is a reliable technique for the determination of ^{90}Sr down to low levels. With an average background of 4.1 cpm and the typically encountered peak shape, we estimate that the lower level of detection for this technique is 47 dpm, with the level of quantification being 156 dpm. Computer-based methods of peak detection, included with the software used in this research, are useful for identifying and quantifying peaks resulting from this level of activity. Figure 3.7 shows detector traces for various levels of ^{90}Sr activity.

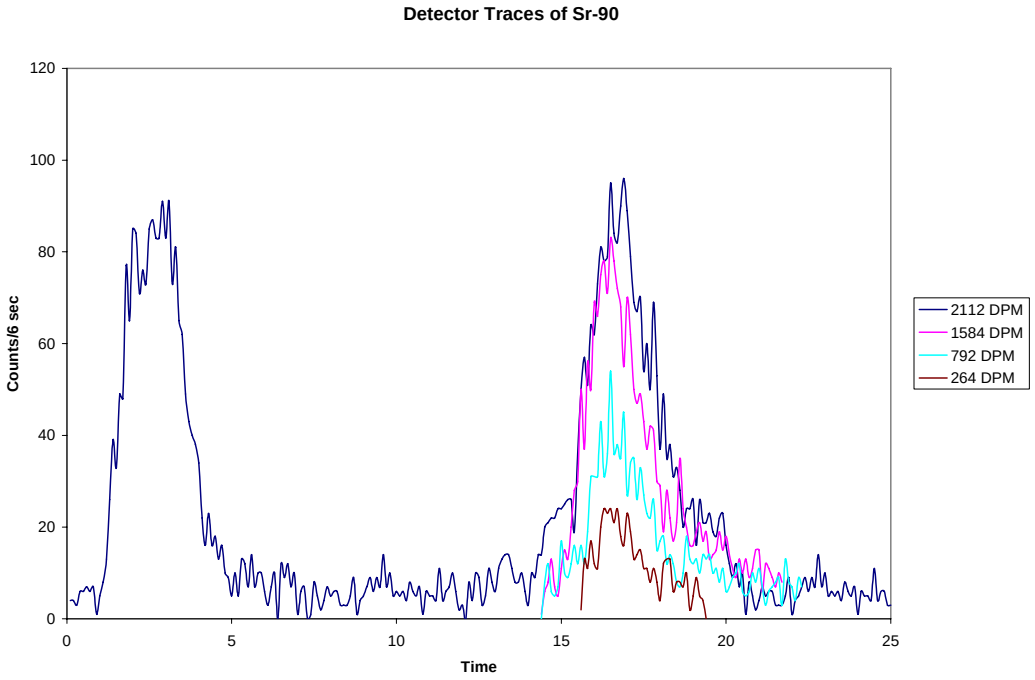

Figure 3.7: Detector traces for various activities of ^{90}Sr as determined by transient-flow counting and a 3cm column. Traces as low as 264 dpm are visually apparent. Computer-aided peak finders are helpful for detecting lower activities of ^{90}Sr.

Stopped-Flow ^{90}Sr Quantification: Assuming no secondary mixing or phase separation effects in the flow cell, the fraction of the sample zone present in the flow cell

at the peak maximum, D_m, can be determined using transient-flow conditions and the following equation:

$$D_m = \frac{C_{\max} t_r}{t_i C_n} \tag{3.5}$$

Where, C_{max}, is the number of net counts per update time at peak maximum and, t_i, is the detector update time. Using the value determined from D_m, a sample of known activity may be run using stopped-flow counting to determine the effective efficiency of the technique. Once D_m and E_{es} are determined, samples of unknown activity may be counted and the resulting values of CPM can be related back to an activity. In this work, D_m was determined to be 0.084 (± 0.004) and E_{es} was 1.025 (± 0.06) for aqueous samples:

$$C_{CPM} = D_m E_{es} A_{dpm} \quad \text{(Stopped-Flow)} \tag{3.6}$$

The value for D_m can also be found by plotting C_{max} versus A_{dpm} (similar to Figure 3.5, but not shown) and noting the slope of the trendline, which is proportional to D_m.

Stopped-flow counting was not actually used in any of the research in this chapter, because low detection limits were obtainable by transient-flow counting means. However, stopped-flow counting is essential for detecting lower efficiency isotopes at the lowest activities.

Urine Matrix Effects: Urine matrix effects on ^{90}Sr determination were studied to determine the suitability of this technique for rapid urine bioassays analysis. To this end, 2mL simulated bioassay samples created using a urine base and various activities of ^{90}Sr. Solutions of 2,112 dpm, 1,056 dpm, and 264 dpm ^{90}Sr were prepared in 10x, 5x, and 2x urine dilutions as well as for full strength urine. These samples were then processed using the elution scheme shown in Table 3.1 and a 15cm column.

Table 3.2: Simulated urine bioassay result. All recoveries activities are within one standard deviation of the activities administered.

URINE CON., %	A (dpm)	DETERMINED A (dpm)	RECOVERY (%)
10	2112	2200 (±140)	104 (±6.6)
10	1056	1076 (±72)	102 (±6.9)
10	264	285 (±24)	108 (±9.1)
20	2112	2217 (±141)	105 (±6.7)
20	1056	975 (±66)	92.4 (±6.3)
20	264	272 (±23)	103 (±8.8)
50	2112	2125 (±136)	101 (±6.4)
50	1056	1071 (±72)	101 (±6.8)
50	264	268 (±23)	101 (±8.8)
100	2112	2095 (±134)	99.2 (±6.3)
100	1056	1000 (±68)	94.7 (±6.4)
100	264	237 (±21)	89.6 (±7.9)

Recoveries of ^{90}Sr in all urine matrices were quantitative, with only a minor decline in recovery in full strength urine. In addition, these urine data highly conform to the existing calibration curve (data not shown) in Figure 3.6. This suggests that similar limits of detection and quantification apply to samples in a urine matrix. These results show excellent potential for applications of this technique to real urine bioassay samples. The ability to tolerate up to 2mL of full strength urine, while performing a nearly quantitative separation and detection of ^{90}Sr in just 30 minutes is highly desirable from the standpoint of simplicity and expediency.

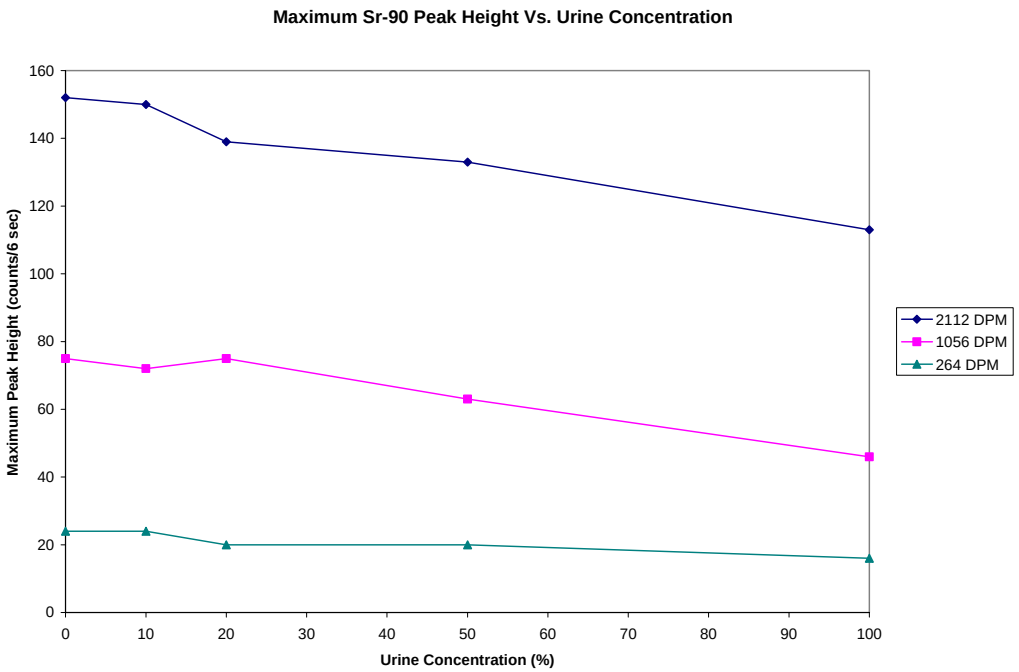

Figure 3.8: Maximum ^{90}Sr peak height for various urine concentrations. Peak height declines with increasing urine concentration as a result of peak broadening.

One irregularity that was noted in the processing of urine matrix samples was a decline in the maximum ^{90}Sr peak heights with increasing urine concentration. This indicates that the peaks are becoming increasingly broad with increasing urine concentration, though not broad enough to significantly affect the overall peak area determination. For the purposes of transient-flow counting, this type of peak broadening is inconsequential. However, any attempts at stopped-flow counting would need to consider the affect the decline in maximum peak height would have at the concentration of urine utilized. This effect would also negatively impact detection limits for the stopped-flow counting technique, since peak maxima would be reduced with respect to background. Figure 3.8 depicts this behavior.

CONCLUSIONS

An automated computer controlled system for the separation and simultaneous detection of ^{90}Sr was optimized for aqueous and simulated urine bioassay samples. An optimal counting window for ^{90}Sr with the β-RAM flow scintillation analyzer was established. Columns of 3cm and 15cm were examined for reproducibility and column life, where it was determined that the 15cm column was superior. This column was capable of accommodating up to 16 analytical cycles with little ^{90}Sr peak drift. In addition, peak shape was improved by transitioning from a 3cm to 15cm column though it was necessary to add 5 minutes to the detection cycle. A calibration curve of detector response to various low activity samples was plotted and shown to be highly linear for both aqueous and urine samples. The resulting lower limit of detection by transient-flow counting was estimated to be 47 dpm, while the lower level of quantification was estimated to be 156 dpm. The time for total analysis and column washing and reconditioning was 30 minutes for transient-flow counting.

The results of the simulated urine bioassay experiments were highly encouraging, with no loss of recovery for urine samples diluted to 50% and little loss of recovery for fully concentrated urine samples. Some peak broadening, with associated decrease in peak maximum counts, was noted. We intend to conduct further research into optimizing column parameters (length, resin size, and packing pressure) for urine bioassays. We also anticipate experimenting with octanol saturated reagents, as suggested by Grate, to determine the suitability of this technique to enhance column performance and reproducibility.

Chapter 4: Flow Scintillation Analysis of ^{210}Po

An automated procedure for the determination of ^{210}Po in aqueous matrices has been developed using a technique called flow scintillation analysis (FSA). This technique employs high performance extraction chromatography (HPEC) and an on-line liquid scintillation counter to provide automated separation and simultaneous detection of low levels of ^{210}Po. Using Sr-Spec resin, ^{210}Po was concentrated on the column from the matrix and potential radiological interferences with 2M HCl and selectively eluted with 6M nitric acid and instantly quantified by FSA. A counting technique called stopped-flow detection was used to improve detection limits. The lowest limit of quantification achieved by this technique was 100 dpm, or 1.67 Bq, per sample for a 30 minute stopped flow counting time. The total analysis time is 60 min per sample. Dilute urine samples, spiked with ^{210}Po, were also processed by this method to test the application of this technique for bioassay monitoring. The advantages of FSA are faster analysis, greater precision, reduced labor commitment, and improved safety due to the fact that chemical and radiological hazards are mostly contained and automated. The stopped-flow counting techniques employed are advantageous in that sensitivity is improved and scintillation cocktail is conserved.

INTRODUCTION

^{210}Po is considered to be one of the most toxic naturally occurring radionuclides (Al-Masri 2004) and a major contributor of natural radioactivity in human foodstuffs, contributing an estimated annual effective dose of 11 μSv per year—22% of the total average effective dose (UNSCEAR 2000). Recently, ^{210}Po was identified as poisoning agent in the high profile death of Alexander Litvinenko in London, England on November 23rd, 2006 (Harrison 2007). Since this time, government health agencies have

been working with radioanalytical laboratories to develop rapid methods of ^{210}Po analysis that could be used to screen large numbers of people for uptake. The most convenient excretion pathway of ^{210}Po for analysis is through the urine, where approximately 1% of the body burden is cleared per day (Stannard 1964). Currently, separation and analysis is performed manually in two separate and distinct time-consuming and labor-intensive processes. In addition, these methods expose technicians to chemical hazards and unsealed sources of radioactivity. For this reason, a rapid and automated combined separation and detection technique is desired for the determination of ^{210}Po in an aqueous matrix.

^{210}Po is a virtually pure α-emitter (5304 keV, 100% intensity) with a half-life of 138.38 days and a specific activity of 4.60 Ci/mg, which decays to the stable isotope ^{208}Pb (KAPL 2002). ^{210}Po can only be determined isotopically by alpha spectrometry, a valuable technique due to its excellent energy resolution, compact size, and low background (Matthews 2007). However, there are some disadvantages to using alpha spectrometry including lengthy source preparation methods. Even when utilizing polonium's well-known ability to autodeposite, the reported mean deposition time is 5-6 h (Matthews 2007). In addition, polonium is notorious for its ability to "creep," whereby an unsealed source will distribute itself and contaminate the area it surrounds (Roessler 2007). As a result, contamination of alpha spectrometers can be a potentially serious problem for large batch samples of ^{210}Po. Finally, the count times that are often employed for alpha spectrometry can add up to 24 hours to the procedure, and can cause a bottle neck in the batch analysis if the capacity of the lab is limited. Therefore, an automated analytical technique that is capable of rapid sample screening is a desirable capability to compliment alpha spectrometry.

Flow scintillation analysis (FSA) with high performance extraction chromatography (HPEC) is a technique that has evolved from its progenitors, sequential injection (Ruzicka 1990; Ivaska 1993; Christian 1994) and flow injection (Ruzicka 1988; Ruzicka 1994). This technique employs a gradient pump and a column packed with an extractive resin, coupled with an on-line liquid scintillation counter. In this manner, the wet chemistry separation is combined with the detection instrumentation. The process allows for the analyte to be concentrated on the stationary phase, which is housed in a chromatography column, and eluted in a sample zone that is carried by the mobile phase to the detector flow cell. Variations on this technique for the analysis of several radionuclides are numerous: ^{90}Sr (Grate 1996; Grate 1999b; Paulenova 2001; Roane 2003; Fjeld 2005), ^{99}Tc (Egorov 1998; Grate 2005), actinides (Reboul 2002; Roane 2002; Hughes 2003; Fjeld 2005). The advantages of FSA include automated sample pre-treatment, removal of interferences and matrix components, preconcentration, the ability to change solvents on- the-fly, increased sample throughput, and reduced reagent consumption. A full and detailed description of flow scintillation analysis principles and applications is available in a chapter of the Handbook of Radioactivity Analysis (L'Annunziata 2003). However, to our knowledge, there is no literature on the determination of ^{210}Po by these techniques.

In this paper, we describe the development of an FSA by HPEC method for the separation and quantification of ^{210}Po. The extractive resin used in this work was Sr-Spec resin, developed and previously described by Horwitz (Horwitz 1992b). The resin consists of the compound, 4,4'(5')-bis(tert-butylcyclohexano)-18-crown-6, impregnated on polymer support beads, and serves as the stationary phase where the polonium is retained and eluted. A stopped-flow counting technique developed by Grate and Egorov was used to improve the detection limits (Grate 1996; Egorov 1998b; Grate 1999b). The

stopped-flow technique improves method sensitivity by extending—indefinitely—the residence time of the largest part of the sample zone within the flow cell, allowing a statistically meaningful number of counts to accumulate before the sample is permitted to exit the detector. An automated column packing device, described in a previous work by the authors, was used to maintain the reproducibility of resin packing from column to column (Peterson 2007). This work characterizes the effectiveness of the technique while optimizing several counting parameters for the determination of low levels of ^{210}Po in aqueous samples. In addition, limited experimentation was done to demonstrate the feasibility of utilizing this technique for urine bioassay samples.

EXPERIMENTAL

High Performance Extraction Chromatography System: A Dionex GP50 gradient pump (Dionex, Sunnyvale, CA) was configured with a Rheodyne 7725i dual mode analytical injector and a 2000 µL sample loop (Precision Flow Products, Lake Elsinore, CA). A 2500 µL Gastight syringe (Hamilton Co, Reno, NV) was used to inject samples into the loop. Sr-Spec resin (EIChroM Industries, Inc., Darren, IL) of bead size 50-100 µm was slurried overnight with deionized water (18 MΩ..Nanopure Water System, Barnstead, Dubuque, IA) and packed into a PEEK lined column, 4.6mm I.D. x 30mm, hardware (Alltech Associates, Deeerfield, IL) using an Alltech Model 1666 slurry packer. The packing pressure was 1000 psi and the calculated volume of the resin was 1.99 mL. Elution schemes for the HPEC system were manually programmed into the gradient pump and controlled through the instrument interface. The scheme used for this procedure can be seen in Table 4.1.

Table 4.1: Gradient used in this study.

Time(min)	Eluent(mL/min)	Composition	Cocktail(mL/min)	Comments
0	1.00	2M HCl	0.0	Inject/Load
5	1.00	6M HNO_3	2.0	Stripping
12.5	0.0	N/A	0.0	Counting
42.5	1.00	6M HNO_3	2.0	Strip Cont.
45	1.50	Water	0.0	Wash
50	1.35	2M HCl	0.0	Condition
60	0.0	N/A	0.0	End Cycle

On-Line Liquid Scintillation Counting: Flow scintillation analysis was accomplished using a β-Ram 4B (IN/US Systems Inc., Tampa, FL). This model possesses an internal cocktail pump and can be fitted with flow cells of various types and sizes. All experiments in this work were done using a 2500 μL liquid flow cell. The device was configured with the HPEC so that the column effluent was mixed with the scintillator in controllable ratios. The detector counting parameters were controlled using Scint Flow SA software (IN/US) run on desktop PC and connected to the detector by a serial port. The detector was signaled to begin cocktail flow and counting by a closed contact connection to the analytical injector when it was turned to the "inject" position. The detector integration time, t_i, was 6s to allow enough counts to accumulate for each data point. Figure 4.1 shows a block diagram of the flow scintillation analysis system.

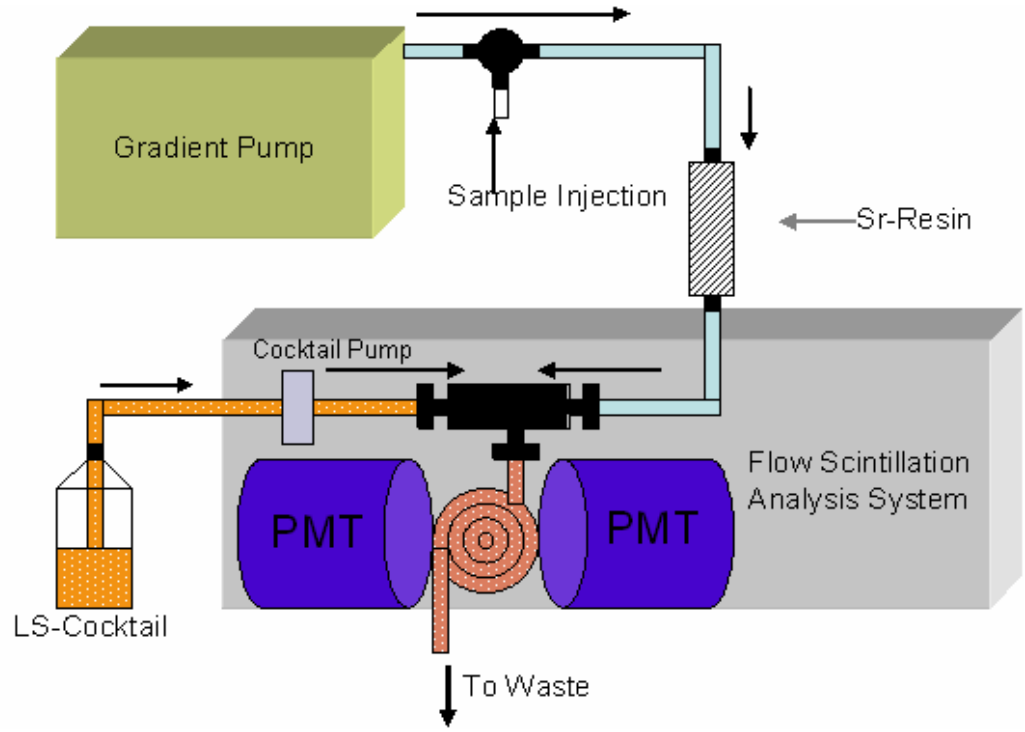

Figure 4.1: A Block Diagram of the Flow Analysis System

Off-Line Liquid Scintillation Counting: All off-line liquid scintillation counting was performed using a Tri Carb 2750 TR/LL Liquid Scintillation Analyzer (Packard Instrument Co., Meriden, CT).

Reagents and Standards: All chemicals used were analytical grade. Deionized water was used in all dilutions. A low-viscosity liquid scintillation cocktail (In-Flow 2:1, IN/US) was used for all flow scintillation measurements because this cocktail can be mixed with eluents at low ratios without gelling. Ultima Gold LLT (Packard) cocktail was used for all off-line liquid scintillation counting. A ^{210}Po working standard was prepared from a well-aged ^{210}Pb standard (Amersham International, Amersham, UK) using a method adapted from a plutonium separation procedure (Talvitie 1971). Originally in 1M nitric acid, an aliquot of the ^{210}Pb solution was evaporated to a just dry

state on a hotplate at 90 °C. It should be noted that polonium solutions must not be heated over 100 °C because losses of polonium occur at temperatures above this point, with more than 90% of polonium lost due to volatization at temperatures greater than 300 °C (Martin 1969).

The ^{210}Pb residue was brought up with a volume of 9M HCl. A 5 mL resin bed of Bio-Rad AG 1-X4 (Bio-Rad, Hercules, CA) in HCl was prepared in a Teflon column. After conditioning the column with three 15mL 9M HCl washes, the sample was loaded onto the column at a rate of 3 mL/min. Three additional washes of 15 mL of 9M HCl are then run through the column. ^{210}Pb is not retained on the column and is found in the 45 mL of HCl load solution. ^{210}Bi is then removed from the column by stripping with 7.5M HNO_3 at a rate of 3 mL/min and can be found in the first 50 mL of strip effluent. Finally, ^{210}Po is eluted in a subsequent addition of 100 mL of 7.5M HNO_3 at a rate of 3 mL/min. Working stock solutions of ^{210}Po can then be prepared from this product.

Urine Matrix Preparation: Samples were prepared to simulate urine bioassay from patients with ^{210}Po exposure by mixing portions of water spiked with ^{210}Po with a urine base (provided by the Centers for Disease Control and Prevention, Atlanta, GA). The resulting samples contained the desired levels of ^{210}Po and dilute concentrations of other urine matrix components. Even at a dilute strength, there are still significant levels of salts and organic compounds present to reasonably simulate bioassay samples.

RESULTS AND DISCUSSION

Preparation of the ^{210}Po Stock: The original intent of the Talvitie separation procedure used here was to remove polonium from biological samples so that plutonium could be analyzed. Nevertheless, we have determined that this method is also effective at separating the ^{210}Pb/^{210}Bi/^{210}Po decay series into its component isotopes. The ^{210}Pb standard solution was originally prepared over 15 years prior to the time of separation,

allowing sufficient time for secular equilibrium to be established with its daughters. Using the previously described method, polonium separation from the aged ^{210}Pb solution was accomplished with an 89.0% recovery. Analysis of aliquots of the ^{210}Pb, ^{210}Bi, and ^{210}Po fraction solutions were done by the off-line liquid scintillation analyzer. The three isotopes studied can easily be identified by observing their spectral energies and peak shapes. Samples of the Bio-Rad column effluent were collected at regular intervals and counted with the mean results of duplicate runs shown in Table 4.2.

Table 4.2: Percent of each isotope recovered in the column effluent. Lead is not retained on the column and is found entirely within the effluent of the HCl load solution. Bismuth is found entirely within the first 50 mLs of the nitic strip. Polonium is eluted with subsequent additions of nitric acid, with diminishing returns after 150 mLs of nitric acid.

ACID, VOL. mL	% OF RECOV. ^{210}Pb	% OF RECOV. ^{210}Bi	% OF RECOV. ^{210}Po
HCl, 0-45	100	0	0
HNO_3, 0-25	0	53.5	0
HNO_3, 26-50	0	46.5	0
HNO_3, 51-75	0	0	43.6
HNO_3, 76-100	0	0	39.4
HNO_3, 101-125	0	0	11.4
HNO_3, 126-150	0	0	8.6
HNO_3, 151-175	0	0	2.5
HNO_3, 176-200	0	0	2.0
HNO_3, 201-225	0	0	1.6

All of the fractions that contained polonium were then combined and evaporated to near dryness to concentrate the polonium and drive off the nitric acid. The residue was then brought up in 100 mL of 1M HCl in a volumetric flask. Aliquots of this solution

were mixed with Ultima Gold at a ratio of 1:15 and counted via standard off-line liquid scintillation counting for 1,000 minutes. The final working standard was determined to have an activity of 468 dpm/mL (± 3.7 dpm). Since ^{210}Po has a reasonably short half-life, the actual stock activity needs to be recalculated on a daily basis to correct for loss due to radioactive decay.

^{210}Po Observation: The first setting that requires optimization is ^{210}Po channel window setting so that only the ^{210}Po peak area is counted, minimizing background noise. 2500 µL of a solution of a known activity of ^{210}Po was mixed with cocktail at a 2:1 ratio and manually injected directly into the flow cell. The pulse hight analysis feature of the β-RAM was used to determine the spectral appearance of the ^{210}Po within the instrument. This spectrum is shown below in Figure 4.2.

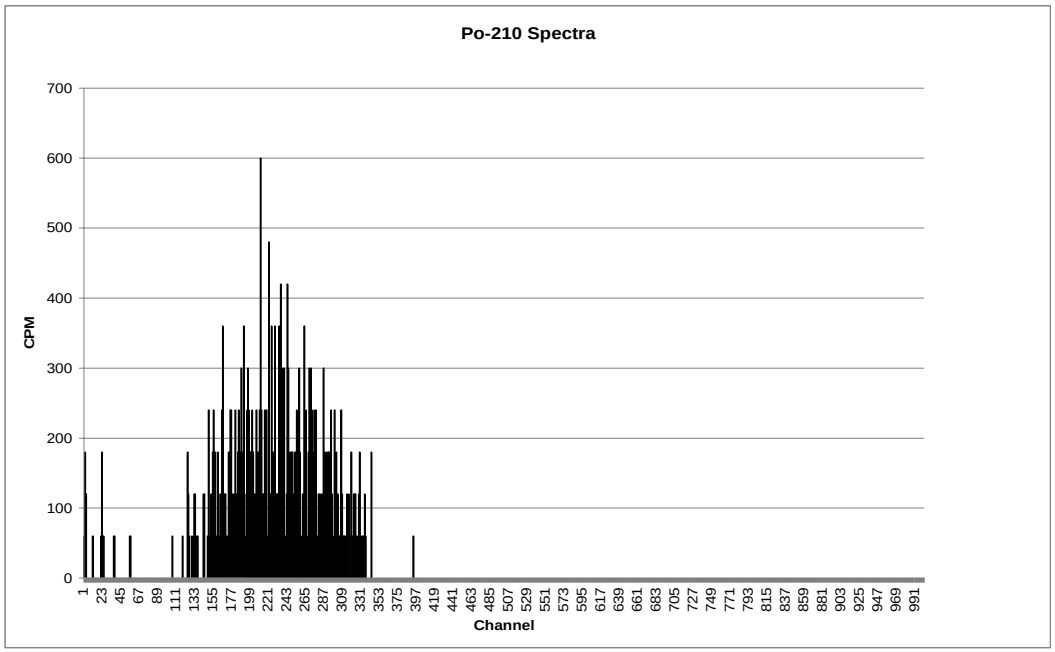

Figure 4.2: The spectral appearance of ^{210}Po within the β-RAM. Most of the signal occurs within channels 100-350.

While the optimum channel setting would appear to be with a window of 100-350 channels, there was significant loss of efficiency at this setting during actual runs. This may be due to increased quench occurring in actual samples. Extra quench may be present due to organic components of the column washing off and/or as a result of freshly mixed on-the-fly cocktail eluent solutions. Therefore, it was necessary to utilize a counting window of 0-350 channels to restore the desired counting efficiency.

In order to determine the time at which the ^{210}Po peak elutes from the column under the gradient scheme shown in Table 4.1, a test injection of the analyte was made. In this test, 936 dpm of ^{210}Po was injected with a volume of 2mL. Figure 4.3 shows the resulting chromatogram.

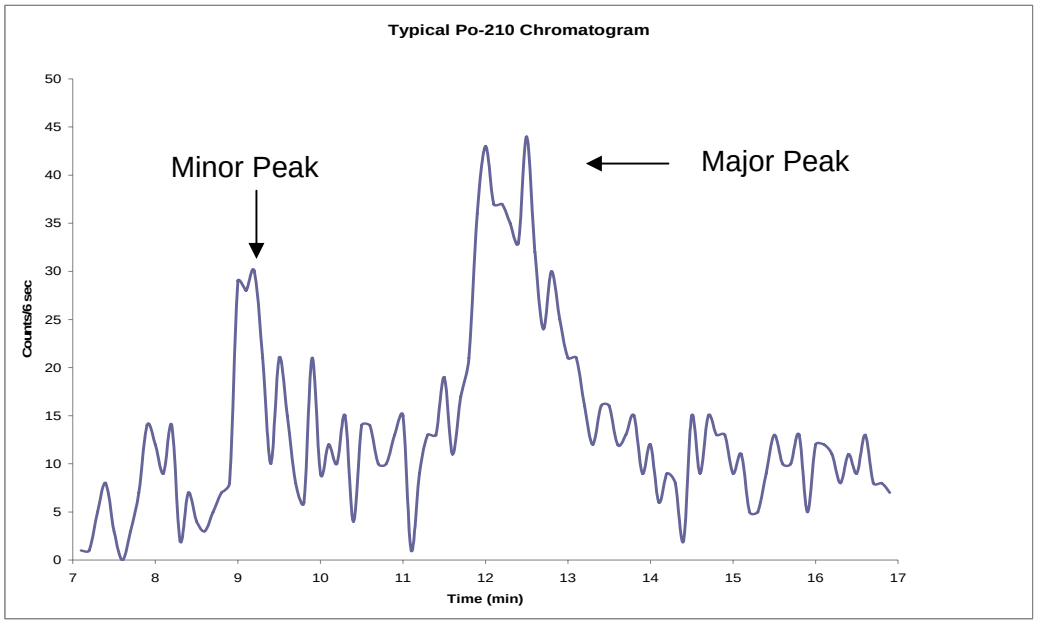

Figure 4.3: Sample chromatogram showing the ^{210}Po peak location. Note, that two distinct peaks occur. A minor peak at ~9 min. and the major peak at ~12 min.

The ^{210}Po peak occurs in two parts at approximately the 9 minute mark and the 12 minute mark. The persistent occurrence of two distinct peaks may be due to different complexes of the polonium with various matrix and solid phase constituents. While this situation is not ideal for optimum counting, the major peak can be targeted for analysis and allowances for the activity of the total polonium output can be accounted for by an efficiency correction. Thus, the flow of the system can be stopped at the 12.5 minute mark so that the peak maximum—and most of the total peak area—is within the flow cell during the stopped flow counting time.

Transient-Flow ^{210}Po Quantification: The polonium elutes from the column in a sample zone (or in this case, two sample zones), where it is mixed on-the-fly with scintillation cocktail at a specified ratio prior to entering the detector flow cell. The flow cell consists of a calibrated volume of optically transparent Teflon tubing that is placed within a fixed geometry between two photomultiplier tubes. Scintillations from the radiation are "seen" by the detector only when the sample zone present in the flow cell. Assuming that there is no secondary mixing in the flow cell, the residence time, t_r, of the eluted sample zone in the flow cell is described by:

$$t_r = \frac{V_c}{F} \tag{4.1}$$

where, V_c, is the volume of the flow cell and, F, is the combined flow rate of the eluent/cockatil mixture. For transient flow counting the peak area is summed and the background count for the area is subtracted to derive a net number of counts for the peak, C_n. The net CPM for the peak can then be determined by:

$$C_{CPM} = \frac{C_n}{t_r} \quad \text{(Transient-Flow)} \tag{4.2}$$

If a known activity of ^{210}Po is introduced to the system, the net count rate can be related to the sample activity, A_{dpm}, to determine the effective efficiency, E_{es} (which combines the efficiency of the separation and the detector).

$$C_{CPM} = E_{es} A_{dpm} \quad \text{(Transient-Flow)} \tag{4.3}$$

In this way, the figure of merit, FM, described by Knoll, can be determined for any given set of experimental conditions, allowing specific parameters to be optimized (Knoll, 1979).

$$FM = \frac{E_{es}^2}{B} \tag{4.4}$$

Counting Parameter Optimization: The effects of different loading and eluent solutions were studied to determine the optimum conditions for retaining and stripping ^{210}Po from the column. Previous works cite the optimum loading solution for polonium on the Sr-Sprec resin to be 2M HCl and the optimum strip solution to be 6M HNO_3 (Vajda, 1997, Vrecek, 2004). These concentrated strong acids can be detrimental to the life of the column and system parts. Therefore, we sought to determine the merit of using more dilute reagents in our work. Data relating to polonium behavior with Sr-Spec resin shows that polonium is not retained for very high and very low molarities of nitric acid (eichrom.com). After loading ^{210}Po on the column with 2M HCl, various strip reagents were applied to determine the optimum eluent. Solutions of 8M HNO_3, 6M HNO_3, 0.5 M HNO_3, 0.1M HNO_3, and water were used to strip ^{210}Po from the column. A plot of the resulting figures of merit for the peaks resulting from these experiments is shown in Figure 4.4.

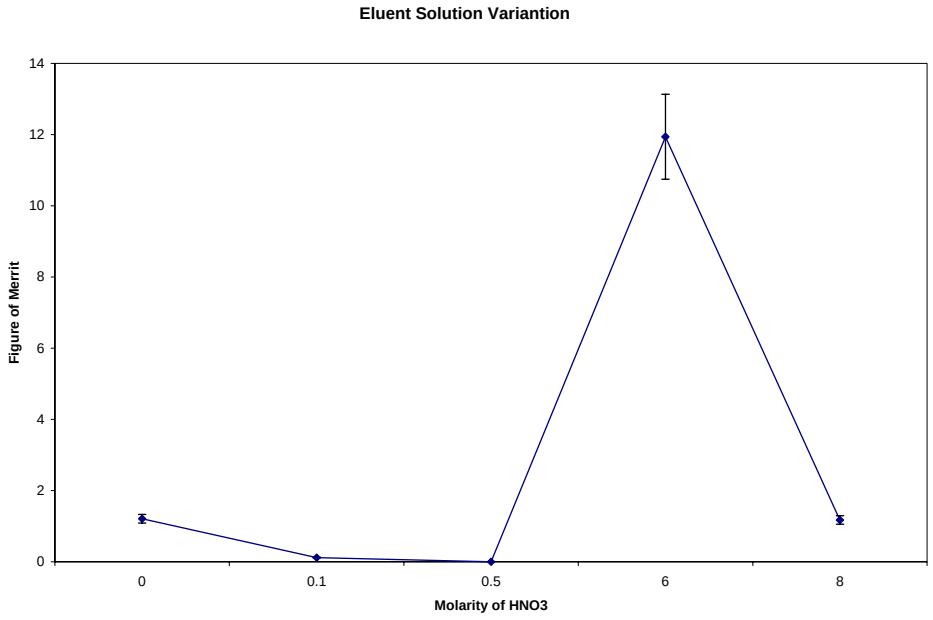

Figure 4.4: Figures of merit resulting from the ^{210}Po peak resulting from various eluents. The 6M HNO_3 strip solution is clearly the best reagent to remove polonium from the Sr-Spec resin.

The superior strip reagent is 6M HNO_3. While water was a better eluent than low molarities of nitric acid, it is significantly inferior to 6M HNO_3. It was, therefore, determined to continue using 6M HNO_3 as the eluent for all subsequent trails.

An unfortunate consequence of the gradient scheme is that the 2M HCl, used to load the ^{210}Po, is destructive to the stainless steel components and plastic seals of the on-line detector. It was, therefore, desirable to determine if a lower molarity of HCl or any molarity of HNO_3 (which is less destructive to the components concerned) could be used to effectively load the ^{210}Po onto the column. Columns were loaded with 0.5M HCl, 1M HCl, 0.5M HNO_3, 1M HNO_3, and 1.5M HNO_3 and stripped with 6M HNO_3 to determine the optimum loading reagent. A plot of the resulting figures of merit for the peaks resulting from these trials is shown in Figure 4.5.

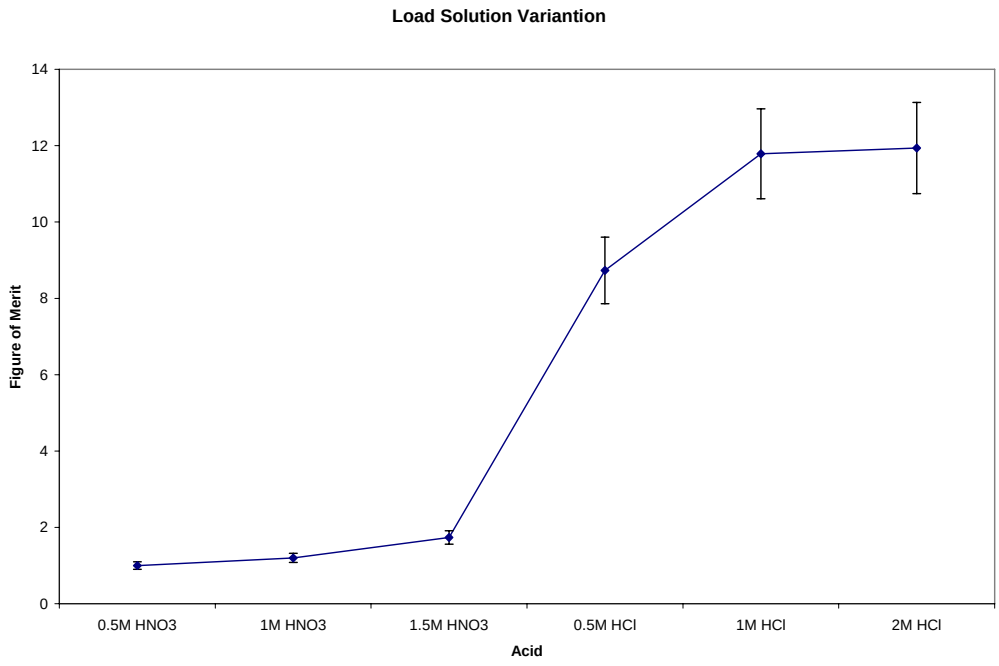

Figure 4.5: Plots of the figures of merit for the peaks resulting from various load solutions.

As expected, the greater the molarity of HCl that is used, the better the retention, and subsequent elution of polonium. While none of the nitric acid molarities can be recommended for use as a load solution, 1M HCl may be used effectively as a load solution. The use of 1M HCl over 2M HCl may result in an extension of the column life and a reduction of steel and plastic corrosion.

The best cocktail/eluent ratio must also be determined to optimize the ^{210}Po analysis. This was done by determining the ^{210}Po efficiencies resulting from cocktail/eluent ratios of: 1, 1.75, 2, and 3. Background activity values were also obtained for these ratios so that figure of merit could be determined. Figure 4.6 shows the results of these experiments.

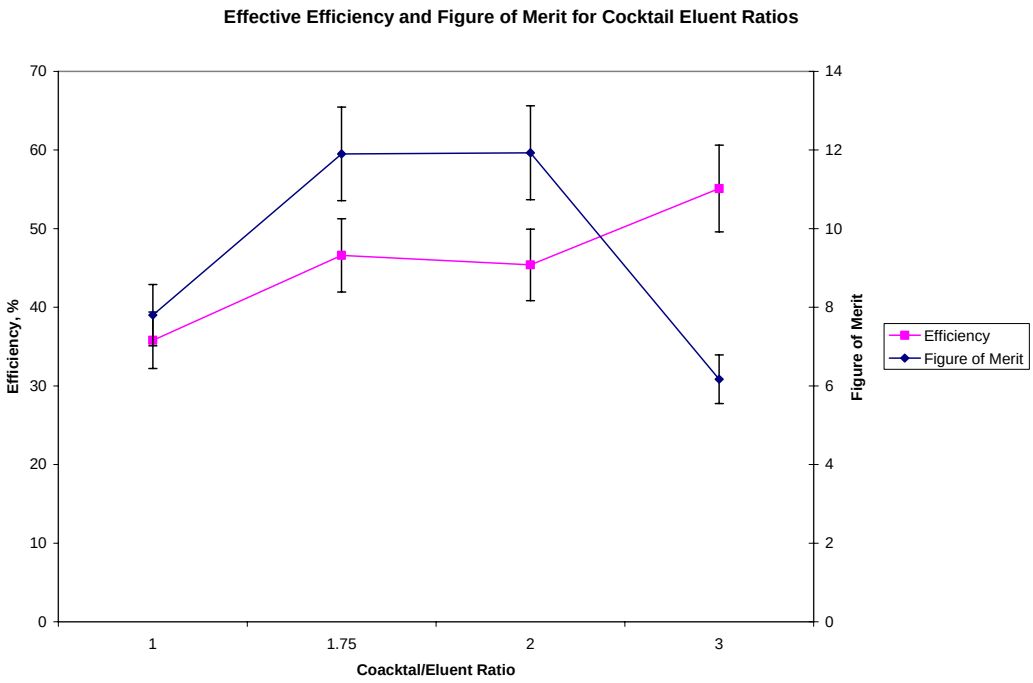

Figure 4.6: Plots of effective efficiency and figure of merit at peak maximum for various cocktail/eluent ratios. The optimum ratio is between 1.75 and 2.

The optimum cocktail/eluent ratio is between 1.75 and 2. The range is small and insignificant; either a ratio of 1.75 or 2 could be used effectively. The figure of merit resulting from higher or lower ratios drops quickly. It is interesting to note that while detection efficiency increases for a ratio of 3, the figure of merit depreciates due to the increase in background that also results.

Stopped-Flow ^{210}Po Quantification: The optimum counting conditions were utilized in the final stopped-flow counting experiments. Using the known position of the ^{210}Po peak, flow could be stopped at the peak maximum point and held indefinitely in the flow cell for counting. For the purposes of this research a stopped-flow counting time of 30 minutes was used to collect enough counts for low level ^{210}Po determination. A background count was conducted to determine the average background activity and the

standard deviation of this activity. To demonstrate the principle of stopped-flow counting, a plot of identical traces are shown via transient-flow and stopped-flow in Figure 4.7.

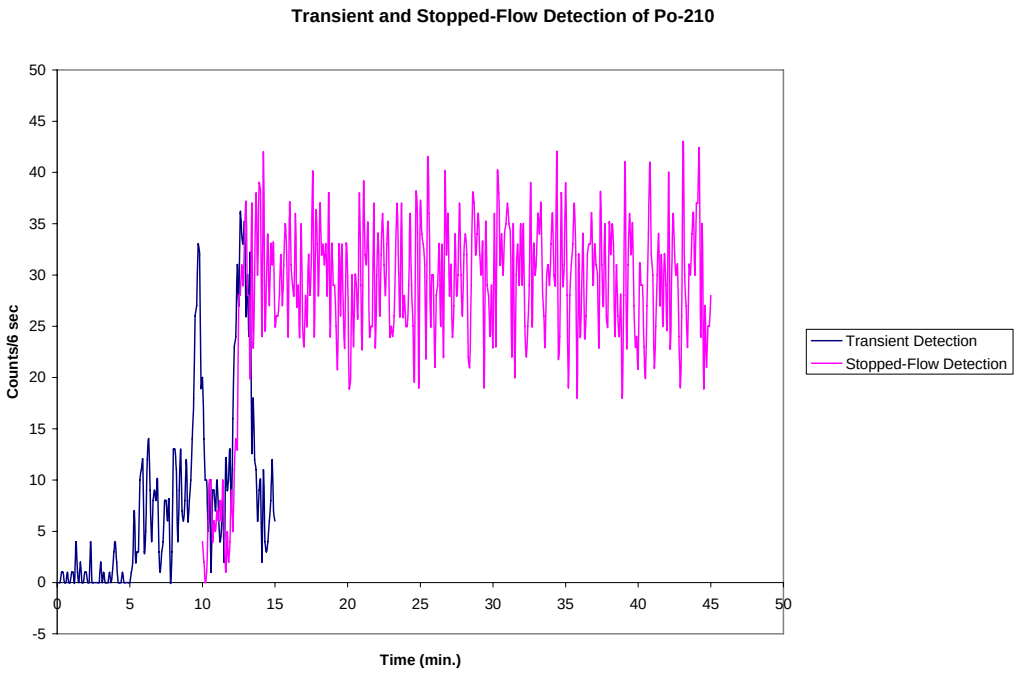

Figure 4.7: A trace of ^{210}Po as determined by transient-flow counting and by stopped-flow counting.

Assuming no secondary mixing or phase separation effects in the flow cell, the fraction of the sample zone present in the flow cell at the peak maximum, D_m, can be determined using transient-flow conditions and the following equation:

$$D_m = \frac{C_{\max} t_r}{t_i C_n} \tag{4.5}$$

where, C_{max}, is the number of net counts per update time at peak maximum and, t_i, is the detector update time. Using the value determined from D_m, a sample of known activity

may be run using stopped-flow counting to determine the effective efficiency of the technique. Once D_m and E_{es} are determined, samples of unknown activity may be counted and the resulting values of CPM can be related back to an activity. In this work, D_m was determined to be 0.068 (± 0.003) and E_{es} was 0.615 (± 0.07).

$$C_{CPM} = D_m E_{es} A_{dpm} \quad \text{(Stopped-Flow)} \tag{4.6}$$

The usefulness of transient-counting methods for radionuclide determination is limited to samples with relatively high activities (>500 dpm) due to the uncertainty introduced by the low number of counts observed. Radiation counting errors are proportional to the square root of the number of decay events, assuming Poisson statistics, and therefore increase dramatically with a low number of observed counts. One can reason that increasing the residence time of the sample in the flow cell will reduce uncertainties and improve sensitivities, since more counts will be observed. Therefore, by stopping the flow of the system while the peak maximum is in the detector, sample residence time can be increased indefinitely to accumulate as many counts as desired. The results are lower detection limits and reduced uncertainty in the results.

Various levels of ^{210}Po activity were injected into the system to determine if these levels register an average activity that is more than 3 standard deviations from the background count rate of 2.2 (± 0.22) CPM . The results are shown in Figure 4.8.

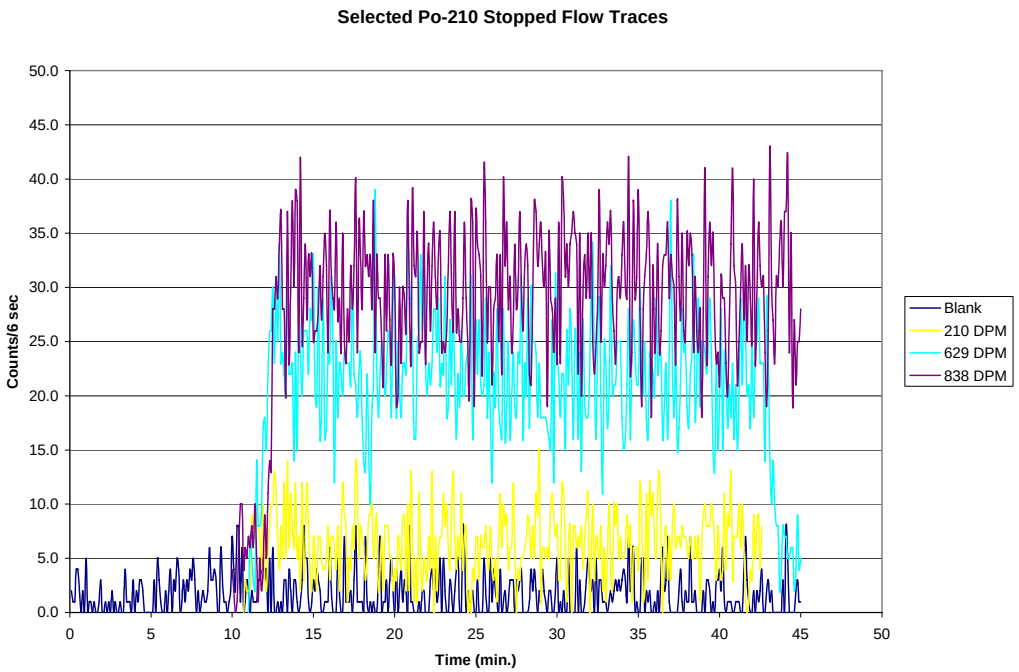

Figure 4.8: Various activities of ^{210}Po determined by stopped-flow counting. While not shown for clarity, a trace of 104 DPM registered an average CPM of 4.2.

Given the efficiency, peak fraction, and background level, the limit of detection, L_D, was determined to be 8 DPM of ^{210}Po per sample. The limit of quantitation, L_q, was determined to be 84 DPM.

Finally, a plot was made to show the calibration curve of the detector and its response to various levels of ^{210}Po. This plot is used to determine if there are any non-linear effects in the detector response that would cause detection limits to deviate from theoretical values. This plot is shown in Figure 4.9.

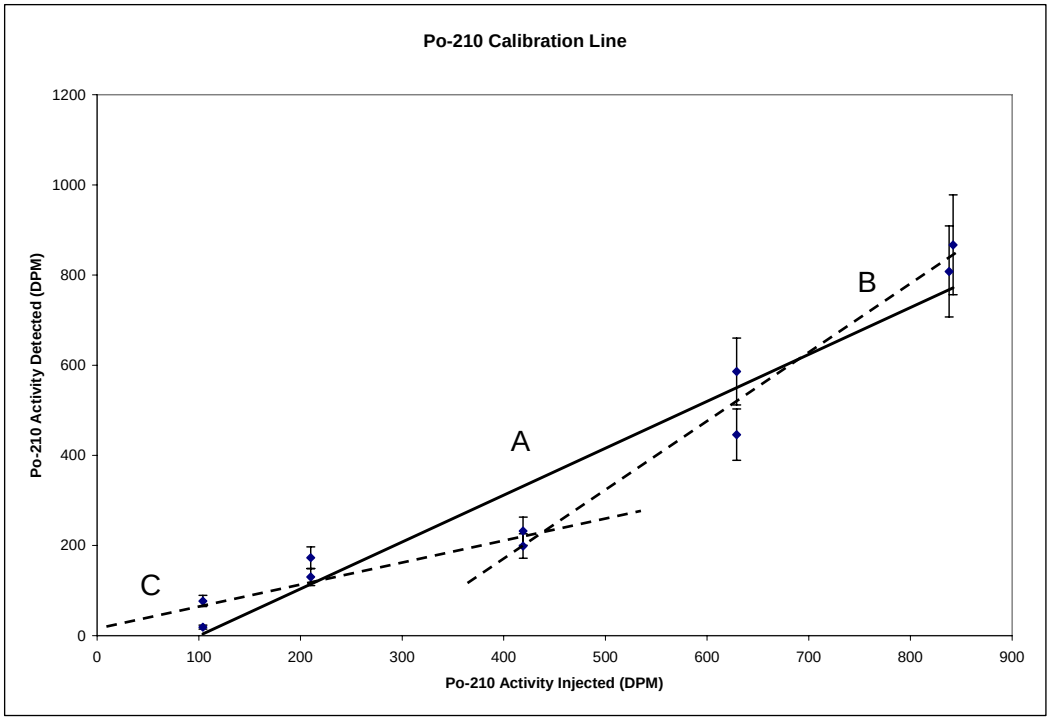

Figure 4.9: A calibration curve of detector response to various levels of ^{210}Po activity as determined by stopped-flow counting. Non-linear detector responses seem to persist for activities of < 400 DPM. Three possible trendlines are shown. A) Includes all points, y = 1.0398x -104.24, R^2 = 0.93. B) Includes activities >400 DPM, y = 1.4781x -407.2, R^2 = 0.9702. C) Includes activities <400 DPM, y = 0.5002x +16.1, R^2.

There is a definite non-linear appearance to the distribution of the calibration curve, indicating that the detector is biased to low values for the range of activities studied. This not a surprising result, given that the FSA is an instrument that is designed for radiolabeling experiments, where activities are typically in the range of nCi-mCi (2,200 to 2.2 x 10^9 dpm) per sample. The main trendline, shown in Figure 4.9, includes all the data points and is within one standard deviation of all activities tested, except for those with an activity of 419 DPM. In an effort to better model the detector response, the calibration curve can be broken into two parts. In Figure 4.9, line B, models activities >400 DPM well. Line C models activities <400 DPM. The failure of the total data to be

linear may be indicative of two competing processes that are introducing systematic error in the detector, one that is most prevalent for higher activities and one that dominates at lower activities. The factors that influence this behavior is presently unknown to the authors, however, we believe that results from samples within the activity range studied are still valid, given proper consideration of the identified biases. Given the evidence of the system bias, we recommend revising the limit of quantification upward to 100 DPM per sample.

Urine Bioassay: Finally, the optimized counting techniques were applied to the urine bioassay samples to determine the effects of the urine matrix on the anticipated results. Two samples were run with the results of this trial shown in Table 4.3.

Table 4.3: Dilute urine bioassay results. The bias corrected activities of the samples are shown with their determined recoveries. Both sample recoveries are within one standard deviation of expected values. For the 10x dilution with 417 DPM, calibration curve C was used to correct for the bias. For the 5x dilution with 500 DPM, calibration curve B was used.

U. DIL.	A (dpm)	DETERMINED A (dpm)	BIAS CORRECTED A (dpm)	RECOVERY, %
10x	417	228 (± 31)	424 (± 57)	102 (± 14)
5x	500	353 (± 45)	514 (± 66)	103 (± 13)

Recoveries were excellent for the two urine samples once the bias corrections were applied. This indicates that the discontinuous calibration curve theory has merit and that good results can be obtained from its use in aqueous and dilute urine matrices. One important point to note is that a shift in the peak position occurred for the 5x dilute urine sample. The peak maximum was shifted from the expected 12.5 minute mark to 14.2 minutes. More work needs to be done to determine if there is any consistent peak

shifting for a range of urine concentrations. In addition more work is needed to determine any effects of more concentrated urine matrices on polonium recovery.

CONCLUSIONS

An automated computer controlled system for the separation and simultaneous detection of ^{210}Po was created and optimized for aqueous samples. A method of ^{210}Po recovery from well-aged ^{210}Pb solutions was detailed. Obtaining ^{210}Po from ^{210}Pb is an easy and convenient way of maintaining a stock of ^{210}Po without having to be concerned with significant decay of the stock activity over time. A loading and elution protocol was developed and optimized for acid concentration to permit effective loading and elution of ^{210}Po. Cocktail/eluent ratios were also optimized to obtain results with the best figures of merit. An optimal counting window for ^{210}Po with the β-RAM flow scintillation analyzer was also established. A calibration curve of detector response to various low activity samples was plotted and a non-linearity in the curve was noted. A discontinuous calibration curve was deemed to be the best fit for the data. Detector biases for activities above and below 400 DPM were identified. The system allows for quantification of ^{210}Po in samples with at least 100 DPM of activity, using the stopped-flow counting technique and a 30 minute count time. The time for total analysis and column washing and reconditioning was 60 minutes. While no experiments were performed in this work to determine column longevity, we believe that a column life of 10 cycles, as determined elsewhere, can be recommended here (Vajda 1997; Vreček 2003). The feasibility of analysis of ^{210}Po in dilute urine matrices was also briefly examined, with encouraging results. Much more work is needed to study the method efficacy for urine analysis of ^{210}Po and to optimize counting parameters.

Chapter 5: Flow Gamma Analysis of ^{60}Co and ^{137}Cs

An automated method for the determination of ^{60}Co and ^{137}Cs in aqueous samples by a new technique, called flow gamma analysis (FGA) was examined. This new technique detects the activity of gamma-emitting nuclides in a flowing system with a NaI(Tl) detector. FGA is closely related to the similar method of flow scintillation analysis (FSA), which was also used in this work to determine ^{60}Co and ^{137}Cs. By employing high performance extraction chromatography (HPEC) to separate the analytes from the sample matrix and carry them to a flow cell, they can be counted by gamma spectroscopy. The all-in-one system would enable the separation of certain gamma-emitting nuclides from matrix constituents and possible interferences by using columns filled with extractive chromatographic resin. In this work, Eichrom's Sr-Spec resin (which cobalt and cesium have not affinity for) was used to clean up the sample stream prior to gamma counting. While the advantages of removing Sr, Po, and certain actinides has negligible effect on the effectiveness of ^{60}Co and ^{137}Cs determination by gamma counting, there are several scenarios where it may be of interest to remove these gamma emitters to facilitate ^{90}Sr, ^{210}Po, and actinide determination by other methods. To this end we have examined the feasibility of ^{60}Co and ^{137}Cs detection by FGA. We also examined FSA as a method for low-level ^{60}Co and ^{137}Cs determination with applications to bioassay. Advantages to this method over traditional methods of bioassay gamma analysis include rapid quantification, and simplified batch sample processing. Disadvantages of the technique as it is currently developed include high detection limits and poor energy resolution. These disadvantages may be mitigated by future work that would continue to optimize the detector setup and counting parameters.

INTRODUCTION

Many gamma-emitting radionuclides are formed as byproducts of nuclear power generation, and weapons production. Two of the most significant gamma-emitting isotopes are ^{60}Co and ^{137}Cs because these nuclides are produced in relatively large quantities and have relatively long half-lives. ^{60}Co is a β/γ emitter with a half-life of 5.27 years (β_{max} = 317.88 keV, γ_1 = 1173.24 keV, γ_2 = 1332.5 keV) that produces two energetic gamma rays with each disintegration, decaying into stable ^{60}Ni (KAPL 2002). ^{137}Cs is also β/γ emitter with a half-life of 30.07 years (β_{max} = 514 keV, γ = 661.66 keV) that produces one energetic gamma ray in 94.4% of its transitions as it decays to ^{137m}Ba which emits the 662 keV gamma ray with a half-life of 2.55 minutes as it transitions to stable ^{137}Ba (KAPL 2002).

In addition to being found in nuclear waste streams, these isotopes have found wide-spread uses in medicine and industry. Curie-level quantities of ^{60}Co and ^{137}Cs are used as radiation therapy sources, sterilizers for food and medical equipment, x-ray machine, thickness gauges, and to check pipe welding. Because of the availability of high-level sources of these isotopes, there is great concern for public health if there should be an industrial accident or terrorist event involving these isotopes.

Recent history has already witnessed the devastating effects of an accidental release of ^{137}Cs from a discarded teletherapy source in Goiania, Brazil in 1987. Members of the public who tried to salvage the medical equipment unknowingly ruptured a vessel containing approximately 1400 Ci of ^{137}Cs and spread its contents among friends and family members, causing some of them to become sick with radiation poisoning. About 112,000 people were sequestered in the Olympic stadium and surveyed with hand meters; 250 were identified as contaminated, 50 of which were further monitored, including 20 that were hospitalized, of which 4 died as a result of their exposure (IAEA 1998). Both

whole body in vivo counting and in vitro counting of patient excreta were done assess internal uptake and Prussian Blue (ferric ferrocyanide) was administered to some patients to enhance elimination.

Because of the potential for future accidental releases or the intentional terrorist use of a radiological dispersal device (RDD) involving ^{60}Co or ^{137}Cs, there would be great usefulness for a rapid urine bioassay method capable of detecting these radionuclides. To this end, we have examined the feasibility of using a new technique, called flow gamma analysis (FGA) to separate ^{60}Co and ^{137}Cs from the urine matrix and simultaneously detect these nuclides using a flow-through NaI(Tl) detector. This system would be capable of processing large batches of urine samples and providing rapid results, while preserving the gamma-emitting analytes for further analysis.

Existing methods of determining gamma-emitting nuclides in urine bioassays involve placing urine samples into vessels of standardized geometries for which backgrounds and efficiencies are well characterized; where the best sensitivities are achieved by evaporating 24-hour void samples down to small volumes or residues (AEC 1971; Rich 1990). Since the gamma rays emitted by ^{60}Co and ^{137}Cs are not significantly attenuated by the urine residue or high concentrations of salts, it is feasible to maximize counting efficiency by condensing large samples. However, the process of evaporating a 24-hour void (Reference Man 24-hour urine void is 1440 mL (Cember 1996)) is slow, since boiling of the samples during evaporation is avoided. While counting of the 24-hour void in its entirety is possible, counting efficiency is sacrificed and no further analysis on the urine can be done while the sample is counted.

Therefore, it would be advantageous to have a method that could accomplish a rapid preliminary analysis of a small sample of uncondensed urine to aid in triaging patients by identifying those with the most activity in their urine. This may be

accomplished by FGA. Due to the fact that the flow cell size and its placement with respect to the detector are constant, the counting geometry is fixed and variable amounts of sample can be counted without compromising the known counting parameters.

Detection of gamma-emitters in a flowing system has been previously accomplished by various scintillation methods. This is typically accomplished by using specialized counting flow cells, e.g., Cerenkov, BGO (Anonymous 1995), CaF_2 (Anonymous 1995), and PET (Takei 2001). Homogeneous liquid flow cells have also been used to detect various gamma emitters(Fjeld 1995; Desmartin 1997; Egorov 1998b). However, these systems often employ only rudimentary multi-channel analysis, capable of discriminating between up to two radionuclides, whose gamma emission energies are well separated. These methods instead rely on chromatograms and previous knowledge of chromatographic behavior of analytes to determine the identity of an observed peak. This precludes most types of multi-isotopic analysis when two or more analytes co-elute. This is the case with ^{60}Co and ^{137}Cs and the Sr-Spec resin; neither analyte has any affinity for the resin and so they both elute with the passing of the sample zone through the column and are thus unresolvable chromatographically (Horwitz 1992b).

An instrument capable of performing more sophisticated multi-channel analysis is needed to be able to discriminate between ^{60}Co and ^{137}Cs based on gamma emission energy rather than chromatography. NaI(Tl) detectors are able to accomplish such energy discrimination. The full-with-half-max of a typical NaI(Tl) detector at the ^{137}Cs emission peak, 662 keV, is approximately 56 keV (Friedlander 1981). While this resolution is worse than that of a typical germanium detector by a factor of 30, it is nonetheless suitable for our goals of resolving ^{60}Co and ^{137}Cs (Kahn 2007).

Flow NaI(Tl) counters are available commercially and are primarily utilized in the pharmaceutical and biotechnology fields for counting radio-labeled compounds.

However, the activities of radio-labeled compounds that are typically used in these applications is on the order of mCi, which is much high than levels that would be found urine bioassays of even those with lethal uptake of ^{60}Co or ^{137}Cs. Therefore, it is uncertain if a flow gamma detector that was designed for use with radio-labeled compounds can be used for much lower activity urine bioassay samples. In addition, these instruments are built for chromatographic purposes and function as gross gamma counters with the advantage of improved counting efficiency. Therefore, it was necessary to modify one of these instruments with an after market amplifier and multi-channel analyzer to convert the gross gamma output signal from the detector into a signal that could create a gamma energy spectrum.

In this paper we describe the modification of a commercially available flow gamma counter into one that can be used to obtain a gamma spectrum of analytes as they travel through the flow cell. The purpose of utilizing a Sr-Spec chromatography column with these analytes is to show analysis of ^{60}Co and ^{137}Cs may be performed in conjunction with the previously described ^{90}Sr and ^{210}Po determination by FSA. We also examined the possibility of determining ^{60}Co and ^{137}Cs by FSA to detect the associated beta particles of these analytes. While, transient-flow counting was the method of flow analysis used in the experiments presented in this paper, stopped-flow counting may also be used to achieve better detection limits for these analytes (Grate 1996; Egorov 1998b; Grate 1999b).

EXPERIMENTAL

High Performance Extraction Chromatography System: A Dionex GP50 gradient pump (Dionex, Sunnyvale, CA) was configured with a Rheodyne 7725i dual mode analytical injector and a 2000 µL sample loop (Precision Flow Products, Lake Elsinore, CA). A 2500 µL Gastight syringe (Hamilton Co, Reno, NV) was used to inject samples

into the loop. Sr-Spec resin (EIChroM Industries, Inc., Darren, IL) of bead size 50-100 μm was slurried overnight with deionized water (18 MΩ..Nanopure Water System, Barnstead, Dubuque, IA) and packed into one of two PEEK lined columns, 4.6mm I.D. x 30mm or 150mm, hardware (Alltech Associates, Deeerfield, IL) using an Alltech Model 1666 slurry packer. The packing pressure was 1000 psi and the calculated volume of the resin was 0.499 mL for the 3cm columns, and 2.49 mL for the 15cm columns. Samples were loaded with 1 mL/min of 8M HNO_3 and were not retained by the resin. The column effluent was either fed directly into the FGA for gamma counting or mixed with scintillation cocktail at a 2:1 scintillatior/eluenet ratio.

On-Line Liquid Scintillation Counting: Flow scintillation analysis was accomplished using a β-Ram 4B (IN/US Systems Inc., Tampa, FL). This model possesses an internal cocktail pump and can be fitted with flow cells of various types and sizes. All experiments in this work were done using a 2500 μL liquid flow cell. The device was configured with the HPEC so that the column effluent was mixed with the scintillator in controllable ratios. The detector counting parameters were controlled using Scint Flow SA software (IN/US) and Laura Lite 3.4 (IN/US) run on desktop PC and connected to the detector by a serial port. The detector was signaled to begin cocktail flow and counting by a closed contact connection to the analytical injector when it was turned to the "inject" position. The detector integration time, t_i, was 6s to allow enough counts to accumulate for each data point.

Flow Gamma Counting: A tandem NaI(Tl) gamma counting unit was obtained from (IN/US Systems) and interfaced to function with the support of our β-Ram 4B as the intelligent front end of the system. The tandem gamma counter consists of a Bicron (Saint-Gobain Crystals, Newbury, OH) well-type thallium-activated NaI detector. The crystal dimensions were 1.5" dia. x 2" long with a well of approximately 5/8" dia. x 1.5"

deep. This detector was optically coupled via a quartz light-guid to a 1.5" dia. PMT. The thickness of the aluminum casing on the well was 0.005" to permit maximum penetration of low-energy gamma rays. The detector was placed within a single piece of formed lead shielding (~35 lbs.) that was approximately 4" x 4" with a 2" dia. hole cut in the center to accommodate the detector. The detector comes in a casing with its in-house high voltage supply and pre-amplifier. The detector out put is intended to connect to the β-Ram 4B, where the signal is processed as a gross gamma count. Instead, the detector output signal was split, with one end going to the β-Ram 4B and the other end going to an after market amplifier and multi-channel analyzer. The amplifier used was an Ortec (Ortec, Oak Ridge, TN) positive NaI detector interface module (DIM). This was connected to an Ortec DSpec Pro multi-channel analyzer. Typical counting parameters were a high voltage setting of 600 V, a rise time of 6 μs, and 1024 channels. Acquisition and analysis were performed using Maestro 32 v. 6.05 MCA Emulator (Ortec). The detector was energy calibrated using a mixed ^{60}Co and ^{137}Cs. The detector was periodically re-calibrated and pole-zeroed when the peak position drifted.

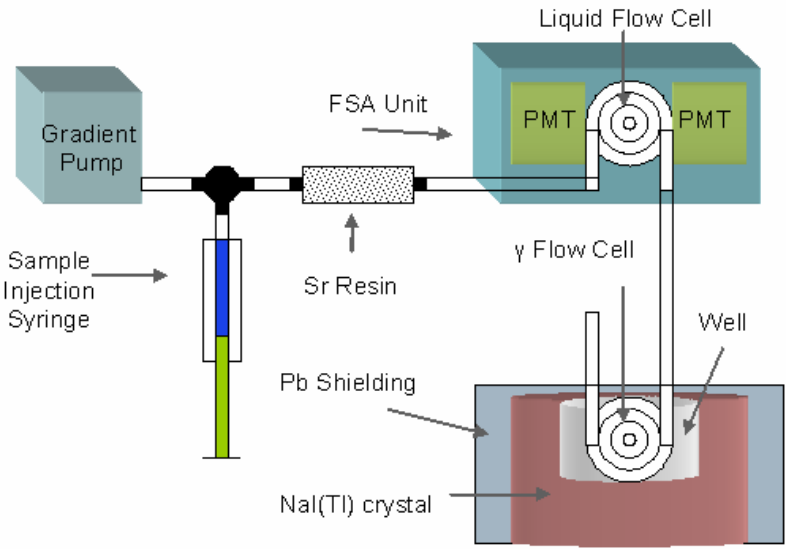

Figure 5.1: Block diagram of the FSA and FGA units.

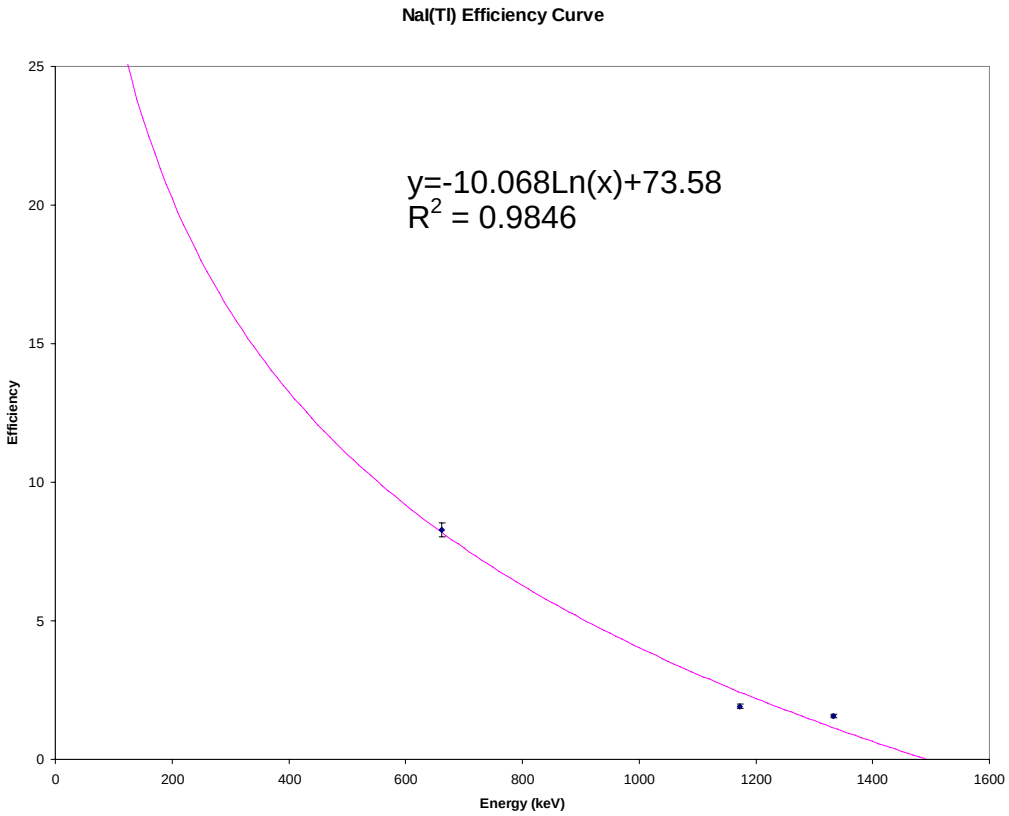

Figure 5.2: NaI(Tl) efficiency curve.

Detector background was established by performing a 1000 minute count with no source present in the well and noting background counts in the regions of interest (ROIs) that were previously established for ^{60}Co and ^{137}Cs. Net counts for each peak were determined by averaging the counts in 4 channels to the left and right of the peak continuum and subtracting this average count per channel from the peak ROIs. An efficiency curve (Figure 5.2) for the detector was determined by placing known activities of in-house ^{60}Co and ^{137}Cs liquid standards in the flow cell and counting for 30 minutes in the fixed flow cell geometry. The typically encountered efficiencies for a 1750 µL

geometry were 8.28% for the 662 keV ^{137}Cs γ, 1.92% for the 1173 keV ^{60}Co γ, and 1.56% for the 1332.5 keV ^{60}Co γ. Figure 5.3 shows a 200 μL gamma flow cell.

Figure 5.3: 200 μL gamma flow cell. The sample flows in one end and out the other. The metal spacer ensure that the flow cell is positioned within the well of the NaI(Tl) counter. Larger cells may also be accommodated.

Reagents and Standards: All chemicals used were analytical grade. Deionized water was used in all dilutions. A low-viscosity liquid scintillation cocktail (In-Flow 2:1, IN/US) was used for all flow scintillation measurements because this cocktail can be mixed with eluents at low ratios without gelling. Ultima Gold LLT (Packard) cocktail was used for all off-line liquid scintillation counting. Standard ^{60}Co and ^{137}Cs solutions were prepared by evaporating aliquots of in-house standards to dryness and dissolving the residue in measured volumes of 8M nitric acid.

RESULTS AND DISCUSSION

^{60}Co and ^{137}Cs Chromatography Observation: Individual high activity samples of either ^{60}Co or ^{137}Cs were injected into the syringe port and loaded onto the Sr column with 1mL/min 8M nitric acid for 10 minutes. The column effluent was mixed with scintillation cocktail at a scintillator/eluent ratio of 2:1 to detect beta particle activity. Because the β_{max} energy of ^{60}Co and ^{137}Cs (318 keV and 514 keV) are similar to that of ^{90}Sr (546 keV), a previously established ^{90}Sr counting window of 0-600 channels was used to observe these isotopes. This experiment allowed us to determine the peak position and form of the ^{60}Co and ^{137}Cs elution; samples are shown in Figure 5.4. Both ^{60}Co and ^{137}Cs peaks can be found entering the flow cell approximately 3.5 minutes after sample injection; a finding that is consistent with no significant retention on the column. However, ^{60}Co peaks were generally somewhat broader than ^{137}Cs, indicating that cobalt may have some minimal interaction with the resin. Since ^{60}Co and ^{137}Cs effectively co-elute from the column, there is no way to resolve these peaks chromatographically using FSA. However, discrimination by gamma spectroscopy is possible.

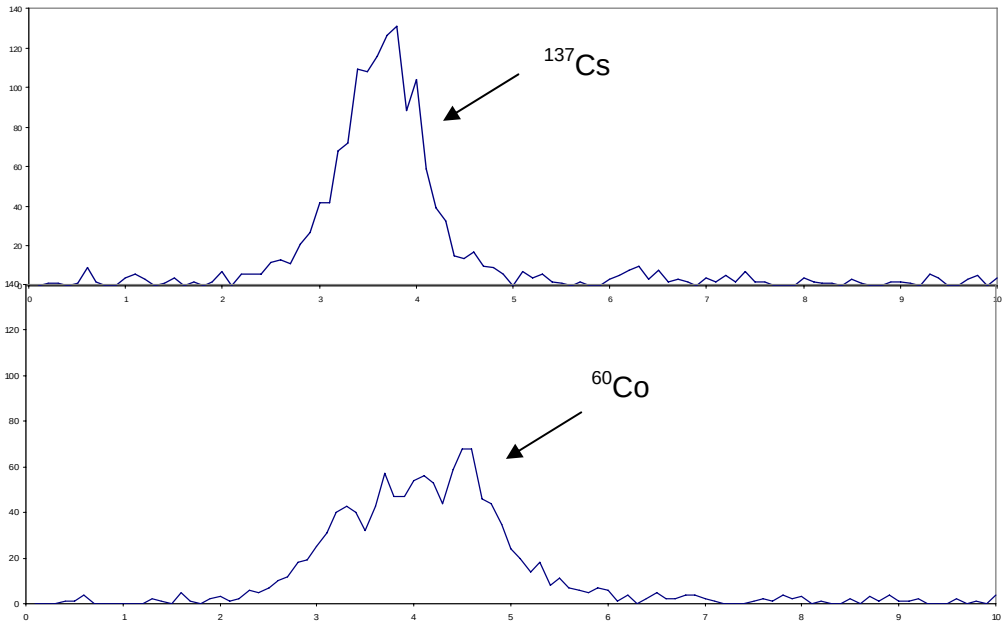

Figure 5.4: Detector traces of ^{60}Co and ^{137}Cs observed by FSA. 2170 dpm of ^{137}Cs and 1662 dpm of ^{60}Co both elute approximately 3.5 minutes after injection. ^{60}Co peaks were generally somewhat broader than ^{137}Cs peaks.

Static ^{60}Co and ^{137}Cs Gamma Spectrometry Observation: Gamma spectroscopy by NaI(Tl) is able to resolve the γ-ray emissions of ^{60}Co and ^{137}Cs by γ energy discrimination because the associated gamma peaks are well-separated. Figure 5.5 shows a typical gamma spectrum of a source that contains both ^{60}Co and ^{137}Cs. The observed ^{137}Cs peak occurs at an energy of 662 keV and has a full-with-half-max (FWHM) of 68 keV, while the 1173 and 1332 keV ^{60}Co peaks have FWHM of 78 and 90 keV respectively. These peaks did drift from their energy calibrated locations from day to day and needed to be recalibrated regularly. This is presumably due to drift in the high voltage, which can significantly affect the peak channel position for a NaI(Tl) detector (Knoll 2000). Figure 5.5 shows the γ-ray peak position and shape for a mixed ^{137}Cs/^{60}Co source.

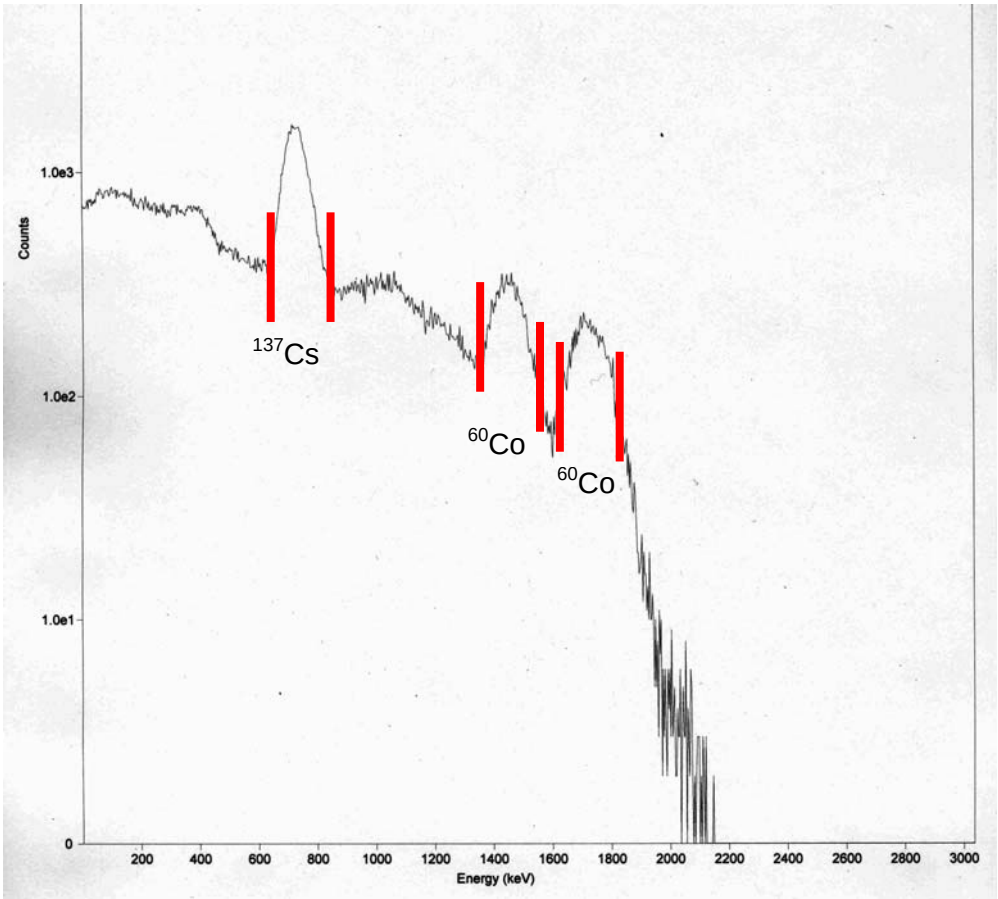

Figure 5.5: The γ-ray energy spectrum of a mixed $^{137}Cs/^{60}Co$ source. Regions of interest (ROIs) are bounded by red lines.

The established ROIs for the ^{60}Co and ^{137}Cs peaks were observed during a 1000 minute background count that was conducted with no sources present in the detector. The ROIs were integrated in for background spectra to determine the number of background counts that can be expected for each ROI. By applying the efficiency calibration of each isotope (efficiency curve reported in Figure 5.2) to the background cpm in each ROI, we determined the background dpm for each γ-ray. The results of these calculations are shown in Table 5.1.

Table 5.1: Background activity for ^{60}Co and ^{137}Cs.

GAMMA E. (keV)	BKGND (cpm)	EFF. (%)	BKGND A (dpm)
662	29.8 (± 0.2)	8.28 (±0.3)	360 (± 13)
1173	8.78 (± 0.09)	1.92 (±0.06)	457 (±15)
1332.5	4.66 (± 0.07)	1.56 (± 0.05)	299 (± 11)

From these background activity rates, we can determine the critical limit, and limits of detection and quantification for static counting of these isotopes for this detector. These limits a shown in Table 5.2 for a hypothetical 30 minute count time.

Table 5.2: Critical, detection, and quantification limits for a 30 minute count of a ^{60}Co or ^{137}Cs source, using the NaI(Tl) detector.

GAMMA E. (keV)	L_C (dpm)	L_D (dpm)	L_Q (dpm)
662	28 (± 1)	59 (± 2)	192 (± 7)
1173	66 (± 2)	136 (± 4)	495 (±16)
1332.5	59 (± 2)	123 (± 5)	480 (± 18)

Transient Gamma Counting of ^{60}Co and ^{137}Cs: The ultimate goal of developing a flow gamma analysis system is to detect ^{60}Co and ^{137}Cs flowing system. This is an inherently more difficult detection problem than static gamma counting because the radioactive sample zone has only a limited time that it can be "seen" by the detector as it passes through the flow cell. Assuming that there is no diffusion of the sample zone in the flow cell, the residence time, t_r, of the eluted sample zone in the flow cell is described by:

$$t_r = \frac{V_c}{F} \tag{5.1}$$

where, V_c, is the volume of the flow cell and, F, is the combined flow rate of the eluent. In this work, 200 and 1750 μL flow cells were used with an eluent flow rate of 1mL/min. Therefore, the residence time used in all calculations is 12s for the 200μL flow cell and 105s for the 1750μL flow cell. We attempted to collect both chromatographic information, using the tandem gamma detector for its intended purpose, and to collect spectral information, using the modified detector output. Collecting chromatographic data proved impossible for the low activity levels utilized in these experiments. This was mainly due to the very high background gross gamma count rate of the NaI(Tl) that the chromatography measurement uses. These backgrounds were typically on the order of 8,000 cpm because counts of any energy were registered.

The γ-ray energy spectra were also of limited use. This was due to the fact that only minimal counts were registered in the ROIs during the short residence time of the sample zone. Using the background ROI count rates, isotope efficiency information, and flow cell residence times, we can determine the limits of detection for ^{60}Co and ^{137}Cs for different sized flow cells. These data are shown in Table 5.3. These limits assume a 1mL/min eluent flow rate. It is not supprising to see that as the flow cells get larger, detection limits for ^{60}Co and ^{137}Cs are lowered. Nevertheless, these detection limits are still higher than is desirable for bioassay monitoring. Better data may be obtained by utilizing a larger NaI(Tl) detector (3" diam. x 3" crystal) to improve the γ-ray detection efficiency. Also, the addition of more Pb shielding for the detector would improve detection limits by lowering the background count rate.

Table 5.3: Detection limits for transient-flow counting of a ^{60}Co or ^{137}Cs samples, versus different flow cell volumes for the NaI(Tl) detector.

GAMMA E. (keV)	200 μL (DPM)	1750 μL (DPM)	2500 μL (DPM)
662	2026 (± 67)	539 (± 18)	440 (± 15)
1173	6032 (± 177)	1408 (± 41)	1134 (±33)
1332.5	6353 (± 258)	1370 (± 56)	1092 (± 44)

Transient-Flow Quantification of ^{60}Co and ^{137}Cs by FSA: Having failed to achieve lower detection limits for ^{60}Co and ^{137}Cs by FGA, we turned to FSA as an alternative detection method for these isotopes. As was previously shown, samples containing both ^{60}Co and ^{137}Cs cannot be resolved into their isotopic composition by this method. However, if there is previous knowledge that the sample contains either only ^{60}Co or only ^{137}Cs, then this method may be used to quantify the isotope in question.

In this work, a 2500 μL flow cell was used with a combined scintillator/eluent flow rate of 3mL/min. Therefore, the residence time used in all calculations is 50s. For transient flow counting, the peak area is summed and the background count for the area is subtracted to derive a net number of counts for the peak, C_n. The net CPM for the peak can then be determined by:

$$C_{CPM} = \frac{C_n}{t_r} \quad \text{(Transient-Flow)} \qquad (5.2)$$

If a known activity of ^{60}Co or ^{137}Cs is introduced to the system, the net count rate can be related to the sample activity, A_{dpm}, to determine the effective efficiency, E_{es} (which combines the efficiency of the separation and the detector).

$$C_{CPM} = E_{es} A_{dpm} \quad \text{(Transient-Flow)} \qquad (5.3)$$

Using the above relations, we can create a calibration curve for the detector and analyte of interest by injecting various ^{60}Co or ^{137}Cs activities and plotting the resulting net peak areas, see Figures 5.6 and 5.7. The slope of the line is related to the effective efficiency, E_{es}, by dividing the slope by the sample residence time, t_r.

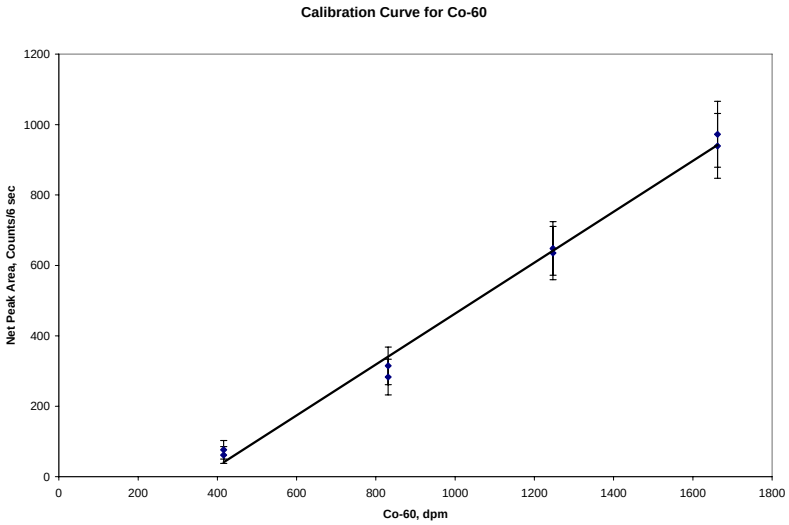

Figure 5.6: ^{60}Co calibration curve. y= 0.723x -260, R^2 = 0.9926. Error bars are 3σ.

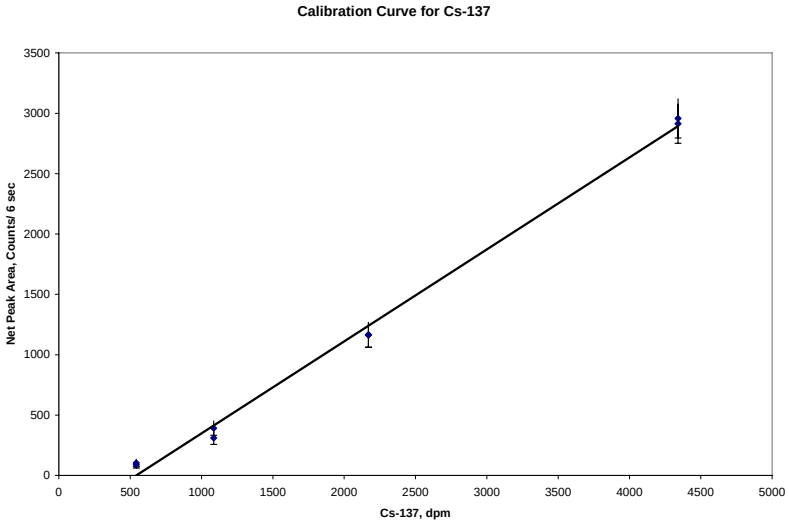

Figure 5.7: ^{137}Cs calibration curve. y= 0.762x -414, R^2 = 0.9954. Error bars are 3σ.

Figures 5.6 and 5.7 indicate that the detection of these isotopes are detected with high efficiency (87% (±4) for ^{60}Co and 91% (±5) for ^{137}Cs), but with a pronounced bias effect that suppresses detector response. This is most likely due to quench effects which can be significant for the 8M HNO_3 eluent (Grate 1999b). Correction for the bias can easily be compensated for by using the calibration curve equations, derived from Figures 5.6 and 5.7, however, overall detection limits are adversely affected by the bias. We estimate that the detection limit for ^{60}Co by FSA is 494 (±25) dpm, while the detection limit for ^{137}Cs by this method is 729 (±36) dpm. So while better detection limits are obtained for ^{60}Co by FSA, FGA is a superior method of detection for ^{137}Cs, if similarly sized flow cells are used for each method.

CONCLUSIONS

An automated method for the determination of ^{60}Co and ^{137}Cs in aqueous samples by a new technique, called flow gamma analysis (FGA) was examined. This method attempted to combine rapid chromatographic separation techniques with the γ energy discrimination properties of a NaI(Tl) detector. This would enable the determination of β/γ emitting nuclides that co-elute from the column; a determination is not possible with established FSA techniques. However, due to low the detection efficiency of the NaI(Tl) detector used in these experiments, the FGA detection limits for ^{60}Co and ^{137}Cs were undesirably high; 1134 (±33) dpm for ^{60}Co and 440 (± 15) for ^{137}Cs for a 2500 μL gamma flow cell. We also conducted experiments to determine these isotopes by FSA, even though we could not resolve samples with mixtures of the two analytes. Better detection limits were achieved for ^{60}Co, 494 (±25) dpm, by this method; however, worse detection limits found for ^{137}Cs, 729 (±36) dpm. Determination by FSA was primarily hampered by an encountered detector response bias that inhibited the determination of these analytes at lower levels.

The authors believe that chemical quenching of the scintillation process by the high concentration of nitric acid eluent, 8M, may be to blame for this effect. It is possible that by lowering the molarity of nitic acid, less bias will be encountered. We believe that we can reduce the load solution nitric acid concentration to 3M, and still be able to achieve retention of ^{90}Sr, a possible interference.

The authors also believe that NaI(Tl) detection efficiency can be improved with the addition of extra lead shielding. If a large lead brick cave is built around the detector the background count rate can be expected to drop, thereby enhancing the signal to noise ratio when a source is present. The addition of a copper or cadmium liner for the detector cave would also further reduce background. This modification can be made easily and without much added cost. Further, we believe that the use of a detector with a larger NaI(Tl) crystal would improve γ-ray detection efficiency since γ-ray stopping power is proportional to the crystal thickness. A well-type NaI(Tl) detector with a 3" diam. x 3" crystal is capable of approximately 32% absolute detection efficiency for the 662 keV γ of ^{137}Cs and approximately 25% absolute detection efficiency for the 1332 keV γ of ^{60}Co (Kahn, 2007). This modification would be more costly that the previous, but would have the added bonus of accommodating larger gamma flow cells in the larger well.

Chapter 6: Optimization of Actinide Analysis By HPEC and ICP-MS

A procedure for the separation and detection of trace levels of actinides using high performance extraction chromatography (HPEC) and inductively coupled plasma mass spectrometry (ICP-MS) has been optimized. Using Eichrom's TRU resin, a mixture of five actinides (^{232}Th, ^{238}U, ^{237}Np, ^{239}Pu, and ^{243}Am) can be separated and detected by mass in under four minutes. Several method parameters were optimized in this research including: resin size, column length, packing pressure, and eluent flow rate. Experiments were also conducted to examine the feasibility of reducing or eliminating oxalic acid from the elution scheme. The use of large quantities of oxalic acid in combination with ICP-MS is undesirable in that this reagent causes a residue buildup on the cones of the mass spectrometer. Overtime, this buildup reduces the performance of the mass spectrometer. A rapid and automated method of trace actinide separation and detection has applications in a number of areas including environmental monitoring, bioassays, expedited routine analysis, and emergency response situations.

INTRODUCTION

The ability to detect trace levels of actinides in biological samples has long been a concern of the nuclear industry, the national lab complex, and public health officials. This is because actinides are most toxic once inside the body where their long biological half-life and alpha radiation is extremely damaging. Actinides can enter the body via ingestion, inhalation, or wounds, and exposure to even small amounts can cause severe health hazards (Price 1973). Analytical techniques that can determine the isotopic composition of internally deposited actinides are critically important because isotopic information is most useful in determining dose calculations, and location the uptake

occured. Isotopic determination of actinides is also valuable for a number of other purposes, such as nuclear forensics and nonproliferation monitoring.

Some commonly utilized techniques for determining isotopic actinide content of samples are alpha spectrometry, thermal ionization mass spectrometry (TIMS), accelerator mass spectrometry (AMS), and neutron activation analysis (NAA). These techniques can be problematic in terms of extensive sample preparation time (alpha spectrometry) or very expensive, high maintenance equipment (TIMS, AMS, NAA). Inductively coupled plasma mass spectrometry (ICP-MS) is a lower cost, more commonly available technique that is extremely useful and widely used for actinide analysis (Lariviere 2006). This technique has the advantage of requiring very little sample preparation (for aqueous samples) and producing fast multi-isotopic analysis with detection limits reported into the low ppq levels for several actinides, including: ^{232}Th, ^{238}U, ^{237}Np, ^{239}Pu, and ^{241}Am (Baglan 2004; Pointurier 2004). A comparison of ICP-MS to various other analytical techniques has shown this method to be superior in many aspects (Dacheux 1997). However, the capabilities of ICP-MS are often limited by the presence of isobars (which produce unresolvable interferences) and polyatomic interferences (some of which are shown in Table 6.1) (Alonso 1995; Egorov 2001).

Table 6.1: Commonly encountered actinide polyatomic interferences.

ISOBARS	POLYATOMIC IONS
^{236}U and ^{236}Np	^{230}ThH and ^{231}Pa
^{238}U and ^{238}Pu	^{236}UH and ^{237}Np
^{241}Pu and ^{241}Am	^{237}NpH and ^{238}U
^{242}Pu and ^{242}Am	^{238}UH and ^{239}Pu
	^{240}PuH and ^{241}Am
	^{242}PuH and ^{243}Am

While the best sensitivities are realized only in “neat” solutions, samples with complex matrices such as environmental (soil, seawater) or biological (urine) samples

reduce sensitivities. This is due to the fact that an increase in the number of matrix molecules in the sample stream leads to increasing interferences. Therefore, it is necessary to remove as many matrix components as possible prior to analysis and to use techniques which separate isobars and potential polyatomic interferences. This necessitates the separation of the actinide elements in the sample stream to as large a degree as possible prior to detection.

Techniques for actinide separation have been developed and applied to alpha spectrometry for many years, while applications to ICP-MS have been more recent (Boulyga 2001). These methods typically involve lengthy, labor-intensive procedures, and there would be great benefit in the development of a fast, automated separation procedure that feeds directly into a mass spectrometer. Previously demonstrated methods involve the use of resins to load analytes onto a column, where they are separated from matrix elements, and then separate them by individually eluting them (Epov 2005). The most commonly used form of this technique is the chromatography column (Choppin 1995). A very effective form of chromatographic separation is through the use of organic liquid extractants (a product of earlier liquid-liquid extraction techniques) that have been immobilized onto polymer beads. Several varieties of these types of extractive resins are commercially available from Eichrom, including: TEVA, U/TEVA, TRU, and Sr. Recently our group demonstrated the rapid separation of five actinides (Th, U, Np, Pu, and Am) on columns packed with either U/TEVA or TRU resin (Hang 2004; 2005). This method enabled the pre-concentration of these analytes onto the column from large volume samples. The separations took approximately 12 minutes to completely resolve these analytes using manually packed 30 cm columns. Equilibration times and hold times for the injection increased the total analytical cycle time to nearly 30 minutes. In addition, this separation method utilized a relatively large quantity of oxalic acid (~0.1g

per cycle) to fully remove the analytes from the column. The use of this much oxalic acid is detrimental to performance of the mass spectrometer since it degrades performance and necessitates frequent cleaning and retuning of the instrument.

In this study we packed columns TRU resin using a commercial slurry packer. This enables us to pack columns uniformly and reproducibly. The use of a slurry packer also enables us to optimize the columns and packing conditions. In this study we have optimized these separations to reduce or eliminate the oxalic acid in the separation. We also examine various parameters on the separation including resin size, packing pressure, column length and flow rate.

EXPERIMENTAL

Instrumentation: Ion chromatography was performed using a high performance ion chromatograph (DX-600, Dionex, Sunnyvale, CA). The IC was equipped with an autosampler (AS50, Dionex) capable of injections up to 1 ml. Elemental detection and identification of the IC eluent was accomplished by a quadrapole ICP-MS (Elan 6100, Perkin Elmer, San Jose, CA). Typical parameters for the ICP-MS were: 0.75 L/min nebulizer gas flow, 10.25 V Lens Voltage, 1225 W ICP-RF power, -2200 V Analog Stage Voltage. The ICP was equipped with a concentric glass nebulizer and a cyclonic spray chamber (Perkin Elmer). The process of sample injection, separation, and detection was automated through the Chromeleon management system (Dionex) and the ICP-MS software was triggered to collect data through a contact closure. Data was collected by peak hopping between the major actinide masses (Th^{232}, U^{235}, U^{238}, Np^{237}, Pu^{239}, Am^{243}).

Reagents and Materials: Trace metal grade nitric acid was obtained from Fisher Scientific (Pittsburgh, PA). Oxalic acid eluent was purchased from Dionex and diluted to the recommended concentration (80 mM oxalic acid, 100 mM tetramethyl ammonium hydroxide, and 50 mM potassium hydroxide). Deionized water (18 MΩNanopure Water

System, Barnstead, Dubuque, IA) was used to dilute acids and standards to the desired concentrations

Ion chromatography columns were prepared using a resin containing octylphenyl-N,N-diisobutyl carbamoylphosphine oxide adsorbed onto the packing beads, which are made of polymethylmethacrylate. This resin is commonly called TRU resin and was obtained from Eichrom Technologies (Darien, IL). These resins were supplied with three different particle sizes; 20-50 μm, 50-100 μm, and 100-150 μm. The resins were packed into PEEK lined column hardware (Alltech Associates, Deeerfield, IL) using an Alltech model 1666 Slurry Packer. Columns were prepared in 30 cm, 10 cm, and 3 cm lengths.

Standard solutions of Np^{237}, Pu^{239}, and Am^{243} were obtained from Isotope Products (Valencia, CA). These standards are normally sold with a specific activity (i.e. 2 μCi/mL), so these values were converted to ppm values so that all standards would be prepared with similar values. A standard 1000 ppm ICP-MS solution of Th was obtained from Alfa Aesar (Ward Hill, MA). A standard 1000 ppm ICP-MS solution of U was obtained from SPEC Certiprep (Methchen, NJ). The thorium solution was confirmed to contain 100% of Th^{232}, the uranium solution was confirmed to contain approximately 0.7% U^{235} and 99.3% U^{238} (natural uranium concentrations). All actinides were diluted to a stock solution of 50 ppt in water with 5% nitric acid.

Column Preparation: Columns were prepared using a commercial slurry packer in order to improve the reproducibility of the packing from column to column. The slurry packer contains a pneumatic amplification pump which enables a low pressure gas supply to be amplified into the liquid of the slurry. The amplification is approximately 1:100. To pack a column the resin was first suspended in approximately 25 ml of deionized water. The slurry was mixed overnight prior to packing. The column and exit frit were then attached to the reservoir, into which the packing slurry was added. The reservoir

was topped off with deionized water and the fluid lines from the slurry packer were attached to the reservoir. After the lines were primed, the air pressure was adjusted to the desired level and the solvent flow was turned on. The slurry packer was allowed to pack each column for approximately five minutes. After the pressure was bled off, frits were installed and the column was rinsed with a flow of 3M nitric acid.

RESULTS AND DISCUSSION

Optimization of Columns: The primary purpose of this study is to optimize the separation of actinides on columns packed with TRU resin. For most testing, the oxalic acid was removed from the gradient as a way to reduce the amount of organic impurities put into the mass spectrometer. Once the oxalic acid was removed from the eluent, the primary parameter that was to be optimized is the retention time. The amount of resolution that will be required will depend largely on the isobaric interferences that are present for each analyte. For instance, it is necessary to separate uranium and plutonium to reduce the isobaric interference from ^{238}UH and ^{239}Pu. It will not be necessary to separate Am from Th as they will not interfere with each other. With these limitations in mind, it was also determined that the amount of hydrochloric acid that needed to be used was around 35%. Table 6.2 shows the various gradients used in this study. The gradient used previously by our group (Hang 2004) is Gradient 1, the gradient with all oxalic acid removed is Gradient 2. A third gradient with a small amount of oxalic acid was also tested (Gradient 3).

Table 6.2: Elution gradients used in this work.

GRADIENT 1			GRADIENT 2			GRADIENT 3		
Time (min)	Flow (mL/min)	Eluent	Time (min)	Flow (mL/min)	Eluent	Time (min)	Flow (mL/min)	Eluent
-11	3	3M HNO_3	-2	3	3M HNO_3	-2	3	3M HNO_3
0	1.5	2M HCl, 50%; H_2O 5%; $H_2C_2O_4$ 40%	0	3	2M HCl, 35%; H_2O 65%	0	3	2M HCl, 35%; H_2O 65%
6	1.5	2M HCl, 0.5%; H_2O 59.5%; $H_2C_2O_4$ 40%	2	3	2M HCl, 0.5% H_2O 99.5%	0.5	3	2M HCl, 15% H_2O 85%
13	1.5	2M HCl, 0.5%; H_2O 59.5%; $H_2C_2O_4$ 40%	6	3	2M HCl, 0.5% H_2O 99.5%	2	3	2M HCl, 0.5%; H_2O 94.5%; $H_2C_2O_4$ 5%
						6	3	2M HCl, 0.5% H_2O 99.5%

Packing Pressure: The slurry packer that was used enables columns to be packed easily and reproducibly. Part of the process in packing high-efficiency columns efficiently is in determining the optimal packing pressure for the packing material being used in a particular application. The slurry packer that we used is capable of generating pressures well over 10,000 psi, however very high pressure would crush the polymeric

resin material on which the active stationary phase is adsorbed to. For our use we packed columns at or below 3000 psi (liquid pressure). We initially packed four columns at 3000 psi and separated the actinides using Gradient 1. This produced very reproducible columns (data not shown). In order to test the effect of packing pressure on the column performance we packed three columns 30 cm long at pressures varying from 1000 psi (the low limit of the slurry packer), up to 3000 psi. We then separated the five actinides on each column using Gradient 2, as seen in Figure 6.1.

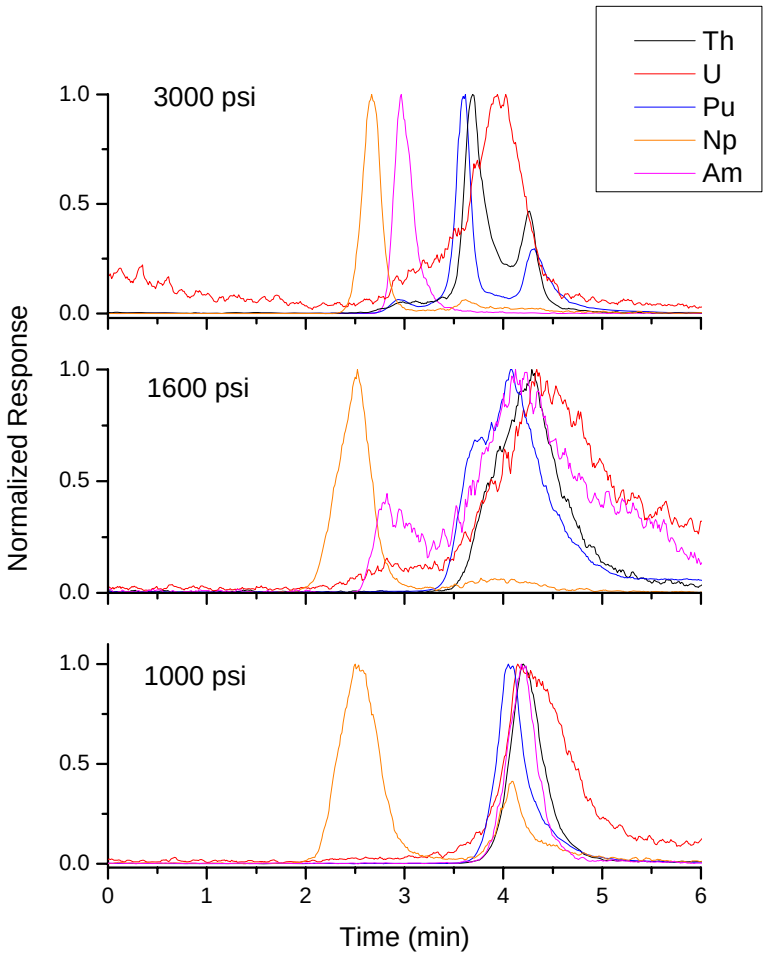

Figure 6.1: Separation of actinide analytes on 30 cm long TRU resin (50-100 µm) packed at pressures between 1000 psi and 3000 psi. Separation using Gradient 2 in Table 6.2.

This data demonstrates several points. First, without the oxalic acid the selectivity between the different actinides is significantly reduced and the actinide peaks tend to co-elute. Second, the faster flow rate combined with the faster gradient causes all five actinides to be eluted in under six minutes, which is approximately twice as fast as our previous study. The data presented in Figure 1 also demonstrates that the effect of a higher packing pressure is to improve the selectivity between the analytes and thus improve the separation. The likely reason for this improvement is that as the resin becomes better packed at higher pressure, there is less void volume in the column, improving the separation. We expect that because a relatively soft polymer is used as the support material that very high packing pressures are unrealistic because the beads would compress and ruin the resin.

Column Length: Another parameter that is expected to have a significant effect on the separation is the column length. As the column length increases there is a larger number of theoretical plates available to enable a good separation. This is simply an effect of there being less material in a shorter column resulting in less opportunities for the analytes to interact with the packing material. A longer column also increases the amount of time that is required for the separation and it also results in broader peaks that result from the band broadening process that occurs within the column.

In order to test the effect of column length, we packed three different columns with the same packing material and under the same packing conditions (50-100 μm resin, 3000 psi packing pressure). The column lengths were 30 cm, 10 cm and 3 cm. Each column was then used to separate the five actinides under the same gradient conditions (Gradient 2). Figure 6.2 shows the effect of column length on the retention of three different actinides (Pu, Am, Np).

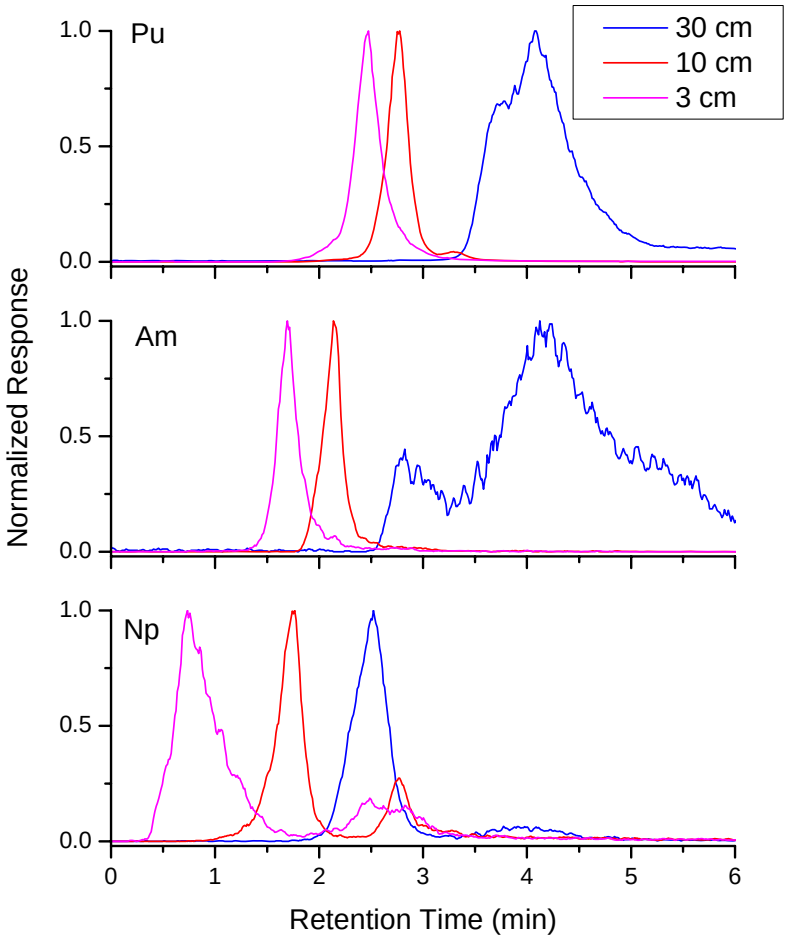

Figure 6.2: Separation of Pu, Am, and Np on columns of 30 cm, 10 cm, and 3 cm. Columns were packed with TRU resin (50-100 µm) at a pressure of 3000 psi. Separation using Gradient 2 in Table 2.

As expected, the shorter column results in a shorter retention time, decreasing from 4.5 minutes to 2 minutes for plutonium and decreasing from 2.5 minutes to under 1 minute for neptunium. For the 30 cm column the peak shape is generally poorer than for the shorter columns. This is probably because the gradient is relatively fast; by the time the gradient is over the analytes are still on the column and they will re-equilibrate under

the less favorable conditions, resulting in significant band broadening. Figure 6.3 shows the effect of the column length on the complete separation of all five actinides. The 30 cm column produces a very poor separation of the analytes for the reasons discussed above. The 10 cm and 3 cm columns both produce reasonable separations of the analytes in under 4 minutes. While these separations do not fully separate all of the analytes, it does a good job of separating most of the analytes that will produce isobaric interferences with each other. The main analytes that can interfere with one another and are not fully resolved are the plutonium and the uranium. These two analytes are separated a little better in the 3 cm column, and there is no major advantage to using the 10 cm column, so the 3 cm column is preferred for the remainder of the tests.

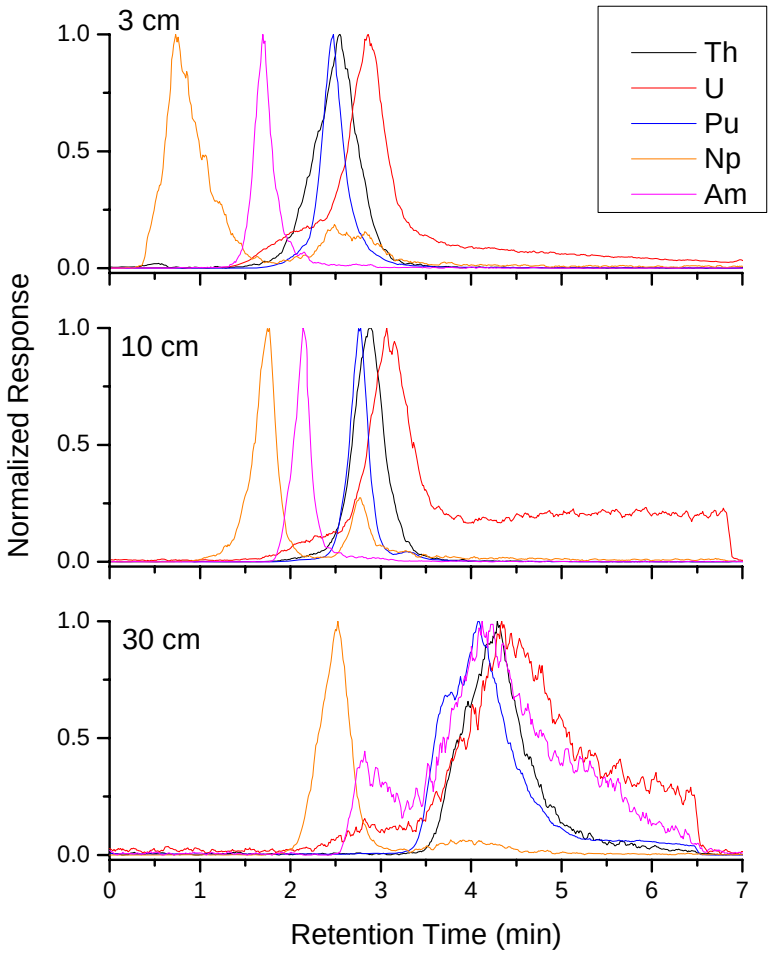

Figure 6.3: Separation of actinide analytes on columns of 3 cm, 10 cm, and 30 cm. Columns were packed with TRU resin (50-100 µm) at a pressure of 3000 psi. Separation using Gradient 2 in Table 6.2.

Resin Size: Another parameter that can be controlled in examining the performance of the resin for separating the actinide analytes is the resin size. In LC it has been demonstrated many times that improved performance is obtained with smaller packing materials. Commercial packings for analytical applications are typically in the range of 3-5 µm. This small size requires that the packing material be composed of non-

compressible silica materials. The resin used in this study is composed of a polymeric methacrylate backbone, which is compressible. In addition the resin is only available in relatively large sizes. With these limitations in mind, we packed three 3 cm columns with each of the resin sizes under identical conditions. The columns were then used to separate the actinide series. These results are presented in Figure 6.4. For all three columns the complete separation is obtained in under 4 minutes, although again the separation does not produce a baseline separation of all analytes. This data shows that as smaller resin is used the result is sharper and more well defined peak shapes. The improvement from the 50-150 μm resin to the 20-50 μm resin is not as pronounced, but the peak shape for the uranium is improved.

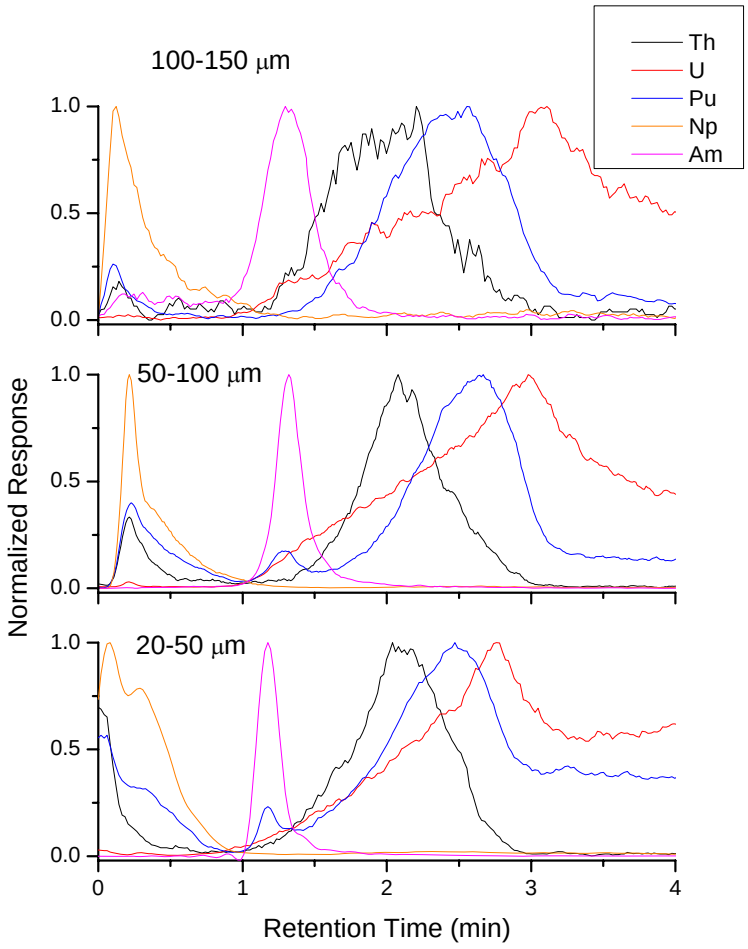

Figure 6.4: Separation of actinide analytes on columns packed with different sizes of TRU resin (100-150 μm, 50-100 μm, 20-50 μm). All columns were 3 cm long and were packed with a packing pressure of 3000 psi. Separation using Gradient 2 in Table 6.2.

Flow Rate: The flow rate of the eluents through the column is a parameter that has multiple effects on the separation. For one, increasing the flow rate will increase the backpressure that the pump produces when pumping the eluent through the column. An increasing flow rate will also decrease the amount of time that the eluent is in the column. This results in a shorter retention time for all analytes. Another result is that there is less

time in which the analytes can come into equilibrium with the stationary phase on the resin. Because full equilibrium is not achieved, the resolution of the separation will be reduced and peak shapes will be affected to differing degrees.

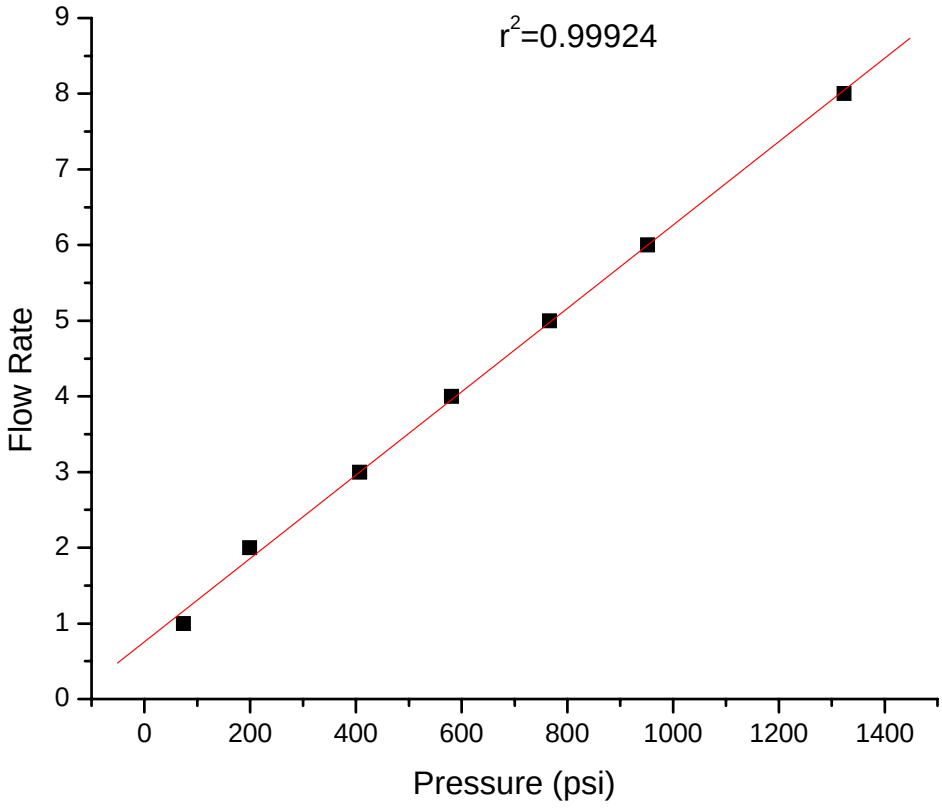

Figure 6.5: Flow rate versus pressure. Note the good linearity up to very high flow rates.

In order to demonstrate these effects, we separated all five actinides on a 3 cm long TRU column with a 50-100 μm resin. These separations were carried out at flow rates ranging from 1 ml/min up to 8 ml/min. Figure 6.5 shows that the backpressure increases linearly with increasing flow rate. This indicates that the resin is not compacting or deforming even at pressures up to approximately 1300 psi. Because the

structure of the underlying resin is not changing, we can assume that the stationary phase should still be performing adequately up to these pressures.

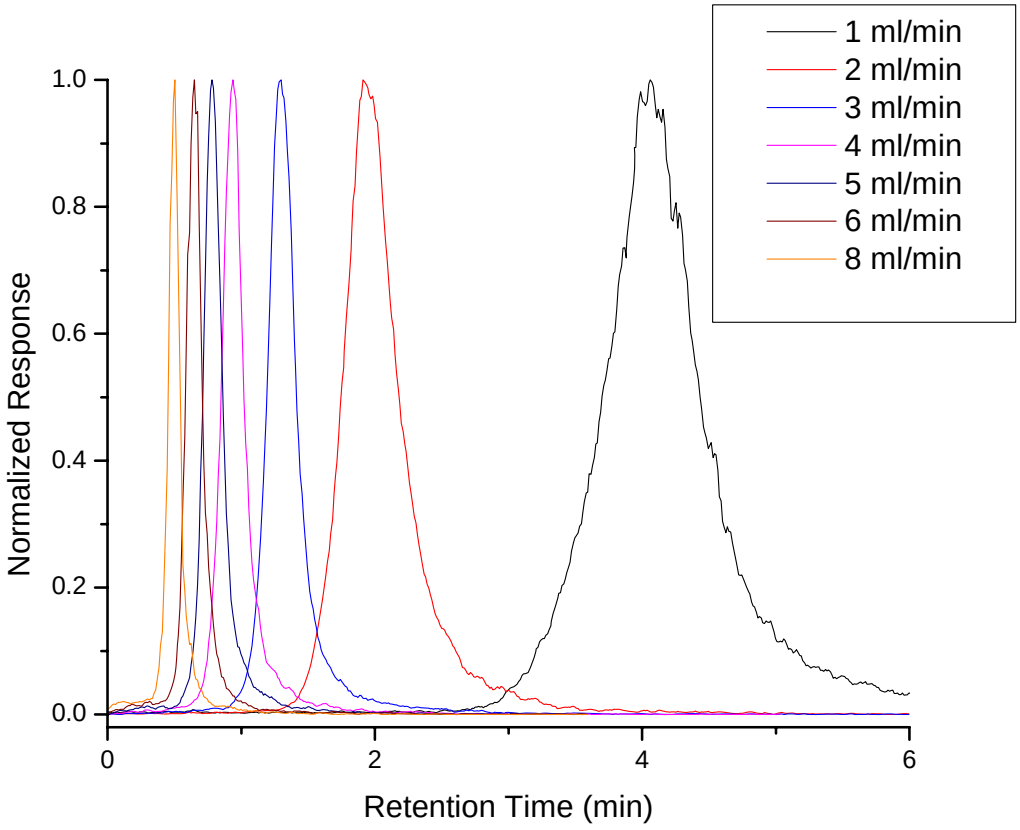

Figure 6.6: Retention of Americium on a 3 cm long TRU column (50-100 µm, 3000 psi packing pressure) at flow rates between 1 ml/min up to 8 ml/min.

Figure 6.6 shows the effect of increasing the flow on the retention of a single analyte, americium. This figure shows that as the flow is increased, the analyte has a shorter and shorter retention time. Also, as the flow is increased, the peak also becomes narrower. Both of these observations are what should be expected as the equilibration time is decreased due to a shorter residence time of the analyte in the column.

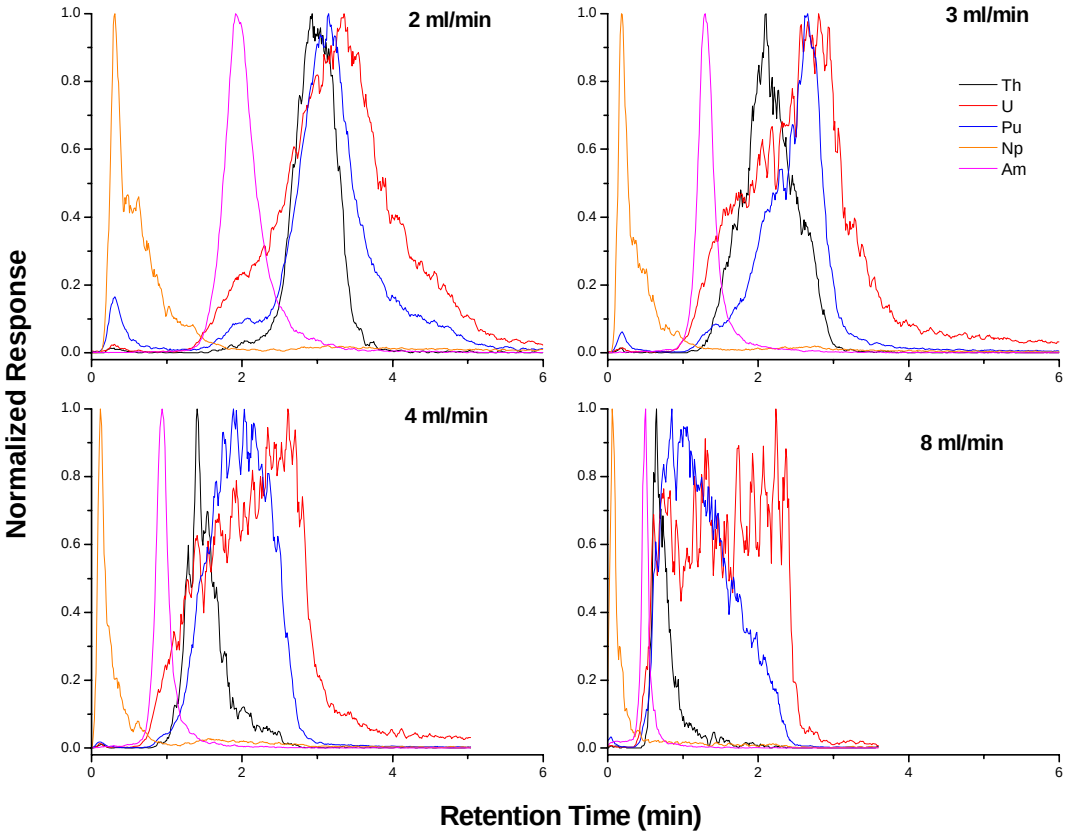

Figure 6.7: : Separation of actinides on a 3 cm long TRU column (50-100 µm, 3000 psi packing pressure). Flow rates were 2 ml/min, 3 ml/min, 4 ml/min and 8 ml/min.

Figure 6.7 shows the separation of the actinides at several flow rates. At the lowest flow rate (2 ml/min) the actinides separate with some co-elution of the Th/U/Pu. As the flow rate is increased, the peak shapes become better and there becomes better separation between the actinides. At the highest flow rates there is very little selectivity between the actinides. It should be noted that at is that at the highest flow rates, the peaks for plutonium and uranium became very distorted. This is because very high flow rates are not ideal for the nebulizer of the ICP-MS. These high flow rates overload the system.

The analytes that are in the spray chamber then take longer to be removed from the system, resulting in broad and overloaded peaks.

Calibration Curve: In addition to being able to separate the actinide analytes it is important to determine how much analyte needs to be injected in order for it to be detected in the ICP-MS. In order to build calibration curves, different volumes of the 50 ppt standard was injected onto a 3cm long column with 20-50 μm resin. The maximum number of counts was plotted versus the amount of actinide injected in pg (data not shown). The amount that was injected was converted to the mass of each actinide that was injected, ranging from 2.5 pg up to 50 pg. The injected mass correlated very well with the detected amount of actinide that was injected onto the column (r^2>0.98). From this data, we can also determine the detection limits by determining the amount of noise for each actinide spectra. The detection limit can be assumed to be 3 times higher than the noise level. We can then use the linear equation for the calibration curve to determine at what amount of analyte this signal will be obtained. We therefore estimate the detection limits to be below 1 pg.

Improving Rapid Separation: Although it is possible to get a basic separation without using a strong stripping agent in the eluent (such as oxalic acid), it has become clear that this is not completely sufficient to enable a satisfactory separation between the plutonium and uranium. In order to get a better separation, we devised an optimal separation gradient for a short (3 cm) TRU column that would include the minimum amount of oxalic acid that would enable a separation. This gradient is shown in Table 6.2 as gradient 3. The modified gradient puts less than 0.002 g of oxalic acid on the column, which is more than 50 times less oxalic acid then Gradient 1. This lesser amount of oxalic acid will therefore allow several hundred analytes to be run before the mass spectrometer will have to be cleaned.

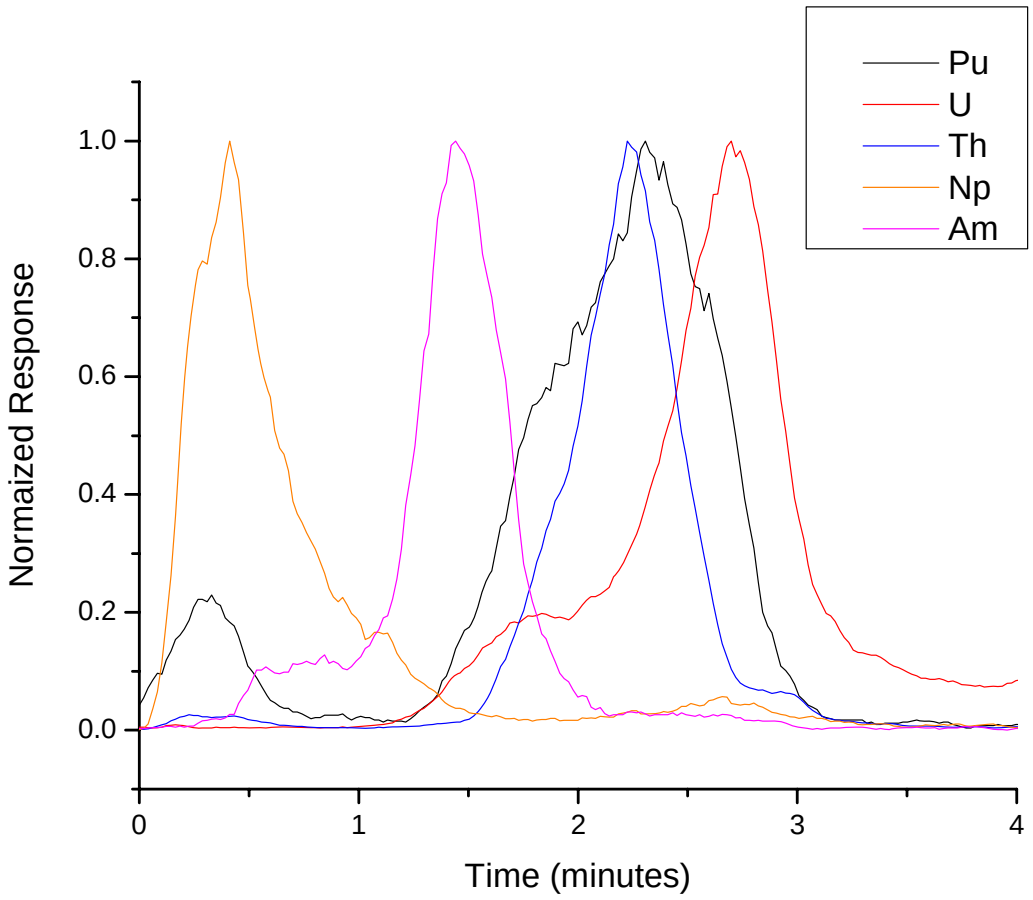

Figure 6.8: : Separation of actinides using Gradient 3 in Table 2. Column used was 3 cm long TRU column (50-100 µm, 3000 psi packing pressure).

The separation of the five actinides was tested on three 3 cm columns with all three resin sizes tested. The resulting separations were better in all cases. Figure 8 shows the separation of the five actinides on the 3 cm column packed with 50-100 µm resin. This data shows a marked improvement in the separation between the uranium and the plutonium. The thorium and the plutonium are still not well separated, but this is less of a concern considering that these two analytes should not produce isobaric interferences with one another.

CONCLUSIONS

In this work, several parameters associated with an on-line separation of actinide compounds utilizing ICP-MS detection have been optimized. First, it was determined that the selectivity between different actinides is significantly reduced with the use of oxalic acid. However, the use of a smaller amount of oxalic acid does permit satisfactory selectivity, while reducing the need for instrument maintenance. Second, it was determined that packing columns under pressure is better than manually packing. Columns that are pressure packed elute the five actinides twice as fast as those packed manually; this likely due to the fact that there is less void space in the column. We determined that while longer columns improve actinide separation, they also increase the overall separation time and result in unacceptably broader peaks. For this reason we recommend using a column of 3-10 cm rather than a 30 cm column. Smaller resin particle size results in sharper, more well defined peaks, though the improvement from 50-150 μm to 20-50 μm is slight. Faster flow rates result in shorter actinide retention time and narrower peaks, though peaks become distorted for flow rates > 4 mL/min and nebulizer efficacy decreases at higher flow rates. For the optimized parameter settings, we were able to achieve detection limits below 1 pg.

Using these improved preparation conditions we anticipate being able to improve the automated separation of actinides for emergency bioassay samples. Future research will consist of examining the properties of other resins and applying results to the separation of actinides from a human urine matrix.

Chapter 7: Actinide Separation and Electrodeposition Using HPEC

A method for the rapid separation of actinides from aqueous samples for electrodeposition by high performance extraction chromatography (HPEC) was developed. Successful actinide analysis by alpha spectrometry requires that samples containing mixtures of actinides be separated and prepared into counting sources in which no interfering isotopes coexist. The system relies on the actinide adsorption characteristics of Eichrom's TRU-Spec resin and a fraction collector to separate a mixed actinide solution (^{229}Th, ^{Nat}U, ^{237}Np, ^{238}Pu, and ^{243}Am) into groupings that are convenient for electrodeposition. The elution profile of the actinides studied was first established and optimized by mass counting using an inductively coupled plasma mass spectrometer (ICP-MS). By knowing the identity and timing of the elution peaks as they exit the column, time windows in a fraction collector were programmed to collect the peak fractions into the appropriate beaker. The samples were then electrodeposited and counted via alpha spectrometry to verify and quantify the isotopes present in each collection beaker. Actinide separation time was reduced from 8 hours to just 15 minutes. The method was shown to effectively separate U, Pu, and Th. Neptunium and americium separations were less successful and will require further research to optimize their separations.

INTRODUCTION

Mass spectrometry is an extremely useful technique for actinide determination due to the low level of sample preparation that is required, relative to alpha spectrometry. The determination of naturally occurring and anthropogenic radionuclides by inductively coupled plasma mass spectrometry (ICP-MS) has gained recognition over the last 15 years, relative to radiometric techniques, particularly for actinide analysis, which

comprise some 88% of the published literature of radionuclide detection by ICP-MS from 1989-2005 (Lariviere 2006). Sensitivities, with regard to activity measurements by mass counting, diminish with the half-life of the isotope to be analyzed. Previous work in this group has shown that, under ideal conditions, ICP mass techniques are suitable for analysis of alpha emitters with half-lives of >70 years (Gonzales 2005). However, under most practical conditions, isotopes with half-lives of <500 years are often difficult to quantify. While sensitivities by other mass counting techniques (TIMS, RIMS, and AMS) are orders of magnitude below those for ICP-MS, these instruments are available in only a very few number of laboratories (Lariviere 2006). Therefore, there is an important set of actinides for which alpha spectrometry remains the best analytical technique for trace and ultra trace analysis required for environmental and in vitro bioassay monitoring.

Isotopic identification and quantification of alpha emitters is accomplished through the detection of characteristic alpha particle energies by a surface barrier detector. Because alpha particles are severely attenuated by sample matrices, they must be chemically isolated and deposited as "massless" samples by electrodeposition to create counting sources. In addition, the alpha particle energies of many actinides are energetically similar and cannot be resolved if they coexist within a source due to the typical alpha detector resolution of 18 keV (L'Annunziata 2003). In practice, alpha-emitters may need a separation of >50 keV to be comfortably quantified due to attenuation from non-ideal counting sources and high-efficiency counting techniques. Therefore, interfering actinides must be separated from each other as well as the sample matrix by a complicated and labor-intensive process that usually takes two working days to accomplish (ASTM 2005a; 2005b).

Table 7.1 presents half-life and alpha particle energy data for the most commonly encountered alpha-emitting actinides. From this table, it can be seen that spectral interferences may be encountered for a number of nuclides. Of particular significance are $^{238}Pu/^{241}Am$ and $^{234}U/^{237}Np$. These nuclides are often found together in samples that are products of nuclear fuel or weapons processes. The problem of $^{238}Pu/^{241}Am$ analysis is particularly acute due to the fact that both of these nuclides are difficult to detect at trace levels by other analytical means (mass spectrometry and gamma spectrometry). Therefore, the efficacy of the separation of americium and plutonium is of greatest importance in developing an automated actinide separation system.

Table 7.1: Commonly encountered alpha-emitting actinides.

ACTINIDE	$T_{1/2}$	PRIM. A (keV)	SECOND. A (keV)	TERT. A (keV)
^{228}Th	1.91 y	5423	5340	N/A
^{229}Th	7340 y	4845	4901	4815
^{230}Th	75380 y	4687	4621	N/A
^{232}Th	1.405E10 y	4012	3947	N/A
^{232}U	68.9 y	5320	5263	N/A
^{233}U	1.592E5 y	4824	4784	4729
^{234}U	2.455E5 y	4775	4722	N/A
^{235}U	7.038E8 y	4398	4215	4596
^{236}U	2.342E7 y	4494	4445	N/A
^{238}U	4.468E9 y	4198	4151	N/A
^{237}Np	2.144E6 y	4788	4771	4766
^{238}Pu	87.7 y	5499	5456	N/A
^{239}Pu	24110 y	5157	5144	5106
^{240}Pu	6564 y	5168	5124	N/A
^{242}Pu	3.733E5 y	4901	4856	N/A
^{241}Am	432.2 y	5486	5443	5388
^{243}Am	7370 y	5275	5233	5181

A faster, automated technique for performing actinide separations would be valuable in reducing sample processing time, reducing costs, and increasing sample throughput. Several important isotopes are too high in specific activity to be detected by

ICP-MS at the trace and ultra trace levels. These include: ^{228}Th, ^{232}U, ^{238}Pu, ^{241}Am, and various curium and californium isotopes. Such a system would expedite the analysis of these isotopes. Potential applications would be environmental monitoring, bioassay monitoring, and routine analytical work. In addition, there is the potential application of using this method in field-analytical work. Since mass spectrometers are not portable, these techniques would be ideal for the analysis of all actinides in remote locations or in emergency response situations.

To achieve these goals, we have examined a method by which a mixed actinide solution, which has previously been separated from its matrix, can be separated into sample fractions of non-interfering isotopes that are ready for electrodeposition and counting. This separation is achieved by high performance extraction chromatography (HPEC). This technique relies on the actinide sorption properties of an extractive resin and a programmable gradient pump to administer an elution scheme to retain and separate individual actinides. Variations on this technique have been used extensively for actinide analysis (Alonso 1995; Fjeld 1995; Smith 1995; Grate 1996; Desmartin 1997; Egorov 1998a; Coates 2001; Unsworth 2001; Reboul 2002; Stricklin 2002; Hang 2004; Fjeld 2005; Grate 2005; Hang 2005; Peterson 2007). The column effluent was first paired with a mass spectrometer to determine the elution profile and timing of the actinide peaks. This practice has been used in other notable works (Thompson 1986; Hollenbach 1994; Aldstadt 1996; Egorov 2001; Hang 2004; 2005; Peterson 2007). By knowledge of the elution peak identity and timing, a fraction collector was programmed with time windows to collect each actinide fraction into a designated beaker. Fraction collection of actinides in this manor has also been used elsewhere (Egorov 1998b; Grate 1999b). The samples were then electrodeposited and counted by alpha spectrometry to verify and quantify the expected isotopes.

The resin used in this work is Eichrom's TRU-Spec resin, developed and characterized by Horwitz (Horwitz 1990; Horwitz 1993b). This resin has high absorption characteristics for Pu(IV), Th(IV), Np (IV) and U(VI), a lower affinity for Am (III), and minimal retention of Np(V) in 3M nitric acid. Neptunium and americium are eluted with dilute concentrations of HCl and oxalic acid. Plutonium, thorium and uranium are eluted with additional oxalic acid. Optimization of actinide separations using this resin and ICP-MS has been done by the authors, demonstrating the feasibility of actinide by actinide separation using this HPEC technique (Hang 2004; Peterson 2007).

The advantages of the automated actinide separation method outlined in this work are many. The length of the actinide separation step in the over all analysis can be reduced from 8 hours to just 15 minutes, resulting in significant increases in sample throughput and reduced labor costs. The number of reagents used in the analysis has been reduced. The technique is simpler and safer to use due to the fact that the handling of chemical and radiological hazards is automated. This technique has many applications including environmental, bioassay, and routine analysis of short-lived actinides. In addition, it has the potential application of being field deployable for emergency response situations where actinide analysis is required.

EXPERIMENTAL

High Performance Extraction Chromatography System: A Dionex GP50 gradient pump (Dionex, Sunnyvale, CA) was configured with a Rheodyne 7725i dual mode analytical injector and a 2000 µL sample loop (Precision Flow Products, Lake Elsinore, CA). A 2500 µL Gastight syringe (Hamilton Co, Reno, NV) was used to inject samples into the loop. Ion chromatography columns were prepared using a resin containing octylphenyl-N,N-diisobutyl carbamoylphosphine oxide adsorbed onto the packing beads, which are made of poly(methyl methacrylate). This resin is commonly called TRU-Spec

resin and was obtained from Eichrom Technologies (Darien, IL) and had particle sizes of 50-100 μm. This resin was packed into a PEEK lined column, 4.6mm I.D. x 150mm, hardware (Alltech Associates, Deeerfield, IL) using an Alltech Model 1666 slurry packer. The packing pressure was 1000 psi and the calculated volume of the resin was 9.97 mL. Elution schemes for the HPEC system were manually programmed into the gradient pump and controlled through the instrument interface. The scheme used for this procedure can be seen in Table 7.2.

Table 7.2: Gradient used in this study.

TIME (MIN)	FLOW (mL/MIN)	ELUENT COMP.	COMMENTS
-11	3	3M HNO_3	Column Conditioning
0	1.5	2M HCl, 50%; H_2O, 10%; $H_2C_2O_4$, 40%	Injection, Actinide Loading
6	1.5	2M HCl, 0.5%; H_2O, 59.5%; $H_2C_2O_4$, 40%	Actinide Stripping
13	1.5	2M HCl, 50%; H_2O, 10%; $H_2C_2O_4$, 40%	End Analysis Cycle

Mass Spectrometer System: Ion chromatography was performed using a high performance ion chromatograph (DX-600, Dionex, Sunnyvale, CA). The IC was equipped with an autosampler (AS50, Dionex) capable of injections up to 1 ml. Elemental detection and identification of the IC eluent was accomplished by a quadrapole ICP-MS (Elan 6100, Perkin Elmer, San Jose, CA). Typical parameters for the ICP-MS were: 0.75 L/min nebulizer gas flow, 10.25 V Lens Voltage, 1225 W ICP-RF power, -2200 V Analog Stage Voltage. The ICP was equipped with a concentric glass nebulizer and a cyclonic spray chamber (Perlin-Elmer). The process of sample injection, separation, and detection was automated through the Chromeleon management system (Dionex) and the ICP-MS software was triggered to collect data through a contact

closure. Data was collected by peak hopping between the major actinide masses (^{232}Th, ^{235}U, ^{238}U, ^{237}Np, ^{239}Pu, ^{243}Am). Thorium and plutonium isotopes are different than those studied in the rest of this work, because these isotopes facilitated mass detection. All elution characteristics for other isotopes of the same element are identical.

Reagents and Standards: Trace metal grade nitric acid was obtained from Fisher Scientific (Pittsburgh, PA). Oxalic acid eluent was purchased from Dionex and diluted to the recommended concentration (80 mM oxalic acid, 100 mM tetramethyl ammonium hydroxide, and 50 mM potassium hydroxide). Deionized water (18 MΩ, Nanopure Water System, Barnstead, Dubuque, IA) was used to dilute acids and standards to the desired concentrations

Standard solutions of ^{237}Np, ^{239}Pu, and ^{243}Am were obtained from Isotope Products (Valencia, CA). These standards are normally sold with a specific activity (i.e. 2 μCi mL^{-1}, equal to 74,000 Bq mL^{-1}), so these values were converted to ppm values so that all standards would be prepared with similar values. A standard 1000 ppm ICP-MS solution of Th was obtained from Alfa Aesar (Ward Hill, MA). A standard 1000 ppm ICP-MS solution of U was obtained from SPEC Certiprep (Methchen, NJ). The thorium solution was confirmed to contain 100% ^{232}Th, the uranium solution was confirmed to contain approximately 0.7% ^{235}U and 99.3% ^{238}U (natural uranium concentrations). All actinides were diluted to a stock solution of 50 ppt in water with 5% nitric acid. Further standards were prepared from dilutions of the stock solution.

For the main experiments, solutions of ^{229}Th, ^{Nat}U, ^{237}Np, ^{238}Pu, and ^{243}Am were prepared from in-house stock solutions with an activity range of 7.35-13.63 dpm/ml. The collected actinide fractions were spiked with the appropriate tracers from the in-house stock solutions of the following isotopes: ^{230}Th, ^{236}U, ^{239}Pu, ^{241}Am. No trace for ^{237}Np

was available so the deposition yield of this isotope was estimated from yields of co-deposited actinides.

Fraction Collector: The fraction collector used in this work was a Foxy 200 (Isco Inc., Lincoln, NE). This unit was plumbed directly in-line with column using PEEK tubing. The collection vessels were disposable 30 mL Pyrex beakers. The collection protocol was manually programmed into the fraction collector's user interface and was based on time windows as established by previous mass spectrometer profiling. The fraction collection protocol was manually initiated at time=0 as described in Table 7.2. A diagram of the sample separation and collection system is shown in Figure 7.1.

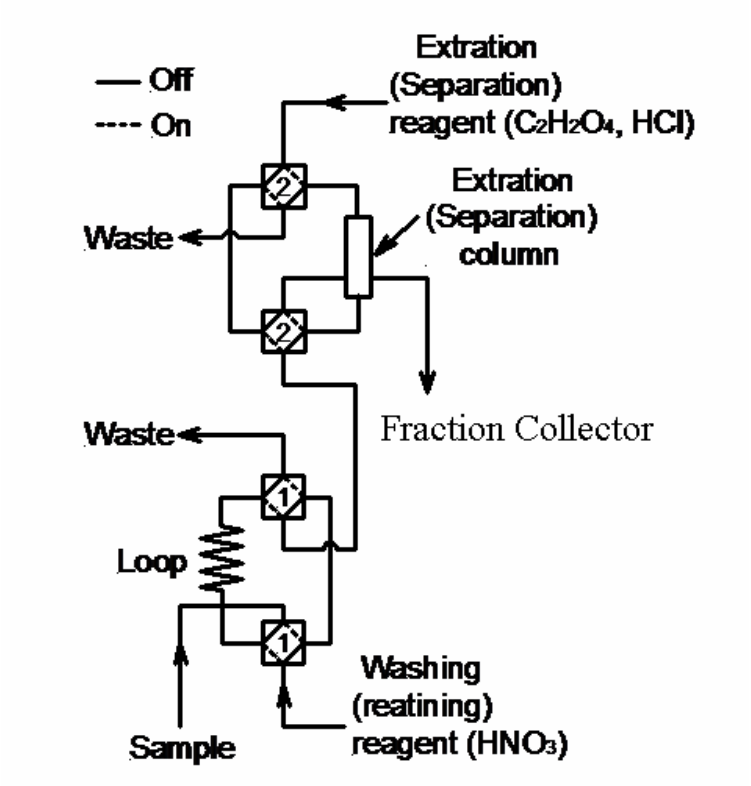

Figure 7.1: A diagram showing the actinide separation and fraction collection system.

Electrodeposition System: The electrodeposition system used for this work was an in-house, custom-built unit that consisted of a plastic cell holder, platinum wires, and a power supply, capable of administering 0.6A to each of 16 cells. The samples were electrodeposited on 5/8" (1.59 cm) stainless steel planchettes (A.F. Murphy Die & Machine Co., Quincy, MA) for 2 hours. A description of the sulfate-based electrolyte and the electrodeposition method is provided by LANL SP-318, R.0 (Plionis, 2005).

Alpha Detection System: The alpha detection system used for all alpha spectrometry measurements was an Ortec EG&G model 920E 16 input MCB Ethernim (Ortec, Oak Ridge, TN). The detectors were Canberra model 7401 alpha spectrometers with a 450 mm detector face (Canberra, Meriden, CT). The electrodeposited counting sources were positioned at the top pedestal height and spectra were acquired using the Ortec acquisition system, Maestro for Windows model A65-B32 v.6.01. The spectra were then analyzed using Ortec's Alpha Vision v5 software.

RESULTS AND DISCUSSION

The separation of mixed actinide samples was first profiled by mass spectrometry to determine the timing and characteristics of the actinide peaks. A chromatogram of the normalized detector response for each actinide is shown in Figure 7.2.

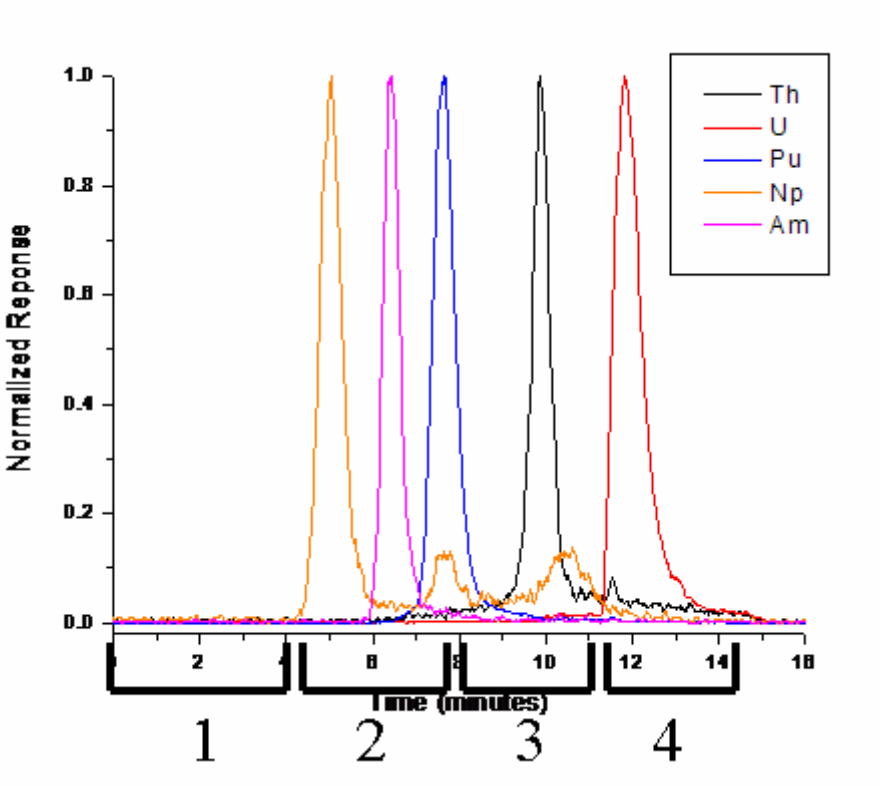

Figure 7.2: A chromatogram of the normalized mass spectrometer detector response to the actinides studied. Note that small portions of the neptunium peak are seen in the region of Pu and Th elution. This figure also shows fraction collection time windows for the collection of the actinide peaks into four separate samples for electrodeposition.

The elution profile, as determined by the mass spectrometer, demonstrates that there is adequate separation between the actinides to effectively resolve each element and facilitate fraction collection of select groups of actinides. Figure 7.2 shows approximate time windows for fraction collection that would conveniently group the actinides for electrodeposition. The first time window would direct the column effluent to a waste container and contains no significant amounts of actinides. The second time window collects and isolates the neptunium and americium into a separate beaker. The third time window would group plutonium and thorium into another counting sample. Finally, a

fourth counting window would provide for the collection of uranium, which is deposited as its own counting source. Table 7.3 shows the parameters of the fraction collection windows.

Table 7.3: Fraction collection windows and associated actinide isotopes.

WINDOW	START (MIN:SEC)	END (MIN:SEC)	EXPECTED ACTINIDES	TRACE ADDED
1	0:0	4:10	None	N/A
2	4:10	7:30	^{237}Np and ^{243}Am	^{241}Am
3	7:30	10:50	^{238}Pu and ^{229}Th	^{239}Pu and ^{230}Th
4	10:50	14:10	^{234}U and ^{238}U	^{236}U

This actinide grouping is convenient, it takes advantage of the natural elution sequence and each actinide pair can be counted together without producing spectral interferences (see Table 7.1). Some high specific-activity actinides, for which this technique was specifically designed, were not used in experiments testing the efficacy of this technique. ^{228}Th was not used because of potential interferences with ^{238}Pu and ^{229}Th was used instead. ^{232}U was not used because this nuclide inevitably contains significant activities of its daughter ^{228}Th; and natural uranium was used instead. ^{237}Np is the only alpha-emitting isotope of any significance of this actinide, therefore it had to be used in this study and could not be traced with the addition of another neptunium isotope. ^{241}Am was not used because of interferences with ^{238}Pu, and ^{243}Am was used instead. Since we wanted to be able to tell if there was any spillover of one Am into Pu, or visa versa, we needed nuclides that we could distinguish from one another.

Triplicate runs of single isotope solutions were conducted. The contents of each collection window were electrodeposited to create counting sources. Since each fraction collected was spiked with the appropriate isotope, a peak for this nuclide should be seen

in each sample. However, the nuclide present in the sample is expected to be seen in only one counting source, which would correspond to the appropriate collection window. The results of a typical thorium solution run are shown in Figure 7.3.

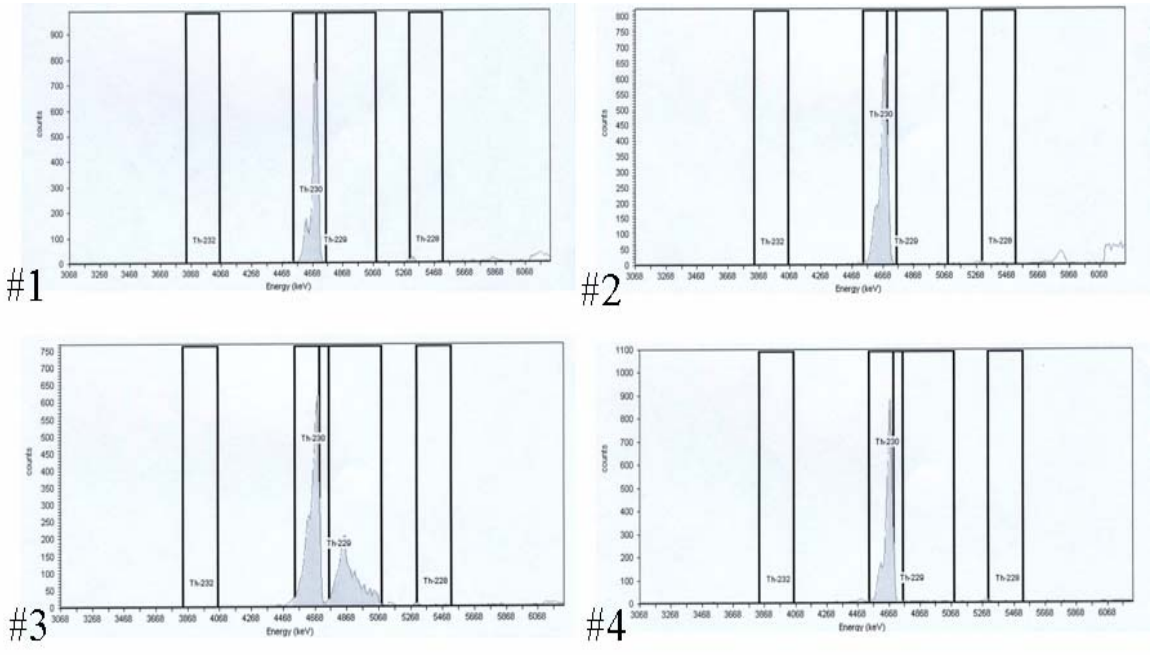

Figure 7.3: The results of a typical Th solution run. Each spectrum shows counts versus energy (keV). Windows 1, 2, and 4 show only the tracer, ^{230}Th, as expected. Window 3 shows both the tracer and the nuclide in the sample, ^{229}Th.

The results from the triplicate runs of each isotope solution are shown in Table 7.4. Window 1 contained no detectable amounts of any radionuclide. This result was expected from the elution profile shown in Figure 7.2. This portion of the eluent need not be collected and may be diverted to waste. Window 2 was intended to contain neptunium and americium fractions. This window was found to contain 58.6% of the total recovered neptunium and 22.0% of the total recovered americium. Window 3 was intended to contain plutonium and thorium fractions. This window was found to contain 29.7% of the total recovered neptunium, 78.0% of the total recovered americium, 98.0% of the

total recovered plutonium, and 100% of the total recovered thorium. Window 4 was intended to contain the uranium fraction. This window was found to contain 11.3% of the total recovered neptunium, 2.0% of the total recovered plutonium, and 100% of the total recovered uranium. Blank runs were conducted between each sample run to determine the extent of any carryover. The only detectable carryover of any nuclides from one run to another was for plutonium, where 0.38% of the total plutonium from the previous run was detected. A second blank run showed no detectable amount of plutonium.

Table 7.4: The total recovered actinide fraction in each collection window.

WINDOW	^{237}Np %	^{243}Am %	^{238}Pu %	^{229}Th %	^{NAT}U %
1	NDA	NDA	NDA	NDA	NDA
2	58.6	22.0	NDA	NDA	NDA
3	29.7	78.0	98.0	100	NDA
4	11.3	NDA	2.0	NDA	100

There was spillover of neptunium into all of the windows that contained actinides, with the majority of neptunium being present in the intended window. This result is not entirely unexpected. As can be seen in Figure 7.2, minor neptunium peaks can be seen at ~7:30 minutes and ~11:00 minutes into the run. This could account for the presence of neptunium within windows 3 and 4. These distinct peaks may be the result of different neptunium oxidation states being present within the neptunium sample solution. The major neptunium oxidation state is +5, but it may also exist in the +3, +4 and +6 oxidation state (Lieser 2001). Actinide solutions are subject to disproportionation, whereby a solution consisting of a single oxidation state will revert to multiple oxidation states over time, depending on acid concentration and the presence of other complexing agents (Katz 1986). This effect may be responsible for the multiple elution peaks observed in the chromatogram (Figure 7.2) and in the electrodeposited actinide fractions

(Table 7.4). The major elution peak (and the one found in Window 1) is likely Np(V), which is not retained by TRU resin. The first minor peak, found at approximately 7:30 min in the chromatogram, is likely Np(IV), which is retained similarly to Pu(IV) and Th(IV) by the TRU resin. The fact that the neptunium co-eluted with the Th and Pu fractions lends credence to the theory that this species is Np (IV). The second minor peak, found at ~11:00 min in the chromatogram, could be Np(VI). There is no data on the retention of Np(VI) on the TRU resin, but it is plausible that this species could co-elute with U(VI) and be found in Window 4.

Unpublished data from experiments performed in our group have shown that the addition of $NaNO_3$ to the sample prior to analysis can act to reduce higher neptunium oxidation states to Np(IV). The addition of this reducing agent to sample solutions may improve the results of our work by forcing all neptunium into the +4 state, which would then co-elute with the plutonium and thorium fractions found in Window 3. The codeposition of Th, Np, and Pu is not ideal, but is acceptable from the standpoint on of spectral interferences. The characteristic alpha energy of ^{237}Np (4788 keV) is ~57 keV from ^{229}Th (4845 keV) and ~101 keV from ^{230}Th (4687 keV). The spectral peaks of these isotopes should be resolvable under counting conditions that optimize FWHM, however, some efficiency would be sacrificed.

Spillover of americium from Window 2 to Window 3 was also problematic. The result of this spillover is not likely to be due to oxidation state effects since americium exists only in the +3 state under commonly encountered conditions. This spillover is like the result of the timing of the collection windows. It is likely that the transition from Window 2 to Window 3 was occurring at the time that americium was being eluted. Experiments incrementally extending the length of the second collection window would

optimize the collection of americium. In this way the critical separation of americium and plutonium could be accomplished.

CONCLUSION

A system was developed that facilitated the automated separation of actinides by HPEC and the collection of actinide fractions into convenient counting groups for electrodeposition and counting by alpha spectrometry. The separation and collection of Pu, Th, and U was successfully demonstrated. Neptunium was found in all three collection windows that contained detectable levels of actinides. This was attributed to oxidation state effects whereby Np(V) was collected in the appropriate window, while Np(IV) was collected with the Pu and Th fractions and Np(VI) was collected with the U fraction. The addition of $NaNO_3$ could reduce higher oxidation states of neptunium to Np(IV), whereby it would be eluted and codepisted with the Pu and Th fractions. Spillover of americium into the Pu and Th collection window was also shown to occur. We anticipate that this could be corrected by incrementally increasing the length of the second counting window until Pu or Th begins to spill over into Window 2. In this way, the collection window for americium may be optimized.

The system described in this work has many potential applications. This technique could provide trace actinide analysis (environmental, bioassay, etc.) of high specific activity isotopes where analysis by ICP-MS is not possible, e.g. ^{228}Th, ^{232}U, ^{238}Pu, ^{241}Am, and various curium and californium isotopes. This system could also be used for routine radioanalytical work, where separations that used to take 8 hours can be accomplished in under 15 minutes. Finally, this system could be used in a mobile laboratory for in-field analysis for environmental monitoring or emergency response situations; since mass spectrometers are not mobile.

Chapter 8: Health Physics Implications

The previous chapters have discussed several rapid analytical techniques for a variety of radionuclides with applications to urine bioassays. These disparate methods are united by the project goal of creating analytical components which could be used to assay victims of a radiological dispersal device (RDD or "dirty bomb") and determine their level and type of uptake. To this end, we need to examine how the detection limits achieved by the featured analytical techniques are related to the medical well-being of people with a radiological uptake. Health physics is the area of environmental health engineering that deals with the protection of individual and population groups against the harmful effects of radiation (Cember 1996). Further, this field studies how to estimate levels of internally deposited radioactivity and relate this quantity to potential adverse health effects; a practice which is commonly called internal dosimetry. The dose associated with the radiological uptake can then be related to immediately observable health effects or the long term risk of developing cancer, through a complex process of modeling. Certain levels of radiological uptake necessitate medical intervention to attempt to remove the internally deposited radionuclides before they inflict their full potential for damage; a practice which typically involves chelation therapy. Chelation therapy is painful and carries its own risk of adverse health effects and should not be applied proactively to any population which might have an exposure (Guilmette 2007). Therefore, the limits of detection for various techniques of determining radionuclide uptake in the body (either rapid or otherwise) have important implications for the practice of health physics and dictating the need for medical intervention. The following chapter provides a brief outline of internal dosimetry practices and relates the detection limits of previously described techniques to their implications for health phyisics.

INTERNAL DOSIMETRY PRACTICES

The need to protect workers and the general population from radiological hazards was first recognized in 1915 by the British Roentgen Society, which introduced proposals for radiation protection even though the concept of absorbed dose was not recognized until 1953 (Hall 2000). Since that time, government bodies have been issuing guidance for estimating "dose factors," or "dose coefficients" for the assessment of biological harm done by radiation. However, these dose-based parameters do not in themselves directly relate to the risk of developing an adverse health effect such as mortality (death in any way hastened by exposure) or morbidity (cancer—fatal or otherwise). Mortality and morbidity are probabilistic effects of radiation exposure and it is, therefore, impossible to predict with absolute certainty whether a given dose will result in either event. By modeling the exposure of a large enough population, we can obtain a population averaged risk assessment for mortality and morbidity for a given radiation dose.

Modeling the risk of radiation dose for the general public is an extremely difficult task that is complicated by five factors:

1. Each of the over 3,000 known isotopes have a unique set of physical parameters that need to be modeled: half-life, radiation types, energies, branching ratios, etc, which contribute to dose estimates.
2. There are varying routes of exposure (inhalation, food, water, external exposure) that result in different metabolic rates and pathways.
3. Isotopes of the over 100 known elements behave differently within the human body and will be dispersed and deposited accordingly. Further, organs within the body have varying levels of sensitivities to radiation and predispositions to forming cancers.

4. There is a large range in body size and metabolic function within the general population that makes it hard to apply one model across all age and gender groups.
5. There is great difficulty in identifying small increases radiologically derived cancer when the incidence of non-radiological cancer is high.

The first point is most easily addressed since copious amounts of physical data exist for most isotopes. Tabulating the physical data for individual isotopes is made easier by limiting the scope of dosimetry modeling to the over 800 radionuclides with half-lives greater than 10 minutes. For the purposes of dosimetry modeling, the most useful physical parameters are half-life, decay mode, branching ratios, radiation energies, and the buildup of any radiological daughter products. This information is most easily accessible from online libraries (Nudat 2007; TON 2007).

Modeling of exposure pathways is more complicated. The main exposure pathways are inhalation, ingestion, and external exposure. External exposure rates are most easily derived by actual irradiation of a phantom based on the Reference Adult standing with no shielding or by modeling the interaction of radioactive emissions on a representation of this phantom using Monte Carlo simulations (EPA 1993). The model for exposure by inhalation is divided into three classes of inhaled particulates: Type F, M, and S, representing fast, medium and slow rates of absorption into the blood stream of these particulates one in the lungs (ICRP 1994; ICRP 1995; ICRP 1996). The modeling assumes that the activity median aerodynamic diameter (AMAD) of the inhaled particles is 1 μm. Ingestion of radionuclides is modeled in a few different matrices for which dose factors for each radionuclide are based: tap water (ICRP 1996), food (ICRP 1996), and cow's milk (UNSCEAR 1982).

Biokinetic models are used to determine the dispersion, deposition, and excretion rates of radionuclides within the body. To accomplish this, two basic systems are modeled: the respiratory tract and the gastrointestinal (GI) tract. After radionuclides enter the lungs or the GI tract, their absorption into the blood stream is dictated by a fractional absorption coefficient, f. Fractional absorption coefficients for each radionuclide are tabulated for the respiratory tract (ICRP 1994; 1995b; 1996) and GI tract, respectively (ICRP 1989; 1993; 1995a; 1995b). These models also track the migration of radionuclide from these systems to their target organs in the body and, finally, their excretion pathway. The excretion pathways modeled are urine and feces.

The same ICRP publications that describe the above biokinetic models for the standard Reference Man also provide figure to augment calculations for various populations that are not accurately modeled by Reference Man. Factors are given to modify the standard model for reference male and female persons for the following age groups: 3 months, 1 year, 5 years, 10 years, 15 years, and adult (17 years and older). In this way general population models are modified to be more relevant for specific segments of the population.

Relating radiation dose factors to mortality and morbidity risk rates is probably the most difficult aspect of modeling. Modelers start by examining cancer mortality data for the US population (NCHS 1992; 1993b; 1993a; 1997) and averaging rates over a stationary population. Then, known data on radiation dose rates and cancer incidence are considered. Much of the existing data on radiation-induced cancer in humans comes from following cohorts of populations with known exposure, such as workers involved in an industrial accident and noting incidences of cancer. Perhaps the most important cohort is the atomic bomb survivors of Hiroshima and Nagasaki; a group of about 270,000 individuals with a wide range of doses ranging from slightly above background to several

grays (Cember 1996). By plotting cancer incidences and mortality rates against known radiation doses and linear no-threshold (LNT) dose response curve is generated. The LNT model is weighted heavily by data in the high dose range, and there is considerable uncertainty in the response for doses less than 0.2 grays (Hall 2000). However, experts have recently validated the LNT model for estimating risk for these low doses (NRPB 1993; UNSCEAR 1993; 1994; NCRP 1997). This does not rule out the possibility that the LNT model seriously over or underestimates the risk for low doses of radiation. Other experts provide some justification for a net beneficial effect of low doses of radiation (Luckey 1990; Jaworowski 1995; Goldman 1996). Despite the uncertainty, for the purposes of this work we will use the LNT model for all risk assessments.

This chapter relies heavily on a recent EPA document, *Cancer Risk Coefficients for Environmental Exposure to Radionuclides* for mortality and morbidity risk rates for the radionuclides studied in the previous chapters (EPA 1999). This report provided mortality and morbidity risk rates (Bq^{-1}) for each radionuclide via inhalation and ingestion pathways. In addition, fractional absorption coefficients for each radionuclide via each pathway were also provided. These factors are specific for the adult Reference Man model and were determined by Keith Eckerman et al. at the Oak Ridge National Laboratory (ORNL) using the DCAL (Dose and Risk Calculation) software developed at ORNL. Urine excretion data for each radionuclide via each pathway was obtained from the library of the MONDAL3 internal dosimetry software (Ishigure 2007), which is available online for free use at the following website, nirs.go.jp:8080/anzendb/RPD/gpmd.php.

Using these data we were able to generate tables featuring the concentration of a particular radionuclide that would be expected to be found the urine of a patient with a given exposure one day after intake. Two tables are provided for each isotope; the first is

for the default inhalation model (typically, Type M particles) and the other is for ingestion based on contaminated tap water. These tables also identify the mortality and morbidity risk for each level of intake. Also, since most bioassay methods concentrate urine samples for better sensitivities, the expected radionuclide activities (Bq/mL) were provided for various degrees of concentration. Finally, we then identified which analytical methods provide the detection limits necessary for quantifying the expected radionuclide activities. These tables are too large and numerous to fit in this chapter so they can be found in Appendix A.

In addition, uncertainties in the inhalation and ingestion risk coefficients for each radionuclide are discussed when that data was available. These uncertainties are graded on an A-F (with A as the most confident and F as the least) scale based on the confidence in the underlying assumptions that were used to create the factors.

^{90}SR RISK ASSESMENT

^{90}Sr is a well-studied radionuclide due to the fact that it is produced in significant quantities by nuclear fission. The inhalation model for ^{90}Sr has a grade of D. For this model, the biokinetics model was deemed equal in confidence to the risk model; both are given greater confidence than the deposition model. The dominant cancer site for this mode is the lungs which, are significantly more affected than the secondary cancer site, bone marrow. Uncertainty in estimating lung dose is due to uncertainty in the range of particles that are classified as Type M. The GI uptake and skeletal biokinetics are considered to be well characterized. The potential migration of the ^{90}Y daughter product adds to dose uncertainty in certain tissues.

The ingestion model is given a grade of B. For this model, the biokinetics model is given equal confidence as the risk model. The dominant cancer site is bone marrow which is significantly more affected than the secondary cancer site, the colon. The GI

uptake and skeletal biokinetics are reasonably well characterized. Some information is available for migration of ^{90}Y from^{90}Sr; the risk estimate for leukemia is relatively insensitive to remaining uncertainties concerning ^{90}Y.

^{90}Sr was evaluated by flow scintillation analysis in chapter 3 of this work, where a quantification limit of 47 dpm per sample was established. Though no experiments were conducted to determine ^{90}Sr by ICP-MS or TIMS, we can assume detection limits of 1 pg and 1 fg, respectively. For ^{90}Sr, these concentrations are equivalent to 306 dpm/mL and 0.306 dpm/mL, respectively. While FSA is a better analytical tool than ICP-MS, it is not as good as TIMS.

Table A.1 shows the inhalation risk analysis of ^{90}Sr. The inhalation of 3.52×10^8 Bq of ^{90}Sr is considered a fatal intake. The fractional absorption of ^{90}Sr via this pathway is 0.1, 0.848% of the body burden is cleared through the urine per day. Thus, we can expect to find 207 dpm of ^{90}Sr per mL of urine in this patient. Without concentration, this level of ^{90}Sr can be detected by TIMS and FSA using just 1 mL of urine. If the full 1440 mL of urine is concentrated and analyzed, ICP-MS can detect ^{90}Sr in patients with uptake sufficient to cause a 1 in 500 chance of mortality; FSA can detect uptakes expected to cause a 1 in 1,000 chance of mortality; TIMS can detect uptakes causing a 1 in 500,000 chance of mortality.

Table A.2 shows the ingestion risk analysis of ^{90}Sr. The ingestion of 6.62×10^8 Bq of ^{90}Sr is considered a fatal intake. The fractional absorption of ^{90}Sr via the GI tract is 0.3 and 5.65% of the body burden is cleared through the urine per day. We can expect to find 7,800 dpm of ^{90}Sr per mL of urine in this patient, an amount detectable by all reviewed techniques. For the concentration of a 24 hour urine sample, ICP-MS can detect ^{90}Sr in patients with a 1:10,000 chance for mortality; FSA can detect uptakes

causing a 1 in 50,000 chance of mortality. TIMS can detect a uptake causing 1 in 1,000,000 chance of mortality using only 50 mLs of urine from exposed patients.

^{210}Po RISK ASSESMENT

^{210}Po is a radionuclide that has garnered attention recently due to the recent high profile murder of former Russian KGB officer, Alexander Litvinenko. It is estimated that Mr. Litvinenko received approximately 2 x 10^{10} Bq of ^{210}Po by ingestion, causing him to die twenty-two days after intake (Guilmette 2007). ^{210}Po was not identified as the poisoning agent until 23 days after Mr. Litvinenko was poisoned (Guilmette 2007). Though it is not know whether early identification of ^{210}Po as the poisoning agent could have prevented his death, it would have been enormously helpful to aid his diagnosis.

Models of ^{210}Po uptake by inhalation or ingestion are not well known. It is known that polonium is virtually evenly distributed within the body after absorption, where it infiltrates all soft tissues. ^{210}Po was evaluated by flow scintillation analysis in chapter 4 of this work, where a quantification limit of 100 dpm per sample was established for this technique. Though no experiments were conducted to determine ^{210}Po by ICP-MS or TIMS, we can assume detection limits of 1 pg and 1 fg, respectively for these techniques. For ^{210}Po, these concentrations are equivalent to 9,970 dpm/mL and 9.97 dpm/mL, respectively. We also evaluated alpha spectrometry as a detection technique for this isotope. Alpha spectrometry has detection limits of approximately .01 pCi (.022 dpm) per sample.

Table A.3 shows the inhalation risk analysis of ^{210}Po. The inhalation of 3.41 x 10^6 Bq of ^{210}Po is considered a fatal intake. The fractional absorption of ^{210}Po via this pathway is 0.1 and approximately 1.0% of the body burden is cleared through the urine per day. We can expect to find 2.37 dpm of ^{210}Po per mL of urine in this patient. Alpha spectrometry is able to detect levels ^{210}Po that can be expected from patients with a 1 in

100 chance of mortality using 1 mL of unconcentrated urine, making it the best analytical tool for ^{210}Po detection. The best rapid method of ^{210}Po detection is FSA which can detect levels of ^{210}Po expected to be found in a full 24 hour urine sample from patients with a 1 in 20 chance of mortality.

Table A.4 shows the ingestion risk analysis of ^{210}Po. The ingestion of 9.8 x 10^7 Bq of ^{210}Po is considered a fatal intake. The fractional absorption of ^{210}Po via the GI tract is 0.1 and approximately 1.0% of the body burden is cleared through the urine per day. We can expect to find 68.1 dpm of ^{210}Po per mL of urine in this patient, an amount detectable by alpha spectrometry and TIMS. For the concentration of a 24 hour urine sample, ICP-MS can detect ^{210}Po in patients with a 1 in 5 chance for mortality; FSA can detect uptakes causing a 1 in 500 chance of mortality and TIMS can detect an uptake causing 1 in 5,000 chance of mortality. Using only 500 mLs of urine from exposed patients, alpha spectrometry can detect ^{210}Po uptake in patients with a 1 in 1,000,000 chance of mortality.

SHORT-LIVED GAMMA EMITTER RISK ASSESMENT

Short-lived gamma emitters are significant in that they pose an external radiation hazard due to their energetic and penetrating gamma rays. Safeguarding the general population from an RDD involving short-lived gamma emitters can be largely accomplished by establishing a safe parameter to which all members of the public should be evacuated. The risk posed by the internal deposition of gamma emitters is less than that for alpha or beta emitters, because a large fraction of the emitted gammas will leave the body without causing ionization. For this reason, there is generally a higher tolerance for these radionuclides in the body though fatal amounts of these isotopes could still be administered with a properly configured RDD.

^{60}Co

^{60}Co is used medically for radiation therapy as implants and as an external source of radiation exposure. It is used industrially as a leveling gauge and to examine welding seams to detect flaws. ^{60}Co is also used to irradiate food and to sterilize medical equipment. For the inhalation model (grade C), the biokinetics model is given the same amount of confidence as the risk model, which is given greater confidence than the deposition model. The dominant cancer site is the lung, which is much more affected than the secondary cancer site, the colon. Lung doses vary considerably as the absorption rate varies within Type M particles. The typical GI intake is moderately well established. Whole body retention of absorbed Co is reasonably well known, but distribution is less well characterized.

For the ingestion model (grade B) the biokinetics model is given the same amount of confidence as the risk model. The dominant cancer site is colon due to the dose from unabsorbed activity that is excreted through the feces. The typical GI uptake moderately well established. Whole body retention is reasonably well known, but distribution is less well characterized.

^{60}Co was evaluated by flow gamma analysis in chapter 5 of this work, where a quantification limit of 500 dpm per sample was established for this technique. Though no experiments were conducted to determine ^{60}Co by ICP-MS or TIMS, we can assume detection limits of 1 pg and 1 fg, respectively for these techniques. For ^{60}Co, these concentrations are equivalent to 2510 dpm/mL and 2.51 dpm/mL, respectively. While FGA is a better analytical tool than ICP-MS, it is not as good as TIMS.

Table A.5 shows the inhalation risk analysis of ^{60}Co. The inhalation of 1.03×10^9 Bq of ^{60}Co is considered a fatal intake. The fractional absorption of ^{60}Co via this pathway is 0.1 and 1.29% of the body burden is cleared through the urine per day.

Therefore, we can expect to find 925 dpm of ^{60}Co per mL of urine in this patient. Without concentration, this level of ^{60}Co can be detected by TIMS and FGA using just 1 mL of urine. If the full 1440 mL of urine is concentrated and analyzed, ICP-MS can detect ^{60}Co in patients with uptake sufficient to cause a 1 in 500 chance of mortality; FGA can detect uptakes expected to cause a 1 in 1000 chance of mortality and TIMS can detect uptakes causing a 1 in 500,000 chance of mortality.

Table A.6 shows the ingestion risk analysis of ^{60}Co. The ingestion of 2.35 x 10^9 Bq of ^{60}Co is considered a fatal intake. The fractional absorption of ^{60}Co via the GI tract is 0.1, 2.75% of the body burden is cleared through the urine per day. Therefore, we can expect to find 2,110 dpm of ^{60}Co per mL of urine in this patient, an amount detectable by FGA and TIMS. For the concentration of a 24 hour urine sample, ICP-MS can detect ^{60}Co in patients with a 1 in 1,000 chance for mortality: FGA can detect uptakes causing a 1 in 5,000 chance of mortality and TIMS can detect an uptake causing 1 in 1,000,000 chance of mortality.

^{137}Cs

^{137}Cs is used in small amounts as a check source of some radiation detection equipment, such as GM counters and liquid scintillation counters. In larger amounts, ^{137}Cs is used in medical radiation therapy devices for treating cancer and in industrial gauges that detect the flow of liquid through pipes and that measure the thickness of materials. For the inhalation model (grade C), the biokinetics model is given the same amount of confidence as the risk model, which is given greater confidence than the deposition model. The data indicate high absorption and fairly uniform distribution of absorbed cesium. The systemic biokinetics of cesium are well established by data in humans, but the potentially rapid migration of ^{137m}Ba from ^{137}Cs yields moderate

uncertainty to doses to some tissues. There are no dominant cancer sites for ^{137}Cs due to the wide distribution of this isotope in the body.

For the ingestion model (grade A) the risk model is given greater confidence than the biokinetics model. It is known that the GI uptake is relatively complete and that the absorbed cesium is fairly uniformly distributed in the body. The systemic biokinetics of cesium are well established, but the potentially rapid migration of ^{137m}Ba from ^{137}Cs yields moderate uncertainty to doses to some tissues. Again, there are no dominant cancer sites.

^{137}Cs was evaluated by flow gamma analysis in chapter 5 of this work, where a quantification limit of 500 dpm per sample was established for this technique. Though no experiments were conducted to determine ^{137}Cs by ICP-MS or TIMS, we can assume detection limits of 1 pg and 1 fg, respectively for these techniques. For ^{137}Cs, these concentrations are equivalent to 193 dpm/mL and 0.193 dpm/mL, respectively. Both ICP-MS and TIMS are better analytical tools for ^{137}Cs detection than FGA.

Table A.7 shows the inhalation risk analysis of ^{137}Cs. The inhalation of 3.12 x 10^9 Bq of ^{137}Cs is considered a fatal intake. The fractional absorption of ^{137}Cs via this pathway is 1 and 0.0639% of the body burden is cleared through the urine per day and we can expect to find 1,380 dpm of ^{137}Cs per mL of urine in this patient. Without concentration, this level of ^{137}Cs can be detected by all methods evaluated using just 1 mL of urine. If the full 1440 mL of urine is concentrated and analyzed, ICP-MS can detect ^{137}Cs in patients with uptake sufficient to cause a 1 in 10,000 chance of mortality: FGA can detect uptakes expected to cause a 1 in 1000 chance of mortality and TIMS can detect uptakes causing a 1 in 1,000,000 chance of mortality using just 250 mLs of urine.

Table A.8 shows the ingestion risk analysis of ^{137}Cs. The ingestion of 1.22 x 10^9 Bq of ^{137}Cs is considered a fatal intake. The fractional absorption of ^{137}Cs via the GI tract

is 1 and 1.58% of the body burden is cleared through the urine per day and we can expect to find 13,300 dpm of ^{137}Cs per mL of urine in this patient, an amount detectable by all methods that were evaluated. For the concentration of a 24 hour urine sample, ICP-MS can detect ^{137}Cs in patients with a 1 in 50,000 chance for mortality: FGA can detect uptakes causing a 1 in 10,000 chance of mortality and TIMS can detect a uptake causing 1 in 1,000,000 chance of mortality using just 25 mLs of urine.

ACTINIDE RISK ASSESMENT

The actinide isotopes evaluated in this study are all alpha emitters with varying degrees of gamma emission. The main threat to public from an RDD involving any of these actinides is from internal uptake where their short-range—but damaging—alpha radiation causes significant harm. Risk assessments were made for the inhalation and ingestion of 9 actinide isotopes: ^{233}U, ^{235}U, ^{238}U, ^{237}Np, ^{238}Pu, ^{239}Pu, ^{242}Pu, ^{241}Am, and ^{243}Am. These isotopes have many commonalities that contribute to their risk assessment.

1. Alpha decay is the decay mode that is overwhelmingly responsible for the assessed dose.
2. The specific activity for these isotopes is generally very low, with the exception of ^{238}Pu and to a lesser extent, ^{241}Am, and ^{243}Am, resulting in mass detection being superior to radiometric detection.
3. Fatal intakes of these nuclides by inhalation are 2 orders of magnitudes lower than those for ingestion.
4. Fractional absorption by both inhalation and ingestion are very low; 0.02 for uranium isotopes and 0.0005 for all other actinides. This results in disproportionately less of the actinides clearing the body

through the urine than for the other, more easily metabolized radionuclides in this study.

Inhalation and ingestion risk assessments for the actinides can be found in Tables A.9-A.26 in Appendix A.

CONCLUSIONS

The ability to determine radionuclides in urine bioassays is critical for the effective and timely management of exposed persons. Table 8.1 summarizes the tables found in the Appendix and gives information regarding radionuclide activity in urine for fatal doses and doses expected to cause a 1 in 1 million chance of mortality. The capability to detect these levels of activity in urine is particularly important for scenarios that involve large uptakes to a large number of people, such as an industrial accident or an RDD event. There are several analytical tools available for the determination of radionuclides in urine bioassays, including: Alpha spectrometry, TIMS, ICP-MS, FSA, and FGA. In addition, there are other methods of in vivo and in vitro assays for radionuclides such as traditional gamma spectroscopy for urinalysis, whole body in vivo counting and fecal analysis. Some of these methods are rapid (ICP-MS, FSA, FGA, and in vivo counting) while others are slow (fecal analysis, alpha spectrometry, TIMS, and traditional gamma spectrometry uninalysis). Though there are many factors to be considered when choosing the optimum technique for determining the uptake of radioactive material. For example, fecal analysis, while inconvenient for both the patient and the analyst, may provide superior results for ingested radionuclides, which have a low fractional absorption coefficient, such as actinides. This is because most of the actinide activity that is ingested is unabsorbed by the body and passes in the feces.

Table 8.1: Summary of urine health physics data. The table shows the activity of each isotope that would be expected in urine from patients with a lethal dose and from those with a 1 in 1M chance of mortality for inhalation and ingestion.

ISOTOPE	INHAL. LD URINE A (Bq/mL)	INHAL. 1:1M MORT. URINE A (Bq/mL)	ING. LD URINE A (Bq/mL)	ING. 1:1M MORT. URINE A (Bq/mL)
^{90}Sr	2.07E+02	2.07E-04	7.80E+03	7.80E-03
^{210}Po	2.37E+00	2.37E-06	6.81E+01	6.81E-05
^{60}Co	9.25E+02	9.25E-04	2.11E+03	2.11E-03
^{137}Cs	1.38E+03	1.38E-03	1.33E+04	1.33E-02
^{233}U	8.12E-01	8.12E-07	9.02E+01	9.02E-05
^{235}U	9.31E-01	9.31E-07	9.16E+01	9.16E-05
^{238}U	1.01E+00	1.01E-06	1.01E+02	1.01E-04
^{237}Np	3.89E-03	3.89E-09	7.08E-05	7.08E-11
^{238}Pu	7.62E-05	7.62E-11	3.30E-04	3.30E-10
^{239}Pu	7.69E-05	7.69E-11	3.21E-04	3.21E-10
^{242}Pu	8.17E-05	8.17E-11	3.38E-04	3.38E-10
^{241}Am	6.99E-04	6.99E-10	3.66E-03	3.66E-09
^{243}Am	7.27E-04	7.27E-10	3.68E-03	3.68E-09

In managing a mass uptake of a potentially harmful amount of radionuclides, one must balance the need for fast results with the need for the best sensitivities. Unfortunately, these needs often are conflicting. One solution to this conundrum may be a two stage analytical approach, whereby a rapid analytical technique is used to screen and triage patients to identify those with the most uptake and the most immediate need for medical attention. Then, as time allows, samples are analyzed by the more sensitive and time-consuming methods to confirm the preliminary assessment and to provide a prognosis to those with lesser amounts of uptake. One must also consider the cost and availability of some techniques, particularly TIMS analysis. While TIMS has proven to be the best analytical method for radionuclide determination for all but ^{210}Po and ^{238}Pu,

there are very few TIMS instruments available in the U.S. and analytical costs can range from $4,000-$8,000 per sample. By comparison, alpha spectrometry is a widely available technique with a cost of less than $500 per sample. The cost for the ICP-MS, FSA, and FGA are expected to be similar or less than the cost of alpha spectrometry.

The poisoning of Mr. Litvinenko with ^{210}Po focused world attention on the dangers of intentional releases of high levels of radioactive material; reigniting fears of terrorism involving RDDs. Aside from the death of Mr. Litvinenko, the most alarming aspect of this case was that ^{210}Po was not identified as the poisoning agent until 23 days after he was poisoned; clearly demonstrating the need for rapid analytical techniques, even if they lack the best sensitivities. During the time after the poisoning, but before his death, Mr. Litvinenko, having ingested approximately 100 lethal dose-equivalents of ^{210}Po *was* effectively an RDD. In addition to traditional excretion pathways, ^{210}Po is also excreted via sweat, where approximately 0.01-0.1% of the total body burden is cleared per day (Harrison 2007). A trail of detectable amounts of ^{210}Po was left around London by Mr. Litvinenko and those persons thought to have poisoned him, prompting the concern that members of the public may have received an uptake of ^{210}Po. Faced with the prospect of tens of thousands of people exposed to ^{210}Po, the British National Health Service (NHS) began fielding calls from concerned citizens. In the aftermath, 2,655 people contacted the NHS with concerns; 799 were found to be legitimately concerned and were offered testing, of which 738 accepted; but only 17 people tested above the level of concern (6mSv or approximately 2,400 Bq ingested) (Guilmette 2007).

The case of Mr. Litvinenko illustrates one further point: Even if an amount of radioactive material is released that could theoretically kill hundreds of people, spreading it in a way that it effects its maximum damage would be difficult. In the event of an actual RDD, we may find that the result is more mass disruption than mass destruction.

In this case, calming public fears becomes an important priority for public health agencies. Here too, rapid screening methods for radionuclides have the potential to be invaluable because of the potential to allay public fears and to identify those in true need of medical intervention.

Chapter 9: Conclusions and Recommendations

The preceding research was commissioned in an effort to provide public health agencies with instrumentation and techniques for the rapid determination of several radionuclides of concern in urine or aqueous matrices. Several analytical methods were investigated including: flow scintillation analysis (FSA) for the determination of ^{90}Sr, ^{210}Po, ^{60}Co, and ^{137}Cs; flow gamma analysis (FGA) for the determination of ^{60}Co, and ^{137}Cs; inductively-coupled mass spectrometry for the determination of actinides; and chromatography-aided separation of actinides for electrodeposition. High performance extraction chromatography (HPEC) was utilized in conjunction with all of the previously mentioned detection methods. This technique enables automated radionuclide separation by passing the sample stream through a chromatographic resin that incorporates extractive ligands that have different retention characteristics for different metal ions. As a result all of the methods developed in this work have a high degree of automation, which, generally, increases sample through put by reducing labor costs and eliminating time-consuming procedures. The expediency of developed techniques is further enhanced by coupling detector systems to the HPEC output, providing simultaneous separation and detection in most cases. Thus, a several components of a comprehensive multi-radionuclide analysis system with combined detection capability were developed. In addition, the individual research projects that comprise this effort have added to the cumulative knowledge of field of radioanalytical chemistry by developing new techniques and by examining novel applications of existing techniques. While the research described herein accomplishes many of the project's objectives, ideas for continued research into further realization of these goals will be discussed later in this chapter.

CONCLUSIONS OF RESEARCH EFFORTS

Flow Scintillation Analysis of ^{90}Sr: An automated computer controlled system for the separation and simultaneous detection of ^{90}Sr was optimized for aqueous and simulated urine bioassay samples. An optimal counting window for ^{90}Sr with the β-RAM flow scintillation analyzer was established. Columns of 3cm and 15cm were examined for reproducibility and column life, where it was determined that the 15cm column was superior. This column was capable of accommodating up to 16 analytical cycles with little ^{90}Sr peak drift. In addition, peak shape was improved by transitioning from a 3cm to 15cm column; however, it was necessary to add 5 minutes to the detection cycle. A calibration curve of detector response to various low activity samples was plotted and shown to be highly linear for both aqueous and urine samples. The resulting lower limit of detection by transient-flow counting was estimated to be 47 dpm, while the lower level of quantification was estimated to be 156 dpm. The time for total analysis and column washing and reconditioning was 30 minutes for transient-flow counting.

The results of the simulated urine bioassay experiments were highly encouraging; with no loss of recovery for urine samples diluted to 50% and little loss of recovery for fully concentrated urine samples. Some peak broadening, with associated decrease in peak maximum counts, was noted.

Flow Scintillation Analysis of ^{210}Po: An automated computer controlled system for the separation and simultaneous detection of ^{210}Po was created and optimized for aqueous samples. A method of ^{210}Po recovery from well-aged ^{210}Pb solutions was detailed. Obtaining ^{210}Po from ^{210}Pb is an easy and convenient way of maintaining a stock of ^{210}Po without having to be concerned with significant decay of the stock activity over time. A loading and elution protocol was developed and optimized for acid

concentration to permit effective loading and elution of ^{210}Po. Cocktail/eluent ratios were also optimized to obtain results with the best figures of merit. An optimal counting window for ^{210}Po with the β-RAM flow scintillation analyzer was also established. A calibration curve of detector response to various low activity samples was plotted and a non-linearity in the curve was noted. A discontinuous calibration curve was deemed to be the best fit for the data. Detector biases for activities above and below 400 DPM were identified. The system allows for quantification of ^{210}Po in samples with at least 100 DPM of activity, using the stopped-flow counting technique and a 30 minute count time. The time for total analysis and column washing and reconditioning was 60 minutes. While no experiments were performed in this work to determine column longevity, we believe that a column life of 10 cycles can be recommended. The feasibility of analysis of ^{210}Po in dilute urine matrices was also briefly examined, with encouraging results.

Flow Gamma Analysis of ^{60}Co and ^{137}Cs: An automated method for the determination of ^{60}Co and ^{137}Cs in aqueous samples by a new technique, called flow gamma analysis (FGA) was examined. This method attempted to combine rapid chromatographic separation techniques with the γ energy discrimination properties of a NaI(Tl) detector. This would enable the determination of β/γ emitting nuclides that co-elute from the column; a determination is not possible with established FSA techniques. However, due to low the detection efficiency of the NaI(Tl) detector used in these experiments, the FGA detection limits for ^{60}Co and ^{137}Cs were undesirably high; 1134 (±33) dpm for ^{60}Co and 440 (± 15) for ^{137}Cs for a 2500 μL gamma flow cell. We also conducted experiments to determine these isotopes by FSA, even though we could not resolve samples with mixtures of the two analytes. Better detection limits were achieved for ^{60}Co, 494 (±25) dpm, by this method; however, worse detection limits found for ^{137}Cs, 729 (±36) dpm. Determination by FSA was primarily hampered by an encountered

detector response bias that inhibited the determination of these analytes at lower levels. The authors believe that chemical quenching of the scintillation process by the high concentration of nitric acid eluent, 8M, may be to blame for this effect.

Optimization of actinide analysis by HPEC and ICP-MS: In this work several parameters associated with an on-line separation of actinide compounds utilizing ICP-MS detection have been optimized. First, it was determined that the selectivity between different actinides is significantly reduced with the use of oxalic acid. However, the use of a smaller amount of oxalic acid does permit satisfactory selectivity, while reducing the need for instrument maintenance. Second, it was determined that packing columns under pressure is better than manually packing. Columns that are pressure packed elute the five actinides twice as fast as those packed manually; this likely due to the fact that there is less void space in the column. We also determined that while longer columns improve actinide separation, they also increase the overall separation time and result in unacceptably broader peaks. For this reason we recommend using a 3-10 cm column rather than a 30 cm column. We also showed that smaller resin particle size results in sharper, more well defined peaks, though the improvement from 50-150 μm to 20-50 μm is slight. We also demonstrated faster flow rates result in shorter actinide retention time and narrower peaks, though peaks become distorted for flow rates > 4 mL/min and nebulizer efficacy decreases at higher flow rates. For the optimized parameter settings we able to achieve detection limits below 1 pg.

Actinide separation and electrodeposition using HPEC: A system was developed that facilitated the automated separation of actinides by HPEC and the collection of actinide fractions into convenient counting groups for electrodeposition and counting by alpha spectrometry. The separation and collection of Pu, Th, and U was successfully demonstrated. Neptunium was found in all three collection windows that contained

detectable levels of actinides. This was attributed to oxidation state effects whereby Np(V) was collected in the appropriate window, while Np(IV) was collected with the Pu and Th fractions and Np(VI) was collected with the U fraction. Spillover of americium into the Pu and Th collection window was also shown to occur.

APPLICABILITY OF DEVELOPED METHODS TO HEALTH PHYSICS

While most of the individual experiments presented in this work appear to stand alone as self-contained research efforts, they are all related to the development of rapid bioassay methods for determination of radiological uptake, the ultimate project goal. Thus, it is important to examine the extent to which each project achieves meaningful application to internal dosimetry assessment.

^{90}Sr was evaluated by flow scintillation analysis in chapter 3 of this work, where a quantification limit of 47 dpm per sample was established for this technique. The detection limits for ^{90}Sr by ICP-MS and TIMS was found to be 306 dpm and 0.306 dpm, respectively. Therefore, while FSA is a better analytical tool than ICP-MS, it is not as good as TIMS. However, FSA has the distinction of being the best rapid analysis technique for determining ^{90}Sr. Tables A.1 and A.2 show us that by processing 2 mL of straight urine by FSA, we can detect levels of ^{90}Sr from an inhalation uptake that would be expected to cause a 1 in 250 chance of mortality and an ingestion uptake that related to a 1 in 5,000 chance of mortality. Therefore, FSA would be a very useful screening method to identify and assess patients with moderate levels of ^{90}Sr.

^{210}Po was evaluated by flow scintillation analysis in chapter 4 of this work, where a detection limit of 100 dpm per sample was established for this technique. The detection limits for ^{210}Po by ICP-MS and TIMS was found to be 9,970 dpm and 9.97 dpm, respectively. Alpha spectrometry has a detection limit of 0.022 dpm for ^{210}Po with a 24 hour count time. Again, FSA has the distinction of being the best rapid analysis

technique for ^{210}Po. Tables A.3 and A.4 show us that by processing 2 mL of straight urine by FSA, we can detect levels of ^{210}Po from an inhalation uptake that would be expected to cause a 1 in 2 chance of mortality and an ingestion uptake that related to a 1 in 20 chance of mortality. Detection limits for ^{210}Po are much better if more than 2 mL of urine is available for concentration on the column. Therefore, FSA would be a very useful screening method to identify and assess patients with the most serious levels of ^{210}Po.

^{60}Co was evaluated by FGA and FSA in chapter 5 of this work, where a detection limit of 1134 dpm was established for FGA and a detection limit of 494 dpm per sample was determined for FSA. The detection limits for ^{60}Co by ICP-MS and TIMS was found to be 2510 dpm and 2.51 dpm, respectively. FSA is also the best rapid determination technique for this isotope. Tables A.5 and A.6 show us that by processing 2 mL of straight urine by FSA, we can detect levels of ^{60}Co from an inhalation uptake that would be expected to cause a 1 in 100 chance of mortality and an ingestion uptake that related to a 1 in 500 chance of mortality. Therefore, FSA would be a very useful screening method to identify and assess patients with serious levels of ^{60}Co.

^{137}Cs was evaluated by FGA and FSA in chapter 5 of this work, where a detection limit of 440 dpm was established for FGA and a detection limit of 729 dpm per sample was determined for FSA. The detection limits for ^{137}Cs by ICP-MS and TIMS was found to be 193 dpm and 0.193 dpm, respectively. For this isotope, ICP-MS is the best rapid determination technique. Tables A.7 and A.8 show us that by processing 2 mL of straight urine by ICP-MS, we can detect levels of ^{137}Cs from an inhalation uptake that would be expected to cause a 1 in 500 chance of mortality and an ingestion uptake that related to a 1 in 5000 chance of mortality. Therefore, ICP-MS would be a very useful screening method to identify and assess patients with moderate levels of ^{137}Cs.

Actinide isotopes were evaluated by ICP-MS in chapter 6 of this work and by chromatography-aided electrodeposition in chapter 7. Detection limits for these actinides by alpha spectrometry is 0.022 dpm for all isotopes, assuming that they are deposited in counting samples that are free from spectral interferences. Detection limits are more or less constant because backgrounds are uniformly very low and detection efficiency is relatively insensitive to the range of alpha particle energies. The ICP-MS detection limits are also fairly constant at 1 pg; though the activity associated with 1 pg varies widely with the half-life of the actinide from a low of 7.46×10^{-7} dpm for ^{238}U to a high of 38 dpm for ^{238}Pu. Tables A.9-A26 show that for all actinides studied, ICP-MS is the best rapid determination technique; it is capable of detecting very low levels of uptake for all uranium isotopes studied. However, this technique is relatively insensitive for ^{237}Np, ^{239}Pu, ^{242}Pu, ^{241}Am, and ^{243}Am, where it is of limited used unless urine samples are significantly concentrated prior to analysis. ICP-MS is of no use at all in determining ^{238}Pu levels in patients with even lethal uptakes of this isotope; so TIMS or alpha spectrometry must be used if ^{238}Pu uptake is suspected. While both TIMS and alpha spectrometry take 2-3 days to process a sample, alpha spectrometry is likely to be faster because of the greater availability of these instruments. In addition, the technique of chromatography aided electrodeposition, developed in chapter 7, may be able to reduce sample processing time to a firm 2 days for this method.

RECOMMENDATIONS FOR INTERPRETATION AND APPLICATION OF THIS RESEARCH

It is recommended that readers of this work interpret the results and implications of this research in a manor that is consistent with the project goals; which are to create radionuclide screening techniques that are relevant to urine bioassay samples and that are both as rapid and automated as possible. In this context, the best techniques for our purposes are almost never the most sensitive and rigorous techniques available. In the

event that the methods and recommendations developed in this work are put into practice by a public health agency or an analytical lab, it is important to remember that these techniques are intended to be used as rapid screening methods only. There is great benefit in utilizing a rapid analysis method if a mass public uptake is suspected. This allows public health officials to quickly identify persons with the most radioactive uptake so that they may be triaged for appropriate medical intervention, if necessary. However, these initial screenings provide only a limited analysis and follow-up screenings should be made with the most sensitive techniques available, as time permits. In this way, the results of the rapid screening method can be confirmed or refuted. In addition, those with certain low levels of intake may not be identified in the initial screening (due to high detection limits) and may still require some degree of attention. Therefore, if the rapid methods developed herein are used in conjunction subsequent analysis by high sensitivity methods, one can be sure that results will be highly expedient and, eventually, highly accurate. This dual screening approach may be the best way to allay public fears in the event of an RDD event or accident because in the absence of prompt and credible information, people will inevitably fear the worst.

RECOMMENDATIONS FOR FUTURE RESEARCH

The results of the analysis of ^{90}Sr in simulated urine bioassays were highly encouraging; with no loss of recovery for urine samples diluted to 50% and little loss of recovery for fully concentrated urine samples. Some peak broadening, with associated decrease in peak maximum counts, was noted. We recommend conducting further research into optimizing column parameters (length, resin size, and packing pressure) for urine bioassays. We also recomend experimenting with octanol saturated reagents to determine the suitability of this approach to enhance column performance and reproducibility by preserving the integrity of the stationary phase of the Sr columns.

No experiments were performed to determine column longevity with respect to ^{210}Po analysis. A recommended column life of 10 cycles was promoted, but there is really no data to determine column life with any certainty. Therefore, we recommend that further research be conducted to determine the Sr column life as it applies to ^{210}Po analysis. The feasibility of analysis of ^{210}Po in dilute urine matrices was also briefly examined, with encouraging results. Much more work is needed to study the method efficacy for urine analysis of ^{210}Po and to optimize counting parameters. It is also highly recommended that trails involving octanol saturated reagents be conducted to determine if there is enhancement of the ^{210}Po peak shape. Specifically, if one can establish a way of forcing ^{210}Po to elute as one peak, instead of two, detection limits would be substantially enhanced. One may also try to employ various oxidizing and reducing agents as a sample pre-treatment to determine if multiple oxidation states of polonium are causing the analyte to elute in two distinct peaks.

In the FSA analysis of ^{60}Co and ^{137}Cs, it was postulated that the observed detector bias was due to quench effects from the 8M nitric acid used in the load solution. It is possible that by lowering the molarity of nitic acid, less bias will be encountered. We believe that one could reduce the load solution nitric acid concentration to 3M, and still be able to achieve retention of ^{90}Sr, a possible interference.

We also believe that NaI(Tl) detection efficiency can be improved with the addition of extra lead shielding. If a large lead brick cave is built around the detector, the background count rate can be expected to drop, thereby enhancing the signal to noise ratio when a source is present. The addition of a copper or cadmium liner for the detector cave would also further reduce background. This modification can be made easily and without much added cost. Further, we believe that the use of a detector with a larger NaI(Tl) crystal would improve γ-ray detection efficiency since γ-ray stopping power is

proportional to the crystal thickness. This modification would be more costly that the previous, but would have the added bonus of accommodating larger gamma flow cells in the larger well.

Using these improved preparation conditions for actinide analysis by ICP-MS, we anticipate one could improve the automated separation of these analytes for emergency bioassay samples. Future research in this area should consist of examining the properties of other resins and applying results to the separation of actinides from a human urine matrix.

In the HPEC driven actinide separation for electrodeposition experiment, we encountered significant spill over of Am into the Pu/Th collection window. We anticipate that this could be corrected by conducting experiments to incrementally increasing the length of the second counting window until Pu or Th begins to spill over into Window 2. In this way, the collection window for americium may be optimized. Further, neptunium was found in all three collection windows that contained detectable levels of actinides. This was attributed to oxidation state effects. The addition of $NaNO_3$ could reduce higher oxidation states of neptunium to Np(IV), whereby it would be eluted and codepisted with the Pu and Th fractions. Experiments should be done to determine if this hypothesis is correct and if the addition of $NaNO_3$ has any effect on Np elution behavior. The system described in this work has many potential applications. This technique could provide trace actinide analysis (environmental, bioassay, etc.) of high specific activity isotopes where analysis by ICP-MS is not possible, e.g. ^{228}Th, ^{232}U, ^{238}Pu, ^{241}Am, and various curium and californium isotopes. This system could also be used for routine radioanalytical work, where separations that used to take 8 hours can be accomplished in under 15 minutes. Finally, this system could be used in a mobile

laboratory for in-field analysis for environmental monitoring or emergency response situations; since mass spectrometers are not mobile.

OUTLINE OF WORK DONE BY THE AUTHOR

Though this work often uses the preposition, "we," and a narrative tone attributed to, "the authors," most of the work featured herein was done by the sole author of this dissertation. The pluralistic tone of the narrative is in anticipation that several of the chapters featured in this work will eventually be published in peer-reviewed journals, where multiple authors will be credited. The purpose of this section is to clearly outline what work was done by the author of this dissertation, and to credit that work which was not done by the author to the appropriate person or persons.

Chapters 1 and 2 of this work were researched and written exclusively by the author; with comments and recommendations by members of the dissertation committee incorporated into the final draft of these chapters.

Chapters 3, 4, and 5 featured the use of the β-RAM model 4B flow scintillation analyzer. The initial set up of this unit, as well as a very basic tutorial, was provided by the vendor. Since the initial setup, the author has personally made all modifications to the unit, flow cells, and associated periphery equipment. All experiments featured in these chapters were conducted exclusively by the author. In addition, all data analysis was done by the author. Finally, the author singularly wrote all sections of these chapters, incorporating input and recommendations by members of the dissertation committee.

Chapter 5 also featured the use of the tandem flow gamma analyzer. The initial setup and of this unit, as well as a very basic tutorial, were provided by the vendor. Since the initial setup of the of the unit, modifications were made to the signal output of the NaI(Tl) detector. The author was aided in these modifications by Kevin Jackman (fellow

UT Nuclear Engineering doctoral student and now LANL postdoc) and Vince Melito (LANL technician and electrical safety officer). The author was provided with limited labor from these individuals to make the needed modifications and ensure the safety of the modified system. Dr. Jackman also provided a tutorial to the author on operation of the detector and good laboratory practices for gamma counting with a NaI(Tl) detector. Further, the author sought and received advice from Dr. Jackman on methods for data analysis concerning the NaI(Tl) detector; though all calculations were performed by the author, alone.

The work featured in Chapter 6 was largely conducted by Dominic Peterson on the mass spectrometer that he setup and maintains. The author contributed to the work by performing experiments testing variable eluent flow rates and noting peak distortions. The author also recorded the pressure on the line as the flow rate was adjusted so that any compression of the resin could be determined. This work was eventually published in the peer reviewed journal, *Journal of Separation Science* (Peterson 2007). The author's name appears second on that publication. The publication was written and submitted by Dr. Peterson, with input and recommendations by the author. The text and figures appearing in Chapter 6 are largely derivative of the aforementioned publication. Only the introduction and conclusion of this chapter are sections that can be solely attributed to the author.

Chapter 7 featured work performed by the author, Edward Gonzales (LANL staff member), and Claudine Armenta (LANL technician). The author was solely responsible for setup of the chromatography and fraction collection systems. The author also performed all actinide separations and collections himself. Mrs. Armenta was responsible for electrodepositing most of the collected actinide fractions; though the author did perform several, himself, as well. Mr. Gonzales the performed all alpha

counting of these prepared samples using the alpha spectrometers that he maintains. All data analysis was performed by the author. The author was also solely responsible for writing Chapter 7.

Chapters 8 and 9 were researched and written exclusively by the author; with comments and recommendations by members of the dissertation committee incorporated into the final draft of these chapters.

Finally, all chromatography columns were packed by Dr. Peterson, using the column packer that he setup and maintains. Column packing had to be done by Dr. Peterson, because he is the only trained and qualified person in the group to operated the column packer, which is a pressure hazard.

IMPACT OF THIS WORK ON THE FIELD

This body of work evaluates several methods of rapid and automated radionuclide detection in urine or aqueous matrices. Some of these methods are novel (FGA and chromatography-aided electrodeposition), while others are novel applications of pre-existing methods (FSA for determination of ^{210}Po and FSA for determination of bioassay levels of ^{90}Sr in urine). In addition we also present research on the optimization of several counting parameters for the established method of actinide detection by ICP-MS.

While FSA has long been used by the biotech sector for radio-labeling organic compounds (mostly with ^{3}H, ^{14}C, ^{32}P, and ^{22}Na), this technique has seen relatively little use in the field of radioanalytical chemistry. The only use of these instruments for radiochemistry, that the author is aware of, is at the Pacific Northwest National Lab (PNNL) and Clemson University. Therefore, the author can be credited with bringing this underutilized capability to LANL. In addition, radiochemistry research using this instrument has mostly been limited to analysis of high-level nuclear waste; a particularly

well-suited type of sample for this instrument, since it was designed to detect with mCi levels of activity.

The author encountered great difficulty adapting this technique for the analysis of samples that contained only nCi and pCi levels of activity. Though, detection limits of ^{90}Sr and ^{99}Tc have been quoted in some publications, no work has been done with samples exclusively in this low activity range. In addition, this work is the first known application of FSA for ^{90}Sr analysis of urine samples. Since the experiments determining ^{90}Sr in urine were highly successful, they should have a positive impact on the field.

This work also featured research describing the first known detection of ^{210}Po by FSA. This analyte is again very popular in the radioanalytical chemistry field, were it is notorious for being difficult to work with. Typical ^{210}Po takes 3 days to accomplish and there are only a few labs that will perform this analysis. This work presents a ^{210}Po analysis method that is accomplished in only 1 hour, and features instrumentation that completely contains the polonium hazard. In addition, the high degree of automation incorporated into the separation and detection, further improve the safety of ^{210}Po analysis. Therefore, it is reasonable to assume that this work will be well-received and have a positive impact on the field.

The flow gamma analysis of ^{60}Co and ^{137}Cs was less successful at detecting pCi-nCi levels of these analytes. However, the techniques developed in this work may be better applied to higher activity samples (such as high-level nuclear waste). Nevertheless, this is the first attempt known to the author of a system that combines chromatography detection with γ-ray energy discrimination. In addition to FAG, these analytes were also quantified by FSA. While detection peaks attributed to ^{60}Co and ^{137}Cs have been observed in other FSA work (nuclear waste samples), these analytes were treated as interferences of the target analyte (^{90}Sr or ^{99}Tc) and were never quantified.

The research into optimization of actinide analysis by ICP-MS, is no doubt an improvement to the collective knowledge of the field. Optimization research is always appreciated, since many established procedures are used for many years without improvement. This work has already been published in a peer reviewed journal, where it will likely have a positive impact on the field.

The research of actinide separation by HPEC for electrodeposition is still very much a work in progress since we are still encountering neptunium and americium spillover into other collection windows. However, if this work can be optimized it has the potential to be a significant improvement on source preparation for alpha counting. Presently, actinide separation takes approximately 8 hours to accomplish, so there would be great advantage to the field if a technique can be perfected to accomplish the same task in just 15 minutes.

Appendix

Table A.1: ^{90}Sr inhalation risk assessment. Colored lines indicated quantification limits for various analytical techniques. TIMS (pink), ICP-MS (blue), FSA (green).

Morbidity (%)	Chance of Mortality	A Ingest (Bq)	A Absd (Bq)	Urine A (Bq/ml)	2x (Bq/ml)	10x (Bq/ml)	25x (Bq/ml)	50x (Bq/ml)	100x (Bq/ml)	250x (Bq/ml)	500x (Bq/ml)	1000x (Bq/ml)	1440x (Bq/ml)
100	1 in 1	3.52E+08	3.52E+07	2.07E+02	4.15E+02	2.07E+03	5.18E+03	1.04E+04	2.07E+04	5.18E+04	1.04E+05	2.07E+05	2.99E+05
53.5	1 in 2	1.76E+08	1.76E+07	1.04E+02	2.07E+02	1.04E+03	2.59E+03	5.18E+03	1.04E+04	2.59E+04	5.18E+04	1.04E+05	1.49E+05
26.75	1 in 4	8.80E+07	8.80E+06	5.18E+01	1.04E+02	5.18E+02	1.30E+03	2.59E+03	5.18E+03	1.30E+04	2.59E+04	5.18E+04	7.46E+04
21.4	1 in 5	7.04E+07	7.04E+06	4.15E+01	8.29E+01	4.15E+02	1.04E+03	2.07E+03	4.15E+03	1.04E+04	2.07E+04	4.15E+04	5.97E+04
10.7	1 in 10	3.52E+07	3.52E+06	2.07E+01	4.15E+01	2.07E+02	5.18E+02	1.04E+03	2.07E+03	5.18E+03	1.04E+04	2.07E+04	2.99E+04
5.35	1 in 20	1.76E+07	1.76E+06	1.04E+01	2.07E+01	1.04E+02	2.59E+02	5.18E+02	1.04E+03	2.59E+03	5.18E+03	1.04E+04	1.49E+04
2.14	1 in 50	7.04E+06	7.04E+05	4.15E+00	8.29E+00	4.15E+01	1.04E+02	2.07E+02	4.15E+02	1.04E+03	2.07E+03	4.15E+03	5.97E+03
1.07	1 in 100	3.52E+06	3.52E+05	2.07E+00	4.15E+00	2.07E+01	5.18E+01	1.04E+02	2.07E+02	5.18E+02	1.04E+03	2.07E+03	2.99E+03
0.428	1 in 250	1.41E+06	1.41E+05	8.29E-01	1.66E+00	8.29E+00	2.07E+01	4.15E+01	8.29E+01	2.07E+02	4.15E+02	8.29E+02	1.19E+03
0.214	1 in 500	7.04E+05	7.04E+04	4.15E-01	8.29E-01	4.15E+00	1.04E+01	2.07E+01	4.15E+01	1.04E+02	2.07E+02	4.15E+02	5.97E+02
0.107	1 in 1000	3.52E+05	3.52E+04	2.07E-01	4.15E-01	2.07E+00	5.18E+00	1.04E+01	2.07E+01	5.18E+01	1.04E+02	2.07E+02	2.99E+02
0.0214	1 in 5000	7.04E+04	7.04E+03	4.15E-02	8.29E-02	4.15E-01	1.04E+00	2.07E+00	4.15E+00	1.04E+01	2.07E+01	4.15E+01	5.97E+01
0.0107	1 in 10000	3.52E+04	3.52E+03	2.07E-02	4.15E-02	2.07E-01	5.18E-01	1.04E+00	2.07E+00	5.18E+00	1.04E+01	2.07E+01	2.99E+01
0.00214	1 in 50000	7.04E+03	7.04E+02	4.15E-03	8.29E-03	4.15E-02	1.04E-01	2.07E-01	4.15E-01	1.04E+00	2.07E+00	4.15E+00	5.97E+00
0.00107	1 in 100000	3.52E+03	3.52E+02	2.07E-03	4.15E-03	2.07E-02	5.18E-02	1.04E-01	2.07E-01	5.18E-01	1.04E+00	2.07E+00	2.99E+00
0.000214	1 in 500000	7.04E+02	7.04E+01	4.15E-04	8.29E-04	4.15E-03	1.04E-02	2.07E-02	4.15E-02	1.04E-01	2.07E-01	4.15E-01	5.97E-01
0.000107	1 in 1000000	3.52E+02	3.52E+01	2.07E-04	4.15E-04	2.07E-03	5.18E-03	1.04E-02	2.07E-02	5.18E-02	1.04E-01	2.07E-01	2.99E-01

Table A.2: ^{90}Sr ingestion risk assessment. Colored lines indicated quantification limits for various analytical techniques. TIMS (pink), ICP-MS (blue), FSA (green).

Morbidity (%)	Chance of Mortality	A Ingest (Bq)	A Absd (Bq)	Urine A (Bq/ml)	2x (Bq/ml)	10x (Bq/ml)	25x (Bq/ml)	50x (Bq/ml)	100x (Bq/ml)	250x (Bq/ml)	500x (Bq/ml)	1000x (Bq/ml)	1440x (Bq/ml)
100	1 in 1	6.62E+08	1.99E+08	7.80E+03	1.56E+04	7.80E+04	1.95E+05	3.90E+05	7.80E+05	1.95E+06	3.90E+06	7.80E+06	1.12E+07
56.5	1 in 2	3.31E+08	9.93E+07	3.90E+03	7.80E+03	3.90E+04	9.74E+04	1.95E+05	3.90E+05	9.74E+05	1.95E+06	3.90E+06	5.61E+06
28.25	1 in 4	1.66E+08	4.97E+07	1.95E+03	3.90E+03	1.95E+04	4.87E+04	9.74E+04	1.95E+05	4.87E+05	9.74E+05	1.95E+06	2.81E+06
22.6	1 in 5	1.32E+08	3.97E+07	1.56E+03	3.12E+03	1.56E+04	3.90E+04	7.80E+04	1.56E+05	3.90E+05	7.80E+05	1.56E+06	2.25E+06
11.3	1 in 10	6.62E+07	1.99E+07	7.80E+02	1.56E+03	7.80E+03	1.95E+04	3.90E+04	7.80E+04	1.95E+05	3.90E+05	7.80E+05	1.12E+06
5.65	1 in 20	3.31E+07	9.93E+06	3.90E+02	7.80E+02	3.90E+03	9.74E+03	1.95E+04	3.90E+04	9.74E+04	1.95E+05	3.90E+05	5.61E+05
2.26	1 in 50	1.32E+07	3.97E+06	1.56E+02	3.12E+02	1.56E+03	3.90E+03	7.80E+03	1.56E+04	3.90E+04	7.80E+04	1.56E+05	2.25E+05
1.13	1 in 100	6.62E+06	1.99E+06	7.80E+01	1.56E+02	7.80E+02	1.95E+03	3.90E+03	7.80E+03	1.95E+04	3.90E+04	7.80E+04	1.12E+05
0.452	1 in 250	2.65E+06	7.95E+05	3.12E+01	6.24E+01	3.12E+02	7.80E+02	1.56E+03	3.12E+03	7.80E+03	1.56E+04	3.12E+04	4.49E+04
0.226	1 in 500	1.32E+06	3.97E+05	1.56E+01	3.12E+01	1.56E+02	3.90E+02	7.80E+02	1.56E+03	3.90E+03	7.80E+03	1.56E+04	2.25E+04
0.113	1 in 1000	6.62E+05	1.99E+05	7.80E+00	1.56E+01	7.80E+01	1.95E+02	3.90E+02	7.80E+02	1.95E+03	3.90E+03	7.80E+03	1.12E+04
0.0226	1 in 5000	1.32E+05	3.97E+04	1.56E+00	3.12E+00	1.56E+01	3.90E+01	7.80E+01	1.56E+02	3.90E+02	7.80E+02	1.56E+03	2.25E+03
0.0113	1 in 10000	6.62E+04	1.99E+04	7.80E-01	1.56E+00	7.80E+00	1.95E+01	3.90E+01	7.80E+01	1.95E+02	3.90E+02	7.80E+02	1.12E+03
0.00226	1 in 50000	1.32E+04	3.97E+03	1.56E-01	3.12E-01	1.56E+00	3.90E+00	7.80E+00	1.56E+01	3.90E+01	7.80E+01	1.56E+02	2.25E+02
0.00113	1 in 100000	6.62E+03	1.99E+03	7.80E-02	1.56E-01	7.80E-01	1.95E+00	3.90E+00	7.80E+00	1.95E+01	3.90E+01	7.80E+01	1.12E+02
0.000226	1 in 500000	1.32E+03	3.97E+02	1.56E-02	3.12E-02	1.56E-01	3.90E-01	7.80E-01	1.56E+00	3.90E+00	7.80E+00	1.56E+01	2.25E+01
0.000113	1 in 1000000	6.62E+02	1.99E+02	7.80E-03	1.56E-02	7.80E-02	1.95E-01	3.90E-01	7.80E-01	1.95E+00	3.90E+00	7.80E+00	1.12E+01

Table A.3: ^{210}Po inhalation risk assessment. Colored lines indicated quantification limits for various analytical techniques. TIMS (pink), ICP-MS (blue), FSA (green), alpha spectrometry (yellow).

Morbidity (%)	Chance of Mortality	A Ingest (Bq)	A Absd (Bq)	Urine A (Bq/ml)	2x (Bq/ml)	10x (Bq/ml)	25x (Bq/ml)	50x (Bq/ml)	100x (Bq/ml)	250x (Bq/ml)	500x (Bq/ml)	1000x (Bq/ml)	1440x (Bq/ml)
100	1 in 1	3.41E+06	3.41E+05	2.37E+00	4.74E+00	2.37E+01	5.93E+01	1.19E+02	2.37E+02	5.93E+02	1.19E+03	2.37E+03	3.41E+03
53	1 in 2	1.71E+06	1.71E+05	1.19E+00	2.37E+00	1.19E+01	2.96E+01	5.93E+01	1.19E+02	2.96E+02	5.93E+02	1.19E+03	1.71E+03
26.5	1 in 4	8.53E+05	8.53E+04	5.93E-01	1.19E+00	5.93E+00	1.48E+01	2.96E+01	5.93E+01	1.48E+02	2.96E+02	5.93E+02	8.53E+02
21.2	1 in 5	6.83E+05	6.83E+04	4.74E-01	9.48E-01	4.74E+00	1.19E+01	2.37E+01	4.74E+01	1.19E+02	2.37E+02	4.74E+02	6.83E+02
10.6	1 in 10	3.41E+05	3.41E+04	2.37E-01	4.74E-01	2.37E+00	5.93E+00	1.19E+01	2.37E+01	5.93E+01	1.19E+02	2.37E+02	3.41E+02
5.3	1 in 20	1.71E+05	1.71E+04	1.19E-01	2.37E-01	1.19E+00	2.96E+00	5.93E+00	1.19E+01	2.96E+01	5.93E+01	1.19E+02	1.71E+02
2.12	1 in 50	6.83E+04	6.83E+03	4.74E-02	9.48E-02	4.74E-01	1.19E+00	2.37E+00	4.74E+00	1.19E+01	2.37E+01	4.74E+01	6.83E+01
1.06	1 in 100	3.41E+04	3.41E+03	2.37E-02	4.74E-02	2.37E-01	5.93E-01	1.19E+00	2.37E+00	5.93E+00	1.19E+01	2.37E+01	3.41E+01
0.424	1 in 250	1.37E+04	1.37E+03	9.48E-03	1.90E-02	9.48E-02	2.37E-01	4.74E-01	9.48E-01	2.37E+00	4.74E+00	9.48E+00	1.37E+01
0.212	1 in 500	6.83E+03	6.83E+02	4.74E-03	9.48E-03	4.74E-02	1.19E-01	2.37E-01	4.74E-01	1.19E+00	2.37E+00	4.74E+00	6.83E+00
0.106	1 in 1000	3.41E+03	3.41E+02	2.37E-03	4.74E-03	2.37E-02	5.93E-02	1.19E-01	2.37E-01	5.93E-01	1.19E+00	2.37E+00	3.41E+00
0.0212	1 in 5000	6.83E+02	6.83E+01	4.74E-04	9.48E-04	4.74E-03	1.19E-02	2.37E-02	4.74E-02	1.19E-01	2.37E-01	4.74E-01	6.83E-01
0.0106	1 in 10000	3.41E+02	3.41E+01	2.37E-04	4.74E-04	2.37E-03	5.93E-03	1.19E-02	2.37E-02	5.93E-02	1.19E-01	2.37E-01	3.41E-01
0.00212	1 in 50000	6.83E+01	6.83E+00	4.74E-05	9.48E-05	4.74E-04	1.19E-03	2.37E-03	4.74E-03	1.19E-02	2.37E-02	4.74E-02	6.83E-02
0.00106	1 in 100000	3.41E+01	3.41E+00	2.37E-05	4.74E-05	2.37E-04	5.93E-04	1.19E-03	2.37E-03	5.93E-03	1.19E-02	2.37E-02	3.41E-02
0.000212	1 in 500000	6.83E+00	6.83E-01	4.74E-06	9.48E-06	4.74E-05	1.19E-04	2.37E-04	4.74E-04	1.19E-03	2.37E-03	4.74E-03	6.83E-03
0.000106	1 in 1000000	3.41E+00	3.41E-01	2.37E-06	4.74E-06	2.37E-05	5.93E-05	1.19E-04	2.37E-04	5.93E-04	1.19E-03	2.37E-03	3.41E-03

Table A.4: ^{210}Po ingestion risk assessment. Colored lines indicated quantification limits for various analytical techniques. TIMS (pink), ICP-MS (blue), FSA (green), alpha spectrometry (yellow).

Morbidity (%)	Chance of Mortality	A Ingest (Bq)	A Absd (Bq)	Urine A (Bq/ml)	2x (Bq/ml)	10x (Bq/ml)	25x (Bq/ml)	50x (Bq/ml)	100x (Bq/ml)	250x (Bq/ml)	500x (Bq/ml)	1000x (Bq/ml)	1440x (Bq/ml)
100	1 in 1	9.80E+07	9.80E+06	6.81E+01	1.36E+02	6.81E+02	1.70E+03	3.40E+03	6.81E+03	1.70E+04	3.40E+04	6.81E+04	9.80E+04
69	1 in 2	4.90E+07	4.90E+06	3.40E+01	6.81E+01	3.40E+02	8.51E+02	1.70E+03	3.40E+03	8.51E+03	1.70E+04	3.40E+04	4.90E+04
34.5	1 in 4	2.45E+07	2.45E+06	1.70E+01	3.40E+01	1.70E+02	4.26E+02	8.51E+02	1.70E+03	4.26E+03	8.51E+03	1.70E+04	2.45E+04
27.6	1 in 5	1.96E+07	1.96E+06	1.36E+01	2.72E+01	1.36E+02	3.40E+02	6.81E+02	1.36E+03	3.40E+03	6.81E+03	1.36E+04	1.96E+04
13.8	1 in 10	9.80E+06	9.80E+05	6.81E+00	1.36E+01	6.81E+01	1.70E+02	3.40E+02	6.81E+02	1.70E+03	3.40E+03	6.81E+03	9.80E+03
6.9	1 in 20	4.90E+06	4.90E+05	3.40E+00	6.81E+00	3.40E+01	8.51E+01	1.70E+02	3.40E+02	8.51E+02	1.70E+03	3.40E+03	4.90E+03
2.76	1 in 50	1.96E+06	1.96E+05	1.36E+00	2.72E+00	1.36E+01	3.40E+01	6.81E+01	1.36E+02	3.40E+02	6.81E+02	1.36E+03	1.96E+03
1.38	1 in 100	9.80E+05	9.80E+04	6.81E-01	1.36E+00	6.81E+00	1.70E+01	3.40E+01	6.81E+01	1.70E+02	3.40E+02	6.81E+02	9.80E+02
0.552	1 in 250	3.92E+05	3.92E+04	2.72E-01	5.45E-01	2.72E+00	6.81E+00	1.36E+01	2.72E+01	6.81E+01	1.36E+02	2.72E+02	3.92E+02
0.276	1 in 500	1.96E+05	1.96E+04	1.36E-01	2.72E-01	1.36E+00	3.40E+00	6.81E+00	1.36E+01	3.40E+01	6.81E+01	1.36E+02	1.96E+02
0.138	1 in 1000	9.80E+04	9.80E+03	6.81E-02	1.36E-01	6.81E-01	1.70E+00	3.40E+00	6.81E+00	1.70E+01	3.40E+01	6.81E+01	9.80E+01
0.0276	1 in 5000	1.96E+04	1.96E+03	1.36E-02	2.72E-02	1.36E-01	3.40E-01	6.81E-01	1.36E+00	3.40E+00	6.81E+00	1.36E+01	1.96E+01
0.0138	1 in 10000	9.80E+03	9.80E+02	6.81E-03	1.36E-02	6.81E-02	1.70E-01	3.40E-01	6.81E-01	1.70E+00	3.40E+00	6.81E+00	9.80E+00
0.00276	1 in 50000	1.96E+03	1.96E+02	1.36E-03	2.72E-03	1.36E-02	3.40E-02	6.81E-02	1.36E-01	3.40E-01	6.81E-01	1.36E+00	1.96E+00
0.00138	1 in 100000	9.80E+02	9.80E+01	6.81E-04	1.36E-03	6.81E-03	1.70E-02	3.40E-02	6.81E-02	1.70E-01	3.40E-01	6.81E-01	9.80E-01
0.000276	1 in 500000	1.96E+02	1.96E+01	1.36E-04	2.72E-04	1.36E-03	3.40E-03	6.81E-03	1.36E-02	3.40E-02	6.81E-02	1.36E-01	1.96E-01
0.000138	1 in 1000000	9.80E+01	9.80E+00	6.81E-05	1.36E-04	6.81E-04	1.70E-03	3.40E-03	6.81E-03	1.70E-02	3.40E-02	6.81E-02	9.80E-02

Table A.5: ^{60}Co inhalation risk assessment. Colored lines indicated quantification limits for various analytical techniques. TIMS (pink), ICP-MS (blue), FGA (orange), FSA (green).

Morbidity (%)	Chance of Mortality	A Ingest (Bq)	A Absd (Bq)	Urine A (Bq/ml)	2x (Bq/ml)	10x (Bq/ml)	25x (Bq/ml)	50x (Bq/ml)	100x (Bq/ml)	250x (Bq/ml)	500x (Bq/ml)	1000x (Bq/ml)	1440x (Bq/ml)
100	1 in 1	1.03E+09	1.03E+08	9.25E+02	1.85E+03	9.25E+03	2.31E+04	4.63E+04	9.25E+04	2.31E+05	4.63E+05	9.25E+05	1.33E+06
60.5	1 in 2	5.17E+08	5.17E+07	4.63E+02	9.25E+02	4.63E+03	1.16E+04	2.31E+04	4.63E+04	1.16E+05	2.31E+05	4.63E+05	6.66E+05
30.25	1 in 4	2.58E+08	2.58E+07	2.31E+02	4.63E+02	2.31E+03	5.78E+03	1.16E+04	2.31E+04	5.78E+04	1.16E+05	2.31E+05	3.33E+05
24.2	1 in 5	2.07E+08	2.07E+07	1.85E+02	3.70E+02	1.85E+03	4.63E+03	9.25E+03	1.85E+04	4.63E+04	9.25E+04	1.85E+05	2.67E+05
12.1	1 in 10	1.03E+08	1.03E+07	9.25E+01	1.85E+02	9.25E+02	2.31E+03	4.63E+03	9.25E+03	2.31E+04	4.63E+04	9.25E+04	1.33E+05
6.05	1 in 20	5.17E+07	5.17E+06	4.63E+01	9.25E+01	4.63E+02	1.16E+03	2.31E+03	4.63E+03	1.16E+04	2.31E+04	4.63E+04	6.66E+04
2.42	1 in 50	2.07E+07	2.07E+06	1.85E+01	3.70E+01	1.85E+02	4.63E+02	9.25E+02	1.85E+03	4.63E+03	9.25E+03	1.85E+04	2.67E+04
1.21	1 in 100	1.03E+07	1.03E+06	9.25E+00	1.85E+01	9.25E+01	2.31E+02	4.63E+02	9.25E+02	2.31E+03	4.63E+03	9.25E+03	1.33E+04
0.484	1 in 250	4.13E+06	4.13E+05	3.70E+00	7.40E+00	3.70E+01	9.25E+01	1.85E+02	3.70E+02	9.25E+02	1.85E+03	3.70E+03	5.33E+03
0.242	1 in 500	2.07E+06	2.07E+05	1.85E+00	3.70E+00	1.85E+01	4.63E+01	9.25E+01	1.85E+02	4.63E+02	9.25E+02	1.85E+03	2.67E+03
0.121	1 in 1000	1.03E+06	1.03E+05	9.25E-01	1.85E+00	9.25E+00	2.31E+01	4.63E+01	9.25E+01	2.31E+02	4.63E+02	9.25E+02	1.33E+03
0.0242	1 in 5000	2.07E+05	2.07E+04	1.85E-01	3.70E-01	1.85E+00	4.63E+00	9.25E+00	1.85E+01	4.63E+01	9.25E+01	1.85E+02	2.67E+02
0.0121	1 in 10000	1.03E+05	1.03E+04	9.25E-02	1.85E-01	9.25E-01	2.31E+00	4.63E+00	9.25E+00	2.31E+01	4.63E+01	9.25E+01	1.33E+02
0.00242	1 in 50000	2.07E+04	2.07E+03	1.85E-02	3.70E-02	1.85E-01	4.63E-01	9.25E-01	1.85E+00	4.63E+00	9.25E+00	1.85E+01	2.67E+01
0.00121	1 in 100000	1.03E+04	1.03E+03	9.25E-03	1.85E-02	9.25E-02	2.31E-01	4.63E-01	9.25E-01	2.31E+00	4.63E+00	9.25E+00	1.33E+01
0.000242	1 in 500000	2.07E+03	2.07E+02	1.85E-03	3.70E-03	1.85E-02	4.63E-02	9.25E-02	1.85E-01	4.63E-01	9.25E-01	1.85E+00	2.67E+00
0.000121	1 in 1000000	1.03E+03	1.03E+02	9.25E-04	1.85E-03	9.25E-03	2.31E-02	4.63E-02	9.25E-02	2.31E-01	4.63E-01	9.25E-01	1.33E+00

Table A.6: ^{60}Co ingestion risk assessment. Colored lines indicated quantification limits for various analytical techniques. TIMS (pink), ICP-MS (blue), FGA (orange), FSA (green).

Morbidity (%)	Chance of Mortality	A Ingest (Bq)	A Absd (Bq)	Urine A (Bq/ml)	2x (Bq/ml)	10x (Bq/ml)	25x (Bq/ml)	50x (Bq/ml)	100x (Bq/ml)	250x (Bq/ml)	500x (Bq/ml)	1000x (Bq/ml)	1440x (Bq/ml)
100	1 in 1	2.35E+09	2.35E+08	2.11E+03	4.22E+03	2.11E+04	5.27E+04	1.05E+05	2.11E+05	5.27E+05	1.05E+06	2.11E+06	3.04E+06
77.5	1 in 2	1.18E+09	1.18E+08	1.05E+03	2.11E+03	1.05E+04	2.63E+04	5.27E+04	1.05E+05	2.63E+05	5.27E+05	1.05E+06	1.52E+06
38.75	1 in 4	5.88E+08	5.88E+07	5.27E+02	1.05E+03	5.27E+03	1.32E+04	2.63E+04	5.27E+04	1.32E+05	2.63E+05	5.27E+05	7.59E+05
31	1 in 5	4.71E+08	4.71E+07	4.22E+02	8.43E+02	4.22E+03	1.05E+04	2.11E+04	4.22E+04	1.05E+05	2.11E+05	4.22E+05	6.07E+05
15.5	1 in 10	2.35E+08	2.35E+07	2.11E+02	4.22E+02	2.11E+03	5.27E+03	1.05E+04	2.11E+04	5.27E+04	1.05E+05	2.11E+05	3.04E+05
7.75	1 in 20	1.18E+08	1.18E+07	1.05E+02	2.11E+02	1.05E+03	2.63E+03	5.27E+03	1.05E+04	2.63E+04	5.27E+04	1.05E+05	1.52E+05
3.1	1 in 50	4.71E+07	4.71E+06	4.22E+01	8.43E+01	4.22E+02	1.05E+03	2.11E+03	4.22E+03	1.05E+04	2.11E+04	4.22E+04	6.07E+04
1.55	1 in 100	2.35E+07	2.35E+06	2.11E+01	4.22E+01	2.11E+02	5.27E+02	1.05E+03	2.11E+03	5.27E+03	1.05E+04	2.11E+04	3.04E+04
0.62	1 in 250	9.41E+06	9.41E+05	8.43E+00	1.69E+01	8.43E+01	2.11E+02	4.22E+02	8.43E+02	2.11E+03	4.22E+03	8.43E+03	1.21E+04
0.31	1 in 500	4.71E+06	4.71E+05	4.22E+00	8.43E+00	4.22E+01	1.05E+02	2.11E+02	4.22E+02	1.05E+03	2.11E+03	4.22E+03	6.07E+03
0.155	1 in 1000	2.35E+06	2.35E+05	2.11E+00	4.22E+00	2.11E+01	5.27E+01	1.05E+02	2.11E+02	5.27E+02	1.05E+03	2.11E+03	3.04E+03
0.031	1 in 5000	4.71E+05	4.71E+04	4.22E-01	8.43E-01	4.22E+00	1.05E+01	2.11E+01	4.22E+01	1.05E+02	2.11E+02	4.22E+02	6.07E+02
0.0155	1 in 10000	2.35E+05	2.35E+04	2.11E-01	4.22E-01	2.11E+00	5.27E+00	1.05E+01	2.11E+01	5.27E+01	1.05E+02	2.11E+02	3.04E+02
0.0031	1 in 50000	4.71E+04	4.71E+03	4.22E-02	8.43E-02	4.22E-01	1.05E+00	2.11E+00	4.22E+00	1.05E+01	2.11E+01	4.22E+01	6.07E+01
0.00155	1 in 100000	2.35E+04	2.35E+03	2.11E-02	4.22E-02	2.11E-01	5.27E-01	1.05E+00	2.11E+00	5.27E+00	1.05E+01	2.11E+01	3.04E+01
0.00031	1 in 500000	4.71E+03	4.71E+02	4.22E-03	8.43E-03	4.22E-02	1.05E-01	2.11E-01	4.22E-01	1.05E+00	2.11E+00	4.22E+00	6.07E+00
0.000155	1 in 1000000	2.35E+03	2.35E+02	2.11E-03	4.22E-03	2.11E-02	5.27E-02	1.05E-01	2.11E-01	5.27E-01	1.05E+00	2.11E+00	3.04E+00

Table A.7: ^{137}Cs inhalation risk assessment. Colored lines indicated quantification limits for various analytical techniques. TIMS (pink), ICP-MS (blue), FGA (orange), FSA (green).

Morbidity (%)	Chance of Mortality	A Ingest (Bq)	A Absd (Bq)	Urine A (Bq/ml)	2x (Bq/ml)	10x (Bq/ml)	25x (Bq/ml)	50x (Bq/ml)	100x (Bq/ml)	250x (Bq/ml)	500x (Bq/ml)	1000x (Bq/ml)	1440x (Bq/ml)
100	1 in 1	3.12E+09	3.12E+09	1.38E+03	2.76E+03	1.38E+04	3.46E+04	6.91E+04	1.38E+05	3.46E+05	6.91E+05	1.38E+06	1.99E+06
73.5	1 in 2	1.56E+09	1.56E+09	6.91E+02	1.38E+03	6.91E+03	1.73E+04	3.46E+04	6.91E+04	1.73E+05	3.46E+05	6.91E+05	9.95E+05
36.75	1 in 4	7.79E+08	7.79E+08	3.46E+02	6.91E+02	3.46E+03	8.64E+03	1.73E+04	3.46E+04	8.64E+04	1.73E+05	3.46E+05	4.98E+05
29.4	1 in 5	6.23E+08	6.23E+08	2.76E+02	5.53E+02	2.76E+03	6.91E+03	1.38E+04	2.76E+04	6.91E+04	1.38E+05	2.76E+05	3.98E+05
14.7	1 in 10	3.12E+08	3.12E+08	1.38E+02	2.76E+02	1.38E+03	3.46E+03	6.91E+03	1.38E+04	3.46E+04	6.91E+04	1.38E+05	1.99E+05
7.35	1 in 20	1.56E+08	1.56E+08	6.91E+01	1.38E+02	6.91E+02	1.73E+03	3.46E+03	6.91E+03	1.73E+04	3.46E+04	6.91E+04	9.95E+04
2.94	1 in 50	6.23E+07	6.23E+07	2.76E+01	5.53E+01	2.76E+02	6.91E+02	1.38E+03	2.76E+03	6.91E+03	1.38E+04	2.76E+04	3.98E+04
1.47	1 in 100	3.12E+07	3.12E+07	1.38E+01	2.76E+01	1.38E+02	3.46E+02	6.91E+02	1.38E+03	3.46E+03	6.91E+03	1.38E+04	1.99E+04
0.588	1 in 250	1.25E+07	1.25E+07	5.53E+00	1.11E+01	5.53E+01	1.38E+02	2.76E+02	5.53E+02	1.38E+03	2.76E+03	5.53E+03	7.96E+03
0.294	1 in 500	6.23E+06	6.23E+06	2.76E+00	5.53E+00	2.76E+01	6.91E+01	1.38E+02	2.76E+02	6.91E+02	1.38E+03	2.76E+03	3.98E+03
0.147	1 in 1000	3.12E+06	3.12E+06	1.38E+00	2.76E+00	1.38E+01	3.46E+01	6.91E+01	1.38E+02	3.46E+02	6.91E+02	1.38E+03	1.99E+03
0.0294	1 in 5000	6.23E+05	6.23E+05	2.76E-01	5.53E-01	2.76E+00	6.91E+00	1.38E+01	2.76E+01	6.91E+01	1.38E+02	2.76E+02	3.98E+02
0.0147	1 in 10000	3.12E+05	3.12E+05	1.38E-01	2.76E-01	1.38E+00	3.46E+00	6.91E+00	1.38E+01	3.46E+01	6.91E+01	1.38E+02	1.99E+02
0.00294	1 in 50000	6.23E+04	6.23E+04	2.76E-02	5.53E-02	2.76E-01	6.91E-01	1.38E+00	2.76E+00	6.91E+00	1.38E+01	2.76E+01	3.98E+01
0.00147	1 in 100000	3.12E+04	3.12E+04	1.38E-02	2.76E-02	1.38E-01	3.46E-01	6.91E-01	1.38E+00	3.46E+00	6.91E+00	1.38E+01	1.99E+01
0.000294	1 in 500000	6.23E+03	6.23E+03	2.76E-03	5.53E-03	2.76E-02	6.91E-02	1.38E-01	2.76E-01	6.91E-01	1.38E+00	2.76E+00	3.98E+00
0.000147	1 in 1000000	3.12E+03	3.12E+03	1.38E-03	2.76E-03	1.38E-02	3.46E-02	6.91E-02	1.38E-01	3.46E-01	6.91E-01	1.38E+00	1.99E+00

Table A.8: ^{137}Cs ingestion risk assessment. Colored lines indicated quantification limits for various analytical techniques. TIMS (pink), ICP-MS (blue), FGA (orange).

Morbidity (%)	Chance of Mortality	A Ingest (Bq)	A Absd (Bq)	Urine A (Bq/ml)	2x (Bq/ml)	10x (Bq/ml)	25x (Bq/ml)	50x (Bq/ml)	100x (Bq/ml)	250x (Bq/ml)	500x (Bq/ml)	1000x (Bq/ml)	1440x (Bq/ml)
100	1 in 1	1.22E+09	1.22E+09	1.33E+04	2.67E+04	1.33E+05	3.34E+05	6.67E+05	1.33E+06	3.34E+06	6.67E+06	1.33E+07	1.92E+07
72.5	1 in 2	6.08E+08	6.08E+08	6.67E+03	1.33E+04	6.67E+04	1.67E+05	3.34E+05	6.67E+05	1.67E+06	3.34E+06	6.67E+06	9.61E+06
36.25	1 in 4	3.04E+08	3.04E+08	3.34E+03	6.67E+03	3.34E+04	8.34E+04	1.67E+05	3.34E+05	8.34E+05	1.67E+06	3.34E+06	4.81E+06
29	1 in 5	2.43E+08	2.43E+08	2.67E+03	5.34E+03	2.67E+04	6.67E+04	1.33E+05	2.67E+05	6.67E+05	1.33E+06	2.67E+06	3.84E+06
14.5	1 in 10	1.22E+08	1.22E+08	1.33E+03	2.67E+03	1.33E+04	3.34E+04	6.67E+04	1.33E+05	3.34E+05	6.67E+05	1.33E+06	1.92E+06
7.25	1 in 20	6.08E+07	6.08E+07	6.67E+02	1.33E+03	6.67E+03	1.67E+04	3.34E+04	6.67E+04	1.67E+05	3.34E+05	6.67E+05	9.61E+05
2.9	1 in 50	2.43E+07	2.43E+07	2.67E+02	5.34E+02	2.67E+03	6.67E+03	1.33E+04	2.67E+04	6.67E+04	1.33E+05	2.67E+05	3.84E+05
1.45	1 in 100	1.22E+07	1.22E+07	1.33E+02	2.67E+02	1.33E+03	3.34E+03	6.67E+03	1.33E+04	3.34E+04	6.67E+04	1.33E+05	1.92E+05
0.58	1 in 250	4.87E+06	4.87E+06	5.34E+01	1.07E+02	5.34E+02	1.33E+03	2.67E+03	5.34E+03	1.33E+04	2.67E+04	5.34E+04	7.69E+04
0.29	1 in 500	2.43E+06	2.43E+06	2.67E+01	5.34E+01	2.67E+02	6.67E+02	1.33E+03	2.67E+03	6.67E+03	1.33E+04	2.67E+04	3.84E+04
0.145	1 in 1000	1.22E+06	1.22E+06	1.33E+01	2.67E+01	1.33E+02	3.34E+02	6.67E+02	1.33E+03	3.34E+03	6.67E+03	1.33E+04	1.92E+04
0.029	1 in 5000	2.43E+05	2.43E+05	2.67E+00	5.34E+00	2.67E+01	6.67E+01	1.33E+02	2.67E+02	6.67E+02	1.33E+03	2.67E+03	3.84E+03
0.0145	1 in 10000	1.22E+05	1.22E+05	1.33E+00	2.67E+00	1.33E+01	3.34E+01	6.67E+01	1.33E+02	3.34E+02	6.67E+02	1.33E+03	1.92E+03
0.0029	1 in 50000	2.43E+04	2.43E+04	2.67E-01	5.34E-01	2.67E+00	6.67E+00	1.33E+01	2.67E+01	6.67E+01	1.33E+02	2.67E+02	3.84E+02
0.00145	1 in 100000	1.22E+04	1.22E+04	1.33E-01	2.67E-01	1.33E+00	3.34E+00	6.67E+00	1.33E+01	3.34E+01	6.67E+01	1.33E+02	1.92E+02
0.00029	1 in 500000	2.43E+03	2.43E+03	2.67E-02	5.34E-02	2.67E-01	6.67E-01	1.33E+00	2.67E+00	6.67E+00	1.33E+01	2.67E+01	3.84E+01
0.000145	1 in 1000000	1.22E+03	1.22E+03	1.33E-02	2.67E-02	1.33E-01	3.34E-01	6.67E-01	1.33E+00	3.34E+00	6.67E+00	1.33E+01	1.92E+01

Table A.9: ^{233}U inhalation risk assessment. Colored lines indicated quantification limits for various analytical techniques. TIMS (pink), ICP-MS (blue), alpha spectrometry (yellow). For this isotopes the limits for ICP-MS and alpha spectrometry are very similar, so only the limit for ICP-MS is shown.

Morbidity (%)	Chance of Mortality	A Ingest (Bq)	A Absd (Bq)	Urine A (Bq/ml)	2x (Bq/ml)	10x (Bq/ml)	25x (Bq/ml)	50x (Bq/ml)	100x (Bq/ml)	250x (Bq/ml)	500x (Bq/ml)	1000x (Bq/ml)	1440x (Bq/ml)
100	1 in 1	3.19E+06	6.39E+04	8.12E-01	1.62E+00	8.12E+00	2.03E+01	4.06E+01	8.12E+01	2.03E+02	4.06E+02	8.12E+02	1.17E+03
53	1 in 2	1.60E+06	3.19E+04	4.06E-01	8.12E-01	4.06E+00	1.02E+01	2.03E+01	4.06E+01	1.02E+02	2.03E+02	4.06E+02	5.85E+02
26.5	1 in 4	7.99E+05	1.60E+04	2.03E-01	4.06E-01	2.03E+00	5.08E+00	1.02E+01	2.03E+01	5.08E+01	1.02E+02	2.03E+02	2.92E+02
21.2	1 in 5	6.39E+05	1.28E+04	1.62E-01	3.25E-01	1.62E+00	4.06E+00	8.12E+00	1.62E+01	4.06E+01	8.12E+01	1.62E+02	2.34E+02
10.6	1 in 10	3.19E+05	6.39E+03	8.12E-02	1.62E-01	8.12E-01	2.03E+00	4.06E+00	8.12E+00	2.03E+01	4.06E+01	8.12E+01	1.17E+02
5.3	1 in 20	1.60E+05	3.19E+03	4.06E-02	8.12E-02	4.06E-01	1.02E+00	2.03E+00	4.06E+00	1.02E+01	2.03E+01	4.06E+01	5.85E+01
2.12	1 in 50	6.39E+04	1.28E+03	1.62E-02	3.25E-02	1.62E-01	4.06E-01	8.12E-01	1.62E+00	4.06E+00	8.12E+00	1.62E+01	2.34E+01
1.06	1 in 100	3.19E+04	6.39E+02	8.12E-03	1.62E-02	8.12E-02	2.03E-01	4.06E-01	8.12E-01	2.03E+00	4.06E+00	8.12E+00	1.17E+01
0.424	1 in 250	1.28E+04	2.56E+02	3.25E-03	6.50E-03	3.25E-02	8.12E-02	1.62E-01	3.25E-01	8.12E-01	1.62E+00	3.25E+00	4.68E+00
0.212	1 in 500	6.39E+03	1.28E+02	1.62E-03	3.25E-03	1.62E-02	4.06E-02	8.12E-02	1.62E-01	4.06E-01	8.12E-01	1.62E+00	2.34E+00
0.106	1 in 1000	3.19E+03	6.39E+01	8.12E-04	1.62E-03	8.12E-03	2.03E-02	4.06E-02	8.12E-02	2.03E-01	4.06E-01	8.12E-01	1.17E+00
0.0212	1 in 5000	6.39E+02	1.28E+01	1.62E-04	3.25E-04	1.62E-03	4.06E-03	8.12E-03	1.62E-02	4.06E-02	8.12E-02	1.62E-01	2.34E-01
0.0106	1 in 10000	3.19E+02	6.39E+00	8.12E-05	1.62E-04	8.12E-04	2.03E-03	4.06E-03	8.12E-03	2.03E-02	4.06E-02	8.12E-02	1.17E-01
0.00212	1 in 50000	6.39E+01	1.28E+00	1.62E-05	3.25E-05	1.62E-04	4.06E-04	8.12E-04	1.62E-03	4.06E-03	8.12E-03	1.62E-02	2.34E-02
0.00106	1 in 100000	3.19E+01	6.39E-01	8.12E-06	1.62E-05	8.12E-05	2.03E-04	4.06E-04	8.12E-04	2.03E-03	4.06E-03	8.12E-03	1.17E-02
0.000212	1 in 500000	6.39E+00	1.28E-01	1.62E-06	3.25E-06	1.62E-05	4.06E-05	8.12E-05	1.62E-04	4.06E-04	8.12E-04	1.62E-03	2.34E-03
0.000106	1 in 1000000	3.19E+00	6.39E-02	8.12E-07	1.62E-06	8.12E-06	2.03E-05	4.06E-05	8.12E-05	2.03E-04	4.06E-04	8.12E-04	1.17E-03

Table A.10: ^{233}U ingestion risk assessment. Colored lines indicated quantification limits for various analytical techniques. TIMS (pink), ICP-MS (blue), alpha spectrometry (yellow).

Morbidity (%)	Chance of Mortality	A Ingest (Bq)	A Absd (Bq)	Urine A (Bq/ml)	2x (Bq/ml)	10x (Bq/ml)	25x (Bq/ml)	50x (Bq/ml)	100x (Bq/ml)	250x (Bq/ml)	500x (Bq/ml)	1000x (Bq/ml)	1440x (Bq/ml)
100	1 in 1	5.15E+08	1.03E+07	9.02E+01	1.80E+02	9.02E+02	2.26E+03	4.51E+03	9.02E+03	2.26E+04	4.51E+04	9.02E+04	1.30E+05
77	1 in 2	2.58E+08	5.15E+06	4.51E+01	9.02E+01	4.51E+02	1.13E+03	2.26E+03	4.51E+03	1.13E+04	2.26E+04	4.51E+04	6.49E+04
38.5	1 in 4	1.29E+08	2.58E+06	2.26E+01	4.51E+01	2.26E+02	5.64E+02	1.13E+03	2.26E+03	5.64E+03	1.13E+04	2.26E+04	3.25E+04
30.8	1 in 5	1.03E+08	2.06E+06	1.80E+01	3.61E+01	1.80E+02	4.51E+02	9.02E+02	1.80E+03	4.51E+03	9.02E+03	1.80E+04	2.60E+04
15.4	1 in 10	5.15E+07	1.03E+06	9.02E+00	1.80E+01	9.02E+01	2.26E+02	4.51E+02	9.02E+02	2.26E+03	4.51E+03	9.02E+03	1.30E+04
7.7	1 in 20	2.58E+07	5.15E+05	4.51E+00	9.02E+00	4.51E+01	1.13E+02	2.26E+02	4.51E+02	1.13E+03	2.26E+03	4.51E+03	6.49E+03
3.08	1 in 50	1.03E+07	2.06E+05	1.80E+00	3.61E+00	1.80E+01	4.51E+01	9.02E+01	1.80E+02	4.51E+02	9.02E+02	1.80E+03	2.60E+03
1.54	1 in 100	5.15E+06	1.03E+05	9.02E-01	1.80E+00	9.02E+00	2.26E+01	4.51E+01	9.02E+01	2.26E+02	4.51E+02	9.02E+02	1.30E+03
0.616	1 in 250	2.06E+06	4.12E+04	3.61E-01	7.22E-01	3.61E+00	9.02E+00	1.80E+01	3.61E+01	9.02E+01	1.80E+02	3.61E+02	5.20E+02
0.308	1 in 500	1.03E+06	2.06E+04	1.80E-01	3.61E-01	1.80E+00	4.51E+00	9.02E+00	1.80E+01	4.51E+01	9.02E+01	1.80E+02	2.60E+02
0.154	1 in 1000	5.15E+05	1.03E+04	9.02E-02	1.80E-01	9.02E-01	2.26E+00	4.51E+00	9.02E+00	2.26E+01	4.51E+01	9.02E+01	1.30E+02
0.0308	1 in 5000	1.03E+05	2.06E+03	1.80E-02	3.61E-02	1.80E-01	4.51E-01	9.02E-01	1.80E+00	4.51E+00	9.02E+00	1.80E+01	2.60E+01
0.0154	1 in 10000	5.15E+04	1.03E+03	9.02E-03	1.80E-02	9.02E-02	2.26E-01	4.51E-01	9.02E-01	2.26E+00	4.51E+00	9.02E+00	1.30E+01
0.00308	1 in 50000	1.03E+04	2.06E+02	1.80E-03	3.61E-03	1.80E-02	4.51E-02	9.02E-02	1.80E-01	4.51E-01	9.02E-01	1.80E+00	2.60E+00
0.00154	1 in 100000	5.15E+03	1.03E+02	9.02E-04	1.80E-03	9.02E-03	2.26E-02	4.51E-02	9.02E-02	2.26E-01	4.51E-01	9.02E-01	1.30E+00
0.000308	1 in 500000	1.03E+03	2.06E+01	1.80E-04	3.61E-04	1.80E-03	4.51E-03	9.02E-03	1.80E-02	4.51E-02	9.02E-02	1.80E-01	2.60E-01
0.000154	1 in 1000000	5.15E+02	1.03E+01	9.02E-05	1.80E-04	9.02E-04	2.26E-03	4.51E-03	9.02E-03	2.26E-02	4.51E-02	9.02E-02	1.30E-01

Table A.11: ^{235}U inhalation risk assessment. Colored lines indicated quantification limits for various analytical techniques. ICP-MS (blue), alpha spectrometry (yellow).

Morbidity (%)	Chance of Mortality	A Ingest (Bq)	A Absd (Bq)	Urine A (Bq/ml)	2x (Bq/ml)	10x (Bq/ml)	25x (Bq/ml)	50x (Bq/ml)	100x (Bq/ml)	250x (Bq/ml)	500x (Bq/ml)	1000x (Bq/ml)	1440x (Bq/ml)
100	1 in 1	3.66E+06	7.33E+04	9.31E-01	1.86E+00	9.31E+00	2.33E+01	4.66E+01	9.31E+01	2.33E+02	4.66E+02	9.31E+02	1.34E+03
53	1 in 2	1.83E+06	3.66E+04	4.66E-01	9.31E-01	4.66E+00	1.16E+01	2.33E+01	4.66E+01	1.16E+02	2.33E+02	4.66E+02	6.70E+02
26.5	1 in 4	9.16E+05	1.83E+04	2.33E-01	4.66E-01	2.33E+00	5.82E+00	1.16E+01	2.33E+01	5.82E+01	1.16E+02	2.33E+02	3.35E+02
21.2	1 in 5	7.33E+05	1.47E+04	1.86E-01	3.72E-01	1.86E+00	4.66E+00	9.31E+00	1.86E+01	4.66E+01	9.31E+01	1.86E+02	2.68E+02
10.6	1 in 10	3.66E+05	7.33E+03	9.31E-02	1.86E-01	9.31E-01	2.33E+00	4.66E+00	9.31E+00	2.33E+01	4.66E+01	9.31E+01	1.34E+02
5.3	1 in 20	1.83E+05	3.66E+03	4.66E-02	9.31E-02	4.66E-01	1.16E+00	2.33E+00	4.66E+00	1.16E+01	2.33E+01	4.66E+01	6.70E+01
2.12	1 in 50	7.33E+04	1.47E+03	1.86E-02	3.72E-02	1.86E-01	4.66E-01	9.31E-01	1.86E+00	4.66E+00	9.31E+00	1.86E+01	2.68E+01
1.06	1 in 100	3.66E+04	7.33E+02	9.31E-03	1.86E-02	9.31E-02	2.33E-01	4.66E-01	9.31E-01	2.33E+00	4.66E+00	9.31E+00	1.34E+01
0.424	1 in 250	1.47E+04	2.93E+02	3.72E-03	7.45E-03	3.72E-02	9.31E-02	1.86E-01	3.72E-01	9.31E-01	1.86E+00	3.72E+00	5.36E+00
0.212	1 in 500	7.33E+03	1.47E+02	1.86E-03	3.72E-03	1.86E-02	4.66E-02	9.31E-02	1.86E-01	4.66E-01	9.31E-01	1.86E+00	2.68E+00
0.106	1 in 1000	3.66E+03	7.33E+01	9.31E-04	1.86E-03	9.31E-03	2.33E-02	4.66E-02	9.31E-02	2.33E-01	4.66E-01	9.31E-01	1.34E+00
0.0212	1 in 5000	7.33E+02	1.47E+01	1.86E-04	3.72E-04	1.86E-03	4.66E-03	9.31E-03	1.86E-02	4.66E-02	9.31E-02	1.86E-01	2.68E-01
0.0106	1 in 10000	3.66E+02	7.33E+00	9.31E-05	1.86E-04	9.31E-04	2.33E-03	4.66E-03	9.31E-03	2.33E-02	4.66E-02	9.31E-02	1.34E-01
0.00212	1 in 50000	7.33E+01	1.47E+00	1.86E-05	3.72E-05	1.86E-04	4.66E-04	9.31E-04	1.86E-03	4.66E-03	9.31E-03	1.86E-02	2.68E-02
0.00106	1 in 100000	3.66E+01	7.33E-01	9.31E-06	1.86E-05	9.31E-05	2.33E-04	4.66E-04	9.31E-04	2.33E-03	4.66E-03	9.31E-03	1.34E-02
0.000212	1 in 500000	7.33E+00	1.47E-01	1.86E-06	3.72E-06	1.86E-05	4.66E-05	9.31E-05	1.86E-04	4.66E-04	9.31E-04	1.86E-03	2.68E-03
0.000106	1 in 1000000	3.66E+00	7.33E-02	9.31E-07	1.86E-06	9.31E-06	2.33E-05	4.66E-05	9.31E-05	2.33E-04	4.66E-04	9.31E-04	1.34E-03

Table A.12: ^{235}U ingestion risk assessment. Colored lines indicated quantification limits for various analytical techniques. ICP-MS (blue), alpha spectrometry (yellow).

Morbidity (%)	Chance of Mortality	A Ingest (Bq)	A Absd (Bq)	Urine A (Bq/ml)	2x (Bq/ml)	10x (Bq/ml)	25x (Bq/ml)	50x (Bq/ml)	100x (Bq/ml)	250x (Bq/ml)	500x (Bq/ml)	1000x (Bq/ml)	1440x (Bq/ml)
100	1 in 1	5.24E+08	1.05E+07	9.16E+01	1.83E+02	9.16E+02	2.29E+03	4.58E+03	9.16E+03	2.29E+04	4.58E+04	9.16E+04	1.32E+05
77	1 in 2	2.62E+08	5.24E+06	4.58E+01	9.16E+01	4.58E+02	1.15E+03	2.29E+03	4.58E+03	1.15E+04	2.29E+04	4.58E+04	6.60E+04
38.5	1 in 4	1.31E+08	2.62E+06	2.29E+01	4.58E+01	2.29E+02	5.73E+02	1.15E+03	2.29E+03	5.73E+03	1.15E+04	2.29E+04	3.30E+04
30.8	1 in 5	1.05E+08	2.09E+06	1.83E+01	3.66E+01	1.83E+02	4.58E+02	9.16E+02	1.83E+03	4.58E+03	9.16E+03	1.83E+04	2.64E+04
15.4	1 in 10	5.24E+07	1.05E+06	9.16E+00	1.83E+01	9.16E+01	2.29E+02	4.58E+02	9.16E+02	2.29E+03	4.58E+03	9.16E+03	1.32E+04
7.7	1 in 20	2.62E+07	5.24E+05	4.58E+00	9.16E+00	4.58E+01	1.15E+02	2.29E+02	4.58E+02	1.15E+03	2.29E+03	4.58E+03	6.60E+03
3.08	1 in 50	1.05E+07	2.09E+05	1.83E+00	3.66E+00	1.83E+01	4.58E+01	9.16E+01	1.83E+02	4.58E+02	9.16E+02	1.83E+03	2.64E+03
1.54	1 in 100	5.24E+06	1.05E+05	9.16E-01	1.83E+00	9.16E+00	2.29E+01	4.58E+01	9.16E+01	2.29E+02	4.58E+02	9.16E+02	1.32E+03
0.616	1 in 250	2.09E+06	4.19E+04	3.66E-01	7.33E-01	3.66E+00	9.16E+00	1.83E+01	3.66E+01	9.16E+01	1.83E+02	3.66E+02	5.28E+02
0.308	1 in 500	1.05E+06	2.09E+04	1.83E-01	3.66E-01	1.83E+00	4.58E+00	9.16E+00	1.83E+01	4.58E+01	9.16E+01	1.83E+02	2.64E+02
0.154	1 in 1000	5.24E+05	1.05E+04	9.16E-02	1.83E-01	9.16E-01	2.29E+00	4.58E+00	9.16E+00	2.29E+01	4.58E+01	9.16E+01	1.32E+02
0.0308	1 in 5000	1.05E+05	2.09E+03	1.83E-02	3.66E-02	1.83E-01	4.58E-01	9.16E-01	1.83E+00	4.58E+00	9.16E+00	1.83E+01	2.64E+01
0.0154	1 in 10000	5.24E+04	1.05E+03	9.16E-03	1.83E-02	9.16E-02	2.29E-01	4.58E-01	9.16E-01	2.29E+00	4.58E+00	9.16E+00	1.32E+01
0.00308	1 in 50000	1.05E+04	2.09E+02	1.83E-03	3.66E-03	1.83E-02	4.58E-02	9.16E-02	1.83E-01	4.58E-01	9.16E-01	1.83E+00	2.64E+00
0.00154	1 in 100000	5.24E+03	1.05E+02	9.16E-04	1.83E-03	9.16E-03	2.29E-02	4.58E-02	9.16E-02	2.29E-01	4.58E-01	9.16E-01	1.32E+00
0.000308	1 in 500000	1.05E+03	2.09E+01	1.83E-04	3.66E-04	1.83E-03	4.58E-03	9.16E-03	1.83E-02	4.58E-02	9.16E-02	1.83E-01	2.64E-01
0.000154	1 in 1000000	5.24E+02	1.05E+01	9.16E-05	1.83E-04	9.16E-04	2.29E-03	4.58E-03	9.16E-03	2.29E-02	4.58E-02	9.16E-02	1.32E-01

Table A.13: ^{238}U inhalation risk assessment. Colored lines indicated quantification limits for various analytical techniques. ICP-MS (blue), alpha spectrometry (yellow).

Morbidity (%)	Chance of Mortality	A Ingest (Bq)	A Absd (Bq)	Urine A (Bq/ml)	2x (Bq/ml)	10x (Bq/ml)	25x (Bq/ml)	50x (Bq/ml)	100x (Bq/ml)	250x (Bq/ml)	500x (Bq/ml)	1000x (Bq/ml)	1440x (Bq/ml)
100	1 in 1	3.97E+06	7.94E+04	1.01E+00	2.02E+00	1.01E+01	2.52E+01	5.04E+01	1.01E+02	2.52E+02	5.04E+02	1.01E+03	1.45E+03
53	1 in 2	1.98E+06	3.97E+04	5.04E-01	1.01E+00	5.04E+00	1.26E+01	2.52E+01	5.04E+01	1.26E+02	2.52E+02	5.04E+02	7.26E+02
26.5	1 in 4	9.92E+05	1.98E+04	2.52E-01	5.04E-01	2.52E+00	6.30E+00	1.26E+01	2.52E+01	6.30E+01	1.26E+02	2.52E+02	3.63E+02
21.2	1 in 5	7.94E+05	1.59E+04	2.02E-01	4.03E-01	2.02E+00	5.04E+00	1.01E+01	2.02E+01	5.04E+01	1.01E+02	2.02E+02	2.90E+02
10.6	1 in 10	3.97E+05	7.94E+03	1.01E-01	2.02E-01	1.01E+00	2.52E+00	5.04E+00	1.01E+01	2.52E+01	5.04E+01	1.01E+02	1.45E+02
5.3	1 in 20	1.98E+05	3.97E+03	5.04E-02	1.01E-01	5.04E-01	1.26E+00	2.52E+00	5.04E+00	1.26E+01	2.52E+01	5.04E+01	7.26E+01
2.12	1 in 50	7.94E+04	1.59E+03	2.02E-02	4.03E-02	2.02E-01	5.04E-01	1.01E+00	2.02E+00	5.04E+00	1.01E+01	2.02E+01	2.90E+01
1.06	1 in 100	3.97E+04	7.94E+02	1.01E-02	2.02E-02	1.01E-01	2.52E-01	5.04E-01	1.01E+00	2.52E+00	5.04E+00	1.01E+01	1.45E+01
0.424	1 in 250	1.59E+04	3.17E+02	4.03E-03	8.07E-03	4.03E-02	1.01E-01	2.02E-01	4.03E-01	1.01E+00	2.02E+00	4.03E+00	5.81E+00
0.212	1 in 500	7.94E+03	1.59E+02	2.02E-03	4.03E-03	2.02E-02	5.04E-02	1.01E-01	2.02E-01	5.04E-01	1.01E+00	2.02E+00	2.90E+00
0.106	1 in 1000	3.97E+03	7.94E+01	1.01E-03	2.02E-03	1.01E-02	2.52E-02	5.04E-02	1.01E-01	2.52E-01	5.04E-01	1.01E+00	1.45E+00
0.0212	1 in 5000	7.94E+02	1.59E+01	2.02E-04	4.03E-04	2.02E-03	5.04E-03	1.01E-02	2.02E-02	5.04E-02	1.01E-01	2.02E-01	2.90E-01
0.0106	1 in 10000	3.97E+02	7.94E+00	1.01E-04	2.02E-04	1.01E-03	2.52E-03	5.04E-03	1.01E-02	2.52E-02	5.04E-02	1.01E-01	1.45E-01
0.00212	1 in 50000	7.94E+01	1.59E+00	2.02E-05	4.03E-05	2.02E-04	5.04E-04	1.01E-03	2.02E-03	5.04E-03	1.01E-02	2.02E-02	2.90E-02
0.00106	1 in 100000	3.97E+01	7.94E-01	1.01E-05	2.02E-05	1.01E-04	2.52E-04	5.04E-04	1.01E-03	2.52E-03	5.04E-03	1.01E-02	1.45E-02
0.000212	1 in 500000	7.94E+00	1.59E-01	2.02E-06	4.03E-06	2.02E-05	5.04E-05	1.01E-04	2.02E-04	5.04E-04	1.01E-03	2.02E-03	2.90E-03
0.000106	1 in 1000000	3.97E+00	7.94E-02	1.01E-06	2.02E-06	1.01E-05	2.52E-05	5.04E-05	1.01E-04	2.52E-04	5.04E-04	1.01E-03	1.45E-03

Table A.14: ^{238}U ingestion risk assessment. Colored lines indicated quantification limits for various analytical techniques. ICP-MS (blue), alpha spectrometry (yellow).

Morbidity (%)	Chance of Mortality	A Ingest (Bq)	A Absd (Bq)	Urine A (Bq/ml)	2x (Bq/ml)	10x (Bq/ml)	25x (Bq/ml)	50x (Bq/ml)	100x (Bq/ml)	250x (Bq/ml)	500x (Bq/ml)	1000x (Bq/ml)	1440x (Bq/ml)
100	1 in 1	5.78E+08	1.16E+07	1.01E+02	2.02E+02	1.01E+03	2.53E+03	5.06E+03	1.01E+04	2.53E+04	5.06E+04	1.01E+05	1.46E+05
76.5	1 in 2	2.89E+08	5.78E+06	5.06E+01	1.01E+02	5.06E+02	1.26E+03	2.53E+03	5.06E+03	1.26E+04	2.53E+04	5.06E+04	7.28E+04
38.25	1 in 4	1.45E+08	2.89E+06	2.53E+01	5.06E+01	2.53E+02	6.32E+02	1.26E+03	2.53E+03	6.32E+03	1.26E+04	2.53E+04	3.64E+04
30.6	1 in 5	1.16E+08	2.31E+06	2.02E+01	4.05E+01	2.02E+02	5.06E+02	1.01E+03	2.02E+03	5.06E+03	1.01E+04	2.02E+04	2.91E+04
15.3	1 in 10	5.78E+07	1.16E+06	1.01E+01	2.02E+01	1.01E+02	2.53E+02	5.06E+02	1.01E+03	2.53E+03	5.06E+03	1.01E+04	1.46E+04
7.65	1 in 20	2.89E+07	5.78E+05	5.06E+00	1.01E+01	5.06E+01	1.26E+02	2.53E+02	5.06E+02	1.26E+03	2.53E+03	5.06E+03	7.28E+03
3.06	1 in 50	1.16E+07	2.31E+05	2.02E+00	4.05E+00	2.02E+01	5.06E+01	1.01E+02	2.02E+02	5.06E+02	1.01E+03	2.02E+03	2.91E+03
1.53	1 in 100	5.78E+06	1.16E+05	1.01E+00	2.02E+00	1.01E+01	2.53E+01	5.06E+01	1.01E+02	2.53E+02	5.06E+02	1.01E+03	1.46E+03
0.612	1 in 250	2.31E+06	4.62E+04	4.05E-01	8.09E-01	4.05E+00	1.01E+01	2.02E+01	4.05E+01	1.01E+02	2.02E+02	4.05E+02	5.83E+02
0.306	1 in 500	1.16E+06	2.31E+04	2.02E-01	4.05E-01	2.02E+00	5.06E+00	1.01E+01	2.02E+01	5.06E+01	1.01E+02	2.02E+02	2.91E+02
0.153	1 in 1000	5.78E+05	1.16E+04	1.01E-01	2.02E-01	1.01E+00	2.53E+00	5.06E+00	1.01E+01	2.53E+01	5.06E+01	1.01E+02	1.46E+02
0.0306	1 in 5000	1.16E+05	2.31E+03	2.02E-02	4.05E-02	2.02E-01	5.06E-01	1.01E+00	2.02E+00	5.06E+00	1.01E+01	2.02E+01	2.91E+01
0.0153	1 in 10000	5.78E+04	1.16E+03	1.01E-02	2.02E-02	1.01E-01	2.53E-01	5.06E-01	1.01E+00	2.53E+00	5.06E+00	1.01E+01	1.46E+01
0.00306	1 in 50000	1.16E+04	2.31E+02	2.02E-03	4.05E-03	2.02E-02	5.06E-02	1.01E-01	2.02E-01	5.06E-01	1.01E+00	2.02E+00	2.91E+00
0.00153	1 in 100000	5.78E+03	1.16E+02	1.01E-03	2.02E-03	1.01E-02	2.53E-02	5.06E-02	1.01E-01	2.53E-01	5.06E-01	1.01E+00	1.46E+00
0.000306	1 in 500000	1.16E+03	2.31E+01	2.02E-04	4.05E-04	2.02E-03	5.06E-03	1.01E-02	2.02E-02	5.06E-02	1.01E-01	2.02E-01	2.91E-01
0.000153	1 in 1000000	5.78E+02	1.16E+01	1.01E-04	2.02E-04	1.01E-03	2.53E-03	5.06E-03	1.01E-02	2.53E-02	5.06E-02	1.01E-01	1.46E-01

Table A.15: ^{237}Np inhalation risk assessment. Colored lines indicated quantification limits for various analytical techniques. TIMS (pink), ICP-MS (blue), alpha spectrometry (yellow).

Morbidity (%)	Chance of Mortality	A Ingest (Bq)	A Absd (Bq)	Urine A (Bq/ml)	2x (Bq/ml)	10x (Bq/ml)	25x (Bq/ml)	50x (Bq/ml)	100x (Bq/ml)	250x (Bq/ml)	500x (Bq/ml)	1000x (Bq/ml)	1440x (Bq/ml)
100	1 in 1	2.09E+06	1.04E+03	3.89E-03	7.79E-03	3.89E-02	9.73E-02	1.95E-01	3.89E-01	9.73E-01	1.95E+00	3.89E+00	5.61E+00
57.5	1 in 2	1.04E+06	5.22E+02	1.95E-03	3.89E-03	1.95E-02	4.87E-02	9.73E-02	1.95E-01	4.87E-01	9.73E-01	1.95E+00	2.80E+00
28.75	1 in 4	5.22E+05	2.61E+02	9.73E-04	1.95E-03	9.73E-03	2.43E-02	4.87E-02	9.73E-02	2.43E-01	4.87E-01	9.73E-01	1.40E+00
23	1 in 5	4.18E+05	2.09E+02	7.79E-04	1.56E-03	7.79E-03	1.95E-02	3.89E-02	7.79E-02	1.95E-01	3.89E-01	7.79E-01	1.12E+00
11.5	1 in 10	2.09E+05	1.04E+02	3.89E-04	7.79E-04	3.89E-03	9.73E-03	1.95E-02	3.89E-02	9.73E-02	1.95E-01	3.89E-01	5.61E-01
5.75	1 in 20	1.04E+05	5.22E+01	1.95E-04	3.89E-04	1.95E-03	4.87E-03	9.73E-03	1.95E-02	4.87E-02	9.73E-02	1.95E-01	2.80E-01
2.3	1 in 50	4.18E+04	2.09E+01	7.79E-05	1.56E-04	7.79E-04	1.95E-03	3.89E-03	7.79E-03	1.95E-02	3.89E-02	7.79E-02	1.12E-01
1.15	1 in 100	2.09E+04	1.04E+01	3.89E-05	7.79E-05	3.89E-04	9.73E-04	1.95E-03	3.89E-03	9.73E-03	1.95E-02	3.89E-02	5.61E-02
0.46	1 in 250	8.35E+03	4.18E+00	1.56E-05	3.11E-05	1.56E-04	3.89E-04	7.79E-04	1.56E-03	3.89E-03	7.79E-03	1.56E-02	2.24E-02
0.23	1 in 500	4.18E+03	2.09E+00	7.79E-06	1.56E-05	7.79E-05	1.95E-04	3.89E-04	7.79E-04	1.95E-03	3.89E-03	7.79E-03	1.12E-02
0.115	1 in 1000	2.09E+03	1.04E+00	3.89E-06	7.79E-06	3.89E-05	9.73E-05	1.95E-04	3.89E-04	9.73E-04	1.95E-03	3.89E-03	5.61E-03
0.023	1 in 5000	4.18E+02	2.09E-01	7.79E-07	1.56E-06	7.79E-06	1.95E-05	3.89E-05	7.79E-05	1.95E-04	3.89E-04	7.79E-04	1.12E-03
0.0115	1 in 10000	2.09E+02	1.04E-01	3.89E-07	7.79E-07	3.89E-06	9.73E-06	1.95E-05	3.89E-05	9.73E-05	1.95E-04	3.89E-04	5.61E-04
0.0023	1 in 50000	4.18E+01	2.09E-02	7.79E-08	1.56E-07	7.79E-07	1.95E-06	3.89E-06	7.79E-06	1.95E-05	3.89E-05	7.79E-05	1.12E-04
0.00115	1 in 100000	2.09E+01	1.04E-02	3.89E-08	7.79E-08	3.89E-07	9.73E-07	1.95E-06	3.89E-06	9.73E-06	1.95E-05	3.89E-05	5.61E-05
0.00023	1 in 500000	4.18E+00	2.09E-03	7.79E-09	1.56E-08	7.79E-08	1.95E-07	3.89E-07	7.79E-07	1.95E-06	3.89E-06	7.79E-06	1.12E-05
0.000115	1 in 1000000	2.09E+00	1.04E-03	3.89E-09	7.79E-09	3.89E-08	9.73E-08	1.95E-07	3.89E-07	9.73E-07	1.95E-06	3.89E-06	5.61E-06

Table A.16: ^{237}Np ingestion risk assessment. Colored lines indicated quantification limits for various analytical techniques. TIMS (pink), ICP-MS (blue), alpha spectrometry (yellow).

Morbidity (%)	Chance of Mortality	A Ingest (Bq)	A Absd (Bq)	Urine A (Bq/ml)	2x (Bq/ml)	10x (Bq/ml)	25x (Bq/ml)	50x (Bq/ml)	100x (Bq/ml)	250x (Bq/ml)	500x (Bq/ml)	1000x (Bq/ml)	1440x (Bq/ml)
100	1 in 1	2.09E+06	1.04E+03	7.08E-05	1.42E-04	7.08E-04	1.77E-03	3.54E-03	7.08E-03	1.77E-02	3.54E-02	7.08E-02	1.02E-01
76	1 in 2	1.04E+06	5.22E+02	3.54E-05	7.08E-05	3.54E-04	8.85E-04	1.77E-03	3.54E-03	8.85E-03	1.77E-02	3.54E-02	5.10E-02
38	1 in 4	5.22E+05	2.61E+02	1.77E-05	3.54E-05	1.77E-04	4.43E-04	8.85E-04	1.77E-03	4.43E-03	8.85E-03	1.77E-02	2.55E-02
30.4	1 in 5	4.18E+05	2.09E+02	1.42E-05	2.83E-05	1.42E-04	3.54E-04	7.08E-04	1.42E-03	3.54E-03	7.08E-03	1.42E-02	2.04E-02
15.2	1 in 10	2.09E+05	1.04E+02	7.08E-06	1.42E-05	7.08E-05	1.77E-04	3.54E-04	7.08E-04	1.77E-03	3.54E-03	7.08E-03	1.02E-02
7.6	1 in 20	1.04E+05	5.22E+01	3.54E-06	7.08E-06	3.54E-05	8.85E-05	1.77E-04	3.54E-04	8.85E-04	1.77E-03	3.54E-03	5.10E-03
3.04	1 in 50	4.18E+04	2.09E+01	1.42E-06	2.83E-06	1.42E-05	3.54E-05	7.08E-05	1.42E-04	3.54E-04	7.08E-04	1.42E-03	2.04E-03
1.52	1 in 100	2.09E+04	1.04E+01	7.08E-07	1.42E-06	7.08E-06	1.77E-05	3.54E-05	7.08E-05	1.77E-04	3.54E-04	7.08E-04	1.02E-03
0.608	1 in 250	8.35E+03	4.18E+00	2.83E-07	5.67E-07	2.83E-06	7.08E-06	1.42E-05	2.83E-05	7.08E-05	1.42E-04	2.83E-04	4.08E-04
0.304	1 in 500	4.18E+03	2.09E+00	1.42E-07	2.83E-07	1.42E-06	3.54E-06	7.08E-06	1.42E-05	3.54E-05	7.08E-05	1.42E-04	2.04E-04
0.152	1 in 1000	2.09E+03	1.04E+00	7.08E-08	1.42E-07	7.08E-07	1.77E-06	3.54E-06	7.08E-06	1.77E-05	3.54E-05	7.08E-05	1.02E-04
0.0304	1 in 5000	4.18E+02	2.09E-01	1.42E-08	2.83E-08	1.42E-07	3.54E-07	7.08E-07	1.42E-06	3.54E-06	7.08E-06	1.42E-05	2.04E-05
0.0152	1 in 10000	2.09E+02	1.04E-01	7.08E-09	1.42E-08	7.08E-08	1.77E-07	3.54E-07	7.08E-07	1.77E-06	3.54E-06	7.08E-06	1.02E-05
0.00304	1 in 50000	4.18E+01	2.09E-02	1.42E-09	2.83E-09	1.42E-08	3.54E-08	7.08E-08	1.42E-07	3.54E-07	7.08E-07	1.42E-06	2.04E-06
0.00152	1 in 100000	2.09E+01	1.04E-02	7.08E-10	1.42E-09	7.08E-09	1.77E-08	3.54E-08	7.08E-08	1.77E-07	3.54E-07	7.08E-07	1.02E-06
0.000304	1 in 500000	4.18E+00	2.09E-03	1.42E-10	2.83E-10	1.42E-09	3.54E-09	7.08E-09	1.42E-08	3.54E-08	7.08E-08	1.42E-07	2.04E-07
0.000152	1 in 1000000	2.09E+00	1.04E-03	7.08E-11	1.42E-10	7.08E-10	1.77E-09	3.54E-09	7.08E-09	1.77E-08	3.54E-08	7.08E-08	1.02E-07

Table A.17: ^{238}Pu inhalation risk assessment. Colored lines indicated quantification limits for various analytical techniques. TIMS (pink), alpha spectrometry (yellow).

Morbidity (%)	Chance of Mortality	A Ingest (Bq)	A Absd (Bq)	Urine A (Bq/ml)	2x (Bq/ml)	10x (Bq/ml)	25x (Bq/ml)	50x (Bq/ml)	100x (Bq/ml)	250x (Bq/ml)	500x (Bq/ml)	1000x (Bq/ml)	1440x (Bq/ml)
100	1 in 1	1.10E+06	5.51E+02	7.62E-05	1.52E-04	7.62E-04	1.90E-03	3.81E-03	7.62E-03	1.90E-02	3.81E-02	7.62E-02	1.10E-01
56.5	1 in 2	5.51E+05	2.76E+02	3.81E-05	7.62E-05	3.81E-04	9.52E-04	1.90E-03	3.81E-03	9.52E-03	1.90E-02	3.81E-02	5.49E-02
28.25	1 in 4	2.76E+05	1.38E+02	1.90E-05	3.81E-05	1.90E-04	4.76E-04	9.52E-04	1.90E-03	4.76E-03	9.52E-03	1.90E-02	2.74E-02
22.6	1 in 5	2.21E+05	1.10E+02	1.52E-05	3.05E-05	1.52E-04	3.81E-04	7.62E-04	1.52E-03	3.81E-03	7.62E-03	1.52E-02	2.19E-02
11.3	1 in 10	1.10E+05	5.51E+01	7.62E-06	1.52E-05	7.62E-05	1.90E-04	3.81E-04	7.62E-04	1.90E-03	3.81E-03	7.62E-03	1.10E-02
5.65	1 in 20	5.51E+04	2.76E+01	3.81E-06	7.62E-06	3.81E-05	9.52E-05	1.90E-04	3.81E-04	9.52E-04	1.90E-03	3.81E-03	5.49E-03
2.26	1 in 50	2.21E+04	1.10E+01	1.52E-06	3.05E-06	1.52E-05	3.81E-05	7.62E-05	1.52E-04	3.81E-04	7.62E-04	1.52E-03	2.19E-03
1.13	1 in 100	1.10E+04	5.51E+00	7.62E-07	1.52E-06	7.62E-06	1.90E-05	3.81E-05	7.62E-05	1.90E-04	3.81E-04	7.62E-04	1.10E-03
0.452	1 in 250	4.41E+03	2.21E+00	3.05E-07	6.09E-07	3.05E-06	7.62E-06	1.52E-05	3.05E-05	7.62E-05	1.52E-04	3.05E-04	4.39E-04
0.226	1 in 500	2.21E+03	1.10E+00	1.52E-07	3.05E-07	1.52E-06	3.81E-06	7.62E-06	1.52E-05	3.81E-05	7.62E-05	1.52E-04	2.19E-04
0.113	1 in 1000	1.10E+03	5.51E-01	7.62E-08	1.52E-07	7.62E-07	1.90E-06	3.81E-06	7.62E-06	1.90E-05	3.81E-05	7.62E-05	1.10E-04
0.0226	1 in 5000	2.21E+02	1.10E-01	1.52E-08	3.05E-08	1.52E-07	3.81E-07	7.62E-07	1.52E-06	3.81E-06	7.62E-06	1.52E-05	2.19E-05
0.0113	1 in 10000	1.10E+02	5.51E-02	7.62E-09	1.52E-08	7.62E-08	1.90E-07	3.81E-07	7.62E-07	1.90E-06	3.81E-06	7.62E-06	1.10E-05
0.00226	1 in 50000	2.21E+01	1.10E-02	1.52E-09	3.05E-09	1.52E-08	3.81E-08	7.62E-08	1.52E-07	3.81E-07	7.62E-07	1.52E-06	2.19E-06
0.00113	1 in 100000	1.10E+01	5.51E-03	7.62E-10	1.52E-09	7.62E-09	1.90E-08	3.81E-08	7.62E-08	1.90E-07	3.81E-07	7.62E-07	1.10E-06
0.000226	1 in 500000	2.21E+00	1.10E-03	1.52E-10	3.05E-10	1.52E-09	3.81E-09	7.62E-09	1.52E-08	3.81E-08	7.62E-08	1.52E-07	2.19E-07
0.000113	1 in 1000000	1.10E+00	5.51E-04	7.62E-11	1.52E-10	7.62E-10	1.90E-09	3.81E-09	7.62E-09	1.90E-08	3.81E-08	7.62E-08	1.10E-07

Table A.18: ^{238}Pu ingestion risk assessment. Colored lines indicated quantification limits for various analytical techniques. TIMS (pink), alpha spectrometry (yellow).

Morbidity (%)	Chance of Mortality	A Ingest (Bq)	A Absd (Bq)	Urine A (Bq/ml)	2x (Bq/ml)	10x (Bq/ml)	25x (Bq/ml)	50x (Bq/ml)	100x (Bq/ml)	250x (Bq/ml)	500x (Bq/ml)	1000x (Bq/ml)	1440x (Bq/ml)
100	1 in 1	2.82E+08	1.41E+05	3.30E-04	6.59E-04	3.30E-03	8.24E-03	1.65E-02	3.30E-02	8.24E-02	1.65E-01	3.30E-01	4.75E-01
64.5	1 in 2	1.41E+08	7.04E+04	1.65E-04	3.30E-04	1.65E-03	4.12E-03	8.24E-03	1.65E-02	4.12E-02	8.24E-02	1.65E-01	2.37E-01
32.25	1 in 4	7.04E+07	3.52E+04	8.24E-05	1.65E-04	8.24E-04	2.06E-03	4.12E-03	8.24E-03	2.06E-02	4.12E-02	8.24E-02	1.19E-01
25.8	1 in 5	5.63E+07	2.82E+04	6.59E-05	1.32E-04	6.59E-04	1.65E-03	3.30E-03	6.59E-03	1.65E-02	3.30E-02	6.59E-02	9.49E-02
12.9	1 in 10	2.82E+07	1.41E+04	3.30E-05	6.59E-05	3.30E-04	8.24E-04	1.65E-03	3.30E-03	8.24E-03	1.65E-02	3.30E-02	4.75E-02
6.45	1 in 20	1.41E+07	7.04E+03	1.65E-05	3.30E-05	1.65E-04	4.12E-04	8.24E-04	1.65E-03	4.12E-03	8.24E-03	1.65E-02	2.37E-02
2.58	1 in 50	5.63E+06	2.82E+03	6.59E-06	1.32E-05	6.59E-05	1.65E-04	3.30E-04	6.59E-04	1.65E-03	3.30E-03	6.59E-03	9.49E-03
1.29	1 in 100	2.82E+06	1.41E+03	3.30E-06	6.59E-06	3.30E-05	8.24E-05	1.65E-04	3.30E-04	8.24E-04	1.65E-03	3.30E-03	4.75E-03
0.516	1 in 250	1.13E+06	5.63E+02	1.32E-06	2.64E-06	1.32E-05	3.30E-05	6.59E-05	1.32E-04	3.30E-04	6.59E-04	1.32E-03	1.90E-03
0.258	1 in 500	5.63E+05	2.82E+02	6.59E-07	1.32E-06	6.59E-06	1.65E-05	3.30E-05	6.59E-05	1.65E-04	3.30E-04	6.59E-04	9.49E-04
0.129	1 in 1000	2.82E+05	1.41E+02	3.30E-07	6.59E-07	3.30E-06	8.24E-06	1.65E-05	3.30E-05	8.24E-05	1.65E-04	3.30E-04	4.75E-04
0.0258	1 in 5000	5.63E+04	2.82E+01	6.59E-08	1.32E-07	6.59E-07	1.65E-06	3.30E-06	6.59E-06	1.65E-05	3.30E-05	6.59E-05	9.49E-05
0.0129	1 in 10000	2.82E+04	1.41E+01	3.30E-08	6.59E-08	3.30E-07	8.24E-07	1.65E-06	3.30E-06	8.24E-06	1.65E-05	3.30E-05	4.75E-05
0.00258	1 in 50000	5.63E+03	2.82E+00	6.59E-09	1.32E-08	6.59E-08	1.65E-07	3.30E-07	6.59E-07	1.65E-06	3.30E-06	6.59E-06	9.49E-06
0.00129	1 in 100000	2.82E+03	1.41E+00	3.30E-09	6.59E-09	3.30E-08	8.24E-08	1.65E-07	3.30E-07	8.24E-07	1.65E-06	3.30E-06	4.75E-06
0.000258	1 in 500000	5.63E+02	2.82E-01	6.59E-10	1.32E-09	6.59E-09	1.65E-08	3.30E-08	6.59E-08	1.65E-07	3.30E-07	6.59E-07	9.49E-07
0.000129	1 in 1000000	2.82E+02	1.41E-01	3.30E-10	6.59E-10	3.30E-09	8.24E-09	1.65E-08	3.30E-08	8.24E-08	1.65E-07	3.30E-07	4.75E-07

Table A.19: ^{239}Pu inhalation risk assessment. Colored lines indicated quantification limits for various analytical techniques. TIMS (pink), ICP-MS (blue), alpha spectrometry (yellow).

Morbidity (%)	Chance of Mortality	A Ingest (Bq)	A Absd (Bq)	Urine A (Bq/ml)	2x (Bq/ml)	10x (Bq/ml)	25x (Bq/ml)	50x (Bq/ml)	100x (Bq/ml)	250x (Bq/ml)	500x (Bq/ml)	1000x (Bq/ml)	1440x (Bq/ml)
100	1 in 1	1.11E+06	5.56E+02	7.69E-05	1.54E-04	7.69E-04	1.92E-03	3.84E-03	7.69E-03	1.92E-02	3.84E-02	7.69E-02	1.11E-01
56.5	1 in 2	5.56E+05	2.78E+02	3.84E-05	7.69E-05	3.84E-04	9.61E-04	1.92E-03	3.84E-03	9.61E-03	1.92E-02	3.84E-02	5.53E-02
28.25	1 in 4	2.78E+05	1.39E+02	1.92E-05	3.84E-05	1.92E-04	4.80E-04	9.61E-04	1.92E-03	4.80E-03	9.61E-03	1.92E-02	2.77E-02
22.6	1 in 5	2.22E+05	1.11E+02	1.54E-05	3.07E-05	1.54E-04	3.84E-04	7.69E-04	1.54E-03	3.84E-03	7.69E-03	1.54E-02	2.21E-02
11.3	1 in 10	1.11E+05	5.56E+01	7.69E-06	1.54E-05	7.69E-05	1.92E-04	3.84E-04	7.69E-04	1.92E-03	3.84E-03	7.69E-03	1.11E-02
5.65	1 in 20	5.56E+04	2.78E+01	3.84E-06	7.69E-06	3.84E-05	9.61E-05	1.92E-04	3.84E-04	9.61E-04	1.92E-03	3.84E-03	5.53E-03
2.26	1 in 50	2.22E+04	1.11E+01	1.54E-06	3.07E-06	1.54E-05	3.84E-05	7.69E-05	1.54E-04	3.84E-04	7.69E-04	1.54E-03	2.21E-03
1.13	1 in 100	1.11E+04	5.56E+00	7.69E-07	1.54E-06	7.69E-06	1.92E-05	3.84E-05	7.69E-05	1.92E-04	3.84E-04	7.69E-04	1.11E-03
0.452	1 in 250	4.45E+03	2.22E+00	3.07E-07	6.15E-07	3.07E-06	7.69E-06	1.54E-05	3.07E-05	7.69E-05	1.54E-04	3.07E-04	4.43E-04
0.226	1 in 500	2.22E+03	1.11E+00	1.54E-07	3.07E-07	1.54E-06	3.84E-06	7.69E-06	1.54E-05	3.84E-05	7.69E-05	1.54E-04	2.21E-04
0.113	1 in 1000	1.11E+03	5.56E-01	7.69E-08	1.54E-07	7.69E-07	1.92E-06	3.84E-06	7.69E-06	1.92E-05	3.84E-05	7.69E-05	1.11E-04
0.0226	1 in 5000	2.22E+02	1.11E-01	1.54E-08	3.07E-08	1.54E-07	3.84E-07	7.69E-07	1.54E-06	3.84E-06	7.69E-06	1.54E-05	2.21E-05
0.0113	1 in 10000	1.11E+02	5.56E-02	7.69E-09	1.54E-08	7.69E-08	1.92E-07	3.84E-07	7.69E-07	1.92E-06	3.84E-06	7.69E-06	1.11E-05
0.00226	1 in 50000	2.22E+01	1.11E-02	1.54E-09	3.07E-09	1.54E-08	3.84E-08	7.69E-08	1.54E-07	3.84E-07	7.69E-07	1.54E-06	2.21E-06
0.00113	1 in 100000	1.11E+01	5.56E-03	7.69E-10	1.54E-09	7.69E-09	1.92E-08	3.84E-08	7.69E-08	1.92E-07	3.84E-07	7.69E-07	1.11E-06
0.000226	1 in 500000	2.22E+00	1.11E-03	1.54E-10	3.07E-10	1.54E-09	3.84E-09	7.69E-09	1.54E-08	3.84E-08	7.69E-08	1.54E-07	2.21E-07
0.000113	1 in 1000000	1.11E+00	5.56E-04	7.69E-11	1.54E-10	7.69E-10	1.92E-09	3.84E-09	7.69E-09	1.92E-08	3.84E-08	7.69E-08	1.11E-07

Table A.20: ^{239}Pu ingestion risk assessment. Colored lines indicated quantification limits for various analytical techniques. TIMS (pink), ICP-MS (blue), alpha spectrometry (yellow).

Morbidity (%)	Chance of Mortality	A Ingest (Bq)	A Absd (Bq)	Urine A (Bq/ml)	2x (Bq/ml)	10x (Bq/ml)	25x (Bq/ml)	50x (Bq/ml)	100x (Bq/ml)	250x (Bq/ml)	500x (Bq/ml)	1000x (Bq/ml)	1440x (Bq/ml)
100	1 in 1	2.75E+08	1.37E+05	3.21E-04	6.43E-04	3.21E-03	8.04E-03	1.61E-02	3.21E-02	8.04E-02	1.61E-01	3.21E-01	4.63E-01
64	1 in 2	1.37E+08	6.87E+04	1.61E-04	3.21E-04	1.61E-03	4.02E-03	8.04E-03	1.61E-02	4.02E-02	8.04E-02	1.61E-01	2.31E-01
32	1 in 4	6.87E+07	3.43E+04	8.04E-05	1.61E-04	8.04E-04	2.01E-03	4.02E-03	8.04E-03	2.01E-02	4.02E-02	8.04E-02	1.16E-01
25.6	1 in 5	5.49E+07	2.75E+04	6.43E-05	1.29E-04	6.43E-04	1.61E-03	3.21E-03	6.43E-03	1.61E-02	3.21E-02	6.43E-02	9.26E-02
12.8	1 in 10	2.75E+07	1.37E+04	3.21E-05	6.43E-05	3.21E-04	8.04E-04	1.61E-03	3.21E-03	8.04E-03	1.61E-02	3.21E-02	4.63E-02
6.4	1 in 20	1.37E+07	6.87E+03	1.61E-05	3.21E-05	1.61E-04	4.02E-04	8.04E-04	1.61E-03	4.02E-03	8.04E-03	1.61E-02	2.31E-02
2.56	1 in 50	5.49E+06	2.75E+03	6.43E-06	1.29E-05	6.43E-05	1.61E-04	3.21E-04	6.43E-04	1.61E-03	3.21E-03	6.43E-03	9.26E-03
1.28	1 in 100	2.75E+06	1.37E+03	3.21E-06	6.43E-06	3.21E-05	8.04E-05	1.61E-04	3.21E-04	8.04E-04	1.61E-03	3.21E-03	4.63E-03
0.512	1 in 250	1.10E+06	5.49E+02	1.29E-06	2.57E-06	1.29E-05	3.21E-05	6.43E-05	1.29E-04	3.21E-04	6.43E-04	1.29E-03	1.85E-03
0.256	1 in 500	5.49E+05	2.75E+02	6.43E-07	1.29E-06	6.43E-06	1.61E-05	3.21E-05	6.43E-05	1.61E-04	3.21E-04	6.43E-04	9.26E-04
0.128	1 in 1000	2.75E+05	1.37E+02	3.21E-07	6.43E-07	3.21E-06	8.04E-06	1.61E-05	3.21E-05	8.04E-05	1.61E-04	3.21E-04	4.63E-04
0.0256	1 in 5000	5.49E+04	2.75E+01	6.43E-08	1.29E-07	6.43E-07	1.61E-06	3.21E-06	6.43E-06	1.61E-05	3.21E-05	6.43E-05	9.26E-05
0.0128	1 in 10000	2.75E+04	1.37E+01	3.21E-08	6.43E-08	3.21E-07	8.04E-07	1.61E-06	3.21E-06	8.04E-06	1.61E-05	3.21E-05	4.63E-05
0.00256	1 in 50000	5.49E+03	2.75E+00	6.43E-09	1.29E-08	6.43E-08	1.61E-07	3.21E-07	6.43E-07	1.61E-06	3.21E-06	6.43E-06	9.26E-06
0.00128	1 in 100000	2.75E+03	1.37E+00	3.21E-09	6.43E-09	3.21E-08	8.04E-08	1.61E-07	3.21E-07	8.04E-07	1.61E-06	3.21E-06	4.63E-06
0.000256	1 in 500000	5.49E+02	2.75E-01	6.43E-10	1.29E-09	6.43E-09	1.61E-08	3.21E-08	6.43E-08	1.61E-07	3.21E-07	6.43E-07	9.26E-07
0.000128	1 in 1000000	2.75E+02	1.37E-01	3.21E-10	6.43E-10	3.21E-09	8.04E-09	1.61E-08	3.21E-08	8.04E-08	1.61E-07	3.21E-07	4.63E-07

Table A.21: ^{242}Pu inhalation risk assessment. Colored lines indicated quantification limits for various analytical techniques. TIMS (pink), ICP-MS (blue), alpha spectrometry (yellow).

Morbidity (%)	Chance of Mortality	A Ingest (Bq)	A Absd (Bq)	Urine A (Bq/ml)	2x (Bq/ml)	10x (Bq/ml)	25x (Bq/ml)	50x (Bq/ml)	100x (Bq/ml)	250x (Bq/ml)	500x (Bq/ml)	1000x (Bq/ml)	1440x (Bq/ml)
100	1 in 1	1.18E+06	5.91E+02	8.17E-05	1.63E-04	8.17E-04	2.04E-03	4.08E-03	8.17E-03	2.04E-02	4.08E-02	8.17E-02	1.18E-01
56.5	1 in 2	5.91E+05	2.96E+02	4.08E-05	8.17E-05	4.08E-04	1.02E-03	2.04E-03	4.08E-03	1.02E-02	2.04E-02	4.08E-02	5.88E-02
28.25	1 in 4	2.96E+05	1.48E+02	2.04E-05	4.08E-05	2.04E-04	5.10E-04	1.02E-03	2.04E-03	5.10E-03	1.02E-02	2.04E-02	2.94E-02
22.6	1 in 5	2.36E+05	1.18E+02	1.63E-05	3.27E-05	1.63E-04	4.08E-04	8.17E-04	1.63E-03	4.08E-03	8.17E-03	1.63E-02	2.35E-02
11.3	1 in 10	1.18E+05	5.91E+01	8.17E-06	1.63E-05	8.17E-05	2.04E-04	4.08E-04	8.17E-04	2.04E-03	4.08E-03	8.17E-03	1.18E-02
5.65	1 in 20	5.91E+04	2.96E+01	4.08E-06	8.17E-06	4.08E-05	1.02E-04	2.04E-04	4.08E-04	1.02E-03	2.04E-03	4.08E-03	5.88E-03
2.26	1 in 50	2.36E+04	1.18E+01	1.63E-06	3.27E-06	1.63E-05	4.08E-05	8.17E-05	1.63E-04	4.08E-04	8.17E-04	1.63E-03	2.35E-03
1.13	1 in 100	1.18E+04	5.91E+00	8.17E-07	1.63E-06	8.17E-06	2.04E-05	4.08E-05	8.17E-05	2.04E-04	4.08E-04	8.17E-04	1.18E-03
0.452	1 in 250	4.73E+03	2.36E+00	3.27E-07	6.53E-07	3.27E-06	8.17E-06	1.63E-05	3.27E-05	8.17E-05	1.63E-04	3.27E-04	4.70E-04
0.226	1 in 500	2.36E+03	1.18E+00	1.63E-07	3.27E-07	1.63E-06	4.08E-06	8.17E-06	1.63E-05	4.08E-05	8.17E-05	1.63E-04	2.35E-04
0.113	1 in 1000	1.18E+03	5.91E-01	8.17E-08	1.63E-07	8.17E-07	2.04E-06	4.08E-06	8.17E-06	2.04E-05	4.08E-05	8.17E-05	1.18E-04
0.0226	1 in 5000	2.36E+02	1.18E-01	1.63E-08	3.27E-08	1.63E-07	4.08E-07	8.17E-07	1.63E-06	4.08E-06	8.17E-06	1.63E-05	2.35E-05
0.0113	1 in 10000	1.18E+02	5.91E-02	8.17E-09	1.63E-08	8.17E-08	2.04E-07	4.08E-07	8.17E-07	2.04E-06	4.08E-06	8.17E-06	1.18E-05
0.00226	1 in 50000	2.36E+01	1.18E-02	1.63E-09	3.27E-09	1.63E-08	4.08E-08	8.17E-08	1.63E-07	4.08E-07	8.17E-07	1.63E-06	2.35E-06
0.00113	1 in 100000	1.18E+01	5.91E-03	8.17E-10	1.63E-09	8.17E-09	2.04E-08	4.08E-08	8.17E-08	2.04E-07	4.08E-07	8.17E-07	1.18E-06
0.000226	1 in 500000	2.36E+00	1.18E-03	1.63E-10	3.27E-10	1.63E-09	4.08E-09	8.17E-09	1.63E-08	4.08E-08	8.17E-08	1.63E-07	2.35E-07
0.000113	1 in 1000000	1.18E+00	5.91E-04	8.17E-11	1.63E-10	8.17E-10	2.04E-09	4.08E-09	8.17E-09	2.04E-08	4.08E-08	8.17E-08	1.18E-07

Table A.22: ^{242}Pu ingestion risk assessment. Colored lines indicated quantification limits for various analytical techniques. TIMS (pink), ICP-MS (blue), alpha spectrometry (yellow).

Morbidity (%)	Chance of Mortality	A Ingest (Bq)	A Absd (Bq)	Urine A (Bq/ml)	2x (Bq/ml)	10x (Bq/ml)	25x (Bq/ml)	50x (Bq/ml)	100x (Bq/ml)	250x (Bq/ml)	500x (Bq/ml)	1000x (Bq/ml)	1440x (Bq/ml)
100	1 in 1	2.89E+08	1.45E+05	3.38E-04	6.76E-04	3.38E-03	8.45E-03	1.69E-02	3.38E-02	8.45E-02	1.69E-01	3.38E-01	4.87E-01
64	1 in 2	1.45E+08	7.23E+04	1.69E-04	3.38E-04	1.69E-03	4.23E-03	8.45E-03	1.69E-02	4.23E-02	8.45E-02	1.69E-01	2.43E-01
32	1 in 4	7.23E+07	3.61E+04	8.45E-05	1.69E-04	8.45E-04	2.11E-03	4.23E-03	8.45E-03	2.11E-02	4.23E-02	8.45E-02	1.22E-01
25.6	1 in 5	5.78E+07	2.89E+04	6.76E-05	1.35E-04	6.76E-04	1.69E-03	3.38E-03	6.76E-03	1.69E-02	3.38E-02	6.76E-02	9.74E-02
12.8	1 in 10	2.89E+07	1.45E+04	3.38E-05	6.76E-05	3.38E-04	8.45E-04	1.69E-03	3.38E-03	8.45E-03	1.69E-02	3.38E-02	4.87E-02
6.4	1 in 20	1.45E+07	7.23E+03	1.69E-05	3.38E-05	1.69E-04	4.23E-04	8.45E-04	1.69E-03	4.23E-03	8.45E-03	1.69E-02	2.43E-02
2.56	1 in 50	5.78E+06	2.89E+03	6.76E-06	1.35E-05	6.76E-05	1.69E-04	3.38E-04	6.76E-04	1.69E-03	3.38E-03	6.76E-03	9.74E-03
1.28	1 in 100	2.89E+06	1.45E+03	3.38E-06	6.76E-06	3.38E-05	8.45E-05	1.69E-04	3.38E-04	8.45E-04	1.69E-03	3.38E-03	4.87E-03
0.512	1 in 250	1.16E+06	5.78E+02	1.35E-06	2.71E-06	1.35E-05	3.38E-05	6.76E-05	1.35E-04	3.38E-04	6.76E-04	1.35E-03	1.95E-03
0.256	1 in 500	5.78E+05	2.89E+02	6.76E-07	1.35E-06	6.76E-06	1.69E-05	3.38E-05	6.76E-05	1.69E-04	3.38E-04	6.76E-04	9.74E-04
0.128	1 in 1000	2.89E+05	1.45E+02	3.38E-07	6.76E-07	3.38E-06	8.45E-06	1.69E-05	3.38E-05	8.45E-05	1.69E-04	3.38E-04	4.87E-04
0.0256	1 in 5000	5.78E+04	2.89E+01	6.76E-08	1.35E-07	6.76E-07	1.69E-06	3.38E-06	6.76E-06	1.69E-05	3.38E-05	6.76E-05	9.74E-05
0.0128	1 in 10000	2.89E+04	1.45E+01	3.38E-08	6.76E-08	3.38E-07	8.45E-07	1.69E-06	3.38E-06	8.45E-06	1.69E-05	3.38E-05	4.87E-05
0.00256	1 in 50000	5.78E+03	2.89E+00	6.76E-09	1.35E-08	6.76E-08	1.69E-07	3.38E-07	6.76E-07	1.69E-06	3.38E-06	6.76E-06	9.74E-06
0.00128	1 in 100000	2.89E+03	1.45E+00	3.38E-09	6.76E-09	3.38E-08	8.45E-08	1.69E-07	3.38E-07	8.45E-07	1.69E-06	3.38E-06	4.87E-06
0.000256	1 in 500000	5.78E+02	2.89E-01	6.76E-10	1.35E-09	6.76E-09	1.69E-08	3.38E-08	6.76E-08	1.69E-07	3.38E-07	6.76E-07	9.74E-07
0.000128	1 in 1000000	2.89E+02	1.45E-01	3.38E-10	6.76E-10	3.38E-09	8.45E-09	1.69E-08	3.38E-08	8.45E-08	1.69E-07	3.38E-07	4.87E-07

Table A.23: ^{241}Am inhalation risk assessment. Colored lines indicated quantification limits for various analytical techniques. TIMS (pink), alpha spectrometry (yellow).

Morbidity (%)	Chance of Mortality	A Ingest (Bq)	A Absd (Bq)	Urine A (Bq/ml)	2x (Bq/ml)	10x (Bq/ml)	25x (Bq/ml)	50x (Bq/ml)	100x (Bq/ml)	250x (Bq/ml)	500x (Bq/ml)	1000x (Bq/ml)	1440x (Bq/ml)
100	1 in 1	1.32E+06	6.58E+02	6.99E-04	1.40E-03	6.99E-03	1.75E-02	3.50E-02	6.99E-02	1.75E-01	3.50E-01	6.99E-01	1.01E+00
57.5	1 in 2	6.58E+05	3.29E+02	3.50E-04	6.99E-04	3.50E-03	8.74E-03	1.75E-02	3.50E-02	8.74E-02	1.75E-01	3.50E-01	5.03E-01
28.75	1 in 4	3.29E+05	1.64E+02	1.75E-04	3.50E-04	1.75E-03	4.37E-03	8.74E-03	1.75E-02	4.37E-02	8.74E-02	1.75E-01	2.52E-01
23	1 in 5	2.63E+05	1.32E+02	1.40E-04	2.80E-04	1.40E-03	3.50E-03	6.99E-03	1.40E-02	3.50E-02	6.99E-02	1.40E-01	2.01E-01
11.5	1 in 10	1.32E+05	6.58E+01	6.99E-05	1.40E-04	6.99E-04	1.75E-03	3.50E-03	6.99E-03	1.75E-02	3.50E-02	6.99E-02	1.01E-01
5.75	1 in 20	6.58E+04	3.29E+01	3.50E-05	6.99E-05	3.50E-04	8.74E-04	1.75E-03	3.50E-03	8.74E-03	1.75E-02	3.50E-02	5.03E-02
2.3	1 in 50	2.63E+04	1.32E+01	1.40E-05	2.80E-05	1.40E-04	3.50E-04	6.99E-04	1.40E-03	3.50E-03	6.99E-03	1.40E-02	2.01E-02
1.15	1 in 100	1.32E+04	6.58E+00	6.99E-06	1.40E-05	6.99E-05	1.75E-04	3.50E-04	6.99E-04	1.75E-03	3.50E-03	6.99E-03	1.01E-02
0.46	1 in 250	5.26E+03	2.63E+00	2.80E-06	5.59E-06	2.80E-05	6.99E-05	1.40E-04	2.80E-04	6.99E-04	1.40E-03	2.80E-03	4.03E-03
0.23	1 in 500	2.63E+03	1.32E+00	1.40E-06	2.80E-06	1.40E-05	3.50E-05	6.99E-05	1.40E-04	3.50E-04	6.99E-04	1.40E-03	2.01E-03
0.115	1 in 1000	1.32E+03	6.58E-01	6.99E-07	1.40E-06	6.99E-06	1.75E-05	3.50E-05	6.99E-05	1.75E-04	3.50E-04	6.99E-04	1.01E-03
0.023	1 in 5000	2.63E+02	1.32E-01	1.40E-07	2.80E-07	1.40E-06	3.50E-06	6.99E-06	1.40E-05	3.50E-05	6.99E-05	1.40E-04	2.01E-04
0.0115	1 in 10000	1.32E+02	6.58E-02	6.99E-08	1.40E-07	6.99E-07	1.75E-06	3.50E-06	6.99E-06	1.75E-05	3.50E-05	6.99E-05	1.01E-04
0.0023	1 in 50000	2.63E+01	1.32E-02	1.40E-08	2.80E-08	1.40E-07	3.50E-07	6.99E-07	1.40E-06	3.50E-06	6.99E-06	1.40E-05	2.01E-05
0.00115	1 in 100000	1.32E+01	6.58E-03	6.99E-09	1.40E-08	6.99E-08	1.75E-07	3.50E-07	6.99E-07	1.75E-06	3.50E-06	6.99E-06	1.01E-05
0.00023	1 in 500000	2.63E+00	1.32E-03	1.40E-09	2.80E-09	1.40E-08	3.50E-08	6.99E-08	1.40E-07	3.50E-07	6.99E-07	1.40E-06	2.01E-06
0.000115	1 in 1000000	1.32E+00	6.58E-04	6.99E-10	1.40E-09	6.99E-09	1.75E-08	3.50E-08	6.99E-08	1.75E-07	3.50E-07	6.99E-07	1.01E-06

Table A.24: ^{241}Am ingestion risk assessment. Colored lines indicated quantification limits for various analytical techniques. TIMS (pink), alpha spectrometry (yellow).

Morbidity (%)	Chance of Mortality	A Ingest (Bq)	A Absd (Bq)	Urine A (Bq/ml)	2x (Bq/ml)	10x (Bq/ml)	25x (Bq/ml)	50x (Bq/ml)	100x (Bq/ml)	250x (Bq/ml)	500x (Bq/ml)	1000x (Bq/ml)	1440x (Bq/ml)
100	1 in 1	3.56E+08	1.78E+05	3.66E-03	7.32E-03	3.66E-02	9.14E-02	1.83E-01	3.66E-01	9.14E-01	1.83E+00	3.66E+00	5.27E+00
70	1 in 2	1.78E+08	8.90E+04	1.83E-03	3.66E-03	1.83E-02	4.57E-02	9.14E-02	1.83E-01	4.57E-01	9.14E-01	1.83E+00	2.63E+00
35	1 in 4	8.90E+07	4.45E+04	9.14E-04	1.83E-03	9.14E-03	2.29E-02	4.57E-02	9.14E-02	2.29E-01	4.57E-01	9.14E-01	1.32E+00
28	1 in 5	7.12E+07	3.56E+04	7.32E-04	1.46E-03	7.32E-03	1.83E-02	3.66E-02	7.32E-02	1.83E-01	3.66E-01	7.32E-01	1.05E+00
14	1 in 10	3.56E+07	1.78E+04	3.66E-04	7.32E-04	3.66E-03	9.14E-03	1.83E-02	3.66E-02	9.14E-02	1.83E-01	3.66E-01	5.27E-01
7	1 in 20	1.78E+07	8.90E+03	1.83E-04	3.66E-04	1.83E-03	4.57E-03	9.14E-03	1.83E-02	4.57E-02	9.14E-02	1.83E-01	2.63E-01
2.8	1 in 50	7.12E+06	3.56E+03	7.32E-05	1.46E-04	7.32E-04	1.83E-03	3.66E-03	7.32E-03	1.83E-02	3.66E-02	7.32E-02	1.05E-01
1.4	1 in 100	3.56E+06	1.78E+03	3.66E-05	7.32E-05	3.66E-04	9.14E-04	1.83E-03	3.66E-03	9.14E-03	1.83E-02	3.66E-02	5.27E-02
0.56	1 in 250	1.42E+06	7.12E+02	1.46E-05	2.93E-05	1.46E-04	3.66E-04	7.32E-04	1.46E-03	3.66E-03	7.32E-03	1.46E-02	2.11E-02
0.28	1 in 500	7.12E+05	3.56E+02	7.32E-06	1.46E-05	7.32E-05	1.83E-04	3.66E-04	7.32E-04	1.83E-03	3.66E-03	7.32E-03	1.05E-02
0.14	1 in 1000	3.56E+05	1.78E+02	3.66E-06	7.32E-06	3.66E-05	9.14E-05	1.83E-04	3.66E-04	9.14E-04	1.83E-03	3.66E-03	5.27E-03
0.028	1 in 5000	7.12E+04	3.56E+01	7.32E-07	1.46E-06	7.32E-06	1.83E-05	3.66E-05	7.32E-05	1.83E-04	3.66E-04	7.32E-04	1.05E-03
0.014	1 in 10000	3.56E+04	1.78E+01	3.66E-07	7.32E-07	3.66E-06	9.14E-06	1.83E-05	3.66E-05	9.14E-05	1.83E-04	3.66E-04	5.27E-04
0.0028	1 in 50000	7.12E+03	3.56E+00	7.32E-08	1.46E-07	7.32E-07	1.83E-06	3.66E-06	7.32E-06	1.83E-05	3.66E-05	7.32E-05	1.05E-04
0.0014	1 in 100000	3.56E+03	1.78E+00	3.66E-08	7.32E-08	3.66E-07	9.14E-07	1.83E-06	3.66E-06	9.14E-06	1.83E-05	3.66E-05	5.27E-05
0.00028	1 in 500000	7.12E+02	3.56E-01	7.32E-09	1.46E-08	7.32E-08	1.83E-07	3.66E-07	7.32E-07	1.83E-06	3.66E-06	7.32E-06	1.05E-05
0.00014	1 in 1000000	3.56E+02	1.78E-01	3.66E-09	7.32E-09	3.66E-08	9.14E-08	1.83E-07	3.66E-07	9.14E-07	1.83E-06	3.66E-06	5.27E-06

Table A.25: ^{243}Am inhalation risk assessment. Colored lines indicated quantification limits for various analytical techniques. TIMS (pink), ICP-MS (blue), alpha spectrometry (yellow).

Morbidity (%)	Chance of Mortality	A Ingest (Bq)	A Absd (Bq)	Urine A (Bq/ml)	2x (Bq/ml)	10x (Bq/ml)	25x (Bq/ml)	50x (Bq/ml)	100x (Bq/ml)	250x (Bq/ml)	500x (Bq/ml)	1000x (Bq/ml)	1440x (Bq/ml)
100	1 in 1	1.37E+06	6.84E+02	7.27E-04	1.45E-03	7.27E-03	1.82E-02	3.63E-02	7.27E-02	1.82E-01	3.63E-01	7.27E-01	1.05E+00
57.5	1 in 2	6.84E+05	3.42E+02	3.63E-04	7.27E-04	3.63E-03	9.08E-03	1.82E-02	3.63E-02	9.08E-02	1.82E-01	3.63E-01	5.23E-01
28.75	1 in 4	3.42E+05	1.71E+02	1.82E-04	3.63E-04	1.82E-03	4.54E-03	9.08E-03	1.82E-02	4.54E-02	9.08E-02	1.82E-01	2.62E-01
23	1 in 5	2.74E+05	1.37E+02	1.45E-04	2.91E-04	1.45E-03	3.63E-03	7.27E-03	1.45E-02	3.63E-02	7.27E-02	1.45E-01	2.09E-01
11.5	1 in 10	1.37E+05	6.84E+01	7.27E-05	1.45E-04	7.27E-04	1.82E-03	3.63E-03	7.27E-03	1.82E-02	3.63E-02	7.27E-02	1.05E-01
5.75	1 in 20	6.84E+04	3.42E+01	3.63E-05	7.27E-05	3.63E-04	9.08E-04	1.82E-03	3.63E-03	9.08E-03	1.82E-02	3.63E-02	5.23E-02
2.3	1 in 50	2.74E+04	1.37E+01	1.45E-05	2.91E-05	1.45E-04	3.63E-04	7.27E-04	1.45E-03	3.63E-03	7.27E-03	1.45E-02	2.09E-02
1.15	1 in 100	1.37E+04	6.84E+00	7.27E-06	1.45E-05	7.27E-05	1.82E-04	3.63E-04	7.27E-04	1.82E-03	3.63E-03	7.27E-03	1.05E-02
0.46	1 in 250	5.47E+03	2.74E+00	2.91E-06	5.81E-06	2.91E-05	7.27E-05	1.45E-04	2.91E-04	7.27E-04	1.45E-03	2.91E-03	4.19E-03
0.23	1 in 500	2.74E+03	1.37E+00	1.45E-06	2.91E-06	1.45E-05	3.63E-05	7.27E-05	1.45E-04	3.63E-04	7.27E-04	1.45E-03	2.09E-03
0.115	1 in 1000	1.37E+03	6.84E-01	7.27E-07	1.45E-06	7.27E-06	1.82E-05	3.63E-05	7.27E-05	1.82E-04	3.63E-04	7.27E-04	1.05E-03
0.023	1 in 5000	2.74E+02	1.37E-01	1.45E-07	2.91E-07	1.45E-06	3.63E-06	7.27E-06	1.45E-05	3.63E-05	7.27E-05	1.45E-04	2.09E-04
0.0115	1 in 10000	1.37E+02	6.84E-02	7.27E-08	1.45E-07	7.27E-07	1.82E-06	3.63E-06	7.27E-06	1.82E-05	3.63E-05	7.27E-05	1.05E-04
0.0023	1 in 50000	2.74E+01	1.37E-02	1.45E-08	2.91E-08	1.45E-07	3.63E-07	7.27E-07	1.45E-06	3.63E-06	7.27E-06	1.45E-05	2.09E-05
0.00115	1 in 100000	1.37E+01	6.84E-03	7.27E-09	1.45E-08	7.27E-08	1.82E-07	3.63E-07	7.27E-07	1.82E-06	3.63E-06	7.27E-06	1.05E-05
0.00023	1 in 500000	2.74E+00	1.37E-03	1.45E-09	2.91E-09	1.45E-08	3.63E-08	7.27E-08	1.45E-07	3.63E-07	7.27E-07	1.45E-06	2.09E-06
0.000115	1 in 1000000	1.37E+00	6.84E-04	7.27E-10	1.45E-09	7.27E-09	1.82E-08	3.63E-08	7.27E-08	1.82E-07	3.63E-07	7.27E-07	1.05E-06

Table A.26: ^{243}Am ingestion risk assessment. Colored lines indicated quantification limits for various analytical techniques. TIMS (pink), ICP-MS (blue), alpha spectrometry (yellow).

Morbidity (%)	Chance of Mortality	A Ingest (Bq)	A Absd (Bq)	Urine A (Bq/ml)	2x (Bq/ml)	10x (Bq/ml)	25x (Bq/ml)	50x (Bq/ml)	100x (Bq/ml)	250x (Bq/ml)	500x (Bq/ml)	1000x (Bq/ml)	1440x (Bq/ml)
100	1 in 1	3.58E+08	1.79E+05	3.68E-03	7.37E-03	3.68E-02	9.21E-02	1.84E-01	3.68E-01	9.21E-01	1.84E+00	3.68E+00	5.30E+00
70	1 in 2	1.79E+08	8.96E+04	1.84E-03	3.68E-03	1.84E-02	4.60E-02	9.21E-02	1.84E-01	4.60E-01	9.21E-01	1.84E+00	2.65E+00
35	1 in 4	8.96E+07	4.48E+04	9.21E-04	1.84E-03	9.21E-03	2.30E-02	4.60E-02	9.21E-02	2.30E-01	4.60E-01	9.21E-01	1.33E+00
28	1 in 5	7.17E+07	3.58E+04	7.37E-04	1.47E-03	7.37E-03	1.84E-02	3.68E-02	7.37E-02	1.84E-01	3.68E-01	7.37E-01	1.06E+00
14	1 in 10	3.58E+07	1.79E+04	3.68E-04	7.37E-04	3.68E-03	9.21E-03	1.84E-02	3.68E-02	9.21E-02	1.84E-01	3.68E-01	5.30E-01
7	1 in 20	1.79E+07	8.96E+03	1.84E-04	3.68E-04	1.84E-03	4.60E-03	9.21E-03	1.84E-02	4.60E-02	9.21E-02	1.84E-01	2.65E-01
2.8	1 in 50	7.17E+06	3.58E+03	7.37E-05	1.47E-04	7.37E-04	1.84E-03	3.68E-03	7.37E-03	1.84E-02	3.68E-02	7.37E-02	1.06E-01
1.4	1 in 100	3.58E+06	1.79E+03	3.68E-05	7.37E-05	3.68E-04	9.21E-04	1.84E-03	3.68E-03	9.21E-03	1.84E-02	3.68E-02	5.30E-02
0.56	1 in 250	1.43E+06	7.17E+02	1.47E-05	2.95E-05	1.47E-04	3.68E-04	7.37E-04	1.47E-03	3.68E-03	7.37E-03	1.47E-02	2.12E-02
0.28	1 in 500	7.17E+05	3.58E+02	7.37E-06	1.47E-05	7.37E-05	1.84E-04	3.68E-04	7.37E-04	1.84E-03	3.68E-03	7.37E-03	1.06E-02
0.14	1 in 1000	3.58E+05	1.79E+02	3.68E-06	7.37E-06	3.68E-05	9.21E-05	1.84E-04	3.68E-04	9.21E-04	1.84E-03	3.68E-03	5.30E-03
0.028	1 in 5000	7.17E+04	3.58E+01	7.37E-07	1.47E-06	7.37E-06	1.84E-05	3.68E-05	7.37E-05	1.84E-04	3.68E-04	7.37E-04	1.06E-03
0.014	1 in 10000	3.58E+04	1.79E+01	3.68E-07	7.37E-07	3.68E-06	9.21E-06	1.84E-05	3.68E-05	9.21E-05	1.84E-04	3.68E-04	5.30E-04
0.0028	1 in 50000	7.17E+03	3.58E+00	7.37E-08	1.47E-07	7.37E-07	1.84E-06	3.68E-06	7.37E-06	1.84E-05	3.68E-05	7.37E-05	1.06E-04
0.0014	1 in 100000	3.58E+03	1.79E+00	3.68E-08	7.37E-08	3.68E-07	9.21E-07	1.84E-06	3.68E-06	9.21E-06	1.84E-05	3.68E-05	5.30E-05
0.00028	1 in 500000	7.17E+02	3.58E-01	7.37E-09	1.47E-08	7.37E-08	1.84E-07	3.68E-07	7.37E-07	1.84E-06	3.68E-06	7.37E-06	1.06E-05
0.00014	1 in 1000000	3.58E+02	1.79E-01	3.68E-09	7.37E-09	3.68E-08	9.21E-08	1.84E-07	3.68E-07	9.21E-07	1.84E-06	3.68E-06	5.30E-06

References

AEC (1971). Annual Report, 1970, Health Services Laboratory. Washington, DC, U.S. Atomic Energy Commission.

Al-Masri, M. S., Al-Bich, F. (2004). "Polonium-210 distribution in Syrian phosphogypsum." Journal of Radioanalytical and Nuclear Chemistry **251**(3): 431-435.

Aldstadt, J. H., Kuo, J. M., Smithh, L. L., Erickson, M. D. (1996). "Determination of Uranium By Flow Injection Inductively Coupled Plasma Mass Spectrometry." Analytica Chimica Acta **319**(1-2): 135-143.

Alfaro, J., Apfel, T., Diercksm H., Knochel, A., Gupta, R., Todter, K. (1995). "Trace Analysis of the Nuclides 90Sr and 89Sr in Environmental Samples III: Development of a Fast Analytical Method " Agnew. Chem. Int. Ed. Eng. **34**: 186-191.

Alonso, J. (1995). "Determination of Fission Products and Actinides By Inductively Coupled Plasma-Mass Spectrometry Using Isotope Dilution Analysis: A Study of Random and Systematic Errors." Analytica Chimica Acta **312**(1): 57-78.

Alonso, J., Ignacio Garcia Sena, F., Arbore, P., Betti, M., Koch, L. (1995). "Determination of Fission Products and Actinides in Spent Nuclear Fuels by Isotope Dilution Ion Chromatography Inductively Coupled Plasma Mass Spectrometry." Journal of Analytical Atomic Spectrometry **10**: 381-393.

Anonymous (1951). Toxicology and Radiation Hazard of Polonium. Oak Ridge, Oak Ridge Y-12 Plant.

Anonymous (1995). Detection of Gamma Emitting Radionuclides Using FSA, Gamma-B and Gamma-C Flow Cells. Boston, Perkin Elmer Life and Analytical Sciences.

ASTM (2005). Standard Practice for Electrodeposition of the Actinides for Alpha Spectrometry. ASTM Standard. C26.05. West Conshohocken, ASTM International.

ASTM (2005). Standard Test Method for Radiochemical Determination of Plutonium in Soil by Alpha Spectroscopy. ASTM Standard. C26.05. West Conshohocken, ASTM International.

Baglan, N., Hemet, P., Pointurier, F., Chiappini, R. (2004). "Evaluation of a Single Collector, Double Focusing Sector Field Inductively Coupled Plasma Mass Spectrometer for the Determination of U and Pu Concentrations and Isotopic Compositions at Trace Level." Journal of Radioanalytical and Nuclear Chemistry **261**(3): 609-617.

Biggin, C., Cook, G., MacKenzie, A., Pates, J. (2002). "Time-Efficient Method for the Determination of 210Pb, 210Bi, and 210Po Activities in Seawater Using Liquid Scintillation Spectrometry." Analytical Chemistry **74**(3): 671-677.

Boulyga, S. F., Testa, C., Desideri, D., Becker, J. S. (2001). "Optimisation and Application of ICP-MS and Alpha-Spectrometry for Determination of Isotopic Ratios of Depleted Uranium and Plutonium in Samples Collected in Kosovo." Journal of Analytical Atomic Spectrometry **16**: 1283-1289.

Brown, R. M., Long, S.E., Pickford, C.J. (1988). "The Measurement of Long Lived Radionuclides By Non-Radiometric Methods." Science of the Total Environement **70**: 265-274.

Brown, S. (2005). "Determination of 210Po and 210Pb in Hydrometallurgical Samples Using Liquid Scintillation Counting." Journal of Radioanalytical and Nuclear Chemistry **264**(2): 505-509.

Cember, H. (1996). Introduction to Health Physics. New York, McGraw-Hill Medical.

Chiarizia, R., Horwitz, E.P., Gatrone, R.C., Alexandratos, S.D., Trochimczuk, A.Q., Crick, D.W. (1993). "Uptake of Metal Ions By a New Chelating Ion-Exchange Resin. Part 2. Acid Dependencies of Transition and Post-Transition Metal Ions." Solvent Extraction and Ion Exchange **11**(5): 967-985.

Choppin, G. R., Nash, K.L. (1995). Radiochimica Acta **70-81**: 225-236.

Christian, G. D. (1994). "Sequential Injection Analysis for Electrochemical Measurements and Process Analysis." The Analyist **119**: 2309-2314.

Coates, J. T., Fjeld, R. A., Paulenova, A., DeVol, T. (2001). "Evaluation of a Rapid Technique for Measuring Actinide Oxidation States in a Ground Water Simulant." Journal of Radioanalytical and Nuclear Chemistry **248**(2): 501-506.

Dacheux, N., Aupiais, J. (1997). "Determination of Uranium, Thorium, Plutonium, Americium, and Curium Ultratraces by Photon Electron Rejecting Liquid Scintillation." Analytical Chemistry **69**(13): 2275-2282.

Desmartin, P., Kopajtic, Z., Haerdi, W. (1997). "Radiostrontium-90 (90Sr) Ultra-Traces Measurements by Coupling Ionic Chromatography (HPIC) and on Line Liquid Scintillation Counting (OLLSC)." Environmental Monitoring and Assessment **44**: 413-423.

Dodson, R. W. (1945). Notes on Discusions About Polonium, Dayton, Ohio - April 11 to 14, 1945. Los Alamos, Los Alamos Scientific Laboratory.

E. P. Horwitz, R. C., and M. L. Dietz (1997). "Dipex: A New Extraction Chromatographic Material for the Separation and Preconcentration of Actinides from Aqueous Solution." Reactive and Functional Polymers **33**: 25-36.

Egorov, O., Fiskum, S., O'Hara, M., Grate, J. (1999). "Radionuclide Sensors Based on Chemically Selective Scintillating Microspheres: Renewable Column Sensor for Analysis of 99Tc in Water." Analytical Chemistry **71**: 5420-5429.

Egorov, O., Grate, J. W., Ruzicka, J. (1998). "Automation of Radiochemical Analysis By Flow Injection Techniques: Am-Pu Separation Using TRU-ResinTM Sorbent Extraction Column." Journal of Radioanalytical and Nuclear Chemistry **234**(1-2): 231-235.

Egorov, O., O'Hara, M. J., Farmer, I., Orville T., Grate, J. W. (2001). "Extraction Chromatographic Separations and Analysis of Actinides Using Sequential Injection Techniques With On-Line Inductively Coupled Plasma Mass Spectrometry (ICP MS) Ddetection." The Analyist **126**: 1594-1601.

Egorov, O., O'Hara, M. J., Ruzicka, J., Grate, J. (1998). "Sequential Injection Separation System with Stopped-Flow Radiometric Detection for Automated Analysis of 99Tc in Nuclear Waste." Analytical Chemistry **70**(5): 977-984.

Egorov, O., O'Hara, M., Grate, J. (1999). "Sequential Injection Renewable Separation Column Instrument for Automated Sorbent Extraction Separations of Radionuclides." Analytical Chemistry **71**: 345-352.

EPA (1993). External Exposure to Radionuclides in Air, Water, and Soil. Federal Guidance Repost No. 12. Washington, DC, U.S. Environmental Protection Agency.

EPA (1999). Estimating Radiogenic Cancer Risks, Addendum: Uncertainty Analysis. Washington, DC, Environmental Protection Agency.

Epov, V. N., Benkhedda, K., Cornett, R.J., Evans, R.D. (2005). "Rapid Determination of Plutonium in Urine Using Flow Injection On-Line Preconcentration and Inductively Coupled Plasma Mass Spectrometry." Journal of Analytical Atomic Spectrometry **20**: 424-430.

Fink, R. M. (1950). Biological Studies with Polonium, Radium, and Plutonium. Rochester, University of Rochester.

Fjeld, R. A., DeVol, T. A., Leyba, J. D., Paulenova, A. (2005). "Measurement of Radionuclides Using Ion Chromatography and On-Line Radiation Detection." Journal of Radioanalytical and Nuclear Chemistry **263**(3): 635-640.

Fjeld, R. A., Guha, S., Devol, T. A., Leyba, J. D. (1995). "Ion Chromatography and On-Line Scintillation Counting for the Analysis of Non-Gamma Emitting Radionuclides in Reactor Coolant." Journal of Radioanalytical and Nuclear Chemistry **194**(1): 51-59.

Friedlander, G., Kennedy, J.W., Macias, E.S., Miller, J.M. (1981). Nuclear and Radiochemistry. New York, John Wiley.

Goldman, M. (1996). "Cancer Risk at Low-Level Exposure." Science **271**: 1821-1822.

Gonzales, E. R., Garcia, S.R., Mahan, C., Hang, W. (2005). "Evaluation of Mass Spectrometry and Radiation Detection for the Analysis of Radionuclides." Journal of Radioanalytical and Nuclear Chemistry **263**(2): 457-465.

Grate, J. (2005). "Automated Radiochemical Analysis of Total 99Tc in Aged Nuclear Waste Processing Streams." Journal of Radioanalytical and Nuclear Chemistry **263**(3): 629-633.

Grate, J., Egorov, O. (1998). "Investigation and Optimization of On-Column Redox Reactions in the Sorbent Extraction Separation of Americium and Plutonium Using Flow Injection Analysis." Analytical Chemistry **70**(18): 3920-3929.

Grate, J., Egorov, O., Fadeff, S. (1999). "Separation-Optimized Sequential Injection Method for Rapid Automated Analytical Separation of 90Sr in Nuclear Waste." The Analyist **124**: 203-210.

Grate, J., Egorov, O., Fiskumb, S. (1999). "Automated Extraction Chromatographic Separations of Actinides Using Separation-Optimized Sequential Injection Techniques." The Analyst **124**: 1143-1150.

Grate, J., Strebin, R., Janata, J. (1996). "Automated Analysis of Radionuclides in Nuclear Waste: Rapid Determination of 90Sr by Sequential Injection Analysis." Analytical Chemistry **68**(2): 333-340.

Grate, J. W. (2001). "Extractive scintillating resin for 99Tc quantification in aqueous solutions." Journal of Radioanalytical and Nuclear Chemistry **249**(1): 181-189.

Grudpan, K., Nacapricha, D., Wattanakanjana, Y. (1991). "Radiometric Detectors For Flow-Injection Analysis." Analytica Chimica Acta **246**: 325-328.

Guilmette, R. (2007). Po-210 and the November 2006 London Homacide Incident. Los Alamos, Los Alamos National Security.

Hall, E. J. (2000). Radiation Biology for the Radiologist. Philadelphia, Lippincott Williams & Wilkins.

Hang, W., Mahan, C., Zhu, L., Gonzales, E. (2005). "Evaluation of Chelation Concentration and Cation Separation of Actinides At Ultra-Trace Levels in Urine Matrix." Journal of Radioanalytical and Nuclear Chemistry **263**(2): 467-475.

Hang, W., Zhu, L., Zhong, W., Mahan, C. (2004). "Separation of Actinides At Ultra-Ttrace Level From Urine Matrix Using Extraction Chromatography-Inductively Coupled Plasma Mass Spectrometry." Journal of Analytical A t omic Spectrometry **19**: 966-972.

Harrison, J., Leggett, R., Lloyd, D., Phipps, A., Scott, B. (2007). "Polonium-210 As a Poison." Journal Of Radiological Protection **27**: 17-40.

Hollenbach, M., Grohs, J., Mamich, S., Kroft, M., Denoyer, E. R. (1994). "Determination of Technetium-99, Thorium-230 and Uranium-234 in Soils By Inductively Coupled Plasma Mass Spectrometry Using Flow Injection Preconcentration." Journal of Analytical Atomic Spectrometry **9**: 927-933.

Horwitz, E. P., Chiarizia, R., Diamond, H., Gatrone, R.C., Alexandratos, S.D., Trochimczuk, A.Q., Crick, D.W. (1993). "Uptake of Metal Ions By a New Chelating Ion-Exchange Resin. Part 1. Acid Dependencies of Actinide Ions." Solvent Extraction and Ion Exchange **11**(5): 943-966.

Horwitz, E. P., Chiarizia, R., Dietz, M. (1992). "A Novel Strontium Selective Extraction Chromatographic Resin." Solvent Extr. Ion Extr **10**: 313-336.

Horwitz, E. P., Chiarizia, R., Dietz, M. (1997). "Dipex: A New Extraction Chromatographic Material for the Separation and Preconcentration of Actinides from Aqueous Solution." Reactive and Functional Polymers **33**: 25-36.

Horwitz, E. P., Chiarizia, R., Dietz, M. L., Diamond, H., Nelson, D. M. (1993). "Separation and preconcentration of actinides from acidic media by extraction chromatography." Analytica Chimica Acta **281**(2): 361-372.

Horwitz, E. P., Dietz, M. L., Chiarizia, R., Diamond, H., Essling, A. M., Graczyk, D. (1992). "Separation and Preconcentration of Uranium From Acidic Media By Extraction Chromatography." Analytica Chimica Acta **266**(1): 25-37.

Horwitz, E. P., Dietz, M. L., Nelson, D. M., LaRosa, J. J., Fairman, W. D. (1990). "Concentration and separation of actinides from urine using a supported bifunctional organophosphorus extractant." Analytica Chimica Acta **238**(0): 263-271.

Horwitz, E. P., Dietz, M. L.,Chiarizia, R., Diamond, H., Maxwell , S. L., Nelson, M. R. (1995). "Separation and Preconcentration of Actinides By Extraction Chromatography Using a Supported Liquid Anion Exchanger: Application to the Characterization of High-Level Nuclear Waste Solutions." Analytica Chimica Acta **310**(1): 63-78.

Horwitz, E. P., Dietz, M., Fisher, D. (1991). "Separation and Preconcentration of Strontium from Biological, Environmental, and Nuclear Waste Samples by

Extraction Chromatography Using a Crown Ether." Analytical Chemistry **63**: 522-525.
Horwitz, E. P., Kailina, D. (1984). "Extraction of Am(III) From Nitric Acid By Octyl(phenyl)-N,N-Diisobutylcarbamoylmethylphosphine Oxide-tri-n-butyl Phosphate Mixtures." Solvent Extraction and Ion Exchange **2**: 179.
Horwitz, E. P., Kalina D., Diamond, H., Vandegrift, G., Schulz, W. (1985). "TRUEX Process - A Process for the Extraction of the Transuranic Elements From Nitric Acid Wastes Utilizing Modified PUREX Solvent." Solvent Extraction and Ion Exchange **3**: 75.
Hughes, L., DeVol, T. A. (2003). "On-Line Gross Alpha Radiation Monitoring of Natural Waters With Extractive Scintillating Resins." Nuclear Instruments and Methods in Physics Research Section A: Accelerators, Spectrometers, Detectors and Associated Equipment **505**: 435-438.
Hughes, L. D., DeVol, T. A. (2006). "Evaluation of Flow Cell Detector Configurations Combining Simultaneous Preconcentration and Scintillation Detection for Monitoring of Pertechnetate in Aqueous Media." Analytical Chemistry **78**(7): 2254-2261.
Hughes, L. D., DeVol, T. A., DeVol, T. A. (2006). "Characterization of a Teflon Semiconductor Detector Flow Cell For Monitoring of Pertechnetate in Groundwater." Journal of Radioanalytical and Nuclear Chemistry **267**(2): 287-295.
IAEA (1998). Dosimetric and Medical Aspects of the Radiological Accident in Goiania in 1987. Geneva, International Atomic Energy Agency.
ICRP (1989). Age-Dependent Doses to Members of the Public from Intake of Radionuclides, Part 1. Oxford, International Committee on Radiological Protection.
ICRP (1993). Age-Dependent Doses to Members of the Public from Intake of Radionuclides, Part 2. Oxford, International Committee on Radiological Protection.
ICRP (1994). Human Respiratory Tract Model fro Radiological Protection. Oxford, Intenational Commission on Radiological Protection.
ICRP (1995). Age-Dependent Doses to Members of the Public from Intake of Radionuclides, Part 3. Oxford, International Committe on Radiological Protection.
ICRP (1995). Age-Dependent Doses to Members of the Public from Intake of Radionuclides, Part 4. Oxford, International Commission on Radiological Protection.
ICRP (1996). Age-Dependent Doses to Members of the Public from Intake of Radionuclides. Oxford, International Commission on Radiological Protection.
Ishigure, N., Matsumoto, M., Nakano, T., Enomoto, H. (2007). Monitoring To Dose Calculation (MONDAL). Chiba, National Institute of Radiological Sciences**:** Internal Dose Calculator.
Ivaska, A., Ruzicka, J. (1993). "From Flow Injection to Sequential Injection: Comparison of Methodologies and Selection of Liquid Drives." The Analyist **118**: 885-889.

Jaworowski, Z. (1995). "Stimulating Effects of Ionizing Radiation: New Issue for Regulatory Policy." Regul. Toxicol. and Pharmacol. **22**: 172-179.
Kahn, B. (2007). Radioanalytical Chemistry. New York, Springer Science + Buisiness Media, LLC.
KAPL (2002). Chart of the Nuclides & Isotopes. Cincinnati, Knolls Atomic Power Laboratory, Inc.
Katz, J., Seaborg, G.T., Morss, L. (1986). The Chemistry of the Actinide Elements
Knoll, G. F. (2000). Radiation Detection and Measurement. New York, John Wiley.
Kuca, L. (1989). Radioanalytical Chemistry II. M. K. J. Tolygyessy. New York, John Wiley and Sons**:** 284-316.
L'Annunziata, M. F. (2003). Flow Scintillation Analysis. Handbook of Radioactivity Analysis. M. F. L'Annunziata. Amsterdam, Academic Press**:** 989-1062.
Lariviere, D., Taylor, V. F., Evans, R. D., Cornett, R. J. (2006). "Radionuclide Determination in Environmental Samples By Inductively Coupled Plasma Mass Spectrometry." Spectrochimica Acta Part B: Atomic Spectroscopy **61**(8): 877-904.
Lieser, K. H. (2001). Nuclear and Radiochemistry: Fundamentals and Applications. New York, Wiley-VCH.
Luckey, T. D. (1990). Radiation Hormesis. Boca Raton, CRC Press.
Luque de Castro, M., Valcarcel, M. (1992). "Flow-Through Sensing Device Based on Derivative Synchronous Fluorescence Measurements for the Multi-Determination of B[6] Vitamers." Analytica Chimica Acta **261**: 11-21.
Martin, A., Blanchard, R.L. (1969). "The Thermal Volatilisation of Caesium-137, Polonium-210 and Lead-210 From in Vivo Labelled Samples." The Analyist **94**: 441-446.
Matthews, K. M., Kim, C., Martin, P. (2007). "Determination of 210Po in Environmental materials: A Review of Analytical Methodology." Applied Radiation and Isotopes **65**(3): 267-279.
McAninch, J. E., Hamilton, T.F. (1999). Measurement of Plutonium and Other Actinide Elements at the Center for Accelerator Mass Spectrometry: A Comprehensive Assessment of Competing Techniques. Livermore, Lawrence Livermore National Laboratory.
NCHS (1992). Vital Statistics Mortality Data, Detail, 1989. Hyattsville, National Center for Health Statistics.
NCHS (1993). Vital Statistics Mortality Data, Detail, 1990. Hyattsville, National Center for Health Statistics.
NCHS (1993). Vital Statistics Mortality Data, Detail, 1991. Hyattsville, National Center for Health Statistics.
NCHS (1997). U.S. Decennial Life Tables for 1989-91, Vol. 1, No. 1. Hyattsville, National Center for Health Statistics.
NCRP (1997). Uncertainties in Fatal Cancer Risk Estimates Used in Radiation Protection. Bethesda, National Council on Radiation Protection and Measurements.
NRPB (1993). Estimates of Late Radiation Risks to the UK Population. Didcot, National Radiological Protection Board.

Nudat (2007). Nudat 2.4, Brookhaven National Laboratory.
Obara, T., Miura, T., Fujita, Y. Ando, Y., Sekimoto, H. (2003). "Preliminary study of the removal of polonium contamination by neutron-irradiated lead-bismuth eutectic " Annals of Nuclear Energy **30**(4): 497-502.
Parvez, H., Reich, A., Lucas-Reich, A, Parvez, S. (1988). Flow Through Radioactivity Detection In HPLC. Utrecht, VSP.
Paulenova, A. (2001). "Combined Extraction Chromatography and Scintillation Detection for Off-Line and On-Line Monitoring of Strontium in Aqueous Solutions." Journal of Radioanalytical and Nuclear Chemistry **249**(2): 295-301.
Pearlman, I. H., Richards, H.T. (1944). The Energies of the Neutrons From Polonium Alphas on Boron. Los Alamos, Los Alamos Scientific Laboratory.
Peterson, D., Plionis, A., Gonzales, E. (2007). "Optimization of Extraction Chromatography Separations of Trace Levels of Actinides with ICP-MS Detection." Journal of Separation Science **30**: 0.
Piltingsrud, H. V., Stencel, J.R. (1972). "Determination Of 90Y, 90Sr, And 89Sr In Samples By Use Of Liquid Scintillation Beta Spectroscopy." Health Physics **23**(1): 121.
Pointurier, F., Baglan, N., Hemet, P. (2004). "Ultra Low-Level Measurements of Actinides By Sector Field ICP-MS." Applied Radiation and Isotopes **60**(2-4): 561-566.
Price, K. (1973). "A Review of Transuranic Elements in Soils, Plants, and Animals." Journal of Environmental Quality **2**(1): 62-66.
Reboul, S. H., Borai, E. H., Fjeld, R. A. (2002). "Sequential Separation of Actinides By Ion Chromatography Coupled With On-Line Scintillation Detection." Analytical and Bioanalytical Chemistry **374**(6): 1096-1100.
Rich, B. L. (1990). Internal Dosimetry and Control. U. D. o. Energy. Idaho Falls, Idaho National Engineering Laboratory.
Roane, J., DeVol, T. (2002). "Simultaneous Separation and Detection of Actinides in Acidic Solutions Using an Extractive Scintillating Resin." Analytical Chemistry **74**: 5629-5634.
Roane, J. E., DeVol, T.A., Leyba, J.D., Fjeld, R.A. (2003). "The Use of Extraction Chromatography Resins to Concentrate Actinides and Strontium From Soil for Radiochromatographic Analyses." Journal of Environmental Radioactivity **66**: 227-245.
Robbins, M. C. (1955). The Determination of Polonium in Urine. Los Alamos, Los Alamos Scientific Laboratory.
Roessler, G. (2007). "Why 210Po?" Health Physics News **35**(2): 1-9.
Ruzicka, J. (1994). "Discovering Flow Injection: Journey From Sample to a Live Cell and From Solution To Suspension." The Analyist **119**: 1925-1934.
Ruzicka, J., Hansen, E. (1988). Flow Injection Analysis. New York, Wiley-Interscience.
Ruzicka, J., Marshall, G. D. (1990). "Sequential Injection: A New Concept for Chemical Sensors, Process Analysis and Laboratory Assays." Analytica Chimica Acta **237**: 329-343.
Smith, M. R., Farmer, O. T., Reeves, J. H., Koppenaal, D. W. (1995). "Radionuclide Detection By Ion-Chromatography and On-Line and Beta Detection: Fission

Product Rare Earth Element Measurements." Journal of Radioanalytical and Nuclear Chemistry **194**(1): 7-13.
Stannard, J. N. (1964). Metabolism and Biological Effects of an Alpha Particle Emitter, Polonium-210. Rochester, University of Rochester. Atomic Energy Project.
Stricklin, D. L., Tjarnhage, A., Nygren, U. (2002). "Application of Low Energy Gamma-Spectrometry in Rapid Actinide Analysis for Emergency Preparedness." Journal of Radioanalytical and Nuclear Chemistry **251**(1): 69-74.
Takei, M., Kida, T., Suzuki, K. (2001). "Sensitive Measurement of Positron Emitters Eluted From HPLC." Applied Radiation and Isotopes **55**: 229-234.
Talvitie, N. A. (1971). "Radiochemical Determination of Plutonium in Environmental and Biological Samples by Ion Exchange." Analytical Chemistry **43**(13): 1827.
Thompson, J. J., Houk, R. S. (1986). "Inductively Coupled Plasma Mass Spectrometric Detection for Multielement Flow Injection Analysis and Elemental Speciation By Reversed-Phase Liquid Chromatography." Analytical Chemistry **58**(12): 2541-2548.
Tolgyessy, J., Harangozo, M. (1993). "Flow-Injection Activation Analysis " Journal of Radioanalytical and Nuclear Chemistry **176**: 113-115.
TON (2007). Table of Nuclides, Korea Atomic Energy Research Institute.
U, M., Han, B., Myoe, K., Kywe, A., Tolgyessy, J. (1994). "Modified and Reverse Radiometric Flow Injection Analysis." Journal of Radioanalytical and Nuclear Chemistry Letters **187**(3): 179-184.
U, M., Han, B., Myoe, K., Kywe, A., Tolgyessy, J. (1994). "Radiometric Detection In Flow-Injection Analysis (Radiometric Flow-Injection Analysis)." Journal of Radioanalytical and Nuclear Chemistry Letters **187**(2): 117-122.
U, M., Tolgyessy, J. (1995). "Radiometric Flow-Injection Analysis." Journal of Radioanalytical and Nuclear Chemistry **191**(2): 413-426.
U, M., Tolgyessy, J., Win, N., San, K., Han, B., Myoe, K. (1994). "Radiometric Flow Injection Analysis With an ASIA (Ismatec) Analyzer " Journal of Radioanalytical and Nuclear Chemistry Letters **187**(5): 345-349.
UNSCEAR (1982). Ionizing Radiation: Sources and Biological Effects. New York, United Nations Scientific Committee on the Effects of Atomic Radiation.
UNSCEAR (1993). Sources and Effects of Ionizing Radiation. 1993 Report to General Assembly, with Scientific Annexes. New York, United Nations Scientific Committe on the Effects of Atomic Radiation.
UNSCEAR (1994). Sources and Effects of Ionizing Radiation. 1994 Report to the General Assembly, with Scientific Annexes. New York, United Nations Scientific Committee on the Effects of Atomic Radiation.
UNSCEAR (2000). United Nations. Sources and Effects of Ionizing Radiation. U. N. S. C. o. t. E. o. A. Radiation. New York, United Nations.
Unsworth, E. R., Cook, J. M., Hill, S. J. (2001). "Determination of Uranium and Thorium in Natural Waters With a High Matrix Concentration Using Solid-Phase Extraction Inductively Coupled Plasma Mass Spectrometry." Analytica Chimica Acta **442**(1): 141-146.

Vajda, N., LaRosa, J., Zeisler, R., Danesi, P., Kis-Benedek, G. (1997). "A Novel Technique for the Simultaneous Determination of 210Pb and 210Po Using a Crown Ether." Journal of Environmental Radioactivity **37**(3): 355-372.

Vreček, P., Benedik, L. (2003). "210Pb and 210Po in fossil fuel combustion at the Šoštanj thermal power plant (Slovenia)." Czechoslovak Journal of Physics **53**(1): A51-A55.

Workshop, H. (1986). Radiologische Auswirkungen des Tschernobyl-Unfalls auf die Bundesrepublik Deutschland. Hamburg Workshop. Hamburg.

Wyse, E., MacLellan, J., Lindenmeier, C., Bramson, J., Koppenaal, D. (1998). "Actinide Bioassays By ICPMS." Journal of Radioanalytical and Nuclear Chemistry **234**(1-2): 165-170.

Vita

Alexander Asterios Plionis was born in Washington D.C. on March 21, 1980, the eldest son of Dimitri and Elizabeth Plionis. He was raised in Northern Virginia, where he graduated from high school in Oakton, Virginia. He attended Macalester College in Saint Paul, Minnesota, where he was a National Merit Scholar and a DeWitt Wallace Distinguished Scholar and where he triple majored in Chemistry, Physics, and Classical Languages. During his four years as an undergraduate, he received the NSF Research Experience for Undergraduates grant and a Beltman Summer Research in physical chemistry. He also met fellow Macalester College student, Krista Star Scott, who was to become his wife. Krista and Alex were married on October 14, 2006 in Saint Paul. After receiving his Batchelor of Arts in May of 2002, he decided to continue his studies at the University of Texas at Austin in 2003. He received his Master of Science in Engineering in the field of nuclear engineering in the summer of 2005 and continued to pursue his doctorate. During his time as a graduate student, he spent three summers with the Radiochemistry Team in the Chemical Sciences and Engineering Group at the Los Alamos National Laboratory, eventually achieving a year-round position. The results of his work with LANL, in conjunction with research at the UT, were presented herein.

Permanent address: 4266 River Song Lane, Santa Fe, NM, 87507

This dissertation was typed by the author.